Simulation and Experimental Study of SCM/WDM Optical Systems

Renxiang Huang

B.S.E.E., Beijing University of Posts & Telecommunications, 1993

Submitted to the Department of Electrical Engineering and Computer Science and the Faculty of the Graduate School of the University of Kansas in partial fulfillment of the requirements for the degree of Master of Science

Thesis Committee:

_____
Chairman

_____

_____
Date of Defense: May 23, 2001

Abstract

High-speed data transmission utilizing optical subcarrier multiplexing (SCM) techniques was recently studied by experiments and simulations in several works [1,2,3,4]. SCM may have better spectral efficiency than WDM and SCM system could be less subjected to fiber dispersion than TDM system because the data rate at each subcarrier is low. These works used amplitude shift keying (ASK) as the RF modulation format and used double side band (DSB) as the optical modulation method, they used optical filter to select each subcarrier channel and detect the ASK signal directly. The reported transmission distances were about 500km.

In our study, optical-single-side-band modulation (OSSB) was used since it further increases the spectrum efficiency and significantly decreases the dispersion penalty; Multiple phase shift keying (MPSK) RF modulation was used due to its high spectral efficiency and simple demodulation. We have developed a simulation model and simulated 3 types of SCM systems --- 4-subcarrier binary phase shift keying (BPSK) system, 2-subcarrier quadrant phase shift keying (QPSK) system, 4-subcarrier ASK system. We also show the result of a standard IMDD WDM system for comparison. These 4 types of systems all use 4 wavelengths with 50GHz spacing and have same total capacity (40Gbps). We did an experiment of a single wavelength 4 channel BPSK SCM system (total 10 Gbps capacity) over 75 km standard single mode fiber.

There are two major limiting factors for the system performance, namely nonlinear distortion and accumulated ASE noise. For SCM systems, the nonlinear interference between subcarrier channels is severe because the channel spacing is very narrow and the interference components fall into the signal frequencies. In order to limit nonlinear interference, the signal optical power can not be too high. On the other hand, in order to keep an acceptable signal-to-noise ratio (SNR) in the presence of accumulated ASE noise, the optical power can not be too small. Therefore parameter optimization is essential in the system design. A major benefit of SCM systems is their immunity to fiber dispersion. This type of systems and hence they is

suitable to be used in those situations which require high spectrum efficiency and do not have dispersion compensation.

Polarization walkoff and PMD effects were assessed preliminarily in this work and further simulation and experiments are suggested to determine their exact impact on the system performance.

Our simulation results revealed that with dispersion compensations, the longest transmission distance for BPSK system is 450 km, QPSK system is 1200km, ASK SCM system is 250km, IMDD system is 1100km. If there is no dispersion compensation, these numbers are 250 km, 450 km, 550 km and 100 km respectively.

Acknowledgements

I would like to express my deepest gratitude to my advisor and mentor, Dr. Rongqing Hui, for his invaluable guidance and unwavering support throughout my education at the University of Kansas. Without his encouragement and patience, this work can not be done. I would also like to extent my gratitude to Dr. Kenneth Demarest and Dr. Christopher Allen for serving on my thesis committee and their encouragement.

I would like to thank Dr. Benyuan Zhu and Chris Johnson for valuable discussions on the SCM experiment. I also thank Dr. Kumar (Vijay) Peddanarappagari for those enlightening discussions on simulation methods.

A special thanks to Yonggang Wang for his numerous help and encouragement. My gratitude also goes to other members of the Lightwave Group, in particular, Hok-Yong Pua and Dan Tebben for their friendly help and caring.

Finally, I want to express my gratitude and love to my wife, Ying Tian. Without her loving support and encouragement, I would not have accomplished this goal.

Table of Contents

Chapter One

Background and Introduction

1.1 Introduction and Motivation

The prevalent utilization of Internet by business and consumer has been generating a global demand for huge bandwidth. In recent years, as new bandwidth hungry applications like internet video and audio and new access technologies such as xDSL become more popular, optical communications networks are finally feeling the bandwidth constraints already faced in many other communications networks such as wireless and satellite communication systems. Service providers are searching for ways to increase their fiber optic network capacity.

In order to solve this problem, people have been trying to make full use of the huge bandwidth provided by optical fibers. Technologies like TDM, WDM and their combinations are used and improved.

The TDM strategy is to increase the bit rate carried by a single optical wavelength. These systems use very short pulses to achieve very high bit rate and thus they are subject to the influence of dispersion (because of the wide bandwidth of the signal) and nonlinearities (because of the required high power to overcome the noise). High speed TDM systems are very sensitive to the PMD effect and they are also limited by the achievable speed of electronic components and devices. Because of those constraints, the data rate of commercial optical fiber systems is currently limited at 10Gb/s. For some old fiber plants, the maximum per-channel data rate is 2.5Gb/s due to the limitation in their poor PMD characteristic.

Later, as technology advanced, WDM came along. The WDM strategy is to make better use of optical fiber bandwidth by stacking many TDM channels into the same fiber. The advantage of WDM over TDM is that WDM usually use much lower bit rates and optical power in each channel while achieving a higher total capacity. Hence, the issues in high-speed TDM such as PMD, chromatic dispersion, fiber

nonlinearities become mitigated. However, there are many factors that limit the system performance of WDM. The wavelength stability of semiconductor lasers and selectivity of optical filters limit the minimum channel spacing from 50GHz to 100GHz in current commercial WDM systems. As an example, for a WDM system of 2.5Gb/s per-channel data rate and 50GHz channel spacing, the bandwidth efficiency is only 0.05 bit/Hz. How to further increase the efficiency of bandwidth utilization while maintaining quality transmission? This problem still remains as a challenge to the optical communication society.

1.2 SCM as a viable solution

One technology that can be used to increase the efficiency of bandwidth utilization is the Sub-carrier multiplexing (SCM). It is an old technology that has been studied and applied extensively in microwave and wireless communication systems. In optical domain, the most popular SCM application is the optical analog video transmission and distribution.

SCM technology essentially uses a two step modulation. First, several low bandwidth RF channels carrying analog or digital signal are combined together and they are very close to each other in the frequency domain. Then this composite signal is further modulated onto a higher frequency microwave carrier or optical carrier and can be transmitted through different media.

Because of its simple and low-cost implementation, high-speed optical data transmission using SCM technology attracted the attention of many researchers. The most significant advantage of SCM in optical communications is its ability to place different optical carriers together closely. This is because microwave and RF devices are much more mature than optical devices: the stability of a microwave oscillator is much better than an optical oscillator (laser diode) and the frequency selectivity of a microwave filter is much better than an optical filter. Therefore, the efficiency of bandwidth utilization of SCM is expected to be much better than conventional optical WDM.

First, let us look at the spectrum of optical digital SCM signal and then later we will show an example realization of an optical digital SCM system.

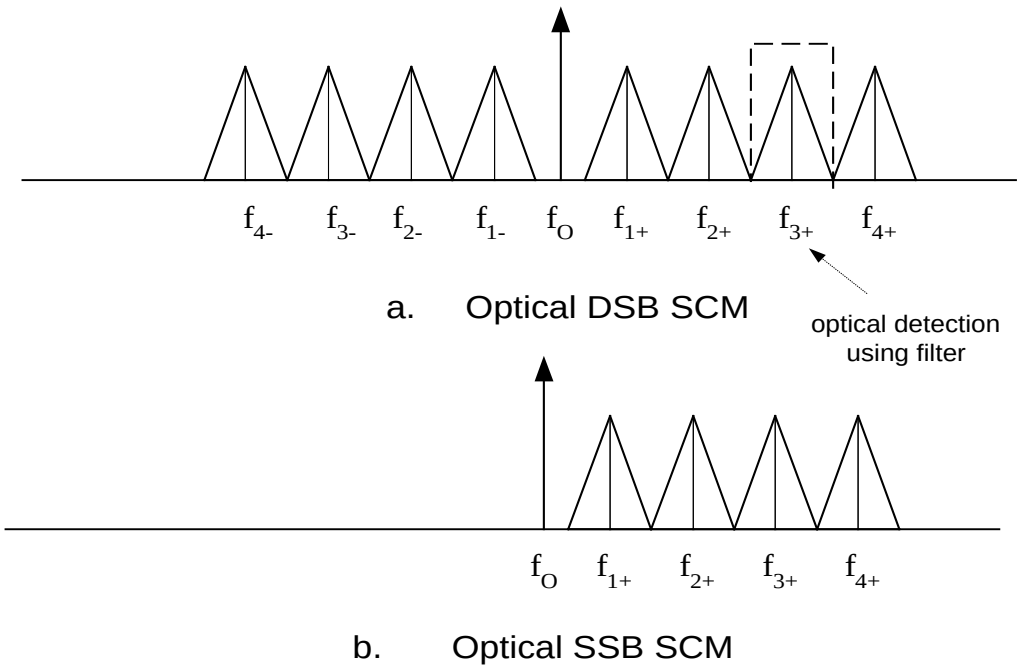

Figure 1.1, Illustration of the spectrums of DSB SCM and SSB SCM signals

Figure 1.1(a) shows the spectrum of traditional SCM system which is double side band modulated (DSB), it is usually generated by direct modulation of a semiconductor laser or an external optical modulator like a Mach Zender modulator. Mach Zender modulator is generally nonlinear in nature. As many different ways to linearize the Mach Zender modulator are found and available [10], more and more systems are using MZ modulator to generate the signal. In the figure, $f_{i\pm}$ is the frequency of the sub carriers i. Signals are on both sides of the carrier, the total optical bandwidth is about twice of the bandwidth of the microwave signal or the modulating signal.

When the bandwidth of the information becomes higher, such as more than several GHz, and the transmission distance is very long, such as more than hundreds of kilometers, the DSB scheme will not work if it still use only a simple photon detector

to detect. This is because the dispersion of the fiber will give quite different delay to f_{i+} and f_{i-} due to the large frequency difference between them. If the relative delay between f_{i+} and f_{i-} is comparable to the duration of a baseband bit, then after photon detector, the two side bands will interfere with each other destructively.

Two methods can be used to solve this problem, one way is to use narrow band optical filter to filter out each subcarrier channel and then detect them separately. This is the method used in previous study of high-speed data transmission utilizing SCM techniques [1,2]. In those studies, DSB is used as the optical modulation method and ASK is used as the RF modulation format. The demodulation of subcarrier is to filter out each subcarrier optically in order to avoid the fiber dispersion effect on the double side band modulation format. ASK RF modulation is used because it makes direct detection possible. The optical spectrums of these systems are very similar to the spectrum showing in Figure 1.1 (a).

Another way is to use optical single side band modulation. Figure 1.1 (b) is the spectrum of optical single side band (OSSB) SCM, the lower side band in the DSB spectrum is removed by ways such as optical filter or special modulating methods. The carrier itself could be remove or kept depending on the preferred demodulating method. The occupied spectrum is only half that of the optical DSB signal.

When optical SSB modulation is used, it will occupy the same bandwidth as the traditional WDM system if they have the same information bit rate. Figure 1.2 (b) is showing the spectrum of a traditional WDM system, Figure 1.2 (a) is the spectrum of a comparable WDM/SCM. Each of the WDM wavelengths carries a SCM composite signal. In this illustration, the signal bandwidths of the two systems are similar if the guard band between two adjacent subcarriers is small enough and can be ignored.

In this example, the bit rate of each subcarrier is only one fourth of the corresponding traditional WDM channel bit rate. 4 subcarriers will give the same capacity as the traditional WDM. They also occupy the same amount of bandwidth.

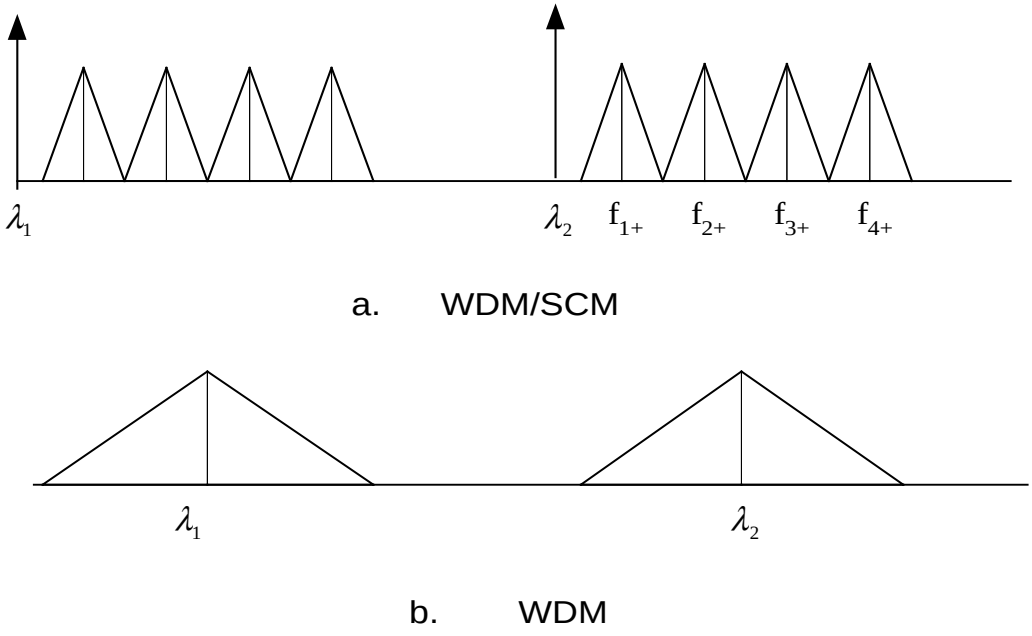

Figure 1.2, Illustration of the spectrums of WDM/SCM and traditional WDM

Because the dispersion effect is proportional to the square of the bit rate in a TDM channel of a WDM system, and the dispersion effect on is 16 times more severe in the traditional WDM system than in the WDM/SCM system, you should be able to transmit the signal longer in WDM/SCM system than in traditional WDM.

In practice, without SCM technology it is not realistic to place two wavelength channels at 5GHz spacing in a WDM system due to wavelength stability of laser diodes and frequency selectivity of optical filters. However, this narrow channel spacing is possible with sub-carrier multiplexing thanks to the maturity of microwave technology. Essentially, WDM/SCM is equivalent to packing more WDM channels in a given optical bandwidth and breaking through the limitations of minimum channel spacing imposed by current optical device technology.

One additional advantage of SCM is that subcarriers can be modulated using various formats including phase modulations because RF carriers have stable phase. It thus can be used in a lot of different network setups and it is easy to be used with

traditional Synchronous Optical Network (SONET) equipment. Also because the bit rate granularity is smaller which facilitates channel add/drop, the combination of WDM and SCM can potentially make optical networks more flexible.

However SCM technology is subject to some important system penalties. Because the channel spacing between subcarrier is so small, you will suffer higher nonlinear distortion. For example, in the lightwave analog video transmission and distribution [11,12], because the analog signal is very sensitive to any type of distortion such as device noise and the inter-modulation distortion (composite second-order (CSO) distortion and composite triple beat (CTO)) due to the nonlinearity of the devices and the fiber, the system has very stringent requirements on the noise and the linearity of the system. In digital sub-carrier multiplexing system, even the linearity of the system and SNR or CNR requirement is not that strict as in analog applications, the major concerns is still the inter-modulation crosstalk due to the devices and fiber.

Little research has been done for a digital SCM system with optical single side band and PSK RF modulation. No systematic comparison between a digital SCM system and a digital binary system has been done. This work will first focus on two types of SCM systems with OSSB and PSK RF modulation and their performance with standard G.652 fiber. In one of the systems, there are 4 wavelength and each wavelength has 4 BPSK subcarriers. Each subcarrier carries OC48 data. In another one, there are 4 wavelength and each wavelength has 2 QPSK subcarriers. Each subcarrier carries 2 OC48 data channels. Then we compared these two systems with a ASK modulated SCM system and a traditional OC192 ASK system.

The motivation to use OSSB and PSK RF modulation is that OSSB can reduce the bandwidth of the signal and increase the spectrum efficiency. Because OSSB will reduce the damage of the chromatic dispersion without optical filtering of each subcarriers, the signal of one wavelength can be converted to electrical signal directly and then demodulate each subcarrier in the microwave domain.

PSK RF modulation is used because BPSK will have 6dB sensitivity gain against ASK. We also used QPSK in our system because it has higher spectrum efficiency.

We didn't consider QAM because in [13], the result of the comparison of QAM and PSK shows that PSK is robust to the nonlinearity of an MZ modulator compared to 16 QAM and 64 QAM, and also the QAM scheme require much higher modulating signal amplitude to reach the same symbol error rate as the PSK. This is because the QAM format needs less bandwidth but higher amplitude.

Simulation is the main way of investigation due to its economical advantage. Experiment was also done for a 1 wavelength 4 subcarriers BPSK SCM system and comparison between this system and a one wavelength ASK OC192 system is also done experimentally.

Figure 1.3 is a demonstrating setup of SCM system, at the left side is the transmitter, in the transmitter, you have m separate optical transmitters, each optical transmitter use n microwave mixer to generate n subcarriers and combine them as a composite signal. Then the composite signal is used to modulate the lightwave.

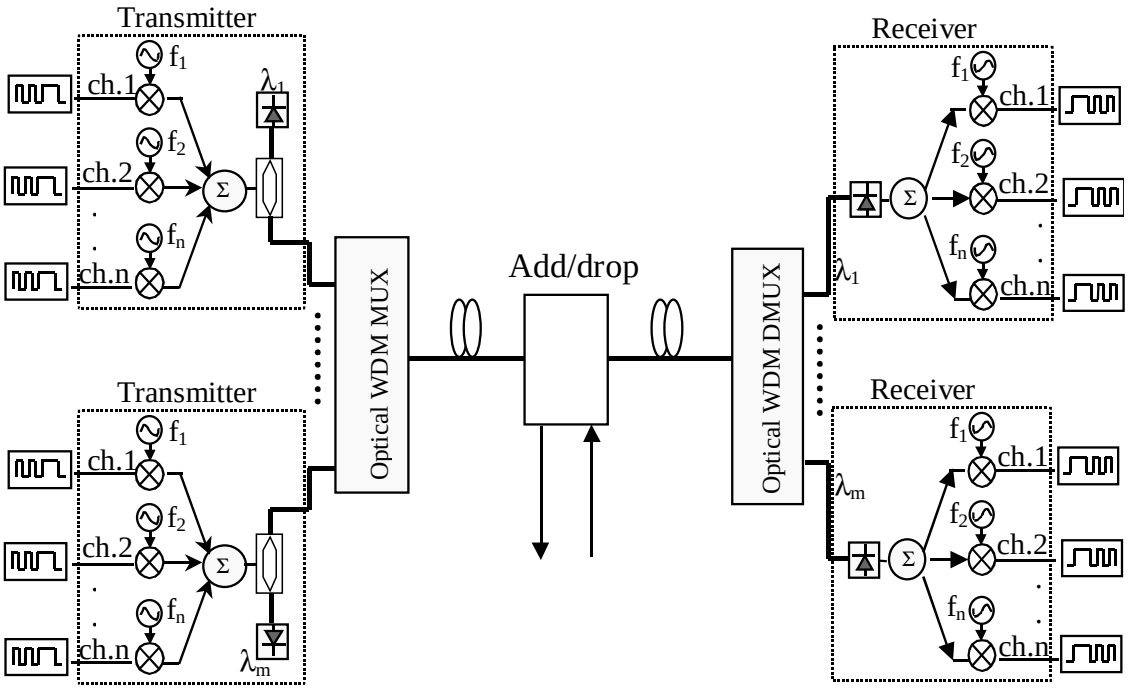

Figure 1.3, A basic configuration of an SCM/WDM optical system

Then the m wavelength channels are combined by an optical WDM multiplexer. At the receiver, an optical WDM demultiplexer is used to separate different wavelength, a separated optical detector is used the convert the optical signal into electrical current, then the electrical signal is sent to n branches. In each branch, the signal is demodulated by a microwave mixer coherently.

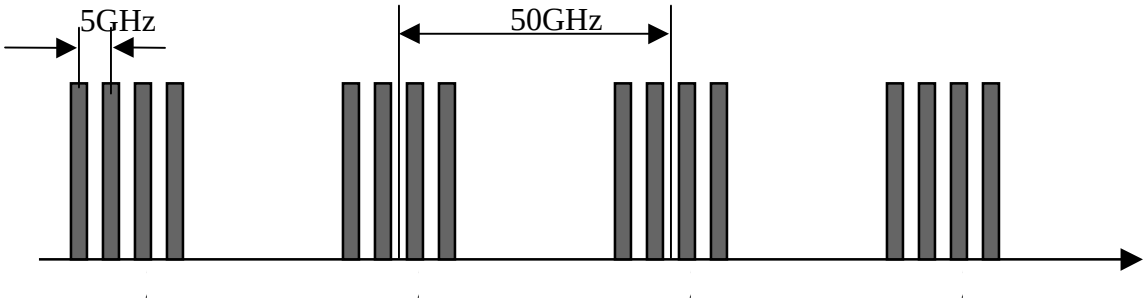

Figure 1.4, Illustration of wavelength arrangement of an SCM/WDM system.

Figure 1.4 is an illustration of wavelength arrangement of an SCM/WDM system when the n=4 and m=4, the subcarrier channel spacing is 5GHz, the wavelength spacing is 50GHz,

It is worth mentioning that here we if an optical carrier is transmitted along with the subcarrier channels then the optical carrier and the subcarrier channels can beat with each other in the photon diode and generate the microwave signal. In this way, you don't have to have a local oscillator like traditional coherent system.

In order to multiplex several sub-carrier digital channels on one wavelength, wideband microwave devices and wideband electro-optic modulators are necessary. Currently, commercially available devices have bandwidths around 20GHz to 30GHz. With a 20GHz modulator bandwidth, 4 SCM channels each carrying OC-48 traffic can be accommodated. In this work, the largest number of SCM channels is 4 because it is limited by the device of the lab and also it is an adequate choice for real applications.

Also, it is not showing in the diagram, since several digital channels are closely packed on one wavelength, we have to use microwave filters both at the transmitter and at the receiver to select the desired channel, and these filters must have good frequency selectivity in order to minimize linear inter-channel crosstalks.

From an optical transmission point of view, as the channel space is much smaller than traditional WDM system, the fiber nonlinearity will generate much higher nonlinear interference. Also because the subcarriers are modulated in one optical wavelength, the nonlinearity of the modulator and the photon detector will also generate inter channel interference too.

1.3 Organization of the thesis

This thesis is organized into 5 chapters. In chapter 2, the simulation model will be presented and the issues involved will be explained in details. These issues include general simulation method; simulation implementation of the modulations, optical fiber, demodulation; noise calculation; polarization walkoff and PMD issues. In chapter 3, the simulation results of 3 different types of SCM systems: 4 wavelength 4 BPSK subcarriers SCM, 4 wavelength 2 QPSK subcarrier SCM, 4 wavelength 4 ASK subcarriers SCM, will be given and the selection of system parameters are examined. Then a traditional 4 wavelength OC192 WDM system is simulated and the results are compared to those of SCM systems. In chapter 4, a one wavelength 4 BPSK subcarriers system is studied experimentally and it is compared with a one wavelength OC192 system.

And finally, in chapter 5, the thesis is concluded and the problems that need further studies are discussed and prospected.

Chapter Two

Numerical model for the SCM system

In order to study the feasibility and performance of the SCM system, both simulation and experiment methods could be used. Due to its economic advantage, simulation method is used very often in studying communication systems.

First of all, simulation does not require any physical devices and equipment. Once the simulation model is built, it is very easy to change the system parameters and the time needed to check a specific setup is usually much smaller comparing to an experimental investigation. Second, in a simulation, the only limitation is the computing power of the computer such as CPU speed and memory size. You can perform a simulation for a complex system while it is very difficult to fulfil in a real experiment, which requires many devices and equipment.

We used both experimental method and numerical modeling method in our investigation of the SCM systems. Since the setup of a multi-wavelength SCM system will require many microwave and optical devices which will cost a lot of money. We only did an experiment of one wavelength SCM system. Then we simulate the performance of several different 4-wavelength SCM systems. We will first present the simulation part in the following two chapters. Then in the fourth chapter, we will present the experimental result.

In order to understand the setup of the simulated SCM systems and the detail of the simulation models of the transmitter, optical fiber, receiver etc., in this chapter, we will introduce the simulation models and discuss some problems that are special to the SCM simulation.

2.1 General Considerations for numerical simulation of optical SCM fiber transmission systems

A numerical modeling or simulation program for a system should include the models of all the components that constitute that specific system. As a system level

simulation, the model for each individual component should be kept as simple as possible when the accuracy requirements allow. It is not necessary to use their detailed models because it will not significantly increase the overall accuracy of the simulation but it would increase complexity dramatically and results in a much lower efficiency. So most of the components in our simulation are assumed to be ideal and doesn't behavior exactly like their physical counterpart. But the effect of this inaccuracy can be ignored because it is very small compare to the distortion of the fiber and will not have big impact on the final result.

Modeling of the optical fiber system is quite different than the modeling of other types of communication systems, such as wireless system, due to its high bit rate, low bit error rate and its transmission media, which needs special consideration.

High bit rate means that the simulation bandwidth has to be very large and the number of bits you can simulate at one time will have to be small due to the limitation of the computing hardware. Low bit error rate means a BER lower than 10^{-9} and you have to run a very long simulation in order to see even a single error bit transmitted. So we use a method called semi-analytical method to calculate the BER of the system. This method will calculate the noise analytically instead of numerically.

Among all the devices and subsystems of an optical transmission system, the optical fiber is usually the main source of the system penalty and its modeling is the most important part of the whole model.

In some situations, analytical calculation can also be used to model the fiber transmission. Because there is no close form solution to the nonlinear transmission equation that guard the waveform evolution along the fiber, linear addition model is applied to the evaluation procedure, every nonlinear effect and the fiber dispersion is considered separately and then all the effects are added together to get the total system performance. The interactions between all these effects are ignored.

Compared to analytical methods, the numerical integration of the propagation equation is generally more accurate and it takes into account all the linear and

nonlinear effects automatically. It became quite popular for the performance evaluation of optical transmission systems.

There are generally two categories of numerical methods which can be used to solve the equation, one of them is the finite difference method and the other is the Pseudo-spectral methods, and pseudo-spectral methods is faster by up to an order of magnitude to achieve the same accuracy. Among the second category, split step Fourier method is used most extensively to solve the pulse propagation problem in nonlinear dispersive media. Its fast speed mainly can be attributed to the use of the fast Fourier transform algorithm. Because its fast speed and easy implementation, we will use the split step Fourier method as the algorithm for the fiber model.

Most previous simulations on fiber systems use single step modulation and demodulation, which is commonly referred to as E/O and O/E conversions. The most often used format is on/off keying modulation. SCM system needs two steps of modulation and demodulation. The first step modulation is the modulation of baseband signal into microwave subcarriers and the second step is the E/O conversion. Demodulation is the reverse of these two steps. Also, SCM can use PSK, QSK and ASK modulation format. We will simulate the first modulation step in the real signal domain and the second modulation in the complex signal domain.

In the remaining of this chapter we will explain the detail of our simulation model.

2.2 Basic information of the numerical model of optical SCM systems:

We have developed a simulation model in MATLAB because it is flexible and has many built-in functions like FFT calculation and array manipulation. This model is capable to simulate a multi-wavelengths sub-carrier multiplexed WDM transmission system. It can use ASK, BPSK and QPSK as the RF modulation format. It simulates a dual-electrod Mach-Zender optical modulator and generates optical DSB or SSB signals. It uses split step Fourier method to simulate the fiber

transmission and it considers the impact of fiber dispersion effect and fiber nonlinear effects such as FWM, XPM, SPM. It calculates the distortion created at various parts of the system, such as modulation, transmission, and demodulation with numerical simulation. An analytic method is used to evaluate the effect of noise. The system performance is evaluated by eye opening and receiver sensitivity.

The simulation model has a graphical user interface and most of the system parameters can be changed through this interface. It also supports a batch mode and the user can change the parameters by editing a text file. In addition to the parameters, The system setup also can be changed through the GUI.

The simulation model considers all the important components of a real system and its structure is very much like that of a real system, which we have showed in chapter 1.

There are several types of SCM systems and the entire simulation models for each type of system can be divided into three parts: the transmitter, fiber path and the receiver. We will first show the diagrams of a 4-subcarrier BPSK SCM system as an example. Other SCM systems like QPSK and ASK SCM will be very similar to it. We use the number 4 as the sub-carrier channel number because it is used in SONET protocols. In fact this number is only limited by the bandwidth of available optical modulator and could be higher.

We will explain the function of each component in the exemplary BPSK system and show some typical signal waveform of spectrum generated by the simulation program.

2.3 Transmitter side simulation models

Figure 2.1 is the diagram for the transmitter side of a 4-subcarrier BPSK system, it only shows the transmitter of one wavelength. Transmitters of all other wavelengths should have the same structure.

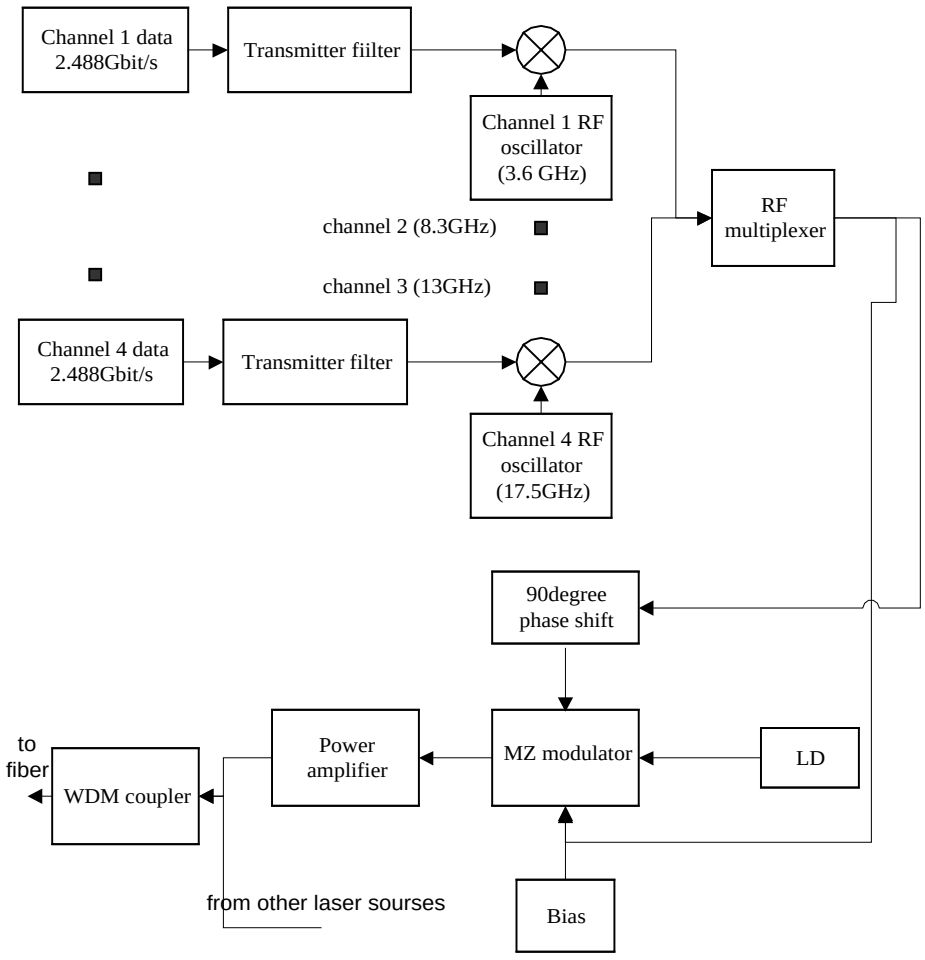

SCM Transmitter Block Diagram

Figure 2.1 Simulation diagram for the transmitter side of a 4 subcarriers BPSK system

In this exemplary transmitter, there are four sub-carrier channels in one wavelength. Data rate is 2.488 Gb/s per sub-carrier channel. The transmitter filters are usually set as 6-order Butterworth filters with 3dB bandwidth of 1.736 GHz. The sub-carrier frequencies are 3.6GHz, 8.3GHz, 13GHz, and 17.5GHz respectively. The RF modulation index of each sub-carrier channel could be different from each other in order to optimize the receiver sensitivity. The RF signals are combined together to modulate a MZ electro-optic modulator. Then the optical output is amplified by an

EDFA. In this diagram, only one wavelength is shown, other channels may be added together through a WDM coupler.

2.3.1 Baseband signal generation

The data rate of each subcarrier can be set to OC48 or other meaningful number. The data bits are generated by a random number generator, it generates a bit sequence of 0 and 1 with equal probability. In this simulation, the length of the bit sequence is usually set to 128. This number is equal to 2^7 and is one of the choices of PRBS (pseudo-random bit sequence) used in most BER tester. This PRBS has 7 consecutive 1s and 6 consecutive 0s. We also used this PRBS in our simulation.

Then an ideal rectangle baseband signal is generated according to the data bits. The number of samples per bit will determine the simulation bandwidth. The simulation bandwidth which is the highest frequency that the simulated signal could be is $0.5/dT$, here dT is the time interval between samples. For nonlinear system, the bandwidth of the output signal is usually larger than that of the input. So one has to consider this situation when selecting the number of samples per bit. Please refer to appendix 1 for the estimation of the bandwidth of a nonlinear system. Usually we use 64 samples in each bit for one wavelength simulation and use 256 samples per bit for four wavelengths simulation.

In order to get rid of the side peaks in the spectrum of an ideal rectangle waveform, we use a transmitter filter to shape the output bit. These transmitter filters are usually are set as 6-order Butterworth filters with 3dB bandwidth of about 0.7*Bitrate. It will effectively remove the second side peak and effectively reduce the inter-channel interference when several subcarriers are multiplexed together.

Figure 2.2, (a) (b) and (c) are the eyediagram, waveform and spectrum of the filtered signal. Figure 2.2 (d) is the spectrum of the rectangle signal before the filtering. (In the program, the amplitude of the signal before the modulation is set to an arbitrary number, so in these plots, only the relative amplitude is relevant.) We can see that the second peak in the spectrum is further suppressed by 15 dB by the filter.

This suppression is very important in subcarrier multiplexing because the frequency difference between adjacent subcarriers is only about 2 times the bit rate and is about 5 GHz in the case of OC48. We will discuss this later.

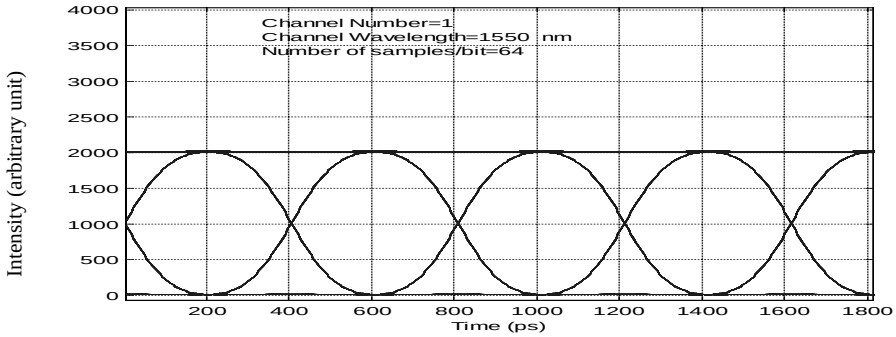

(a)eyediagram of baseband signal after the electrical filter

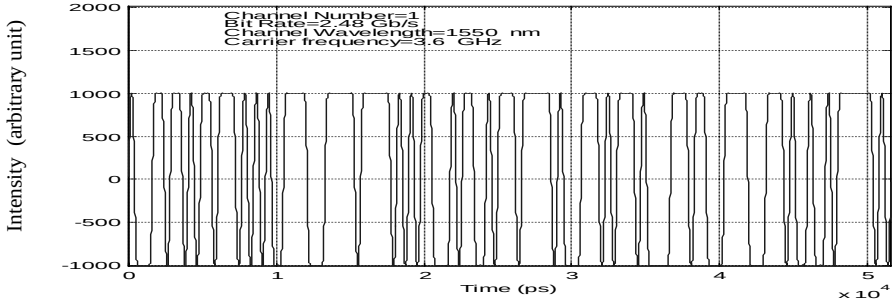

(b) waveform of baseband signal after the electrical filter

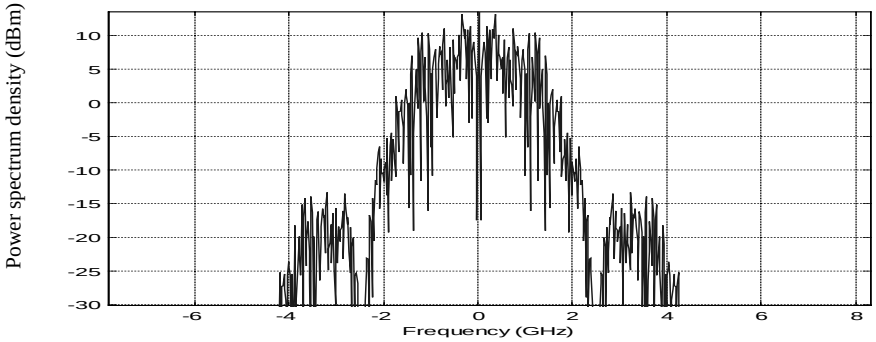

(c)spectrum of of baseband signal after the electrical filter

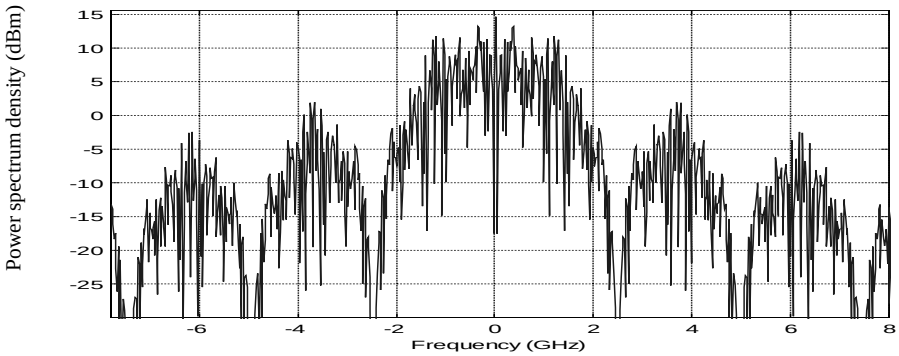

(d) spectrum of of baseband signal before the electrical filter

Figure 2.2 Eyediagram, waveform and spectrum of the baseband signal

2.3.2 Subcarrier signal generation

The most common modulation method in optical fiber communications is on-off keying because it can utilize a rather simple receiver structure and also because it is difficult to utilize those complex modulation methods as used in the microwave communications. This is because of the immaturity of optical technology.

In SCM optical transmission systems, a large variety of modulation schemes become feasible because all those modulation and demodulation can be done in the microwave domain.

The major modulation formats are OOK (on off keying) or ASK (amplitude shift keying), PSK(phase shift keying) and QAM (Quadrature amplitude modulation).

When BPSK is compared with ASK on a peak envelope power (PEP) basis [16], for a given noise value of N_0 (the only detrimental factor is the additive white noise), 6 dB less (peak) signal power is required for BPSK signaling to give the same BER as that for ASK. Even the two are compared on an average power basis, the performance of BPSK has a 3 dB advantage over ASK since the average power of ASK is 3 dB below its PEP. But the average power of BPSK is equal to its PEP.

The BER of BPSK is $BER = Q(\sqrt{\frac{A_C^{\ 2}}{8N_0B}})$ and the BER for ASK is $BER = Q(\sqrt{\frac{A_C^{\ 2}}{2N_0B}})$, where A_C is the peak value of the signal, B is the noise bandwidth, N_0 is the noise power spectrum density and $Q(x)$ represents a complementary error function. The power different here is 6dB.

Although ASK has such a disadvantage, since ASK is the format that was used in previous study [1,2,3] and it is immune to some polarization effects such as PMD effect, which we will discuss in the receiver part, so we still will study its performance.

Also, as discussed in the work by Sen Lin Zhang, etc [13], in a system using a Mach-Zehnder(MZ) modulator for the modulation of an optical carrier, the effect of the nonlinearly of MZ modulator is less serious for a system using QPSK or 8-PSK than for a system using 16 or 64 QAM. Based on these considerations, we will use both PSK and ASK in our study

BPSK can be represented by $s(t) = A_c m(t)\cos(\omega_c t)$, here $m(t)$ is the binary input, which has a value 1 or –1. For ASK, the value should be 1 or 0

Generally MPSK signal can be represented by its complex envelope $g(t) = x(t) + jy(t) = \sum_{-\infty}^{\infty} c_n f(t - nT_s)$ [16], here $x(t)$ is called the I (in-phase) channel baseband signal and $y(t)$ is the Q (quadrate-phase) channel baseband signal. c_n is a complex valued random variable, $f(t)$ is the function for baseband bit shape. For QPSK, baseband complex signal has 4 possible phases, the real or imaginary part of c_n can only have the value of 1 or –1. The real passband signal is represented by $s(t) = A_c x(t)\cos(\omega_c t) - A_c y(t)\sin(\omega_c t)$

In the case that we use rectangular bit shape for $f(t)$, The PSD for the complex envelope of MPSK is $P(f) = A_c^{\ 2} T_S(\frac{\sin(\pi f T_S)}{\pi f T_S}) = lA_c^{\ 2} T_b(\frac{\sin(l\pi f T_b)}{l\pi f T_b})$, here

$T_S = lT_b$, T_S is the symbol time and T_b is the bit duration, for MPSK $l = \log_2 M$. For QPSK, $l = 2$. Use this equation, the 3dB bandwidth of BPSK is 0.88R, Null to Null bandwidth is 2 R, bounded spectrum bandwidth (50dB) is 201.04 R. If a QPSK system uses the same T_s as a BPSK system, the bandwidth of QPSK will be the same of that of the BPSK system. Because in QPSK each symbol represents 2 bits, so the total capacity is doubled. For QPSK, it has the same BER as BPSK when they have the same E_b / N_0, here E_b is the energy of each bit. (matched filter receiver is used here).

In the following, we will discuss the subcarrier modulation for BPSK while QPSK and ASK will be discussed in chapter 3.

For BPSK, after the transmitter filter, each baseband signal is modulated to a sub carrier frequency by a carrier suppressed microwave mixer. The function of the microwave mixer is simply multiplication. The expression for the output of such a mixer is $Y(t) = k * X(t) * \cos(2\pi f_{RF})$, $X(t)$ is the baseband signal, and $\cos(2\pi f_{RF})$ is the microwave carrier. A separate mixer is need for each subcarrier channel at its own frequency. Here the modulation frequency of each channel, f_{RF}, and the modulation index k of each channel can be changed or optimized. The frequencies we use in this example are 3.6GHz, 8.3GHz, 13GHz, and 17.5GHz.

If the baseband signal $X(t)$ is unipolar, then the modulated signal is ASK. If the baseband signal is bipolar, then the modulated signal is phase shifting keyed or BPSK.

The four subcarriers were combined together by a wideband microwave power coupler and is used to modulate the lightwave from the laser.

Figure 2.3 are the waveform and power spectrum of the multiplexed subcarrier signal. The displayed spectrum indicates that the inter-channel interference is less than -27 to -30 dB.

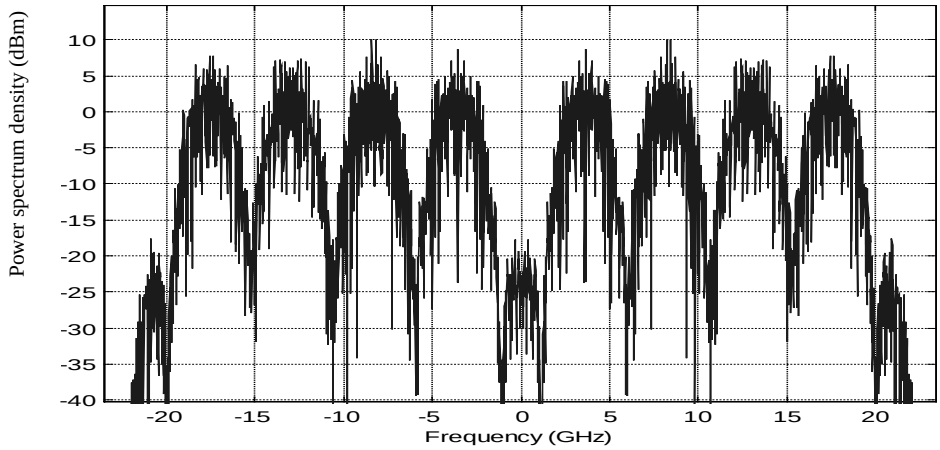

(a)spectrum of the composite microwave subcarriers signal

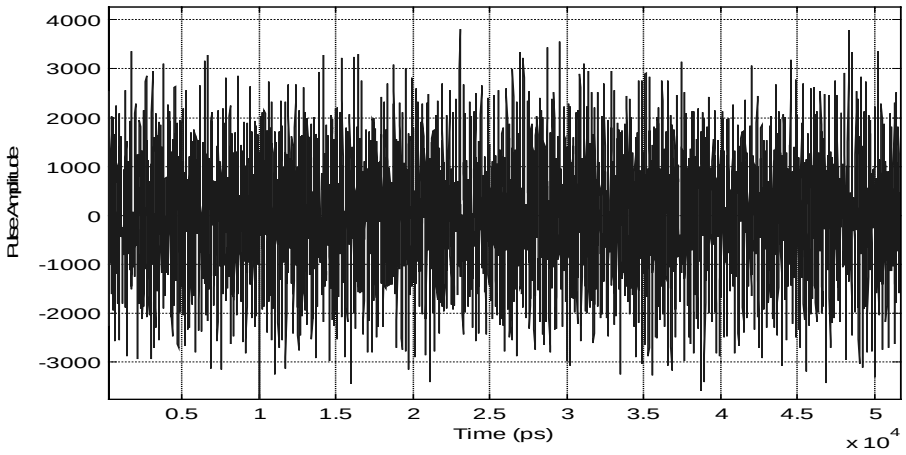

(b)waveform of the composite microwave subcarriers signal

Figure 2.3 Spectrum and waveform of 4 BPSK microwave subcarriers

We should mention that till now, all the baseband and microwave signals are all represented by real functions and no complex numbers are involved. We are going to introduce the optical modulation shortly. In the optical domain, all the optical signal are represented by means of complex envelope, please refer to Appendix 1 for the description of complex signal and complex envelope, also for the power relationship between the complex envelope and the real signal.

2.3.3 Mach-Zehnder modulator

After the microwave subcarrier signal is generated, it is used to modulate the optical carrier. We use a dual drive Mach-Zehnder optical modulator in our system.

2.3.3.1 Principle of MZ modulator,

We only discuss a dual-drive Mach-Zehnder modulator because modulating signals can add to its both arms and this is very important for generating single-side-band optical signal.

The principle of MZ modulator is very simple: an input light is coupled to two waveguide branches of the same length and shape (the lengths could be different for bias purpose), these two branches are fabricated by LiNbO3 and electrical field can be applied on each of them separately. When the electrical field that is applied to these arms changed, the effective refractive index of the waveguide will change, this change can be seen as linearly related to the applied field and the corresponding phase delay change also has a linear relationship with the applied electrical filed intensity. Thus the phase delay of light in each waveguide can be controlled by those external electrical field. The two lightwaves are then coherently added together at the end of the waveguide by another coupler.

If the input is $E_i \exp(-j\omega_0 t)$, the output of such a modulator is

$$
\begin{aligned}
E_o &= \frac{1}{2}(e^{-j\phi_1} - e^{-j\phi_2})E_i \exp(-j\omega_0 t) \\
&= \frac{1}{2}e^{j\phi_0}(e^{-j\Delta\phi/2} - e^{j\Delta\phi/2})E_i \exp(-j\omega_0 t), \\
&= \sin(\frac{\Delta\phi}{2})E_i \exp(-j\phi_0)\exp(-j\omega_0 t)
\end{aligned}
$$

Here, ϕ_1, ϕ_2 are the phase delay of the two arms respectively, $\Delta\phi = \phi_1 - \phi_2$, is the difference between the two arms. $\phi_o = \frac{\phi_1 + \phi_2}{2}$, is the average phase delay of the

two arms. $\sin(\frac{\Delta\phi}{2})$ represents the amplitude modulation, $\exp(-j\phi_0)$ is the phase modulation term. By changing the value and relationship of ϕ_1, ϕ_2, we can achieve many different kind of modulation.

In traditional binary ASK modulation, one important parameter is the chirp of the signal created as a by-product by the modulator. The parameter α of a modulator is defined as the ratio of the phase modulation to the amplitude modulation as $\alpha = 2P_o \frac{(\frac{d\phi_0}{dt})}{(\frac{dP_o}{dt})}$, where $P_o = |E_o|^2 = \sin^2(\frac{\Delta\phi}{2})P_i$. For a symmetrical dual drive Mach-Zehnder modulator, we have $\alpha = \frac{V_1(t)+V_2(t)}{V_1(t)-V_2(t)}$, $V_i(t)$ are the voltages applied to the two arms. To achieve a zero chirp from the modulator, we need $V_1(t) = -V_2(t)$. Thus, in the simulation, when you want to generate chirp free binary ASK signal (traditional intensity modulated signal), one has to apply complementary signals to both input.

2.3.3.2 The realization of single side band optical modulation

In order to increase bandwidth utilization efficiency, and reduce system dispersion penalties, we use single side band (SSB) modulation in our system.

In microwave communications, a single side band signal is a signal that has zero valued spectrum for $f > f_c$,(it is called lower single side band or LSSB) or $f < f_c$ (upper single side band, or USSB) , f_c is the carrier frequency. A SSB signal is usually obtained by using the complex envelope $g(t) = A_c[m(t) \pm j\hat{m}(t)]$, which results in the SSB signal waveform $s(t) = A_c[m(t)\cos\omega_c t \mp \hat{m}(t)\sin\omega_c t]$, where the upper(-) sign is used for USSB and lower (+) sign is used for LSSB, $\hat{m}(t)$ denotes the Hilbert transform of $m(t)$. Hilbert transform is given by $\hat{m}(t) = m(t) * h(t)$, where

$h(t) = \frac{1}{\pi t}$, $H(f) = F[h(t)]$ corresponds to a -90^0 phase shift network:

$$H(f) = \begin{cases} -j, & f > 0 \\ j, & f < 0 \end{cases}$$

Actually, the above formula is called SSB-AM-SC (suppressed carrier) and is only one of many different kinds of SSB formats, yet it is the most popular format.

Although microwave SSB has been studied extensively in the past decades, optical SSB modulation is relatively new. In optical frequency domain, because it is difficult to use the canonical IQ form to generate SSB signal due to the lack of optical mixers, it is also not easy to use the filter to generate the SSB due to the slow rolling off and poor stability of optical filters. Now we explain how to generate the SSB signal using the MZ modulator.

We rewrite the output of the modulator as $E_o(t) = \frac{A}{2}\{\cos[\omega_c t + \phi_1(t)] - \cos[\omega_c t + \phi_2(t)]\}$, using a sinusoid modulation as an example, if we let $\phi_1(t) = \gamma\pi + \beta\pi\cos\Omega t$ and $\phi_2(t) = \beta\pi\cos(\Omega t + \theta)$, $\cos\Omega t$ is the modulating signal, $\cos(\Omega t + \theta)$ is the θ degree phase shifted signal, Ω is the frequency of modulation signal, $\gamma = \frac{V_{dc}}{V_\pi}$ is the bias of one arm, and $\beta = \frac{|V_{ac}|}{V_\pi}$ is the optical modulation index. One should note that to avoid clipping the maximum optical modulation index is 0.5 because the peak-to-peak value of the signal should be less than V_π. Optical SSB is generated by setting $\gamma = \frac{1}{2}$, and $\theta = \frac{\pi}{2}$,

Using the expansions

$$\sin(z\cos x) = 2\sum_{k=0}^{\infty}(-1)^k J_{2k+1}(z)\cos[(2k+1)x],$$

$$\sin(z\sin x) = 2\sum_{k=0}^{\infty} J_{2k+1}(z)\sin[(2k+1)x]$$

$$\cos(z\cos x) = J_0(z) + 2\sum_{k=1}^{\infty}(-1)^k J_{2k}(z)\cos(2kx)$$

$$\cos(z\sin x) = J_0(z) + 2\sum_{k=1}^{\infty} J_{2k}(z)\sin(2kx)$$

and after some manipulation, The modulator output is

$$E_o(t) = -\frac{E_i}{2}\{J_0(\text{bp})[\sin(\text{w}_c t) + \cos(\text{w}_c t)] + 2J_1(\text{bp})\cos(\text{w}_c - \Omega)t + 2J_2(\text{bp}).....\}$$

We can see that there is only one $\cos(\text{w}_c - \Omega)$ term in the output, there is not a $\cos(\text{w}_c + \Omega)$ term in the expression, which means we have only the lower side band in the spectrum.

The difference between this modulation scheme and common double sideband modulation using MZ modulator is that the RF signal applied on the second arm is 90 degree phase shifted signal instead 180 degree shifted signal.

Although in conventional baseband modulated optical systems, optical SSB requires rather complicated implementations due to the difficulty to realize Hilbert transformation over the signal baseband, which includes low frequency components. In sub-carrier optical systems, intermediate frequencies are used and it becomes easier to realize Hilbert transform because there is no very low frequency component in the composite RF signal.

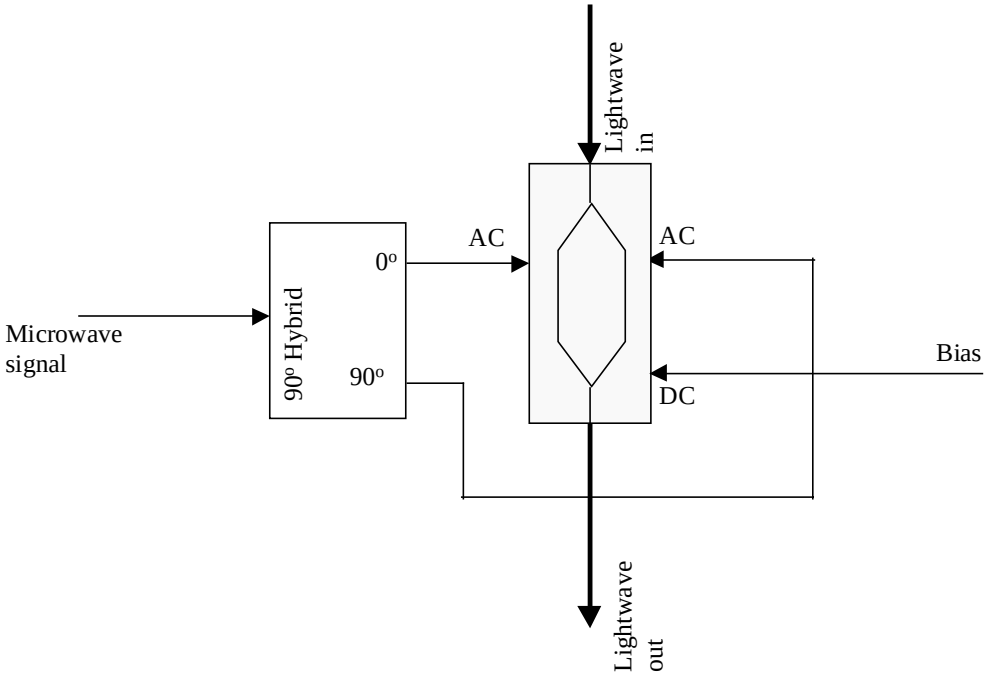

Figure 2.4 Implementation of single sideband optical signal generation using MZ modulator

Figure 2.4 shows the implementation of single sideband optical signal generation using MZ modulator, a 90^o hybrid is used which splits the input signal into two outputs with 90^o phase shift between each other. The two outputs of the hybrid are sent to the two arm of a balanced dual arm M-Z modulator, which has a bandwidth of 20GHz. From now on, the signal is changed from microwave domain into optical domain. Because the optical frequency is too high to be represented as a real signal in the simulation, so we have to use its low pass complex envelope to represent it. Please refer to appendix 1 for details on low pass complex envelope. Below is the spectrum of the generated optical SSB signal.

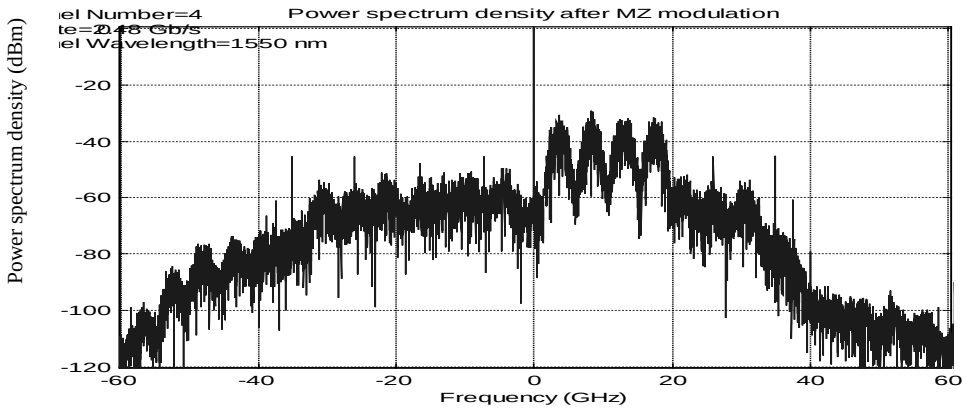

Figure 2.5 Optical SSB spectrum generated by balanced dual-electrode Mach-Zehnder modulator.

In the spectrum shown in Figure 2.5, the side band suppression is about 20dB.

The optical modulation index is defined as the $\frac{\text{maximum phase shift of each arm}}{\pi}$, in the balanced situation, each arm only needs to change the phase by $\pi/2$, so the maximum possible modulation index is 0.5. The RF modulation index is defined as $\frac{\text{peak to peak value of a subcarrier RF signal} * \text{number of subcarriers}}{V_\pi / 2}$. In this particular example, the optical modulation index is 0.4 where the RF modulation index of each channel is 1 for every subcarriers and it is adjustable by changing the amplitude of the baseband signal. We will explain this in more detail later.

2.3.3.3 Nonlinear distortion of unlinearized modulator

The amplitude transfer function of the MZ modulator is sinusoidal. Obviously it is not linear. Generally, nonlinear terms generated by MZ modulator include both composite second order (CSO) and composite triple beat (CTB) which are corresponding to the second and third order nonlinear distortions respectively. However, through the simulation, we found that MZ modulator biased at quadrature point will not generate CSO. We will first proof [10] this point here and show the simulation spectrum later.

First, let's define a normalized notation to simplify the treatment, the normalized modulator output is defined as the AC component of the modulator optical output normalized by the CW component:

$$V(t) = \sum_{q=1}^{N} V_o \cos(\omega_q t + \psi_q) + V_B$$

$p = \dfrac{P - < P >}{< P >} = \sin(\theta + \phi_b)$, with P is the modulator output power, $< P >$ is the average power, ϕ_b as the intrinsic phase biases, θ defined as the normalized modulating $\theta = \dfrac{\pi V}{V_\pi}$, the modulating composite RF signal can be written as $V(t) = \sum_{q=1}^{N} V_o \cos(\omega_q t + \psi_q) + V_B$, ω_q and ψ_q are the frequency and phase of each RF subcarrier, V_B is the bias, V_o is the amplitude of each subcarrier.

Then $p = \sin[\theta + \phi_T] = \cos[\phi_T]\sin[\theta] + \sin[\phi_T]\cos[\theta]$, here $\theta = \sum_{q=1}^{N} \beta \cos(\omega_q t + \psi_q)$, $\beta = \dfrac{\pi V_o}{V_\pi}$, and the bias is $\phi_T = \phi_b + \dfrac{\pi V_B}{V_\pi}$, is defined as the sum of the intrinsic and the applied DC phase biases.

Keeping terms up to third order in the power series expansions of the sine and cosine functions

$$\sin(\theta) = \theta - \frac{1}{6}\theta^3 + \frac{1}{120}\theta^5 + \ldots$$

$$\cos(\theta) = 1 - \frac{1}{2}\theta^2 + \frac{1}{24}\theta^4 + \ldots$$

we have $p = \cos[\phi_T][\theta - \dfrac{1}{6}\theta^3] + \sin[\phi_T][1 - \dfrac{1}{2}\theta^2]$,

and

$$p = \cos[\phi_T][\beta \sum_{q=1}^{N} \cos(\omega_q t + \psi_q) - \frac{1}{6}\beta^3 (\sum_{q=1}^{N} \cos(\omega_q t + \psi_q))^3] + \sin[\phi_T][1 - \frac{1}{2}\beta^2 (\sum_{q=1}^{N} \cos(\omega_q t + \psi_q))^2]$$

the term in β is the desirable linear term, whereas the term in β^2 is the CSO component and the term in β^3 is the CTB component. If ϕ_T is set to zero, the CSO term vanishes while the linear and CTB terms are maximized and the ratio of the linear and CTB terms is independent of the bias point ϕ_T. When the bias point is $\phi_T = 0$, known as the quadrature point, around which the AC transfer characteristic is an odd function. At this point, the even orders of intermodulation are nulled out, in particular CSO distortion becomes negligible.

For SSB modulation in particular, $\theta = \sum_{q=1}^{N} \beta \cos(\omega_q t + \psi_q) - \sum_{q=1}^{N} \beta \sin(\omega_q t + \psi_q) = \sum_{q=1}^{N} \beta \cos(\omega_q t + \psi_q + \frac{\pi}{4})$, the result is the same as that of DSB signal in terms of nonlinear effects.

Figure 2.6 is an illustration of the nonlinear distortion of a MZ modulator generated by computer simulation, where we use two tones as the modulating subcarrier signals, with their frequencies of 5 and 8 GHz. The optical modulation is single side band. In order to demonstrate the effect of modulation index, we used two optical modulation indices here: 0.4 and 0.05 respectively, for each modulation index, the top figure is the optical spectrum and the bottom figure is the electrical power spectrum which is obtained after a photo diode.

From Figure 2.6, one can see the higher the modulation index is, the higher the nonlinear distortion can be generated. In the electrical spectrum, there is no frequency component at 3 or 13 GHz for both modulation indices, which are the product of CSO, this verifies our analytical derivation. Even though there is no CSO in the electrical spectrum, it is quite strong in the optical spectrum. Both CSO and CTB represent nonlinear distortion and create interference between sub-carrier channels.

Figure 2.6(a) is the optical spectrum with OMI of 0.4, Figure 2.6(b) is the electrical spectrum with OMI of 0.4. Figure 2.6(c) is the optical spectrum with OMI of 0.05, figure 2.6(d) is the electrical spectrum with OMI of 0.05. There is a trade off between the signal amplitude and the distortion. The higher the modulation index is, the higher is the signal amplitude, but the distortion is also higher. From the analytical derivation, the ratio of the CTB terms over linear terms is independent of the bias point ϕ_T and proportional to β^2.

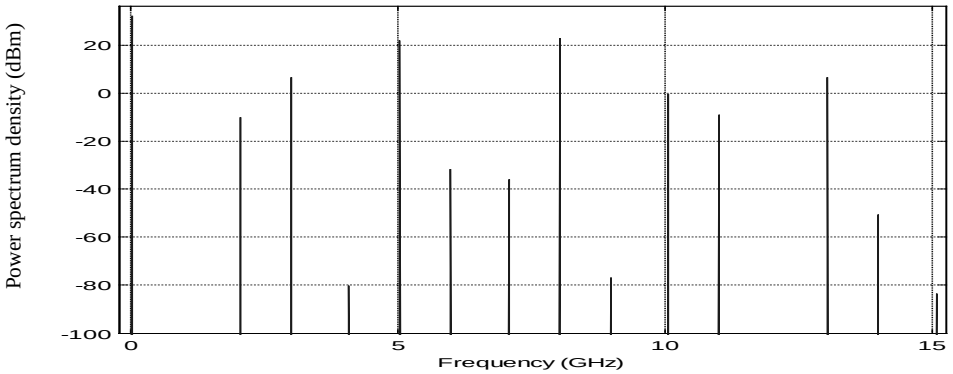

(a) optical spectrum of the MZ modulator output when OMI=0.4

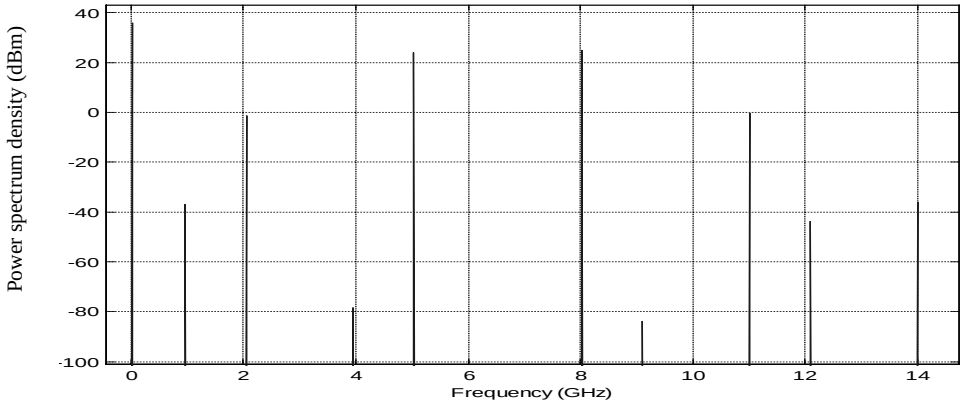

(b) electrical spectrum of the photon dector output when OMI=0.4

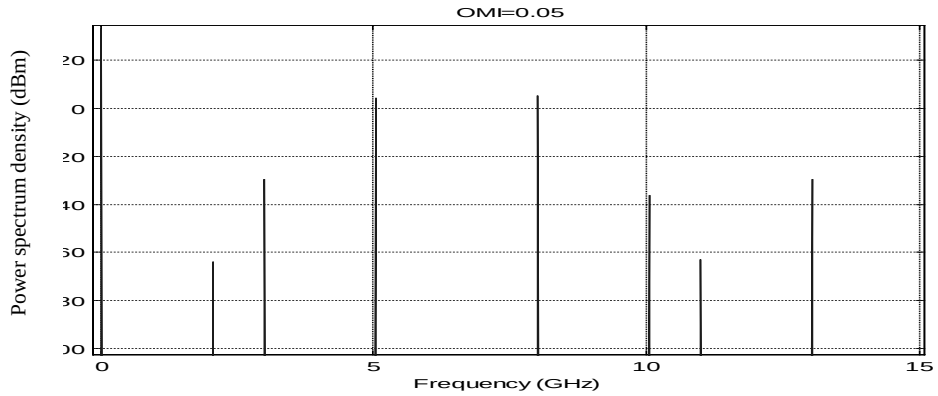

(c) optical spectrum of the MZ modulator output when OMI=0.05

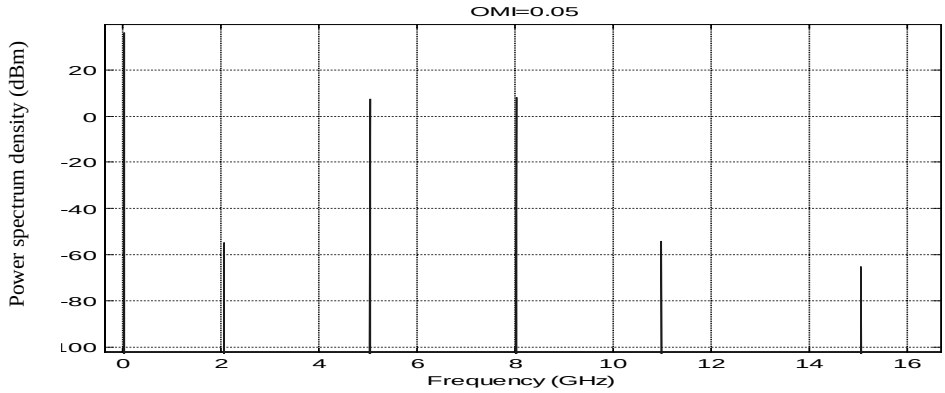

(d) electrical spectrum of the photon detector output when OMI=0.05

Figure 2.6 Illustration of nonlinear distortion of MZ subcarriers modulation

2.3.4 Carrier suppression

As shown in the section, the inter-modulation distortion can be reduced when the optical modulation index (OMI) is small.

When the optical modulation index is small, the signal has a relatively large carrier component and smaller signal components at subcarrier. In order to generate enough signal to noise ratio, the signal component has to be as strong as possible and the optical power of carrier could be very large. This is not very desirable since the carrier power is not carrying any information. Further more, according to the study of F.S.Yang [19], large carrier will result in some undesired effects:

1. For single wavelength, the SBS will clamp the input power and stoke wave will increases the noise floor.
2. For WDM, stimulated Raman scattering (SRS) will deplete the power of high frequency channel and generate interference on low frequency channels. XPM will also lead to crosstalk between wavelength, both the SRS and XPM/GVD crosstalk increase as Pc^2

So it is desirable to have less power in the carrier and more power in the subcarriers. One way to accomplish this is to suppress the carrier component before sending the signal into the fiber. It is worth noting that optical carrier suppression is not useful in non-optically amplified systems because optical carrier suppression does not increase baseband signal energy. In optically amplified systems, on the other hand, without carrier suppression, EDFA output optical power would be limited by the strong carrier component and therefore, carrier suppression will effectively increase signal energy and increase receiver sensitivity.

Fig 2.7 is illustrating the carrier suppression concept.

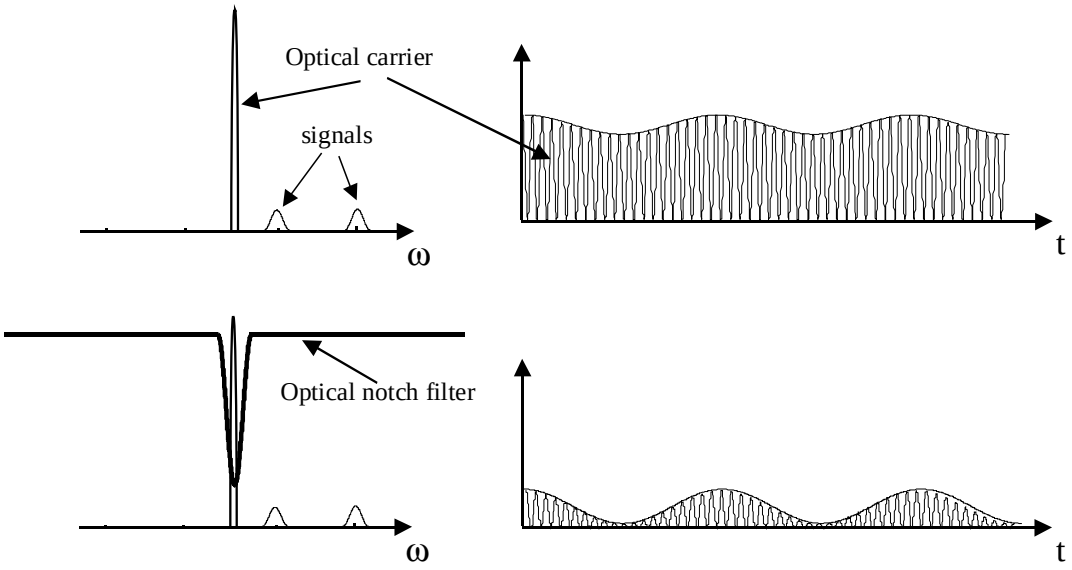

Figure 2.7 Illustration of the carrier suppression

Fig.2.8 shows the experimental set-up for carrier suppression. A fabry-Perot Interferometer (FPI) was used as a wavelength dependent reflector and an optical circulator was used to re-direct the optical signal. The wavelength of the FPI was tuned by its electrical bias in order to obtain an appropriate amount of carrier suppression.

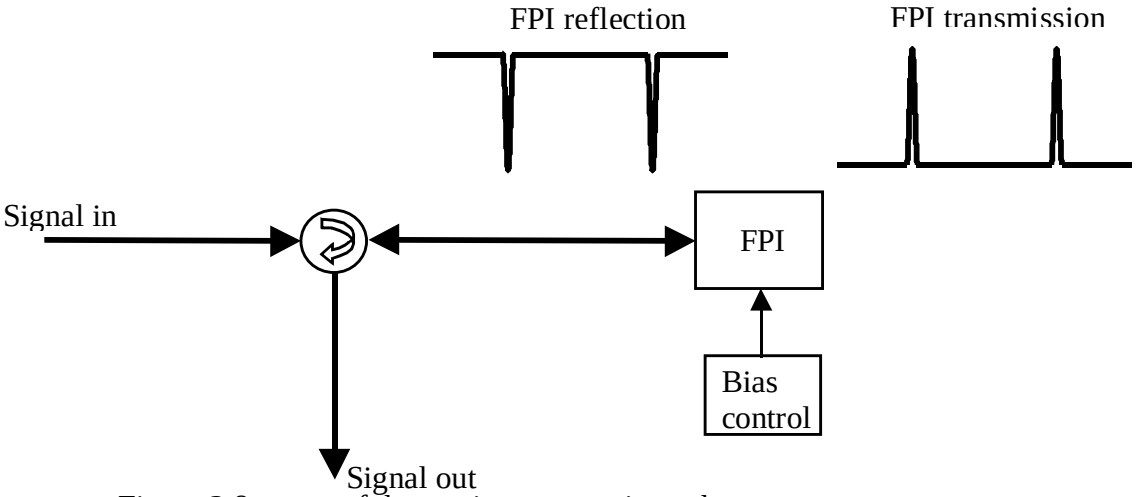

Figure 2.8, setup of the carrier suppression subsystem

The power transfer function of the Fabry-Perot interferometer is

$$T(f) = \frac{(1-A-R)^2}{1+R^2-2R\cos 4\pi f\tau}$$

Here R is the power reflectivity (reflectance of each of the two mirrors). A is the power absorption loss as the light passes through the cavity. The free spectral range $FRSR = \frac{1}{2\tau} = \frac{c}{2nx}$, the 3-dB or HPBW of the peak is given by

$$HPBW = FSR\frac{1-R}{\pi\sqrt{R}} = \frac{c}{2nx}\frac{1-R}{\pi\sqrt{R}},$$

In the experiment, since you only the space between the two mirrors is adjustable, so one can only change the wavelength of the peaks or nulls of the spectrum. The suppression ratio can be changed by move the peaks close or further away from the carrier component. In the simulation, to change the suppression ratio, it is rather easy to keep the bandwidth of the filter unchanged and to change the reflection loss A

Figure 2.9 is the amplitude and phase plot of the system function of a typical FP filter

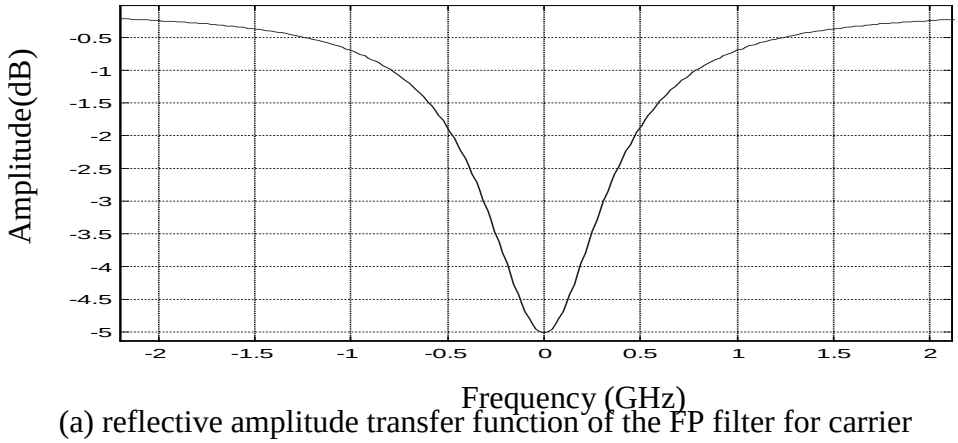

(a) reflective amplitude transfer function of the FP filter for carrier suppression

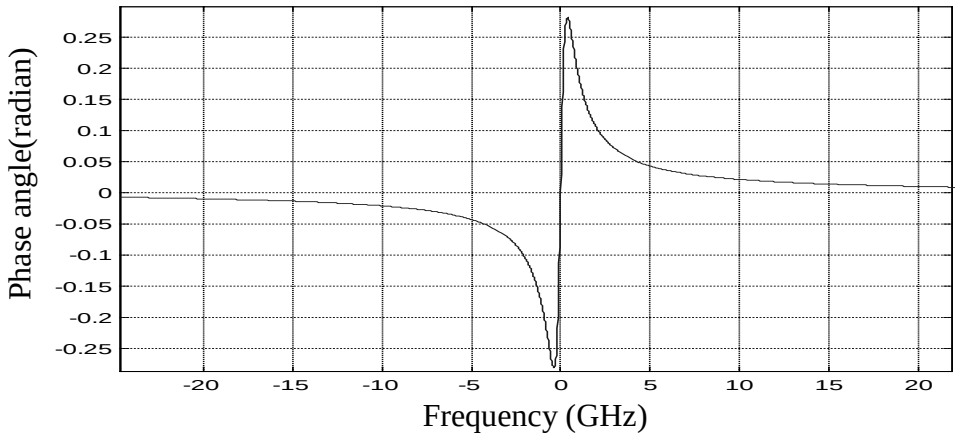

(b) reflective phase transfer function of the FP filter for carrier suppression

Figure 2.9, reflective amplitude and phase transfer function of the FP filter

Figure 2.10 is the optical signal before and after 5 dB suppression of the carrier. The OMI here is 0.25. After the suppression, Figure 2.9(c) shows the optical carrier is reduced about 5 dB compared to Figure 2.9(a). The difference between Figure 2.9(b) and 2.9(d) is that after carrier suppression the maximum signal amplitude is reduced but the AC part of the signal is not distorted

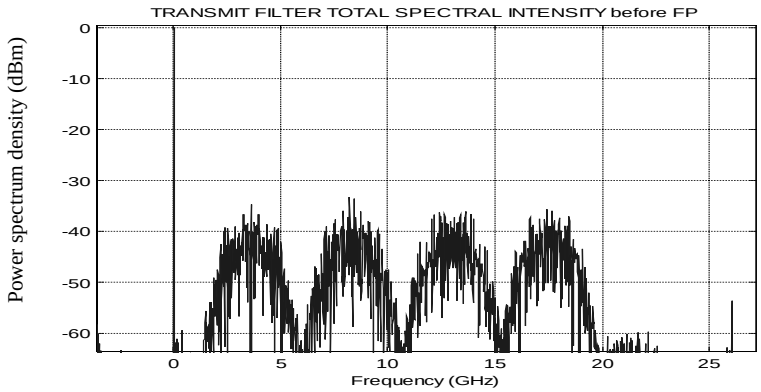

(a) spectrum of the composite optical signal before the carrier suppresion

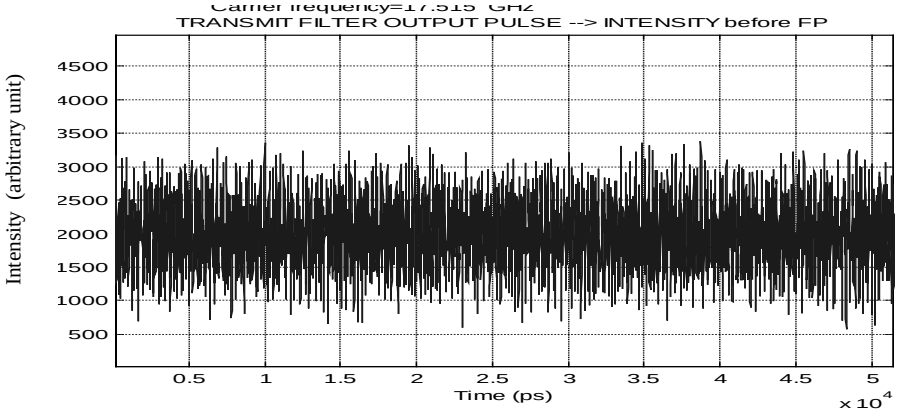

(b) waveform of the composite optical signal before the carrier suppresion

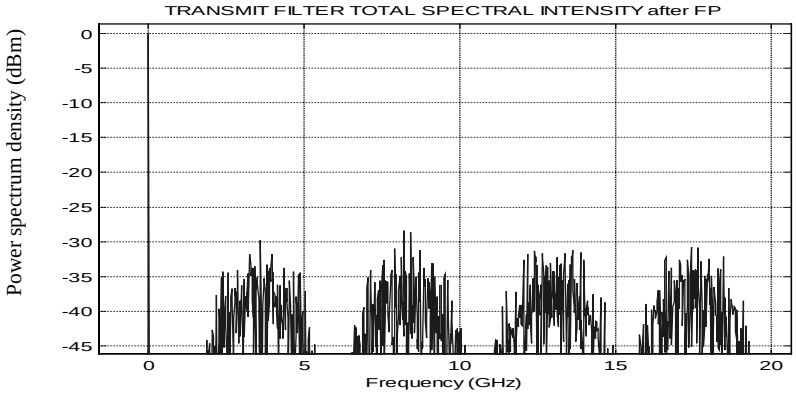

(c) spectrum of the composite optical signal after the carrier suppresion

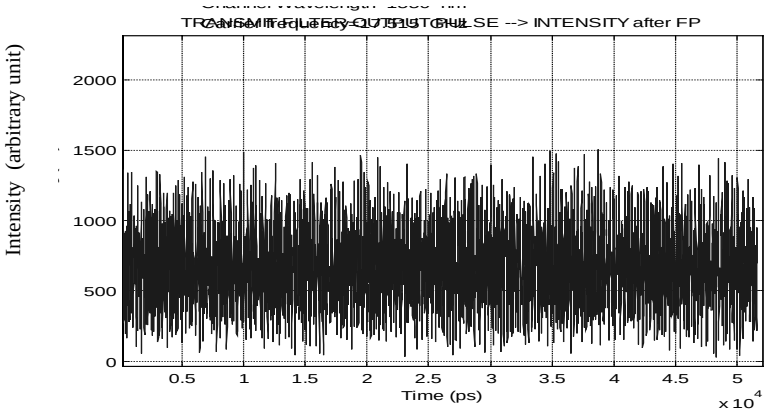

(d) waveform of the composite optical signal after the carrier suppresion

Figure 2.10 Illustration of carrier suppresion: simulation spectrum and waveforms

2.3.5 Transmitter optical filter

Because all the baseband information can be represented by only the upper sideband, a transmitter optical filter can be used to further to filter out residual lower sideband and limit the transmitter bandwidth. It can reduce crosstalk with other wavelength channel in WDM configurations. The filter for this purpose is realized using a Butterworth filter. This is because it has a smaller transition bandwidth compared to the bessel filter. The bandwidth used here is 30GHz, and the order is 15. Below is the spectrum before and after the optical filter, the intensity at –20 GHz is decreased from –60 dBc to –100dBc, the intensity at 30 GHz is decreased from –60 dBc to –65dBc, thus when two wavelengths separated by 50 GHz multiplied together, the crosstalk would be less than -100dBc.

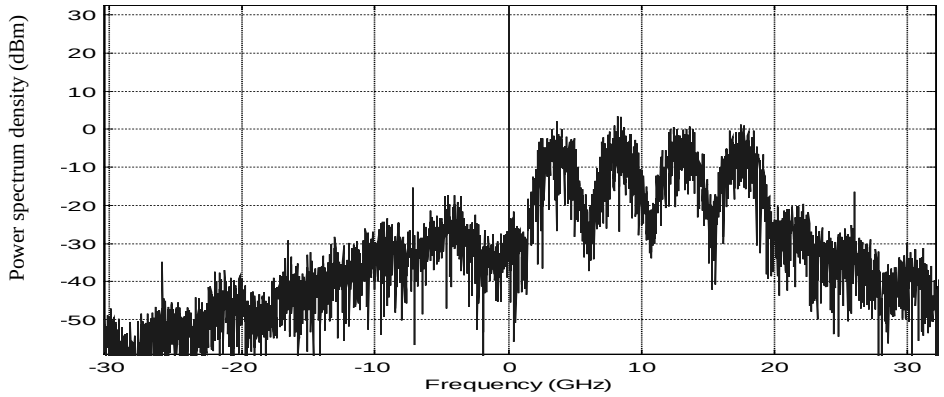

(a) spectrum before the optical filter

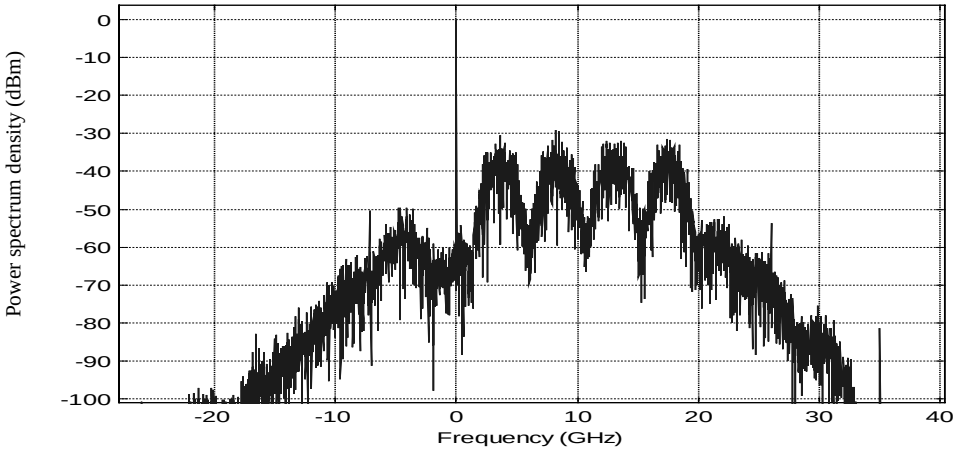

(b) spectrum after the optical filter

Figure 2.11, signal spectrum before and after the WDM filter.

2.3.6 The post optical amplifier

The booster is to model the optical amplifiers that are used in the real systems. We will not study the impact of the gain shape of the EDFA on the system performance. We only use a flat gain EDFA in the simulation and the EDFA is considered only with gain and noise. We do have an input parameter of noise figure, but the noise of the EDFA is not numerically simulated but is calculated by an

analytical method. We will explain this later. Also, all the inline amplifiers are treated the same way as the post amplifier.

2.4 Optical fiber path

In the signal path, the transmitter is followed by the transmission fiber. Figure 2.12 is the diagram of the fiber path

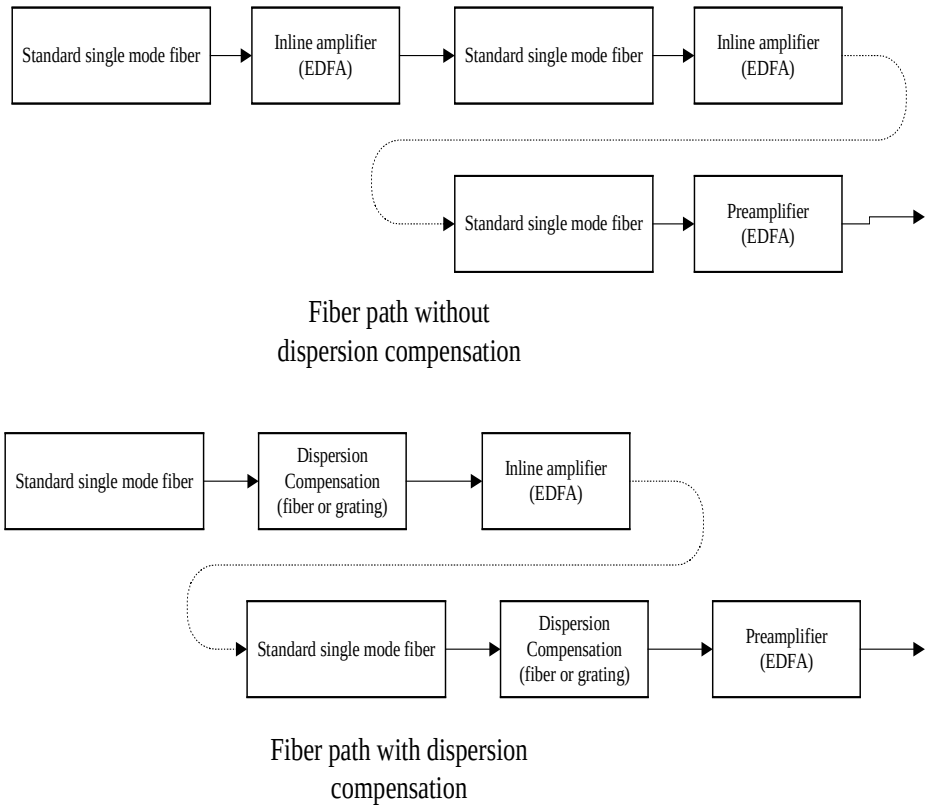

Figure 2.12 setup of the fiber path in the simulation program

This is a multi-span system. Each span is a length of Single made fiber (SMF) followed by an inline amplifier (or preamplifier for the last span), 3 dB additional loss is added for each span except the last span to take into account connection losses. If the dispersion compensation is implemented, an additional loss of 6dB is assumed. This additional attenuation is to used to account for all the attenuations other than optical fiber attenuations, such as coupling, splicing, attenuationof the dispersion compensation module. We assume that the incurred attenuation during each span is fully compensated by the inline amplifier. After each inline amplifier, the total optical power is the same as the power at the output of the transmitter power amplifier (or

post amplifier). By adjusting the additional loss of the last span, we can change the receiver power and find the receiver sensitivity. The sensitivity is defined as the received power when the BER of 10^{-9}, or the Q value of 6.

Dispersion compensation is implemented by adding dispersion compensation module at the end of each fiber span. The dispersion compensation module can be made by DC fiber or fiber bragg gratings. Wehave neglected the nonlinearity of the dispersion compensation components in our study.

The minimum fiber span length in the simulation is 40 km, the number of span is calculated using $N = [\frac{\text{total fiber length}}{\text{maximum span length}}]$, [ ] means round to the nearest integer toward 0. The fiber length of each span is calculated using $\text{span length} = \frac{\text{total fiber length}}{N}$. If the maximum span length is 80, by using such a method, the resulting span length ranges from 40 to 80 km.

The fiber used in the simulation is standard SMF. Its loss factor is 0.25 dB/km, nonlinearity index is 2.36e-20 m^2/W, the effective area is 71 um^2, dispersion parameter D= 18 ps/nm/km. Dispersion slope is 0.093 ps/nm^2/km, the reason to select these parameter values is to find the worst case system performance. We varied the PMD coefficient from 0.1 to 0.5 $ps/\sqrt{km}$ to evaluate its impact.

2.4.1 Nonlinear Schrodinger Equations

Optical fiber is one of the most important components in the whole system. It contributes most to the signal distortion. Here we will introduce the nonlinear propagation equation that governs the transmission characteristics. A numerical method is used to integrate this equation.

Assume the solution of the optical field in the optical fiber has the form

$\tilde{E}(\mathbf{r},\omega-\omega_0)=F(x,y)\tilde{A}(z,\omega-\omega_0)\exp(i\beta_0 z)$, where $F(x,y)$ is the transverse filed. A is the complex envelope of the real signal amplitude. A is normalized such that $|A|^2$ represents the optical power. We then have a differential equation for A.

$$\frac{\partial A}{\partial z}+\beta_1\frac{\partial A}{\partial t}+\frac{i}{2}\beta_2\frac{\partial^2 A}{\partial t^2}+\frac{1}{6}\beta_3\frac{\partial^3 A}{\partial t^3}+\frac{\alpha}{2}A=i\gamma|A|^2 A$$

Here $\gamma=\frac{n_2\omega_0}{cA_{eff}}$, is the nonlinear coefficient, n_2 is the nonlinear refractive index and A_{eff} is the effective fiber core area which depends on the distribution of the transverse field in the fiber. β_i are coefficients of the Talor expansion of the mode propagation constant $\beta(\omega)$, and we have $\beta_i=(\frac{d^i\beta}{d\omega^i})|_{\omega=\omega_0}$,

Wave propagation is sometimes referred to as the nonlinear Schrodinger equation since it can be reduced to that equation under certain conditions.

There is a fundamental assumption in the above equation. We assume the third order nonlinear effects (the nonlinear induced polarization) has an instantaneous impulse response and it can be written by a product of three delta functions. So there are some nonlinear effects can not be explained by this equation, such as stimulated inelastic scattering like SRS and SBS. This equation is only valid for pulse widths $\geq 0.1ps$ or a signal bandwidth of 10^{13} Hz. It will work fine in our simulation since our total bandwidth is only in the order of 10^{11} Hz.

2.4.2 Numerical solution

Split step Fourier method is used extensively to solve the pulse propagation problem in nonlinear dispersive media. Its fast speed can mainly be attributed to the use of the fast Fourier transform algorithm.

The propagation equation can be written as

$$\frac{\partial A}{\partial z}=(\hat{D}+\hat{N})A$$

$$\hat{D} = -\frac{1}{2}\alpha - \frac{i}{2}\beta_2 \frac{\partial^2}{\partial T^2} + \frac{1}{6}\beta_3 \frac{\partial^3}{\partial T^3}$$

$$\hat{N} = i\gamma\left(|A|^2\right)$$

$\hat{D}$ is the differential operator that accounts for dispersion and absorption in a linear medium and $\hat{N}$ is a nonlinear operator that accounts for the fiber nonlinearities

Split step Fourier method obtains an approximate solution by assuming that over a small distance h, the dispersive and nonlinear effects can be pretended to act independently.

There are several variations of to implement this method. The most common one is to use the following approximation

$$A(z+h,T) = \exp(h\hat{D} + h\hat{N})A(z,T) \approx \exp(h\hat{D})\exp(h\hat{N})A(z,T)$$

We ignored the non-commutating nature of the operators $\hat{D}$ and $\hat{N}$, the dominant error term is to the second order of the step size h. We will use this approximation in our simulation program.

In the simulation, the step size h to satisfy the accuracy requirement. One way to reduce the number of step is to utilize the fact that nonlinear distortion mainly occurs at the beginning of the fiber where the optical power is high. At the end of the fiber, due to the attenuation of the fiber, the optical power is low and the nonlineareffect is thus low.

In our simulation, the step size is increased exponentially along the fiber, and the exponential power number is the fiber attenuation.. At the beginning of the fiber span the step size is smallest; at the end of fiber span, the step size is the largest. In all the simulation, the number of steps per span used is 100 and there is no visible change in the results with the increase of the number of steps.

Below is an exemplary spectrum after 80km standard SMF transmission with complete dispersion compensation. The optical power launched into fiber is 3dBm,

and the Optical Modulation Index (OMI) is 0.4. After the fiber transmission, the nonlinearity of fiber generates some new peaks on the other side of the carrier.

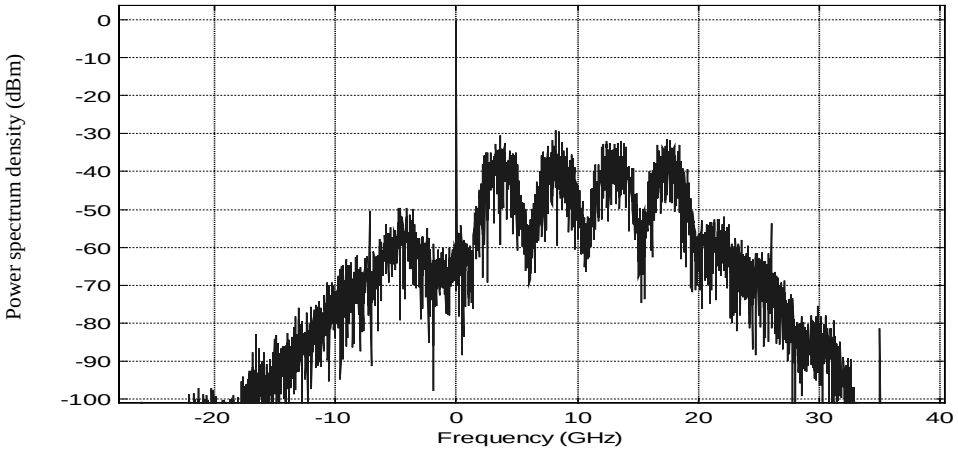

(a) spectrum before the optical fiber

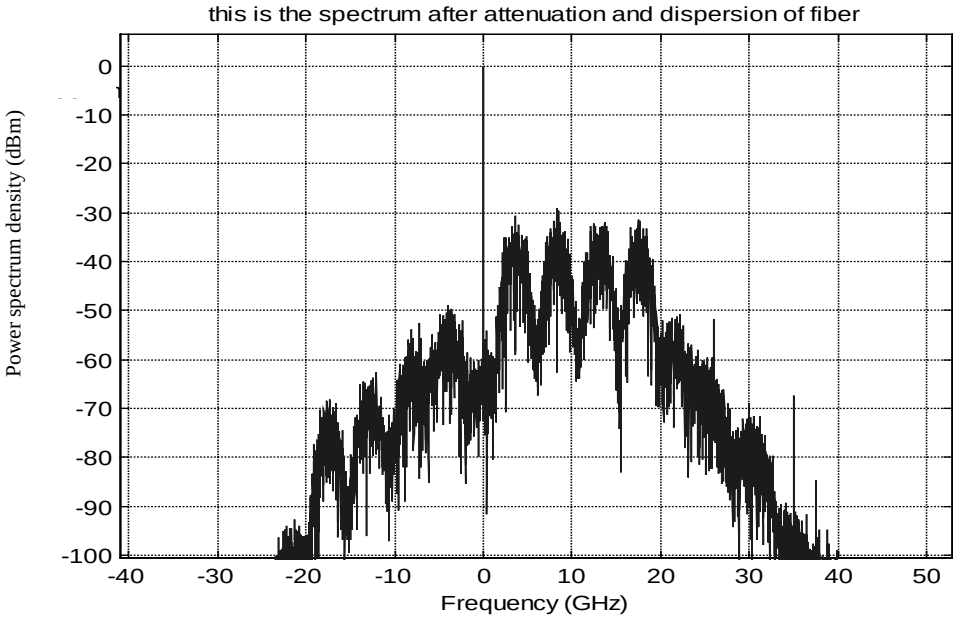

(b) optical spectrum after 80 km fiber transmission

Figure 2.13 optical spectrum before and after 80 km fiber transmission, optical power is 3dBm

2.5 SCM Receiver

Fig 2.14 is the diagram of the SCM receiver. In the receiver side, the EDFA preamplifier output power of each wavelength is fixed at –5dBm for all the simulations. The baseband electrical filters are the same as in the transmitter (6 orders Bessel filters with 3dB bandwidth of 1.736 GHz). The frequencies of RF local oscillators are 2.6GHz, 7.3GHz, 12GHz, and 16.7GHz respectively. The phases of the local oscillators are estimated from the detected input signals. After the electrical filter, we first estimate the total system delay and then search for the best sampling time. The noise is calculated by an analytical method.

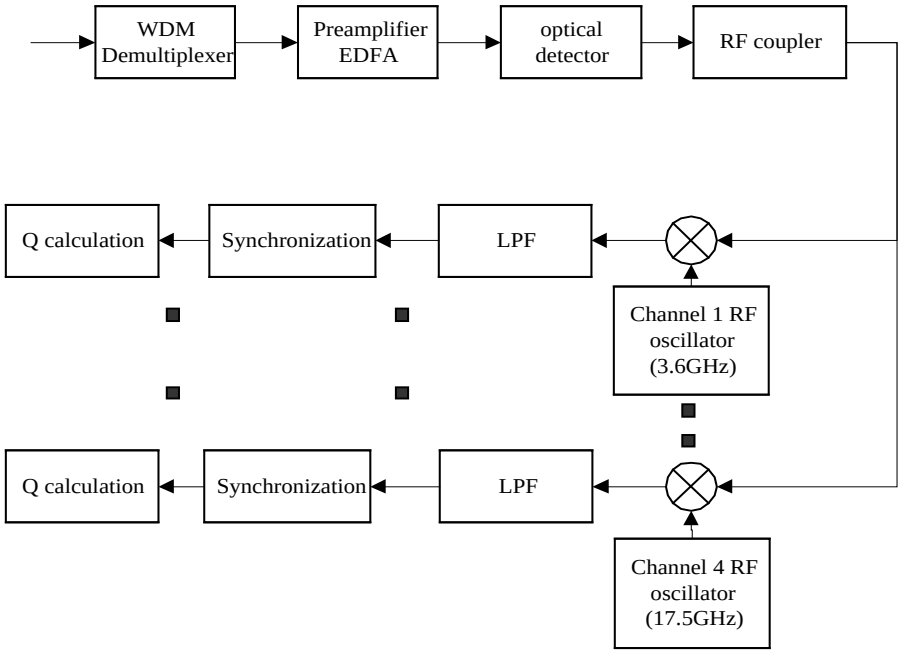

SCM Receiver Block Diagram

Figure 2.14 SCM receiver block diagram

2.5.1 optical demux

After transmission through the optical fiber, optical signal goes to a WDM demultiplexer, it is used to select a single wavelength from the multiwavelength

lightwave signal. We used a Butterworth filter here as in the transmitter side. The bandwidth is about 30GHz and the order is 6.

2.5.2 preamplifier

The optical demultiplexer is followed by an EDFA preamplifier (it may also be put before the optical demultiplexer and this arrangement makes no difference in our simulation). The output power from the preamplifier is fixed at –5dBm for each wavelength. Once again, the amplifier has a flat gain and its ASE is calculated analytically.

2.5.3 Photodiode

After the photo detector, the signal is transformed from a complex signal into a real signal. The function of the photon detector is described by a square operation and then followed by a low pass filter. Fig. 2.15 shows a spectrum of the electrical current after the photon diode. The optical carrier beats with the optical sub carrierat the photo diode, then the optical spectrum is shifted to an RF frequency as shown in Fig. 2.15. The initially SSB optical spectrum is converted to a DSB RF spectrum because of the square-law process of the photo diode.

In practice, there is always an electrical preamplifier after the photo diode, we didn't include it here thus the noise generated by the electrical circuit is neglected.

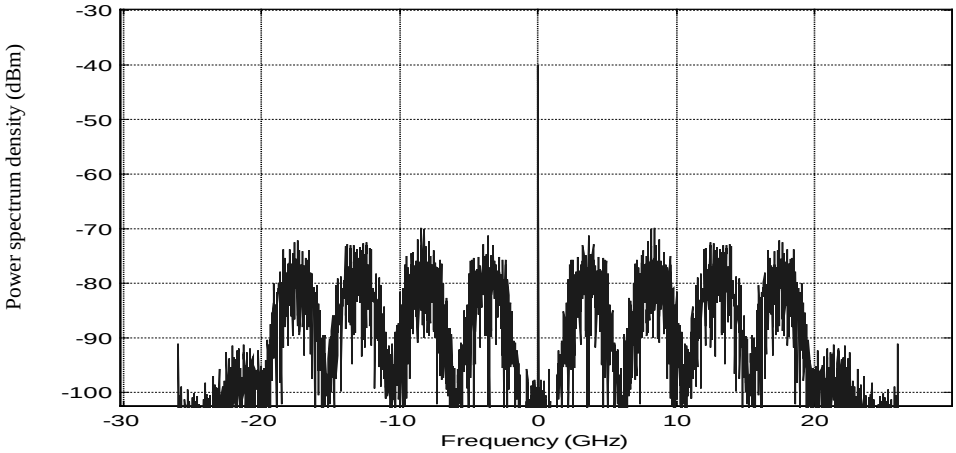

Figure 2.15, electrical spectrum after the photon detector

2.5.4 High pass filter

In Fig. 2.15, we can see that there is a very high DC component. Since the DC component doesn't carry any information, it could be removed. Another reason why we need to remove the DC component is that later during the RF coherent detection, this DC component will move to a nonzero frequency and will interfere with the signal. It will be hard to be removed at that time because of the filter can not be made with very high extinction ratio. In the simulation, we use a high pass RF filter to remove this DC component, the filter is a 5 MHz, 6 order Butterworth high pass filter. In real implementation, this could be done simply by using a capacitor to couple the signal. Figure 2.16 is showing the spectrum after the filter.

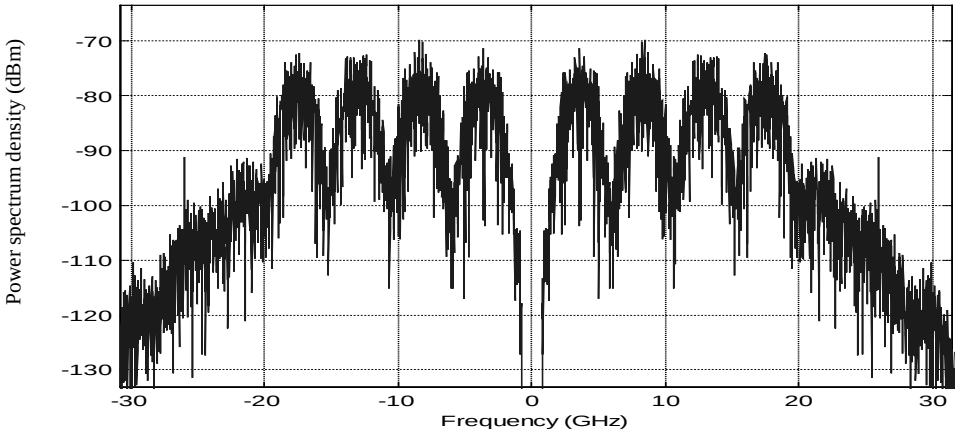

Figure 2.16, electrical spectrum after the high pass filter

2.5.5 Microwave coupler.

A 1×4 microwave (RF) coupler is needed in order to separate four subcarrier channels. The attenuation of the microwave coupler is not considered in the simulation because the SNR is determined before the microwave coupler.

2.5.6 Carrier recovery

After the microwave coupler, the signal at each subcarrier branch is mixed with a local oscillator. The frequencies of local oscillators are the same as they are in

the transmitter side. The phase of the local oscillator is a very important variable to be determined here. Suppose one of the subcarrier is $A(t)*\cos(\omega t+\phi)$, the phase of the local oscillator is ϕ_L, then the useful output signal would be $A(t)\cos(\phi-\phi_L)$, if $\phi-\phi_L=\pi/2$, then the output signal would be 0.

In practice, the phase of the local oscillator can be estimated by methods such as phase lock loop or Mth Power loop. In the simulation, we use the Mth Power loop.

The Mth Power loop is also referred to as the squaring loop. It can be applied to MPSK signal. The MPSK signal can be represented by $s(t)=A\cos(2\pi f_c t+\theta_k+\theta)$. During $kT_S\le t\le(k+1)T_S$, where T_S is the symbol length and θ_k is the angle corresponding to the kth transmitted symbol. θ_k has one of the M values. $\theta_k=0,\frac{2\pi}{M},2\frac{2\pi}{M},3\frac{2\pi}{M},.....,(M-1)\frac{2\pi}{M}$. θ represent the phase delay due to the transmission and processing. Now if we raise $s(t)$ to the power M, and use the fact that $M\theta_k$ is integer multiple of 2π, then we have

$$s^M(t)=A^M\cos(2\pi Mf_c t+M\theta_k+M\theta)+\text{other terms}$$
$$=A^M\cos(2\pi Mf_c t+M\theta)+\text{other terms}$$

The first term is first extracted by a bandpass filter and then a frequency divider.(by a factor of M) can be used to generate a local carrier of the form $C(t)=K\cos(2\pi f_c t+\theta)$,

In the simulation, there is another possible choice to get the exact phase of the received carrier. First, the total delay of the optical fiber can be calculated then the effect of transmitter bias is added which is a random delay for the baseband signal of each subcarrier. From this delay, one can calculate the exact timing of the received signal and fine the phase of the carrier. However, we found that this method is not accurate enough to get a good estimation of the phase due to numerical accuracy.

When the Mth Power loop method is used, the frequency divider is not easy to simulate. One way to get around it is to use the cross-correlation method. From the cross correlation of the filtered Mth harmonic from the Mth loop and an ideal Mth

harmonic, it is possible to find a peak that correspond to the M times exact phase shift of the received carrier. Dividing this phase by M, the exact phase of the received carrier can be obtained.

Figure 2.17(a) is a diagram of the carrier recovery scheme for BPSK system. A bandpass filter is used to select a single subcarrier. This single subcarrier signal is squared by a mixer and then the second order harmonics of the product is selected by a narrow bandpass filter. At last, a frequency divider is used to get the desirable carrier for this subcarrier. Figure 2.17(b) are the waveforms corresponding to those points in the diagram.

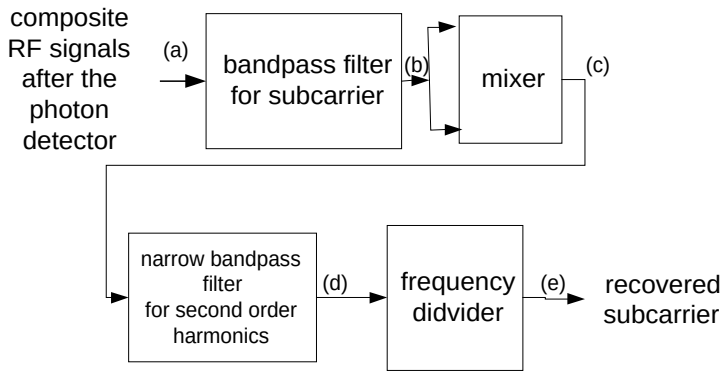

Figure 2.17 (a) diagram of the carrier recovery for BPSK system

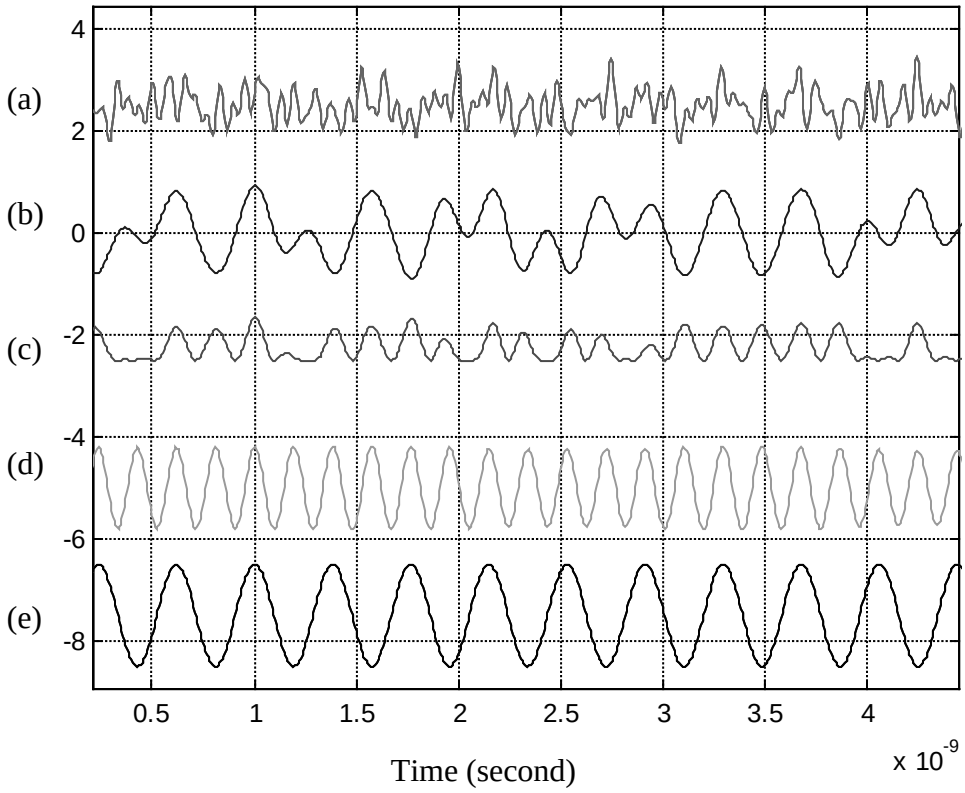

Figure 2.17 (b), illustration of carrier recovery, curves from top to bottom correspond to the signals at (a)-(e) in the diagram (a):

(a) Composite RF signal after the photon diode

(b) Filtered signal for subcarrier 1, central frequency is 2.6 GHz

(c) Squared signal for subcarrier 1, central frequency is 5.2GHz

(d) Filtered Squared signal for subcarrier 1, central frequency is 5.2GHz

(e) Recovered subcarrier 1, central frequency is 2.6GHz

2.5.7 Demodulation

Fig. 2.18 shows the spectrum at the received signal after the mixer, which performs the RF coherent detection.

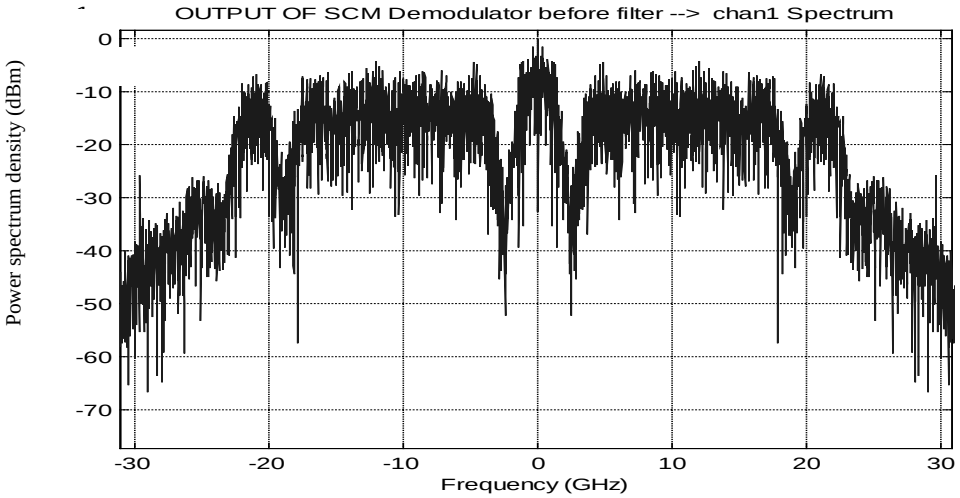

Figure 2.18, signal spectrum after beating with local ossillator

In reality, the output port of the mixer has a certain banwidth, in the simulation we used a 6-order Butterworth low pass filter with a bandwidth of 1.25 times the bitrate. Fig. 2.19 shows the spectrum, waveform and eyediagram after this filter. The eye diagram here is shifted to all positive in Fig2.19(c), this is only for the convenience of comparasion.

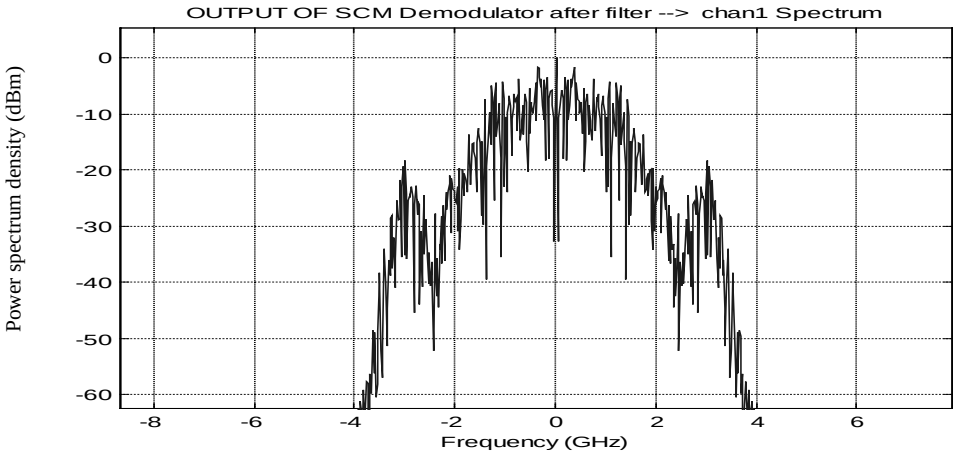

(a) spectrum of the mixer output

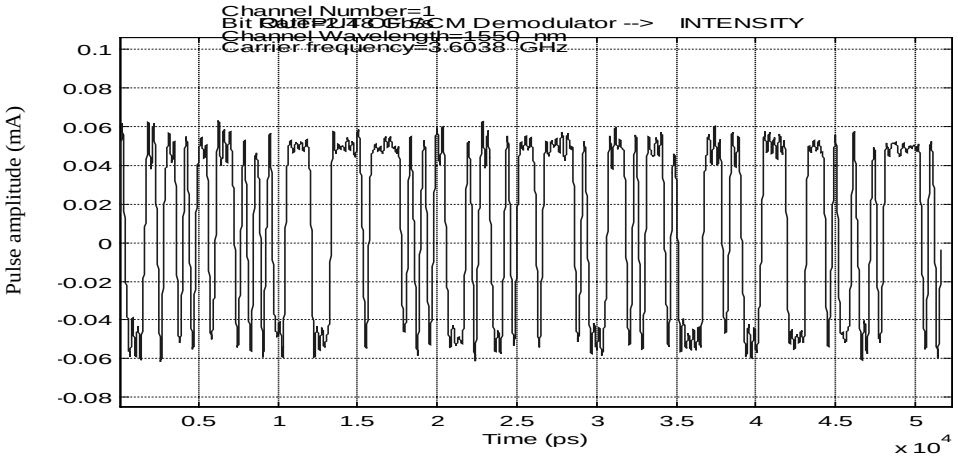

(b) waveform of the mixer output

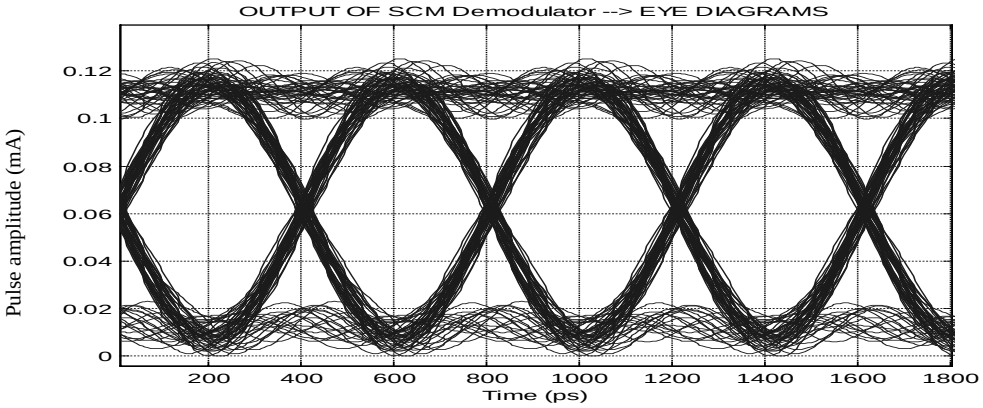

(c) eyediagram of the mixer output

Figure 2.19 spectrum, waveform and eyediagram of the mixer output

2.5.8 Electrical filters

As the bandwidth of the mixer is larger than the signal bit rate, the signal at the mixer output is still distorted by the crosstalk of other subcarriers. We need another narrower baseband to purify our final signal. This electrical filter is the same as that used in the transmitter (6-order Bessel filters with 3dB bandwidth of 1.736 GHz). Fig. 2.20 shows the spectrum, waveform and eyediagram respectively, after the baseband filter. The spectrum shows that the side band here is furthered suppressed compare to the previous spectrum and the eye diagram looks cleaner.

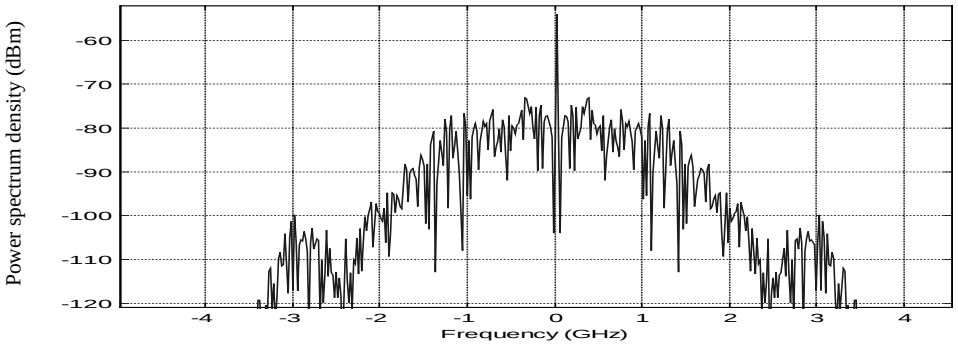

(a) spectrum after electrical filter

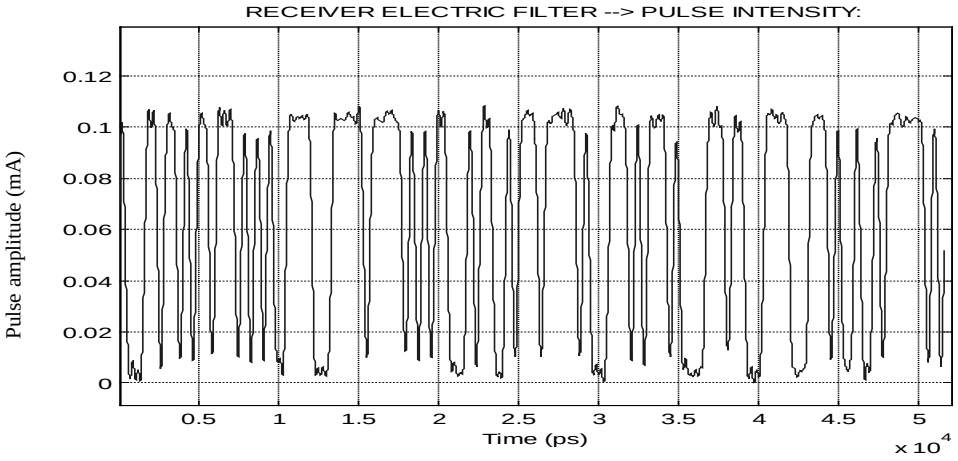

(b) waveform after electrical filter

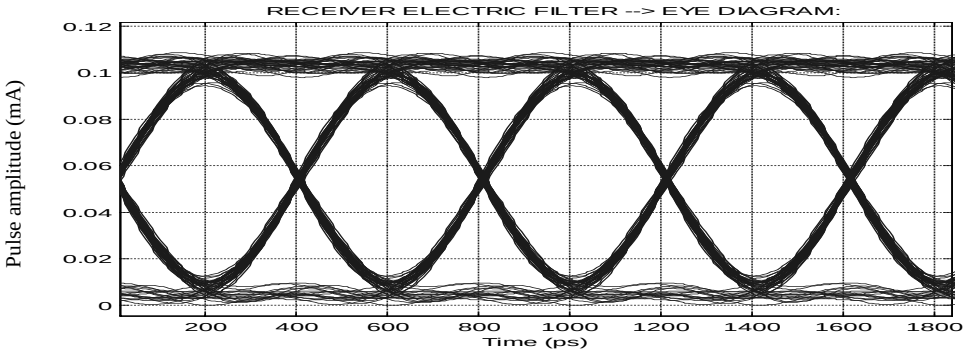

(c) eyediagram after electrical filter

Figure 2.20, spectrum, waveform and eyediagram after electrical filter

2.5.9 Bit Synchronization procedure

After the electrical filter, there is another synchronization procedure that estimates the decision timing of the digital signal. This estimation is based on the delay of the transmission through the optical fiber. Although it does not have to be as accurate as for the estimation of the carrier phase, it needs to be adequate enough.

Suppose the absolute frequency of the chosen subcarrier is f_i, (the frequency shift from the zero or the reference frequency of the simulation. This is the frequency of the wavelength channel plus frequency of the subcarrier within that wavelength channel). The delay can be calculated as $\lambda_o^2 / c * f_i * D * L$, where λ_o is the center wavelength of the simulation which is 1550nm. c is the speed of light, D is the fiber dispersion parameter at frequency f_i. L is the length of the fiber. If there is dispersion compensation in the fiber path, the average value of D has to be changed accordingly by the ratio of the dispersion compensation. Also, the dispersion slope should be considered here too.

2.5.10 Polarization effects in SCM system

2.5.10.1 Polarization walkoff

Optical fiber is not purely a polarization independent transmission media, it has polarization-related effects such as polarization mode dispersion (PMD) and polarization dependent loss (PDL). We will consider the PMD effect here.

In frequency domain, PMD manifests as a frequency dependency of signal polarization at the output of a fiber, the output polarization undergoes a rotation on the Poincare sphere that can be represented by the following differential equation, $\frac{d\hat{s}}{d\omega} = \Omega \otimes \hat{s}$, where $\hat{s}$ is the unit Stokes vector describing the output polarization state, Ω is the rotation vector, which describes the rate of rotation and is also referred to as the dispersion vector. The magnitude of the Ω vector is equal to the differential delay time: $|\Omega| = \Delta\tau$ and the direction of this vector defines an axis whose two

intercepts with the surface of the Poincare sphere correspond to the two principal states of polarization at the fiber output.

In general, both the differential delay and the dispersion vector, Ω, are themselves frequency dependent and may vary over the bandwidth of a signal source. If the first order PMD is considered, Ω can be treated as frequency independent. When the second order dispersion PMD is included, in the frequency domain, it manifests as a linear frequency dependence of the dispersion vector Ω.

In our study, we only consider the first order PMD. The frequency of the highest subcarrier is lower than 20GHz and the wavelength change between the highest subcarrier and the carrier is not considered to be very large. So we can assume the principal state remains fixed for carrier and subcarriers (the Ω is fixed). The differential group delay can be written as $\Delta\tau = \frac{\Delta\theta}{\Delta\omega}$, where the $\Delta\tau$ is the differential group delay (DGD) in seconds, $\Delta\theta$ is the rotation about the principal states axis in radians, and $\Delta\omega$ is the optical frequency change that produced this $\Delta\theta$ rotation, $\Delta\omega$ has a unit of radians/second.

As a first order estimation, in a SCM system that needs the carrier to beat with the subcarrier in the photo diode to reproduce RF signal, the polarization walkoff between the carrier and subcarrier will decrease the amplitude of the signal at the output of the photo detector by a factor of $\cos(\Delta\theta)$. $\Delta\theta$ is the rotation angle between the carrier and the subcarrier. Because of PMD, the beating between the carrier and the subcarrier will generate less microwave signal due to the polarization misalignment between each other in the photon diode.

In the simulation, this walkoff problem is modeled as a reduction in the signal amplitude by a factor of $\cos(\Delta\theta)$.

2.5.10.2 Polarization mode dispersion

PMD also has another detrimental effect on the SCM system. It will distort the microwave signal at the photon detector when the optical signals in two polarization

modes combine together just like in traditional high speed TDM systems. At the fiber output, the signal can be divided into two main polarization modes, these two modes have different transmission delay due to PMD. The higher frequency subcarrier channel will be more subject to PMD effect because the period of that subcarrier is small. We will use the same method, which was used to estimate the PMD effect in binary systems to estimate the PMD effect in SCM systems [18].

To evaluate the impact of PMD in a binary digital system, one usually assumes that pulse bifurcation is the dominant mechanism for pulse broadening. The goal here is to find the maximal allowable mean DGD or $\Delta\tau$ that can ensure the system outrage probability larger than 1 dB system penalty to be less than 30 min per year. We assume a Maxwellian distribution for $\Delta\tau$ and uniform distribution for the power splitting ratio between the two orthogonal state of polarization (SOP). From those assumptions, for a digital system with Chirp Free Gaussian pulses, the DGD between the principal states must be less than 0.14 of the bit period, i.e., $\frac{<\Delta\tau>}{T} <= 0.14$. For a binary system, this can be written as $B^2 L \approx \frac{0.020}{(PMD)^2}$ [18], where B is bit rate, L is the fiber length, PMD is the PMD coefficient .

For SCM systems, the subcarrier is sinusoidal and we assume that has the similar performance compared to a Gaussian pulse. It would be appropriate to substitute B with f_i, which is the subcarrier frequency. Based on this assumption, Figure 2.21 is the estimation of the limitation on SCM system due to the PMD effect. The upper trace is obtained when the sub carrier frequency is 12 GHz and the lower trace is obtained when the sub carrier frequency is 18GHz. The horizontal axis is the PMD parameters. The vertical axis is the maximum transmission distance.

With G.652 SMF, the PMD parameter is <=0.5 $ps/\sqrt{km}$. For some newly installed fiber cables, the PMD parameter could be <=0.1 $ps/\sqrt{km}$. When the PMD is 0.5 $ps/\sqrt{km}$, the distance limits are appropriately 240km and 550km respectively

for these two subcarrier frequencies. When the PMD is 0.1 $ps/\sqrt{km}$, the limits are about 6000 km and 13000 km for these two cases.

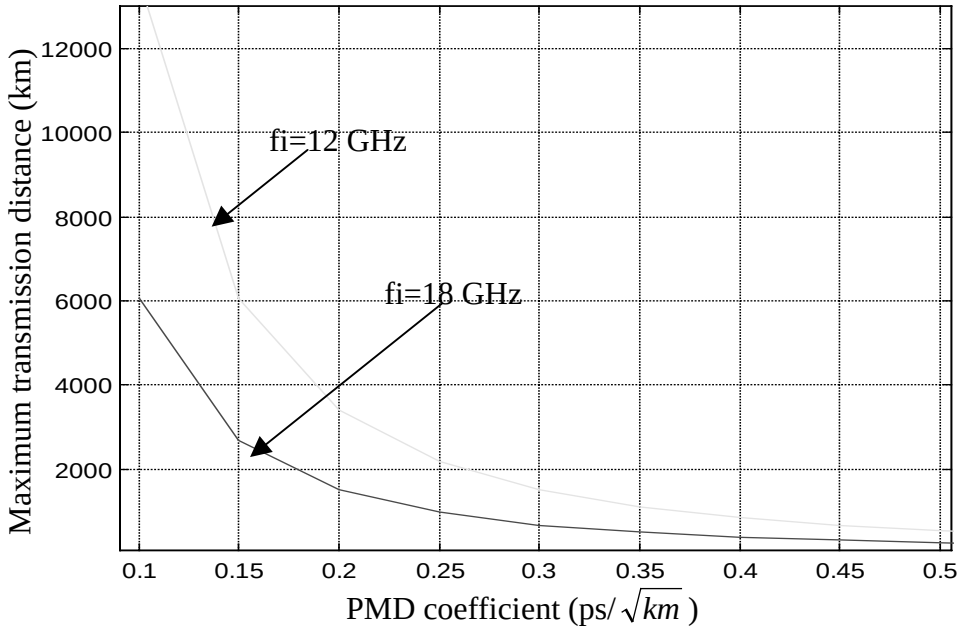

Figure 2.21, Estimation of system limitation due to the polarization effect for subcarriers of 12GHz and 18GHz

2.5.11 Analytical estimation of the Error probability (Bit-Error-Rate)

There are several types of simulation based approaches for estimating the BER[17], such as Monte Carlo simulation, Importance sampling, Extreme value theory, Tail extrapolation (pseudo-thresholds) and Quasi-analytical method, etc. The most common method is the Monte Carlo method that is used frequently in the simulation of wireless systems where the required BER is much higher than that of optical systems.

In Monte Carlo simulation, we take every factor that affects the system performance into account and count the number of successes (by comparing with the source output) and divide by the number of trials. It is very straightforward to implement. But the problem with this method is that it requires a very long symbol

sequence. If the BER is p, the sequence length N should be on the order of $10/p$, and it will produce a 95% confidence that the real BER will be between (1.8* p to 0.55 p), you will see how long it will take for a BER of 10^{-9}. Most other methods are derived from the Monte Carlo method. They produce many more errors per unit time by altering the statistical properties of the noise processes (importance sampling) or by change the decision threshold (Tail extrapolation). But all these methods are relatively difficult to be implemented.

In the simulation, we have used a Quasi-analytical method to estimate the BER. Quasi-analytical (QA) technique is also referred to as semi-analytic. Basically, the QA technique is hybrid in that it combines both numerical simulation and analytical analysis. The simulation is used to generate a noiseless waveform with distortion at the receiver. Given this waveform and assuming that the noise is additive and has a known pdf, one can then calculate the probability of errors with analytical formulas. This is the analytic portion.

The advantage of this method is time efficiency. We don't have to wait for enough errors to occur and we can use much shorter symbol sequence.

In most other BER estimation methods, the waveform contains all of the effects of the system, acting simultaneously on signal and noise. In the QA method we separate the problem into two parts, one dealing with the signal wavelength and the other with the noise contribution to the sampled waveform. We assume all the noise can be considered additive at the input of the decision device, irrespective of how many noise sources there are in the actual system or where they generated. The probability density function of the noise may be specific for different system configurations.

If we know the pdf of the noise is Gaussian, and the decision value I_D is chose such that $Q_1 = \frac{I_1 - I_D}{\sigma_1} = Q_0 = \frac{I_D - I_0}{\sigma_0} = Q$, we have $I_D = \frac{\sigma_0 I_1 + \sigma_1 I_0}{\sigma_1 + \sigma_0}$ is the optimum decision threshold. I_1 is the minimum of symbol "1" and I_0 is the

maximum of symbol "0" at the decision time, σ_0 and σ_1 are the noise variance at signal zero and ones respectively. In the simulation, I_1 and I_0 were obtained by numerical simulation of the system, σ_0 and σ_1 were calculated by the analytical equations. With the values of I_1, I_0, σ_0 and σ_1 known, we can find $BER = \frac{1}{2} erfc(\frac{Q}{\sqrt{2}})$ where $Q = \frac{I_1 - I_0}{\sigma_1 + \sigma_0}$.

In the simulation, the receiver sensitivity can be obtained with the knowledge of eye opening and noise. The sensitivity is defined as the minimum optical power to achieve BER=$10e^{-9}$ or Q=6. The sensitivity can be found by changing the attenuation of the last fiber span. When the input power to the EDFA preamplifier changes, the gain of the amplifier will also change to keep EDFA output to be constant. As will be discussed in the next section, when the EDFA gain changes, the ASE noise will also change. So when the input signal optical power is decreased, the noise will increase and finally there is a point that the noise variance is big enough to make Q=6, this point is our receiver sensitivity.

2.5.12 Calculation of Receiver sensitivity

In an optical communication system with optical amplification, the receiver noise comes from both photo diode and optical amplifiers. In optically pre-amplified receiver, signal-ASE beat noise is usually the dominant noise that leads to performance degradation. We only consider the beat noise in our studies.

2.5.12.1 Noise from optical amplifier

In a long haul transmission system, the use of optical amplifier is inevitable and the noise generated by optical amplifiers is the dominant factor that contributes to the SNR degradation [15]. This noise is commonly referred to as the amplified spontaneous emission (ASE) noise. The optical spectral density of ASE has wide bandwidth (white noise) and is given by $S_{ASE}(f) = \rho_{ASE} = 2n_{sp}hf_o(G-1)$, the factor

2 accounts for two polarizations. Here f_o is the optical frequency, n_{sp} is the spontaneous emission factor which is given by $n_{sp} = \frac{N_2}{N_2 - N_1}$, N_1 and N_2 are the carrier populations at the ground and excited states. The major effect of the ASE noise is that it beats with the signal during the O/E conversion and generates RF noise in the photo current. The noise figure of the amplifier can be expressed as $F_n = 2n_{sp}(G-1)/G \approx 2n_{sp}$, we can calculate n_{sp} through $n_{sp} = 10^{(F_n - 3)/10}$ if we know F_n

The electrical spectrum of signal-spontaneous-beat noise is given by $S_{sig-sp}(f) = 4\frac{q^2\eta^2}{hf} n_{sp} P_{in} G(G-1) = 2R^2 G P_{in} \rho_{ASE}$ (single-side band spectrum), here we have considered that the signal only has one polarization and the ASE noise has two. In addition, ASE noise will also beat with itself and generate spontaneous-spontaneous-beating noise $S_{sp-sp}(f) = 2q^2\eta^2 n^2{}_{sp}(G-1)^2 B_o = (1/2)R^2 \rho_{ASE}{}^2 B_o$, where B_o is the bandwidth of the optical filter before the receiver. We should note that the signal spontaneous beat noise is independent of the optical bandwidth B_o while the spontaneous-spontaneous beat noise is a function of the optical bandwidth. We can not use an optical filter to eliminate signal- spontaneous beat noise. This is because there is always a beat noise between signal and ASE which falls into a bandpass or baseband filter in a receiver and one cannot eliminate this beat noise without eliminating the desired signal at the same time. On the other hand, the spontaneous-spontaneous beat noise is the result of beating among ASE components and is proportional to B_o, which means that the narrower the optical filter is the less the noise is. This noise is usually much smaller than the signal-spontaneous-beating noise. The noise current variance can be expressed by $\sigma^2{}_{s-sp} = 2R^2 G P_{in} \rho_{ASE} B_e$ and $\sigma^2{}_{sp-sp} = (1/2)R^2 \rho_{ASE}{}^2 B_o B_e$, for signal-ASE and ASE-ASE beat noise, respectively, where B_e is the bandwidth of the baseband filter.

When several concatenated amplifiers are used, ASE noise generated by each amplifier has to be added together.

2.5.12.2 Sensitivity estimation for a digital BPSK SCM system:

In this section, we give an analytical estimation of the receiver sensitivity for digital SCM system. We only consider the EDFA preamplifier here and neglect the noise from optical detector and the electrical amplifier.

Fig. 2.22 shows the block diagram of an optically amplified, digital SCM fiber-optic system.

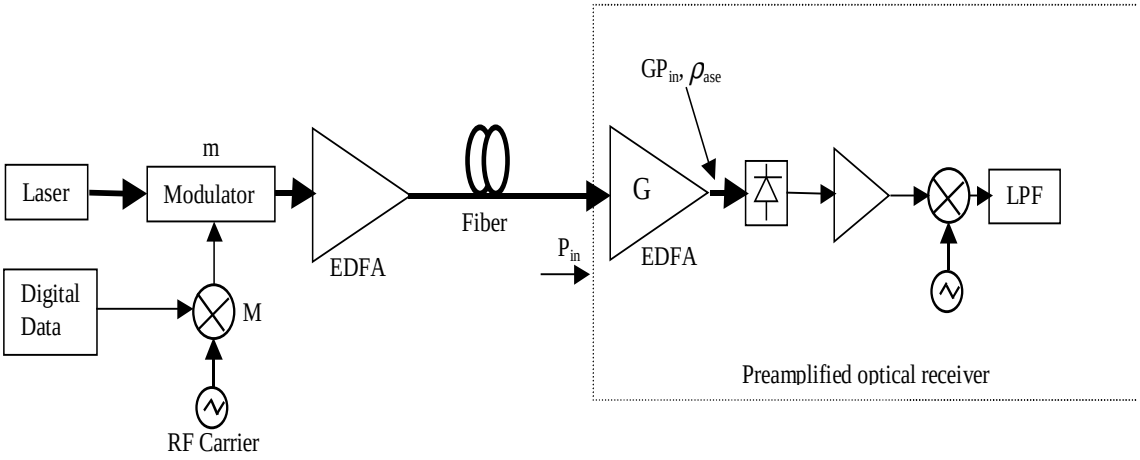

Figure 2.22 , concept model of the SCM system for Q calculation

In the transmitter side, suppose that the electrical modulation index M = 100% and the optical modulation index is m. For a Mach-Zehnder modulator, the transfer function of the optical field is proportional to the input RF signal in a nonlinear way,

$$E_0 = E_i \sin\left[\frac{\pi v(t)}{2V_\pi} + \varphi_b\right]$$

where $v(t)$ is the electrical signal used to modulate the CW optical input E_I. ϕ_b is a constant phase, which depends on the bias point of the modulator.

For a multiple sub-carrier signal, we have,

$$v(t) = \sum_{k=1}^{n} v_k(t) = \sum_{k=1}^{n} v_k u_k(t)\cos(\omega_k t)$$

Where $u_k(t)$ is the normalized digital signal at the kth channel with $u_k(t)$ = -1 and $u_k(t)$ = 1 representing digital signal "0" and "1", respectively and ω_k is the carrier frequency of that channel. If $\phi_b = \pi/4$, which corresponds to biasing the modulator at the quadrature point, we have

$$E_0 = \frac{E_i}{\sqrt{2}}\left\{\left[\sin\frac{\pi}{2v_\pi}\sum_{k=1}^{n} v_k u_k(t)\cos(\omega_k t)\right] + \cos\left[\frac{\pi}{2v_\pi}\sum_{k=1}^{n} v_k u_k(t)\cos(\omega_k t)\right]\right\}$$

Under the assumption of $v(t) << V_\pi$, this expression can be linearized,

$$E_0 = \frac{E_i}{\sqrt{2}}\left\{1+\frac{\pi}{2v_\pi}\sum_{k=1}^{n} v_k u_k(t)\cos(\omega_k t)\right\}$$

Here the first term in the bracket represents the carrier and the second term is the signal. Taking into account the carrier suppression,

$$E_0 = \frac{E_i}{2}\left\{\sqrt{\zeta} + \sum_{k=1}^{n}\frac{m_k}{2}u_k(t)\cos(\omega_k t)\right\}$$

Where ζ is the power suppression ratio of the carrier and m_k is the modulation index of the k^{th} channel and this modulation index is defined by the percentage of the RF signal voltage compared to the modulator's V_π parameter. At the receiver, the photo-current is

$$I_s = \eta|E_0|^2 G\Re \approx I_0\left\{1+\frac{1}{\sqrt{\zeta}}\sum_{k=1}^{n} m_k u_k(t)\cos(\omega_k t)\right\}$$

Where η is the system loss, $\Re$ is the photo-diode responsivity, G is the gain of the optical pre-amplifier, $I_0 = \eta(E_i/2)^2\zeta G\Re = P_{in}G\Re$ is the photo-current and $P_{in} = \eta(E_i/2)^2\zeta$ is the average power of optical signal that reaches the pre-amplified optical receiver. Obviously, the useful signal photo-current for the k^{th} channel is $I_k = P_{in}G\Re m_k u_k(t)\cos(\omega_k t)/\sqrt{\zeta}$.

On the other hand, $\left\langle i^2_{sig-sp}\right\rangle = \Re^2 2\rho_{ase}P_{in}G$ is the power spectral density of signal-spontaneous beat noise. $\left\langle i^2_{sp-sp}\right\rangle = (1/2)\Re^2\rho_{ASE}{}^2 B_o$ is the spectral density of

spontaneous-spontaneous beat noise, where B_o is optical filter bandwidth and ρ_{ASE} is the ASE noise spectral density. Although there are other receiver noises such as thermal noise and shot noise, for optically pre-amplified receiver, signal-spontaneous beat noise is the dominant noise. Therefore, for simplicity, we only take into account the signal-spontaneous beat noise here.

Since the noise is random, it can be decomposed into in-phase component $n_c(t)$ and quadrature component $n_s(t)$ and thus the total AC signal entering the RF demodulator is $U_1 = P_{in} G \Re m_k u_k(t) \cos(\omega_k t) / \sqrt{\zeta} + n_c(t) \cos(\omega_k t) + n_s(t) \sin(\omega_k t)$

Where the total noise power is

$\frac{1}{2}\overline{n}_c^2 + \frac{1}{2}\overline{n}_s^2 = B_e < i_{sig-sp}^2 >= 2\Re^2 \rho_{ase} P_{in} G B_e$, and $\overline{n}_c^2 = \overline{n}_s^2$

B_e is the bandwidth of the receiver baseband electrical filter.

At the demodulator, $U_1(t)$ coherently mixes with a local oscillator $2\cos(\omega_k t)$, the output of the demodulator is:

$U_2 = P_{in} G \Re m_k u_k(t) / \sqrt{\zeta} + n_c(t)$

Here frequency-doubled components have been filtered out. Therefore the signal-to-noise-ratio is

$$SNR = \frac{P_{in} G \Re m_k u_k(t) / \sqrt{\zeta}}{\sqrt{2\Re^2 P_{in} \rho_{ase} G B_e}} = \frac{P_{in} G \Re m_k u_k(t) / \sqrt{\zeta}}{\sqrt{2\Re^2 P_{in} F h \upsilon (G-1) G B_e}} \approx \frac{u_k(t) \sqrt{P_{in} m_k^2}}{\sqrt{2 F h \upsilon B_e \zeta}}$$

Taking into account the fact that $u_k(t) \in (-1,1)$, therefore, without signal waveform distortion, the receiver *Q* value can be approximated as

$$Q = \frac{m_k \sqrt{P_{in}} - (-1) m_k \sqrt{P_{in}}}{2\sqrt{2 F h \upsilon B_e \zeta}} = \frac{m_k \sqrt{P_{in}}}{\sqrt{2 F h \upsilon B_e \zeta}}$$

A BER of 10^{-9} corresponds to Q = 6, therefore the receiver sensitivity at this BER level is $P_{in} = \frac{36 \times 2 \times 1.28 \times 10^{-19} F \zeta B_e}{m_k^2}$

In the ideal case without waveform distortion, suppose the receiver electrical bandwidth is 1.75GHz, optical preamplifier noise figure is 3 (~5dB), modulation index is 25% which is the maximum index for a system with 4 subcarrier channels and there is no carrier suppression, the sensitivity is about -31dBm.

2.5.12.3 Sensitivity Evaluation for QPSK SCM system:

In a QPSK system, for a multiple sub-carrier signal, we have

$$v(t) = \sum_{k=1}^{n} v_k(t) = \sum_{k=1}^{n} \{v_k u_{Ik}(t)\cos(\omega_k t) + v_k u_{Qk}(t)\sin(\omega_k t)\}$$

Where $u_{Ik}(t)$ and $u_{Qk}(t)$ are the normalized digital signal for I and Q baseband channels of the kth subcarrier channel. Similarly as BPSK system, at the receiver, the photo-current is

$$I_s = \eta |E_0|^2 G\Re \approx I_0 \left\{1 + \frac{1}{\sqrt{\zeta}} \sum_{k=1}^{n} m_k \{u_{Ik}(t)\cos(\omega_k t) + u_{Qk}(t)\sin(\omega_k t)\}\right\} \quad ,$$

we note that the peak to peak value of modulating signal for each subcarrier $\{u_{Ik}(t)\cos(\omega_k t) + u_{Qk}(t)\sin(\omega_k t)\}$ is $\sqrt{2}$ times of that of $u_k(t)\cos(\omega_k t)$ in BPSK, in a system with only 2 QPSK subcarriers, the maximum m_k should be $0.25 * 2/\sqrt{2} = 0.25 * \sqrt{2}$, the 2 factor here is to account that there are only 2 subcarriers here and we can double the modulation index for each subcarrier, the $\sqrt{2}$ factor here is to account the difference on the peak to peak value of the modulating signal for each subcarrier for QPSK and BPSK.

The noise calculation for QPSK is the same as BPSK. So a 2 subcarriers QPSK system will have 3 dB improvement on the sensitivity comparing to a 4 subcarriers BPSK system. The sensitivity would be –34 in this case.

2.5.12.4 Sensitivity Evaluation for a binary ASK system:

This section considers both the optically filtered ASK SCM system and the traditional IMDD system. If we only consider one subcarrier in a ASK SCM system,

these two systems essentially have the same signal to noise ratio since they have the same detection schemes. The only difference in their modulation is that ASK SCM system has a carrier component. However, this carrier can be suppressed or removed.

Signal spontaneous beat noise is given by

$S_{ASE}(f) = \rho_{ASE} = 2n_{sp}hf_o(G-1)$,

$S_{sig-sp}(f) = 4\frac{q^2\eta^2}{hf}n_{sp}P_{in}G(G-1) = 2R^2GP_{in}\rho_{ASE}$, here we have considered that the signal only has one polarization and the ASE noise has two.

$Q = \frac{I_S(1) - I_S(0)}{\sqrt{N_{tot}(1)} + \sqrt{N_{tot}(0)}}$, Suppose that there is no waveform distortion and signal spontaneous beat noise is the dominant noise. Q can be reduced to

$Q = \frac{2P_{in}RG}{\sqrt{4R^2hf_o n_{sp} 2P_{in}G(G-1)B_e}} = \sqrt{\frac{P_{in}}{hf_o 2B_e n_{sp}}}$, here the factor 2 before the Pin is because that the average power is half of that of the mark power.

When Q is 6 which corresponding to a BER of 10^{-9}, the sensitivity of OC48 and OC192 binary system is about –46 and –40 if the bandwidth of the electrical filter is only 0.7 times of the bit rate.

Chapter Three
Simulation results of SCM systems

In the last chapter, we have described the basic simulation setup for a 4 subcarriers BPSK system. We also discussed some particular issues for the SCM system and its simulation. Based on the basic setup described in the last chapter, we will use the simulation model to study the performance of three types of SCM system: 4 subcarriers BPSK system, 2 subcarriers QPSK system, 4 subcarriers ASK system. We will also present the result for a traditional OC192 system as a comparison.

First we will make the selections of basic simulation parameters in this chapter, such as the modulation index, RF frequency allocation plan, the bandwidth of the filters etc. This optimization is not necessarily the best, however it will give a possible range within which the system may perform better than out of this range. Or it will give guidance when select the parameters.

It has to be mentioned that there are many factors that are not included or considered in our simulation while they exist in reality, such as the gain tilt of the EDFA, the frequency or wavelength dependence of the dispersion compensation modules etc. Second, though we don't consider all the parameters in a real system, the number of parameters that are considered in the simulation is still large and the combination of different values is huge. We can not simulate all those combinations. We will only consider some meaningful combinations.

After we have some basic idea about how to choose the parameters, we will use one set of the values to find out the performance of an optimized SCM system under different situation such as fiber with different PMD coefficient, with or without dispersion compensation.

As mentioned in the last chapter, we will only study Standard single mode fiber systems because it is most commonly used by large telecos like AT&T, Sprint and Worldcom. Usually newer SMF will have better PMD coefficient which is

typically less than 0.1 ps /sqrt(km) while old SMF may have PMD coefficient as high as 0.5 ps /sqrt(km). Since the SCM systems are sensitive to the PMD effects, we will study fibers with these two different PMD values.

In the next chapter, we will introduce the experiment that we did in the lab, which is a system with 4 BPSK subcarriers. We will discuss the result and compare it with the simulation.

3.1 Performance of an SCM system using 4 BPSK subcarrier each with OC48 data, and with self-coherent detection

In the receiver, if the optical carrier is used to beat with the subcarrier and the subcarrier is demodulated coherently, we will call it a self-coherent detection. We will first study the performance of a SCM system with 4 BPSK subcarriers per wavelength. Each of the subcarriers will carry data at the rate of OC48. This system is the simplest system in the three types of systems we considered in this study. It has simpler modulation format comparing to QPSK system. Compared to direct detection system, it does not require narrow band optical filters. However, we also will see that its performance is the worst in the 3 types of systems.

3.1.1 Bandwidth of the electrical filters

One system parameter is the bandwidth of the baseband electrical filters that are used in the transmitter and the receivers. The wider the bandwidth, the more information the system can preserved and the better eye-opening can be expected, but obviously, less channels could be packed into the same system. In most digital communication systems, the filters bandwidth are set as $0.75 * \text{bit rate}$, for example, for an OC48 system, the filter bandwidth will be 1.86 GHz, and the double side bandwidth is 3.72GHz.

We did a simulation on the effects of the filter bandwidth. In the simulation, the channel spacing between subcarriers is fixed at 4.7 GHz which is about 2 times of the bit rate. Then the bandwidth of the baseband filter is changed from 1 times the bit

rate to 0.4 times of the bit rate. The bandwidths of all the filters are the same in transmitter and receiver. The filters used in the simulation are 6 order butterworth filters. The plot below shows the worst sensitivity of the 4 RF channels vs. the filter bandwidth factor.

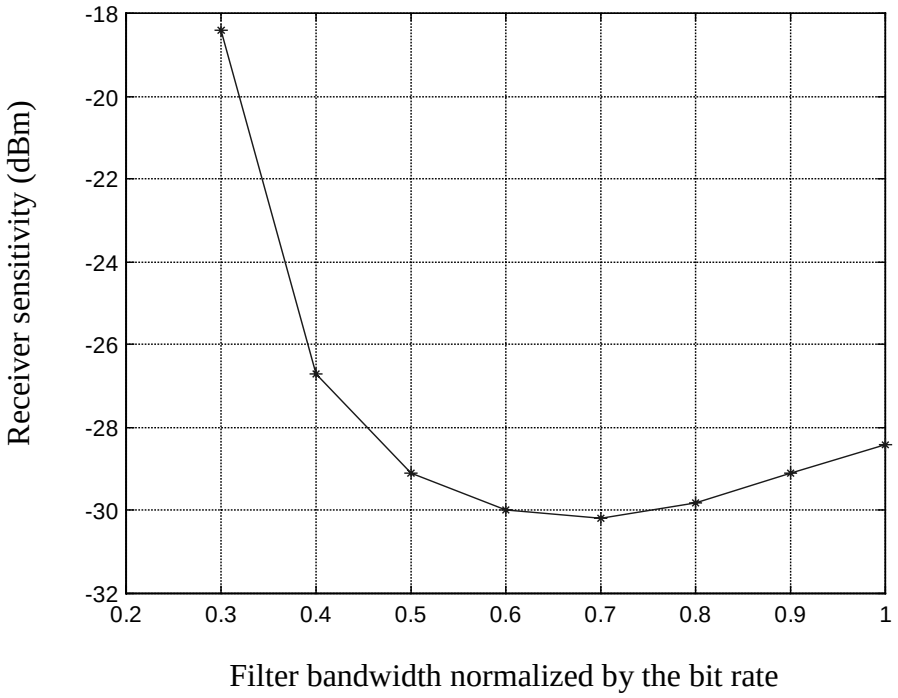

Figure 3.1, worst sensitivity of the 4 subcarrier channels vs. the filter bandwidth factor

From this plot, the best factor is 0.7. In last chapter, we derived an expression of receiver sensitivity. It is shown that the sensitivity is inversely proportional to the bandwidth of the electrical filter. The larger the bandwidth, the more noise is picked up by the receiver. On the other hand, if bandwidth is too small, the signal itself is distorted because the useful information is filtered out. From now on, we will use 0.7 as the factor for the filter in our simulation.

3.1.2 Channel spacing

After determining the minimum bandwidth of the baseband filters, we can now determine the minimum possible channel spacing between the adjacent RF channels so we can have the maximum bandwidth efficiency. Ideally, two adjacent channels should be kept as apart as possible because the leakage from the filtering may result in linear crosstalk between each other. Optimization of channel spacing is necessary to maximize the bandwidth efficiency while keep the inter-channel crosstalk within the tolerable level.

In this simulation, we use four subcarrier channels and change the channel spacing between adjacent subcarrier channels from 1 time the bit rate to 2 times the bit rate. The subcarrier frequency of channel one is set at 2.8 GHz, which is the lowest of the 4 channels. The fiber length here is 0 km and other system parameters remain unchanged.

Figure 3.2 shows the receiver sensitivity vs. channel spacing. Stars, crosses, pluses and circles represent channel 1 to 4 respectively. When the channel spacing is smaller than 4.2 GHz, the subcarriers begin to interfere with each other and degradation begins to appear. The performance of channel 2 and 3 are worse than that of channel 1 and 4 when the channel spacing is small. The reason is that channel 2 and 3 are both interfered from both sides of the spectrum while channel 1 and 4 have crosstalks from one side only.

However when you consider the fiber nonlinearity in the simulation, we found that 4.7 GHz is a relatively better choice as the minimum channel spacing. Also because we used 4.7 GHz in our experiment as the minimum channel spacing. So in the following simulations, we will use 4.7 as the minimum channel spacing.

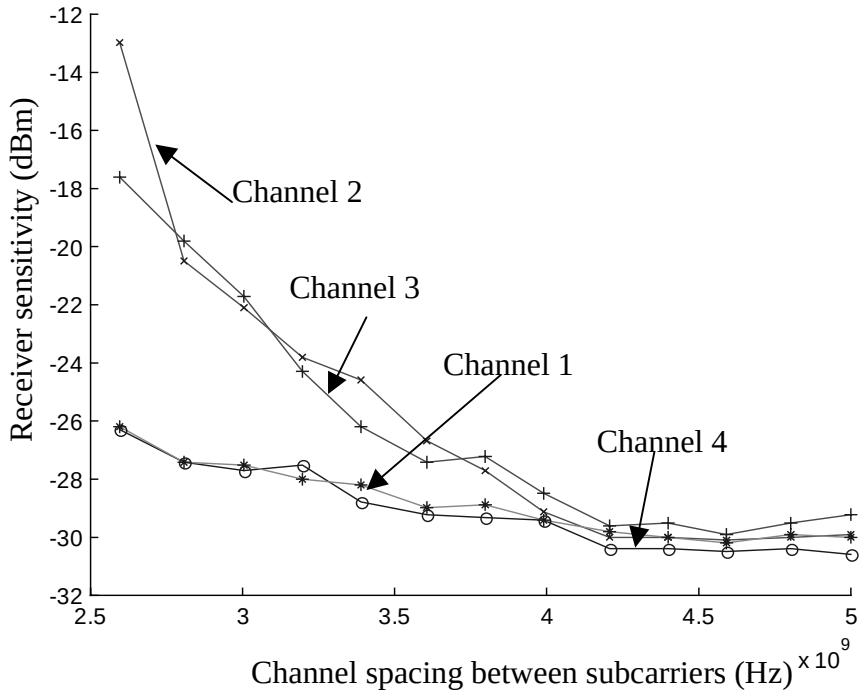

Figure 3.2 Sensitivity vs the channel spacing in a 4 subcarriers BPSK system

3.1.3 frequency plan

After determining the minimum channel spacing, we can now find the frequency of each subcarrier channel. If we use equal spacing among the subcarriers, this essentially is to decide the frequency of the lowest subcarrier. Because of the polarization walkoff problem and the PMD problem, the subcarrier frequency should be kept as low as possible to avoid the damaging effect of these problems.

Based on many observations of the system performance with different parameters such as optical power, frequency plan, modulation index etc. (these results are not presented in this thesis but they can be reproduced easily), if the PMD coefficient of the fiber is 0.1ps/sqrt(km), we found such a single wavelength 4-subcarrier SCM system can transmit roughly about 500 to 600 km depending on different parameters. Considering that the effect of fiber nonlinearity will depend on frequency allocation, so this time we change the frequency of the lowest subcarrier while fixing the RF channel spacing and simulate the system performance in 3

difference transmission distances: 480, 560 and 640km. There is no dispersion compensation used in these simulations.

There are 5 plots shown in Figure 3.3, each of which shows the sensitivity as the function of the frequency of the lowest subcarrier at various transmission fiber lengths of 480km(crosses), 560km(pluses) and 640km(squares). Figure 3.2(a) shows the worst case sensitivity for all the four-subcarrier channels. Figure 3.3 (b) to (e) are the sensitivities for different subcarrier channels. The optical power used in the simulation is 5dBm. There are curves in these plots showing sensitivity of 7 dBm, that is not realistic, it happens because the signal eyes are closed in the simulation.

From Figure 3.3 (a), we can see that when the lowest channel frequency is 2.6GHz, it can transmit to 560km with sensitivity of about –22dBm. Although the system can transmit to 560km when the frequency is 2GHz, but the sensitivity is only –10dBm and that is too small. From figure 3.3 (b) to (e), it is easy to find that channel one (the lowest frequency channel) always has the worst performance among the 4 subcarriers, channel 2 and 3 have better performance and channel 4 is always the best. The reason why the lowest frequency channel always has the worst performance is because of the low frequency noise created by direct detection. In the following study we will use 2.6 GHz for this BPSK system.

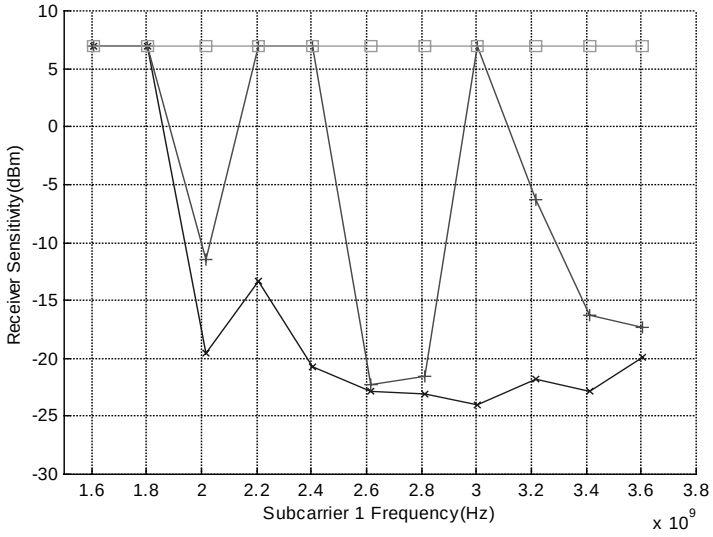

(a) Overall sensitivity

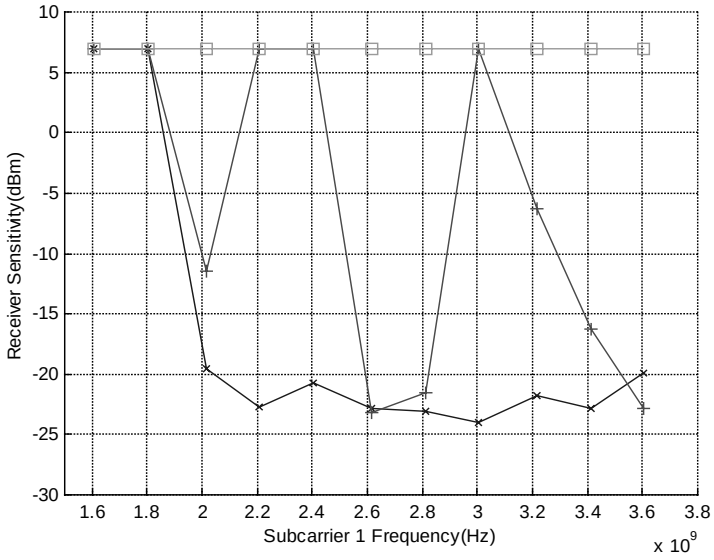

(b) channel 1 sensitivity

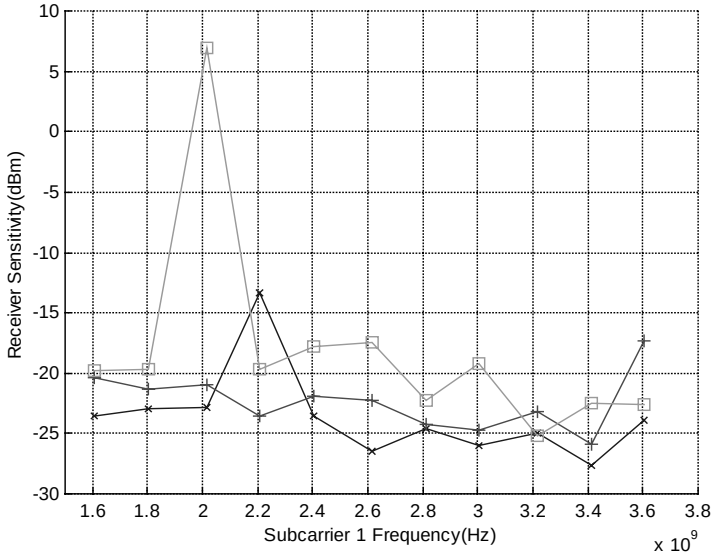

(c) channel 2 sensitivity

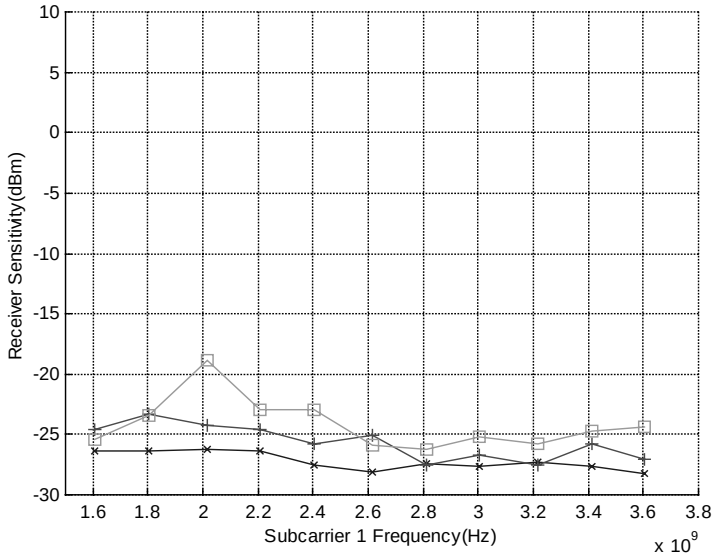

(d) channel 3 sensitivity

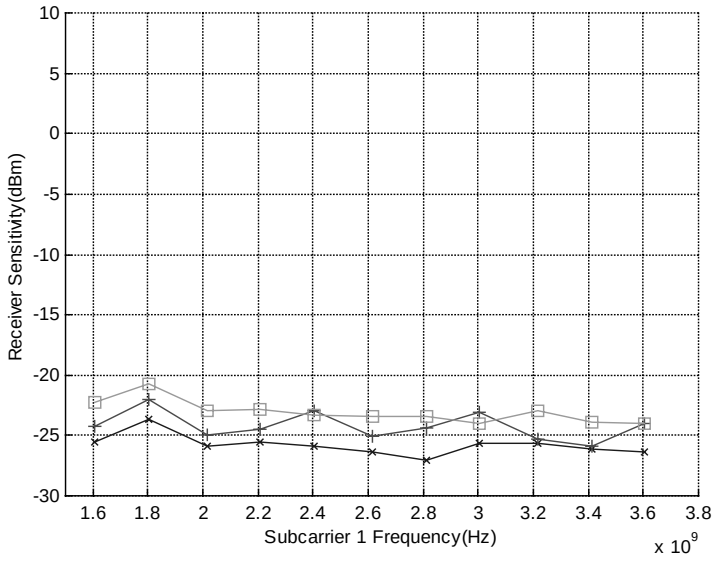

(e) channel 4 sensitivity

Figure 3.3, Sensitivity as the function of the frequency of the first channel at different fiber lengths

The above considerations will give us some guide when we select the frequency plan. It does not give the exact best frequency of each subcarrier channel. However, it will reduce the range of variable values that we can use.

In our simulation, channel 1 frequency is selected as 2.6 GHz which is about the baseband bandwidth of a subcarrier channel. When the frequency spacing is 4.7 GHZ, which is determined earlier, the frequency for 4 channels are 2.6, 7.3, 12, 16.7 GHz respectively.

3.1.4 Effect of Carrier Suppression

In chapter 2, when we calculate the sensitivity using the linear approximation for the MZ modulator, we found the sensitivity could be improved on a dB-per-dB base by carrier suppression when the optical modulation index (OMI) is small. Here, we use numerical simulation to verify that. We use four subcarriers each carrying OC48 data with BPSK modulation. In order to compare with the experimental results, the frequency of the subcarriers is set to 3.6GHz, 8.3GHz, 13GHz, and 17.5GHz. The bandwidth of the electrical filters is 0.7 times the bitrate. The fiber length is 80km, the optical power launched into the fiber is -3dBm, and we use 100% dispersion compensation here. The noise figure of the EDFA is 5dB. We changed the OMI from 0.05 to 0.4 with a step size of 0.05 and keep everything else unchanged. The sensitivity is defined as the sensitivity of the sub carrier channel with the worst performance.

We tested 2 cases, one is with 0 dB carrier suppression, and the other is with 5 dB carrier suppression. Figure 3.4(a) shows the calculated sensitivity result for these two cases. Carrier suppression generally improves the receiver sensitivity. Receiver sensitivity increases with the increase of OMI because the modulation is more efficient. However when the OMI is high enough, the effect of carrier suppression is reduced because the carrier component is already low enough.

Figure 3.4(b) shows the sensitivity difference with and without carrier suppressions. The analytical result of last chapter is more accurate when OMI is small. The maximum sensitivity gain is about 4.2 dB due to carrier suppression. However this max sensitivity gain does not occurred at the minimum OMI of 0.05, we believe this is due to the nonlinearity of the MZ modulator.

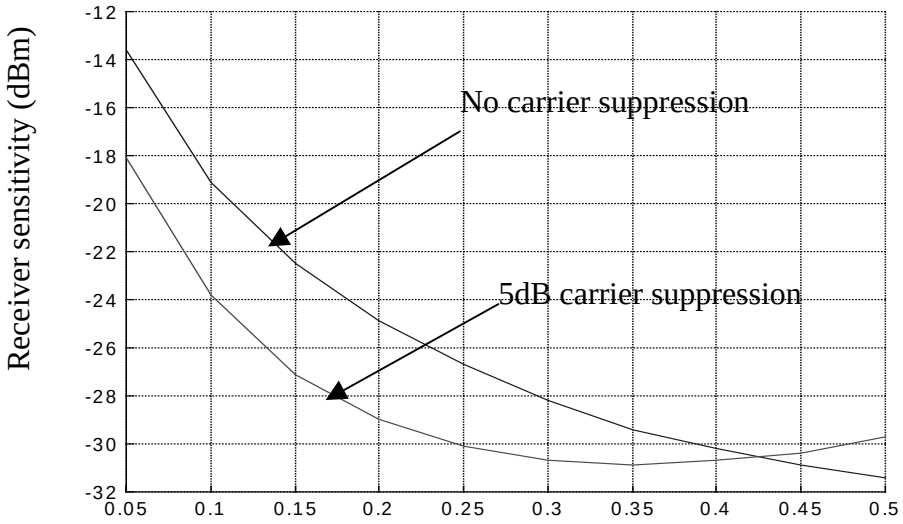

(a)

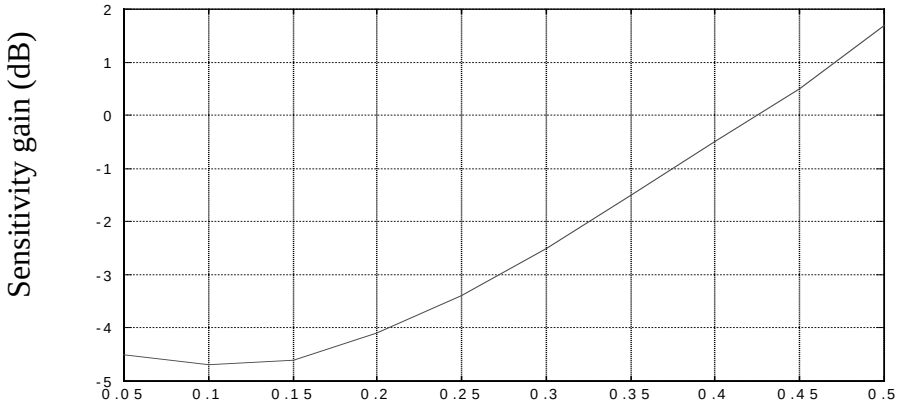

(b)

Figure 3.4, sensitivity improvement due to carrier suppression.

3.1.5 OMI and carrier suppression ratio combination

It was suggested in chapter 2 that we could use a lower OMI with optical carrier suppression to reduce the inter-channel interference as the result of MZ nonlinearity while keep reasonable modulation efficiency.

We have identified that MZ modulator will generate CTB but not generate CSO, the CTB is about –22dBC when the OMI is 0.4 and will decrease to less than –60 dBc when the OMI is 0.05. So we can use a small OMI first to generate a signal that has a large CTB suppression ratio. This signal has very large carrier component because of low modulation index and the total optical power needs to be relatively high in order to have enough signal to noise ratio. If we reduce the amplitude of the carrier without reducing the signal sidebands, then the total optical power is reduced. The ratio between the signal and CTB will not be changed due to carrier suppression. Furthermore, carrier suppression will help to reduce SBS effect.

Now we need to validate our assumption and find what is the best combination of the OMI and carrier suppression ratio. In the simulation, we used the OMI values of 0.05, 0.1, 0.2, 0.3, 0.4 and 0.5. and we vary the optical carrier suppression ratio for each of the OMI values. 3 different transmission fiber length have been used in the simulation: 0, 420 and 500 km. The optical power launched into each fiber span is 5dBm. The purpose to consider nonzero fiber length is to find out what is the impact of fiber nonlinearity at different OMI and carrier suppression. All other parameters are the same as those used in the last section. The calculated receiver sensitivity results are shown in Figure 3.5. The horizontal axis is the carrier suppression ratio and the vertical axis is the sensitivity of the worst subcarrier channel.

In each plot of Figure 3.5, there are 6 curves. From left to right, they correspond to the OMI value of 0.05, 0.1, 0.2, 0.3, 0.4, 0.5 respectively.

At all the distances, For each OMI value, there is a best carrier suppression ratio. A smaller carrier suppression ratio will result in small signal amplitude, while too large suppression ratio will result in signal clipping.

As shown in Figure 3.5 (a), larger OMI and smaller suppression ratio has better performance. However, after transmission through the fiber, smaller OMI and large suppression ratio produce better system performance, this can be seen at Figure 3.5 (b) and (c).

The reason for this could be explained as follows: at 0km, the only nonlinear process is the MZ modulation and this nonlinearity does not significantly degrade system performance and carrier suppression is not helpful. However after 420km or 500km transmission through the fiber, the modulator nonlinearity interacts with fiber nonlinearity and dispersion, thus produces significant sensitivity degradation. In this case, the system performs better with low modulation index and stronger carrier suppression.

Since small carrier suppression ratio is easier to realize, in most of our simulation work we will only show the system performance with OMI=0.3 and 5dB suppression ratio and with OMI=0.4 and no carrier suppression.

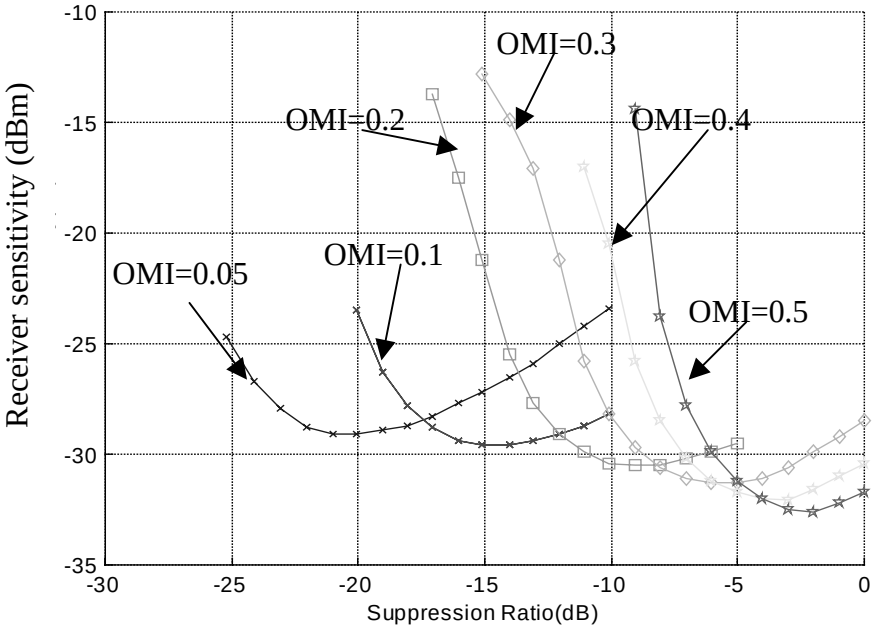

(a) at 0 km

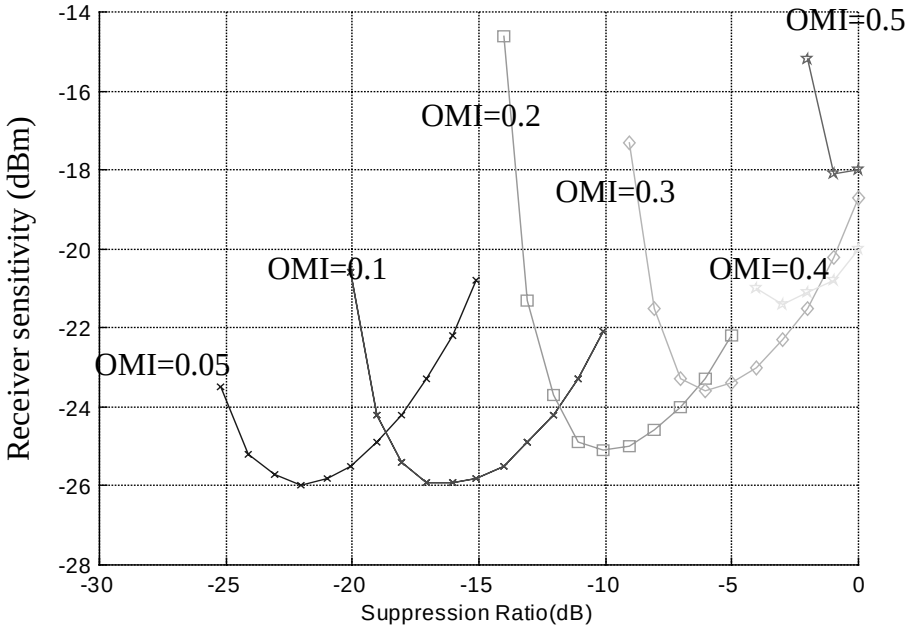

(b) at 420km

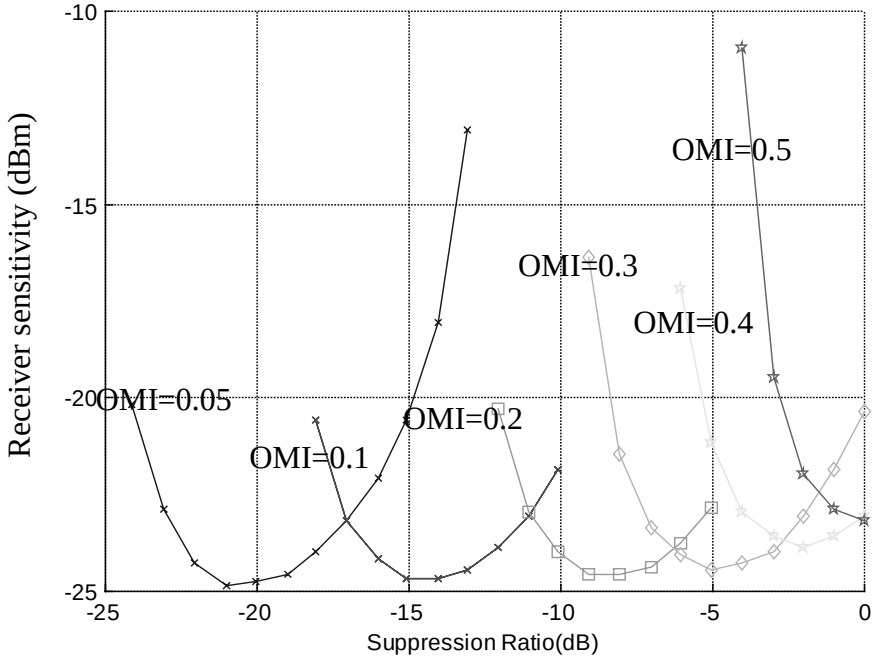

(c) at 500 km

Figure 3.5 BPSK system sensitivity as the function of OMI and carrier suppression for different transmission distance

3.1.6 Simulation results of System sensitivity and eye-opening

Based on the earlier discussion, now we can present some major simulation results for both a single wavelength and a 4 wavelength system with 4 subcarriers per wavelength and using BPSK modulation format. Please see the appendix 2 for all the plots.

For all the results we want to present for both single wavelength and four wavelength systems, the frequencies of subcarriers are 2.6, 7.3, 12, 16.7 GHz. We will use two different OMI values: OMI of 0.4 without suppression and OMI 0f 0.3 with 5 dB carrier suppression. We will use different optical power and investigate the impact of optical power levels. We will give simulated result for systems both without dispersion compensation and with 100 percent dispersion compensation. In four-wavelength cases, spacing between adjacent wavelengths is 50GHz.

The fiber used in the simulation is G.652 fiber. Its attenuation coefficient is 0.25 dB/km, nonlinear index is 2.36e-20 m^2/W, the effective core area is 71 um^2, the dispersion parameter is 18 ps/nm/km and the dispersion slope is 0.093 ps/nm^2/km.

Two types of PMD coefficients are used: 0.1 $ps/\sqrt{km}$ and 0.5 $ps/\sqrt{km}$. The reason why we include PMD effect is that the SCM system is sensitive to the polarization walkoff and system performance is sensitive to PMD characteristic.

The following table summarizes the longest transmission distance for BPSK SCM systems with different system parameters. Results are given for both single wavelength system and 4 wavelength system. In the table, DC means dispersions compensation, OMI means optical modulation index, OP means optical power, RFMI means RF modulation index of each sub-carrier channel, Freq 1 means the frequency of the lowest subcarrier, L means longest transmission distance.

PMD $\frac{ps}{\sqrt{km}}$	DC	OMI	OP dBm	RFMI	Freq1 (GHz)	L (km): Single wavelength	L(km): Four wavelength
0.1	Yes	0.3	5	0.9 0.9 1.15 1.35	2.6	920	450
0.1	yes	0.4	5	0.9 0.9 1.15 1.35	2.6	680	300
0.1	yes	0.3	3	0.9 0.9 1.15 1.35	2.6	640	350
0.1	yes	0.4	3	0.9 0.9 1.15 1.35	2.6	520	400
0.1	yes	0.3	0	0.9 0.9 1.15 1.35	2.6		350
0.1	yes	0.4	0	0.9 0.9 1.15 1.35	2.6		250
0.1	yes	0.3	-3	0.9 0.9 1.15 1.35	2.6		250
0.1	yes	0.4	-3	0.9 0.9 1.15 1.35	2.6		200
0.1	no	0.3	5	1.12 1.05 1.05 0.9	2.6	600	200
0.1	no	0.4	5	1.12 1.05 1.05 0.9	2.6	600	200
0.1	no	0.3	3	1.12 1.05 1.05 0.9	2.6	560	250
0.1	no	0.4	3	1.12 1.05 1.05 0.9	2.6	400	250
0.1	no	0.3	0	1.12 1.05 1.05 0.9	2.6		350
0.1	no	0.4	0	1.12 1.05 1.05 0.9	2.6		350
0.1	no	0.3	-3	1.12 1.05 1.05 0.9	2.6		350
0.1	no	0.4	-3	1.12 1.05 1.05 0.9	2.6		250
0.5	yes	0.3	5	0.9 0.9 1.15 1.35	2.6	440	350
0.5	yes	0.4	5	0.9 0.9 1.15 1.35	2.6	360	350
0.5	yes	0.3	3	0.9 0.9 1.15 1.35	2.6	360	350
0.5	yes	0.4	3	0.9 0.9 1.15 1.35	2.6	280	350
0.5	yes	0.3	0	0.9 0.9 1.15 1.35	2.6		250
0.5	yes	0.4	0	0.9 0.9 1.15 1.35	2.6		250
0.5	yes	0.3	-3	0.9 0.9 1.15 1.35	2.6		250
0.5	yes	0.4	-3	0.9 0.9 1.15 1.35	2.6		150
0.5	no	0.3	5	1.12 1.05 1.05 0.9	2.6	500	200

0.5	no	0.4	5	1.12 1.05 1.05 0.9	2.6	440	200
0.5	No	0.3	3	1.12 1.05 1.05 0.9	2.6	440	250
0.5	No	0.4	3	1.12 1.05 1.05 0.9	2.6	360	250
0.5	No	0.3	0	1.12 1.05 1.05 0.9	2.6		300
0.5	No	0.4	0	1.12 1.05 1.05 0.9	2.6		250
0.5	No	0.3	-3	1.12 1.05 1.05 0.9	2.6		250
0.5	No	0.4	-3	1.12 1.05 1.05 0.9	2.6		200

Table 3.1 longest transmission distance for BPSK SCM systems with different parameters.

From the plots for the single wavelength case in the appendix 2, we can see that when the PMD coefficient is high, the high frequency channels will have smaller eye-openings and poor sensitivity due to the polarization walkoff. Also, since the nonlinear interference introduced from the modulation, demodulation and the fiber transmission have a stronger impact on the lower frequency channels, these channels usually have worse performance compare to high frequency channels. We have used different RF modulation index for each subcarriers in order to compensate for this non-uniform performance.

If the fiber is considered a linear medium, at higher optical power, the signal to noise ratio is higher and the system can transmit longer. But at high optical power level, optical fiber exhibits nonlinear effect, it will generate nonlinear interference between channels. For fiber with 0.1 ps/sqrt(km) PMD coefficient, the longest transmission distance is found to be about 450km with the launched optical power of 5 dBm and with 100% dispersion compensation. Without dispersion compensation, lower optical power level will have better results. In this case nonlinear phase modulation may be converted into amplitude modulation through fiber dispersion and thus further degrade system performance. The longest distance without dispersion compensation is found to be 350 km and optical power used per wavelength are

below 0 dBm. For 0.5 $ps/\sqrt{km}$ fiber, these numbers are 350km and 300km respectively.

When using smaller OMI of 0.3 with carrier suppression, performance is usually better than with higher OMI of 0.4 without carrier suppression. This is because the signal has better linearity at smaller OMI and carrier suppression compensates for the reduction of modulation efficiency.

For the results presented above, only PMD induced polarization walk off was considered, while PMD induced pulse distortion was neglected. If the PMD induced distortion, as discussed in 2.5.10.2, is considered, we know that for G.652 SM fiber, with PMD parameter 0.5 $ps/\sqrt{km}$, the transmission distance is limited to 240 km when the highest sub carrier frequency is 18GHz. Although this PMD effect is not included in the simulation, since it is a very coarse and worst case estimation, we think it will have less effect in an real system.

3.2 Performance of an SCM system using QPSK

We already know that the 4-channel BPSK SCM system suffers from excess nonlinear distortion due to nonlinearity in the transmission path. In this case there are 4 SCM channels closely packed in one wavelength, they generate a lot of nonlinear interference between each other. Furthermore a 4-channel SCM system is sensitive to polarization walkoff and PMD problem. The reason for this is that the frequency difference between the carrier and the highest subcarrier is too high and the polarization effect is proportional to this frequency difference.

In order to reduce the number of SCM channels and also reduce the frequency of the highest subcarrier, QPSK can be used as the modulation format. In order to have a 10Gb/s total capacity per wavelength, only two subcarrier channels are needed, each carries 5 Gb/s signal using QPSK format. The symbol rate of each subcarrier is still 2.5Gbps so that the bandwidth of each subcarrier is still the same as in the BPSK system where 2.5 Gb/s data is carried per subcarrier. In QPSK modulation format, each symbol represents 2 bit information since it has 4 possible phase angle. This makes the total bit rate of each wavelength to be 10Gbps.

Figure 3.6 shows the spectrums and eyediagrams of the signal at different points of a 70km fiber system. They are very similar to that of a 4 subcarriers BPSK system. The only difference is the number of subcarriers. The frequencies of the two subcarriers in the QPSK system are 4 and 11.2. GHz. These two frequency values are chosen through optimizations over system performance. During the optimization of the subcarrier frequencies, we make sure that most newly generated nonlinear components do not coincide with these two subcarriers.

We present the eyediagrams in Figure 3.6 for only one 2.5 Gb/s data channel from each subcarrier. The other channel in that subcarrier should have exactly the same performance. We found the lower frequency subcarrier still has poor eye-opening than the high frequency subcarrier because most nonlinear interference products are located within low frequency range.

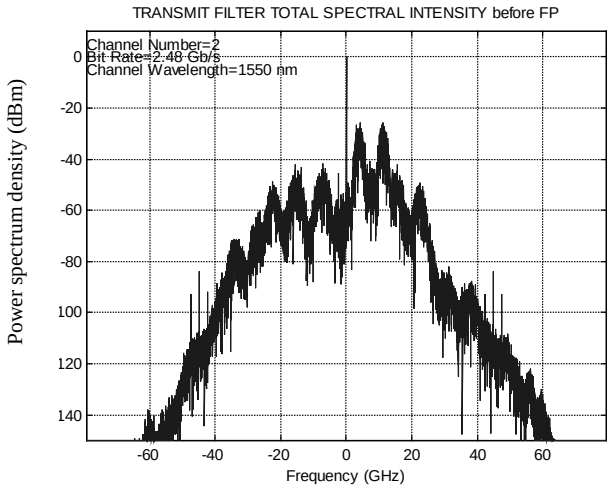

(a) signal spectrum before the WDM optical filter at transmitter

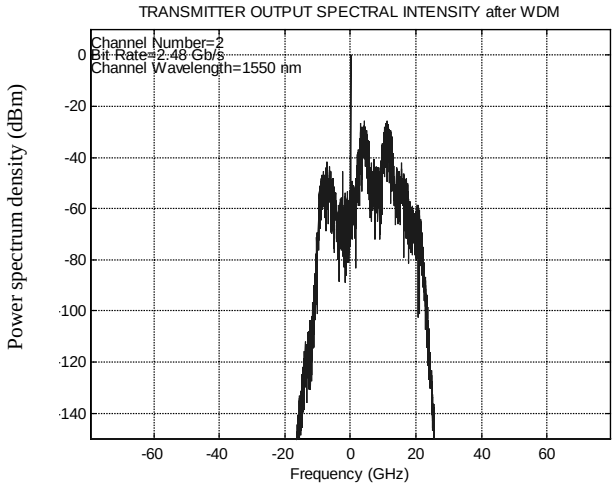

(b) signal spectrum after the WDM optical filter at transmitter

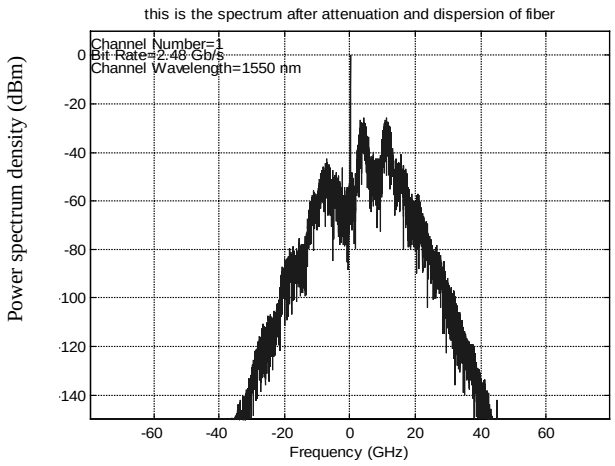

(c) signal spectrum after the transmisssion over 70 km fiber

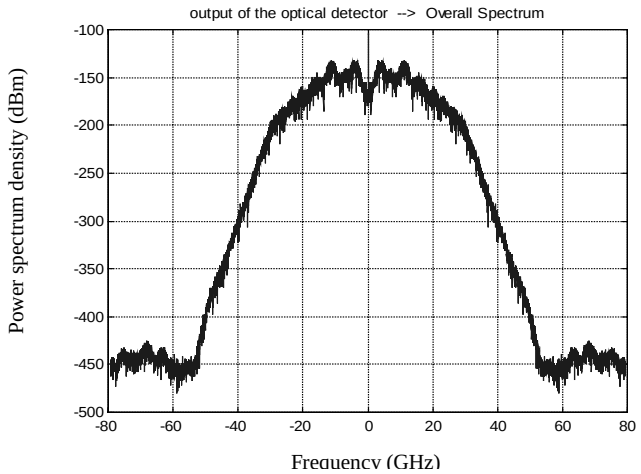

(d) signal electrical spectrum after the photo detector

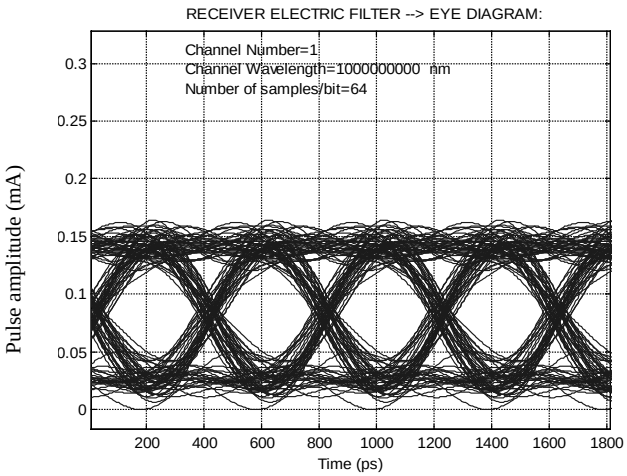

(e) eyediagram of subcarrier one after receiver baseband electrical filter

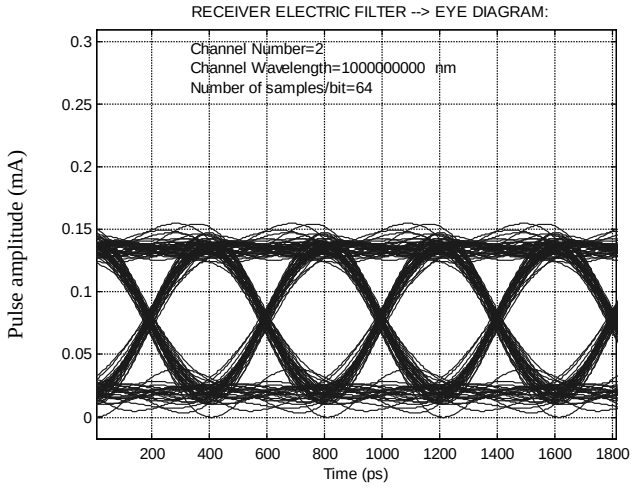

(f) eyediagram of subcarrier two after receiver baseband electrical filter

Figure 3.6, signals for a QPSK system.

The OMI used to make these plots is 0.4. In order to find the impacts of OMI and carrier suppression, we did simulations at different OMIs and carrier suppression ratio similar to what we did in the BPSK systems. Figure 3.7 shows the receiver sensitivity vs carrier suppression ratio at several different OMIs. The simulation were performed for both back to back (figure 3.7(a)) and after 300km SMF (figure 3.7 (b))

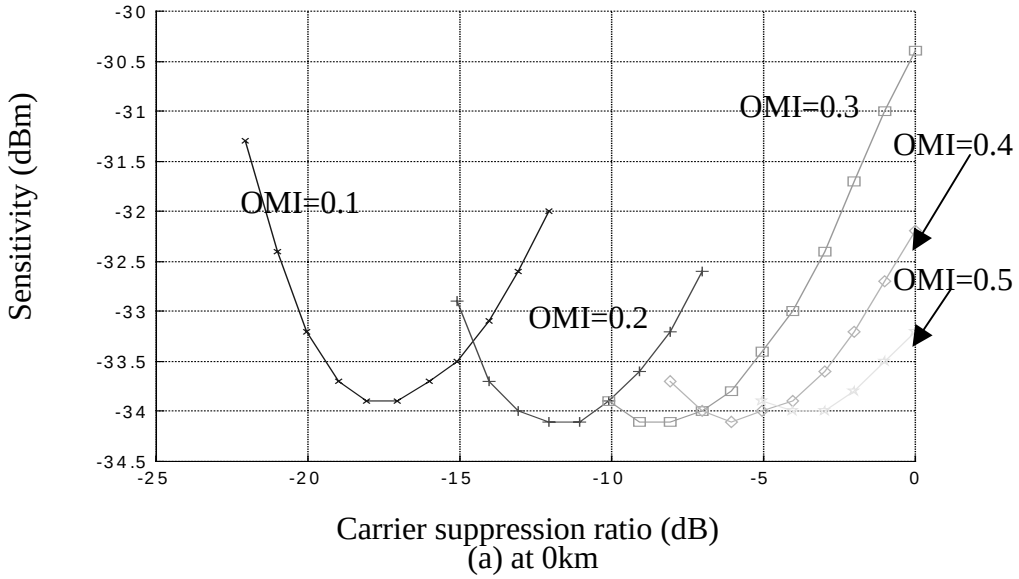

(a) at 0km

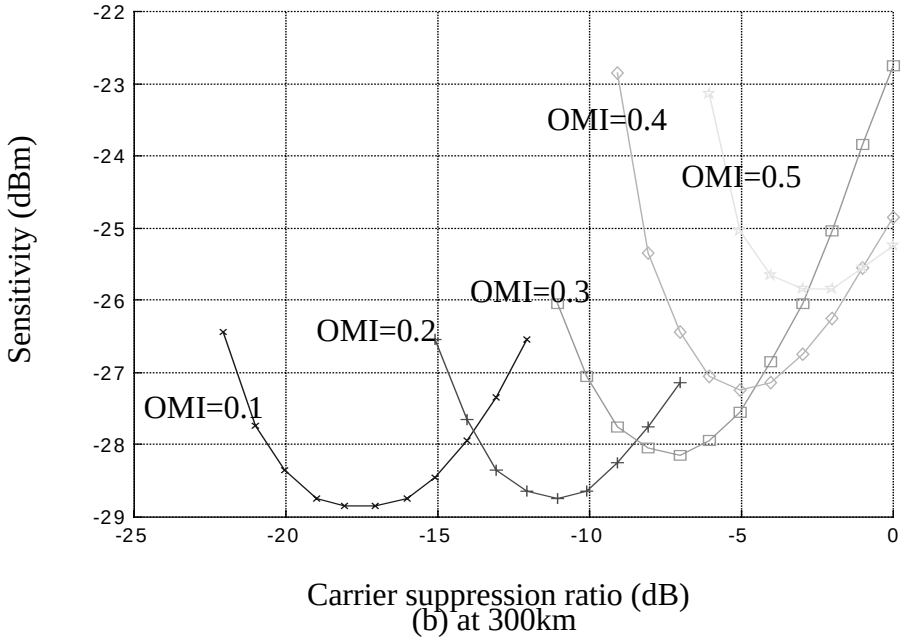

Figure 3.7 QPSK system sensitivity as the function of OMI and carrier suppression for different transmission distance

We found the carrier suppression in QPSK system has similar effect as in the BPSK system. Since we tested 5dB carrier suppression in our experiment, we will still use OMI of 0.3 and 5dB carrier suppression.

Table 3.2 summarizes the QPSK system results for different optical powers levels. Please refer to the appendix 3 for the plots need to generate Tab. 3.2. In this table, DC means dispersions compensation, OMI means optical modulation index, OP means optical power, RFMI means RF modulation index, Freq 1 means the frequency of lower subcarrier, L means longest transmission distance.

For the fiber with PMD parameter of 0.1ps/sqrt(km), the longest transmission distance 1200 km can be achieved with 100% dispersion compensation and 3dBm optical power. Decreasing optical power from 3dBm, the maximum transmission distance will also be decreased. This is different from the situation of BPSK system, where the nonlinearity is more severe and the system works better at smaller optical power.

For the fiber with PMD parameter of 0.5ps/sqrt(km), the longest transmission distance is about 750 km with dispersion compensation and 5dBm optical power. Since the highest subcarrier frequency is 11.2 GHz here which is smaller than 18 GHz used in BPSK system, the PMD walkoff problem is not as severe as in BPSK system.

Without dispersion compensation, the transmission distance is 450 km no matter what is the PMD parameter. Fiber nonlinearity is still one of the limiting factor here.

PMD $ps/\sqrt{km}$	DC	OMI	OP(dBm)	RFMI	Freq1	L(km)
0.1	Yes	0.3	5	1 1	4	1100
0.1	Yes	0.4	5	1 1	4	950
0.1	Yes	0.3	3	1 1	4	1200
0.1	Yes	0.4	3	1 1	4	900
0.1	Yes	0.3	0	1 1	4	750
0.1	Yes	0.4	0	1 1	4	550
0.1	Yes	0.3	-3	1 1	4	500
0.1	Yes	0.4	-3	1 1	4	350
0.1	No	0.3	5	1 1	4	400
0.1	No	0.4	5	1 1	4	400
0.1	No	0.3	3	1 1	4	450
0.1	No	0.4	3	1 1	4	450
0.1	No	0.3	0	1 1	4	250
0.1	No	0.4	0	1 1	4	250
0.1	No	0.3	-3	1 1	4	250
0.1	No	0.4	-3	1 1	4	250
0.5	Yes	0.3	5	1 1	4	750

0.5	Yes	0.4	5	1 1	4	650
0.5	yes	0.3	3	1 1	4	700
0.5	yes	0.4	3	1 1	4	500
0.5	yes	0.3	0	1 1	4	500
0.5	yes	0.4	0	1 1	4	350
0.5	yes	0.3	-3	1 1	4	350
0.5	yes	0.4	-3	1 1	4	250
0.5	no	0.3	5	1 1	4	400
0.5	no	0.4	5	1 1	4	400
0.5	no	0.3	3	1 1	4	450
0.5	no	0.4	3	1 1	4	450
0.5	no	0.3	0	1 1	4	250
0.5	no	0.4	0	1 1	4	250
0.5	no	0.3	-3	1 1	4	250
0.5	no	0.4	-3	1 1	4	250

Table 3.2 longest transmission distance for BPSK SCM systems with different parameters.

3.3 Performance of an SCM system with direct detection

In a 4 subcarriers BPSK system, the highest frequency subcarrier always suffer from the effects of both polarization walk off and polarization mode dispersion. The polarization effects severely limits the max transmission distance.

In order to reduce such undesired effect, we tried to reduce the highest signal frequency by using QPSK modulation format. QPSK has a better PMD tolerance compared to BPSK because the highest subcarrier frequency is reduced form about 17 GHz to 12 GHz. But it is still sensitive to the polarization limitation. One way to overcome this problem is to use coherent detection for each of the subcarriers. This method requires four very stable receiver lasers as the local oscillators, which is obviously a very expensive solution. Another method is to use narrow band optical filter to select the subcarrier directly in optical domains. This method is used in [1] and the authors experimentally transmitted a 10 Gb/s signal through 4 subcarriers each carrying 2.5 Gbps. A direct detection optical receiver was used using narrow band optical filter to make cannel selection. The transmission distance reported was 490km and the sensitivity is about –25dBm. In this work [1] DSB was used. In addition to its sensitivity to chromatic dispersion, the DSB modulation has 3dB intrinsic system penalty due to its four unused subcarriers on the other side of the carrier.

In such a system, the signal subcarrier is selected by optical filtering, so only those modulation formats whose complex envelopes resemble their baseband signals can be demodulated. This requirement implies the use of ASK as the modulation format. Phase modulation format such as PSK or FSK will not give the desired output. Also in the receiver an optical splitter is required to distribute the signal to four different narrow band filters.

The narrow band optical filter we used in the simulation is a simple FP filter. The reflectivity of the mirror is 0.99, which gives the finesse of the filter to be 312.5845. When the bandwidth of the passband is increased or decreased by changing the spacing between the two mirrors, the free-spectral-range (FSR) will be increased

or decreased too. In a system with multiple wavelengths, there is a wideband WDM filter before the optical splitter and the FP filters. This WDM is used to separate different wavelengths and then the FP filter will separate different sub carrier. Because in direct detection system, PMD is not a major limitation, the frequency allocation scheme can be relaxed compare to PSK systems. Choose wider channel spacing will reduce crosstalk caused by optical filter leakage, but will reduce bandwidth efficiency. We choose 2.8GHz as the lowest subcarrier frequency and 4.7GHz as the channel spacing between subcarriers.

In order to illustrate the idea of this direct detection scheme, Figure 3.9 shows the spectrum and signal waveform or eye diagram at different points of the system.

In the transmitter side, the RF modulation is different from that of a PSK system. the envelop of the modulated signal has to resemble the waveform of the baseband signal when the signal bi is "0", there is no output from the transmitter. Figure 3.8 presents the waveform and spectrum of the modulated signal for subcarrier channel 3 in the simulation.

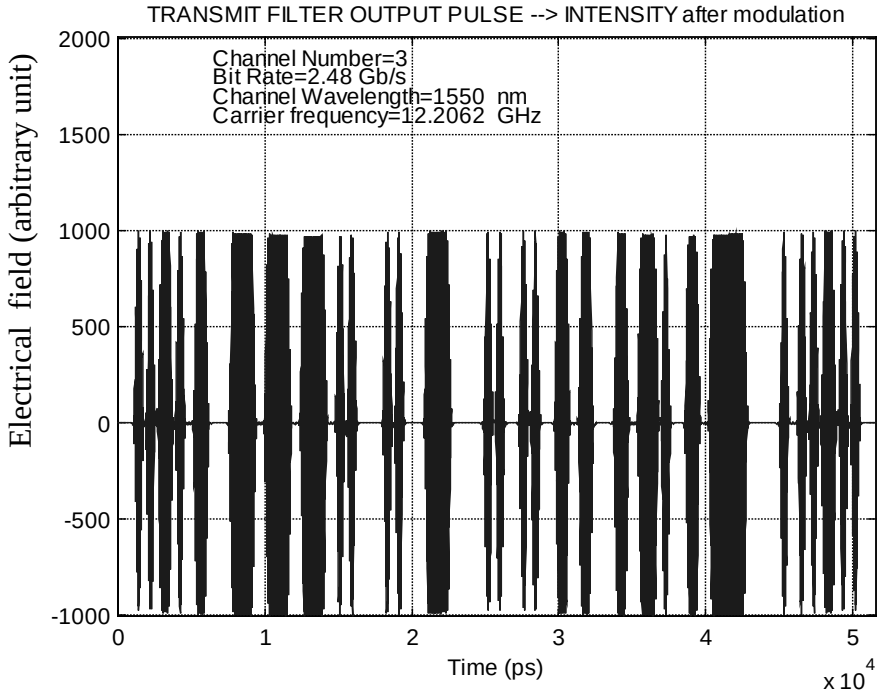

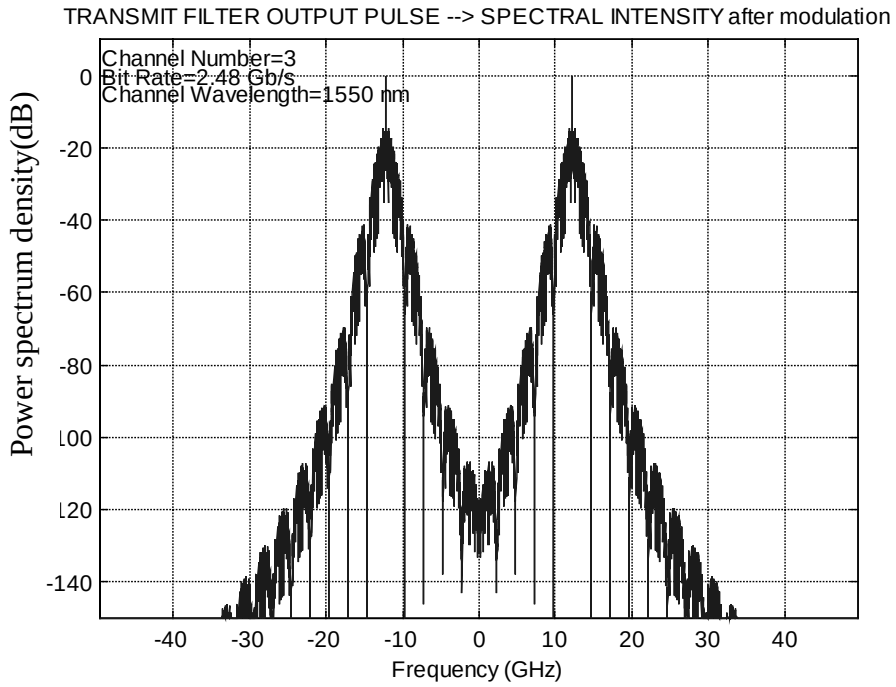

Figure 3.8 waveform and spectrum of the modulated signal for subcarrier 3

Figure 3.9 shows waveform and spectrum of the composite signal with combined four subcarrier channels.

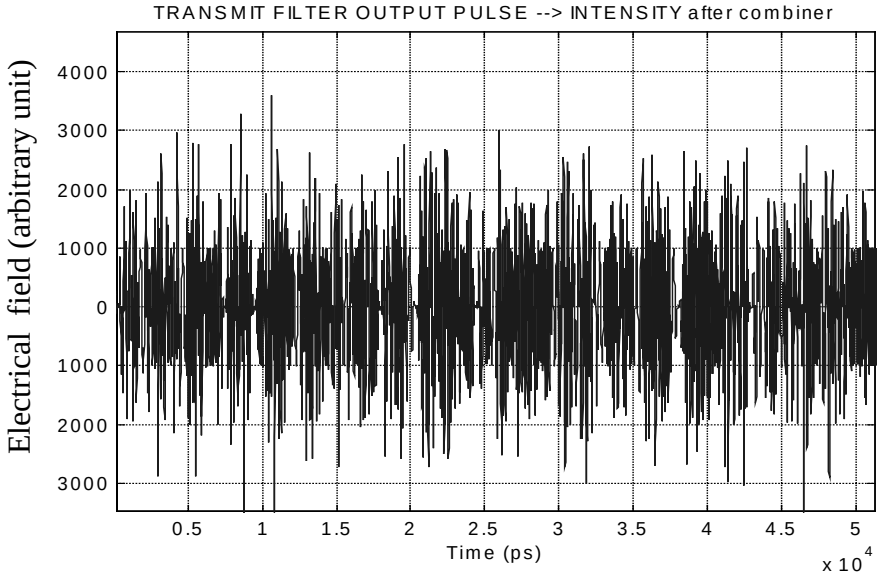

(a)

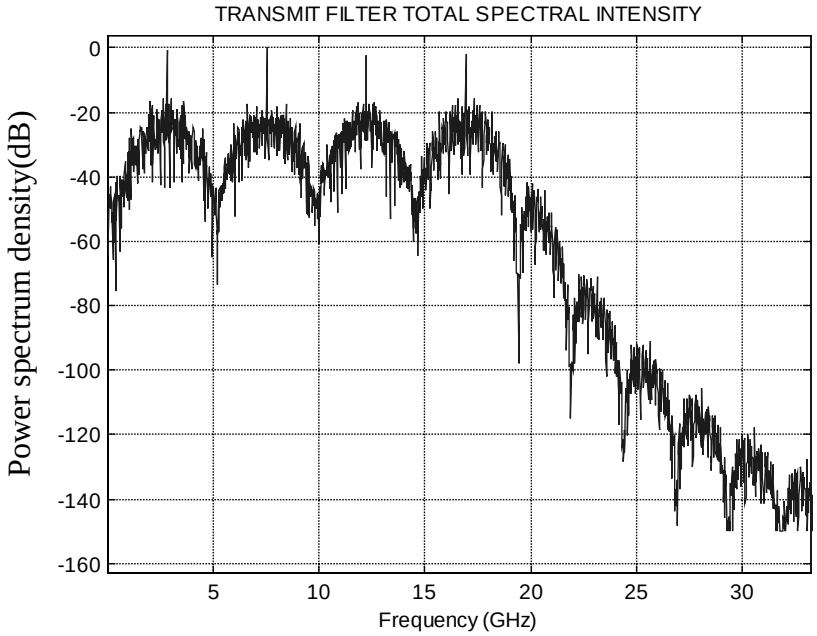

(b)

Figure 3.9 waveform and spectrum of the composite signal

An important difference between the spectrums of the ASK and PSK modulated signals is that ASK spectrum has a strong carrier component at each tone, theis can be observed at Figure 3.9(b).

Figure 3.10 shows the waveform and spectrum of the optical signal with 4 subcarrier channels after the MZ optical modulator. The optical modulation index is 0.3.

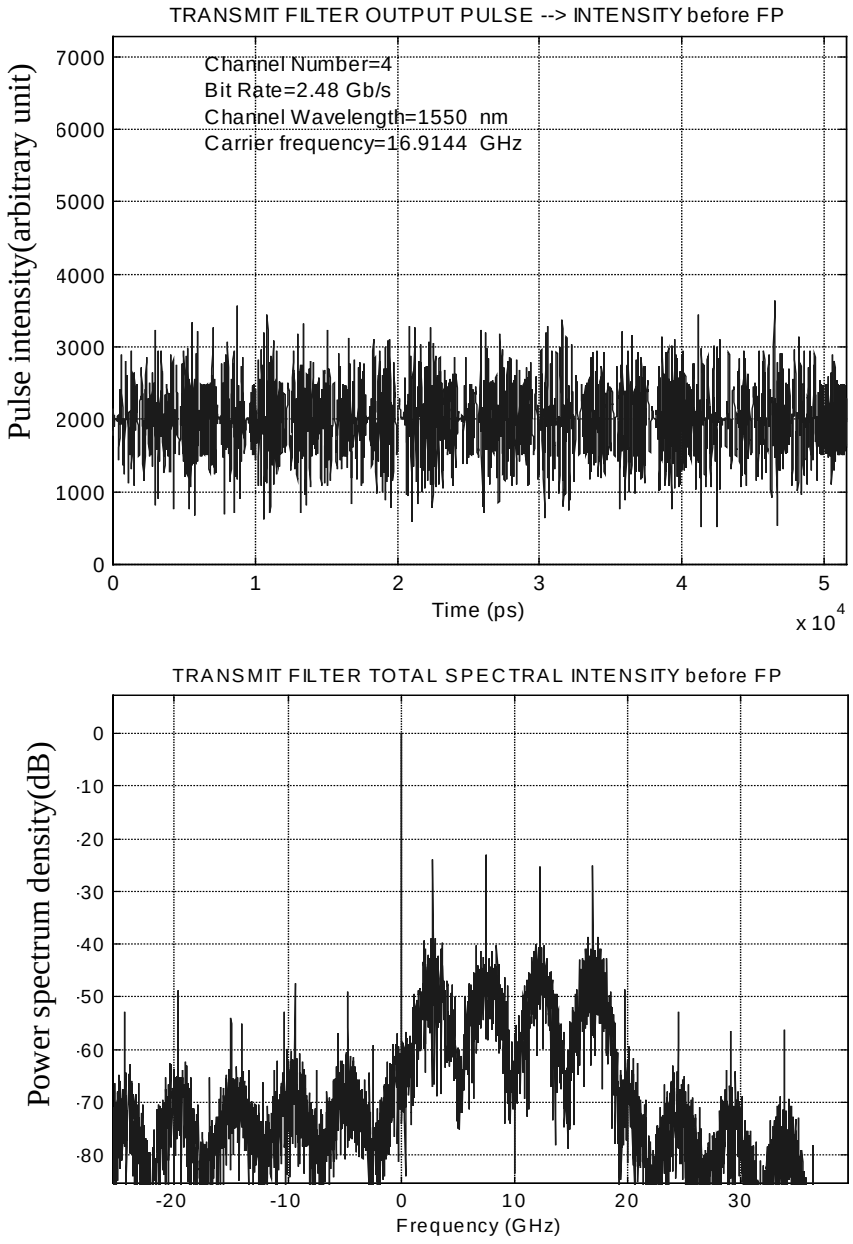

Figure 3.10 spectrum and waveform of the modulated optical signal before carrier suppression

The carrier component which is shown at 0 Hz has a very large amplitude and is almost 25 dB higher than the subcarriers. If such a signal is transmitted, it will be wasting a lot of optical power on the optical carrier and the modulation efficiency is low. In addition, the lowest frequency subcarrier channel will be severely interfered

by the strong carrier component. Avoiding this interference requires a very strong frequency selectivity of the receiver optical filter. Therefore it is useful to suppress the carrier component before it is sent out into the optical fiber.

The carrier suppression is done in the same way as we did in the PSK system. Figure 3.11 shows the waveform and spectrum of the optical signal after 35 dB carrier suppression.

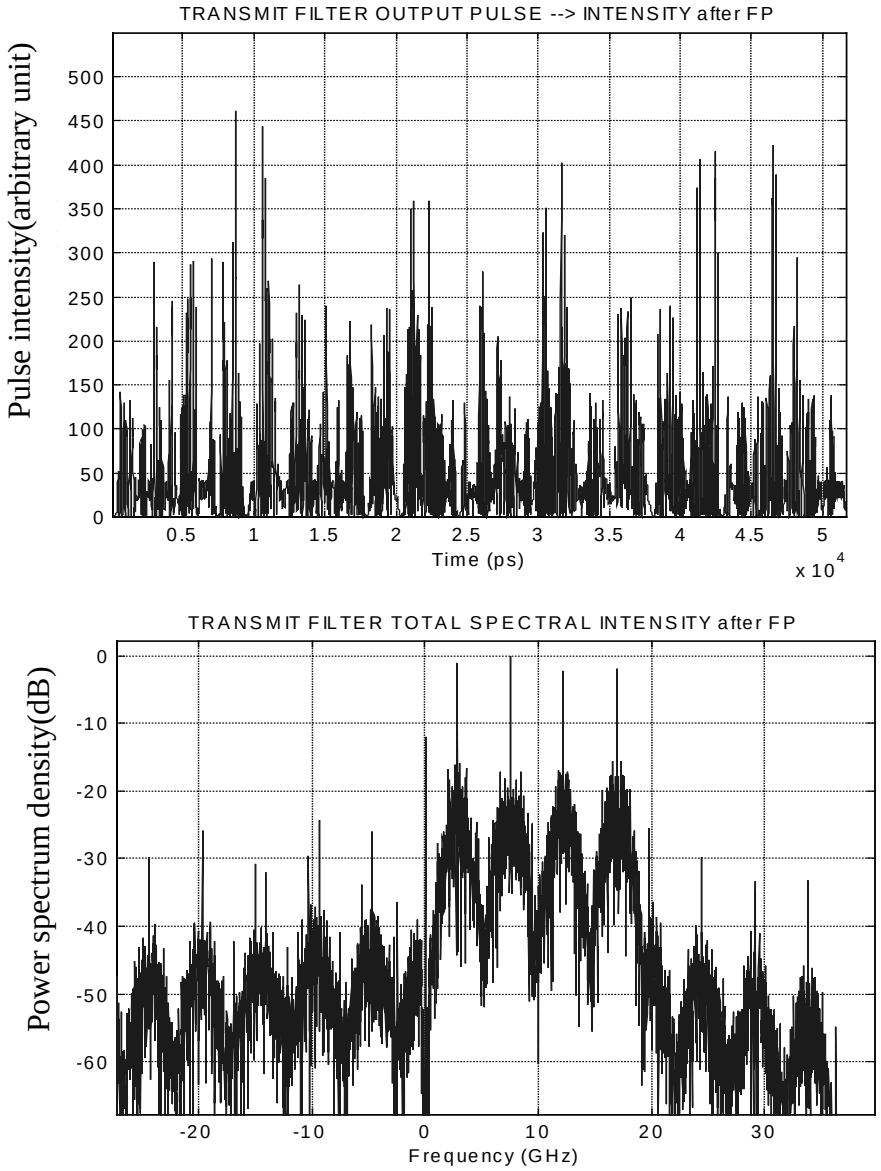

Figure 3.11 spectrum and waveform of the modulated optical signal after carrier suppression

With the carrier suppression implemented, the carrier is almost 10 dB lower than the sub carriers. In order to emphasize the modulation and demodulation procedures, we first look at back-to-back signal performance without passing through any optical fiber.

In the receiver side, the signal is first amplified by a wideband EDFA and then a WDM demultiplexer to separate different wavelength channels. After the WDM DEMUX, a star coupler or splitter has to be used to distribute the optical signal to four narrow bandwidth FP filters each selecting a different subcarrier channel. We should mention here that because the noise and signal has been attenuated by the same amount, so it would not make difference in the sensitivity calculation whether or not the optical filter attenuation is considered. Signal-ASE beat noise is always the dominant noise in the simulation.

In the simulation, we varied the bandwidth of the FP filter by changing the space between the two mirrors of the FP filter. The FSR will then be changed accordingly.

In this particular case, the HPFW of the FP filter is 4GHz which is about 1.6 times the bit rate. Figure 3.12 shows the power and phase transfer function of the filter.

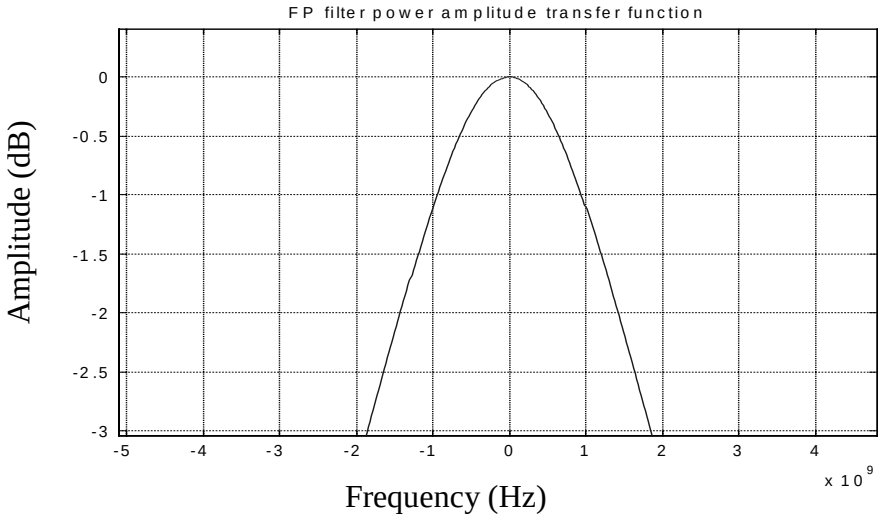

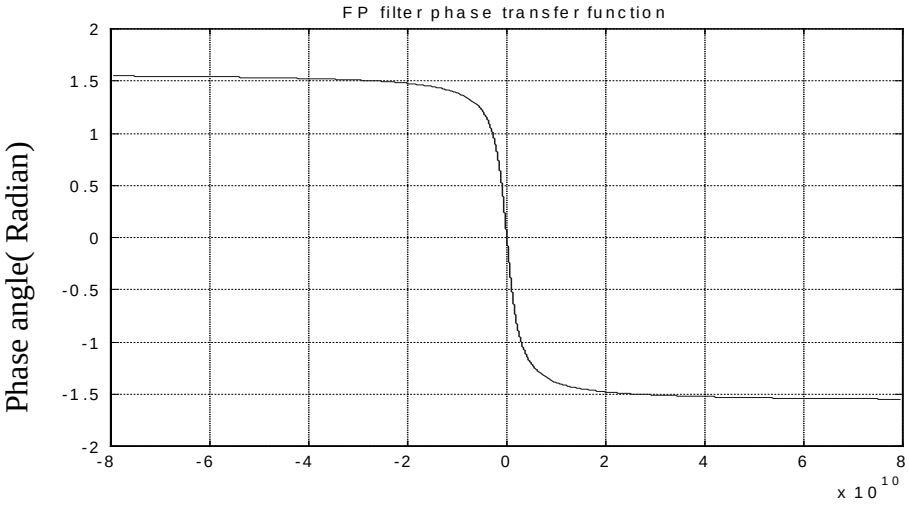

Figure 3.12 Power and phase transfer function of a FP filter

Figure 3.13 is the spectrum and the waveform of the lowest frequency subcarrier channel after the narrowband FP filter. The selectivity of the optical filter is obviously not good. The selected subcarrier is only 10 dB higher than its adjacent subcarrier.

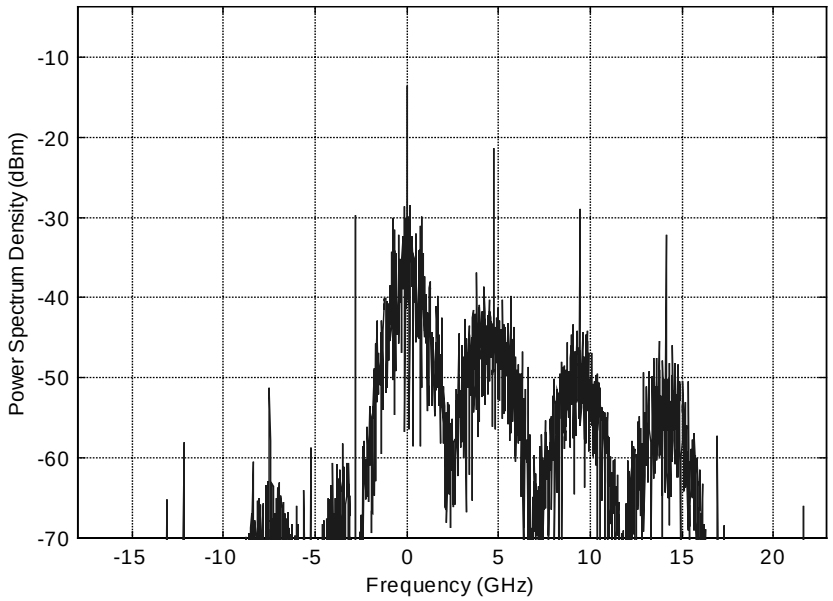

Figure 3.13, spectrum of the signal after the demuxing optical FP filter

Figure 3.14(a) shows electrical spectrum after the O/E conversion. The selected signal power is only about 10 dB higher than the interference channels and therefore the eyediagram has a lot of high frequency components as shown in Figure 3.14(b). The eye seems totally closed. Therefore an additional filtering is necessary to remove high frequency interference.

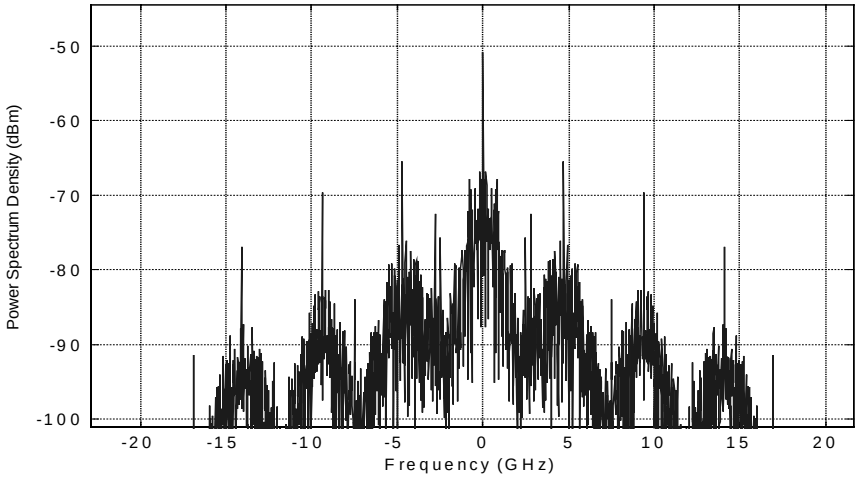

(a)

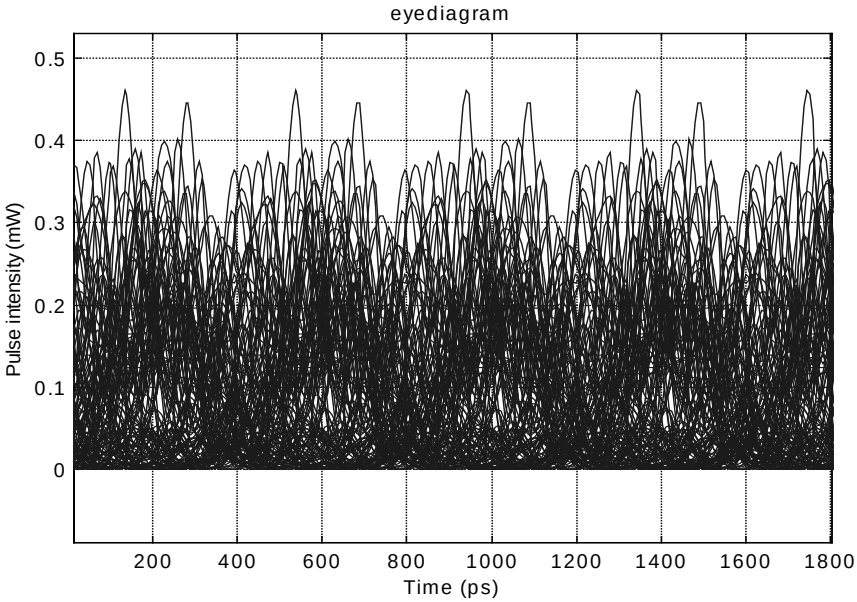

(b)

Figure 3.14, electrical spectrum and eyediagram after the photon diode

To this end we used a baseband electrical filter after the photodiode with bandwidth of 0.7 times the bit rate. It effectively cleans up the eye diagram. Figure 3.15 shows the waveform ,eyediagram and spectrum of the signal after the baseband electrical filter. The electrical filter used here is a 6 order butterworth filter.

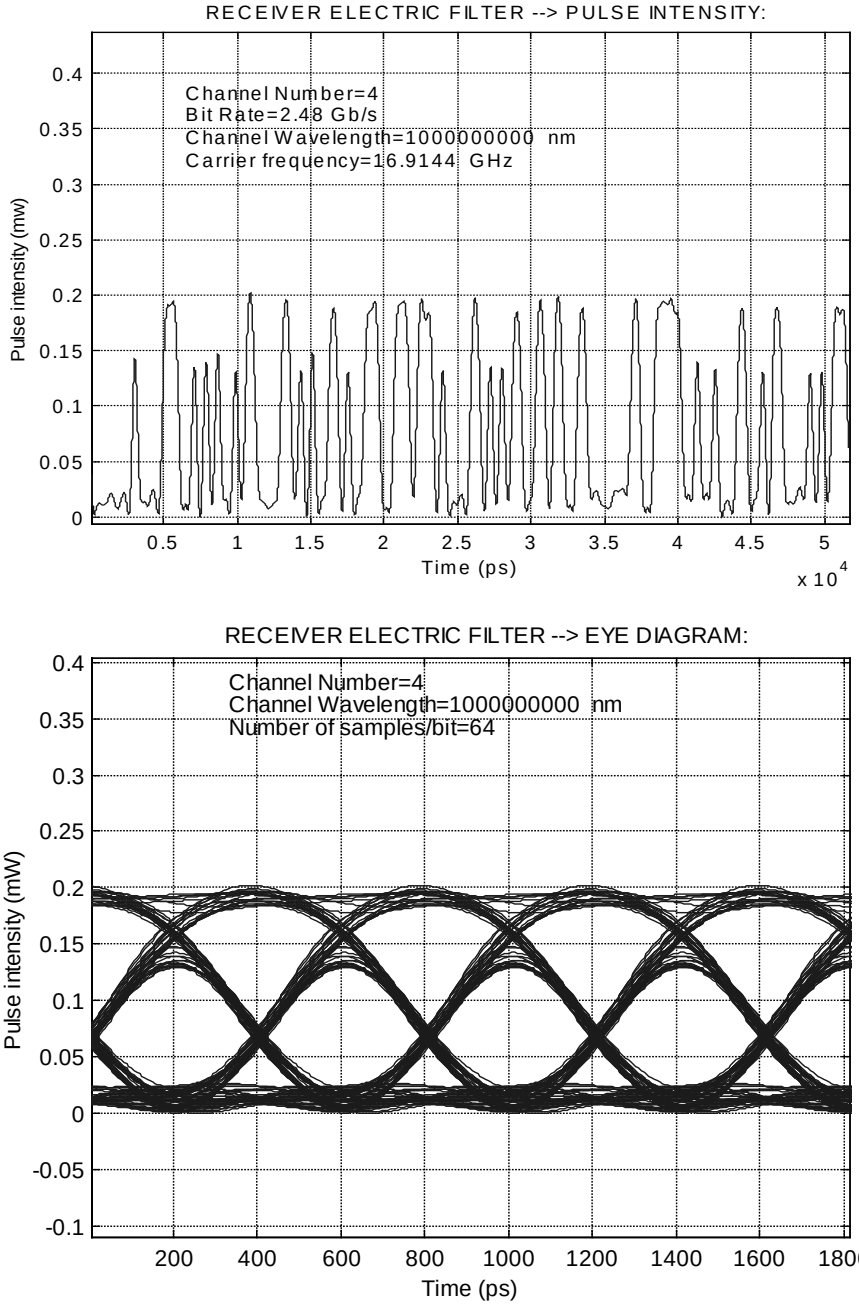

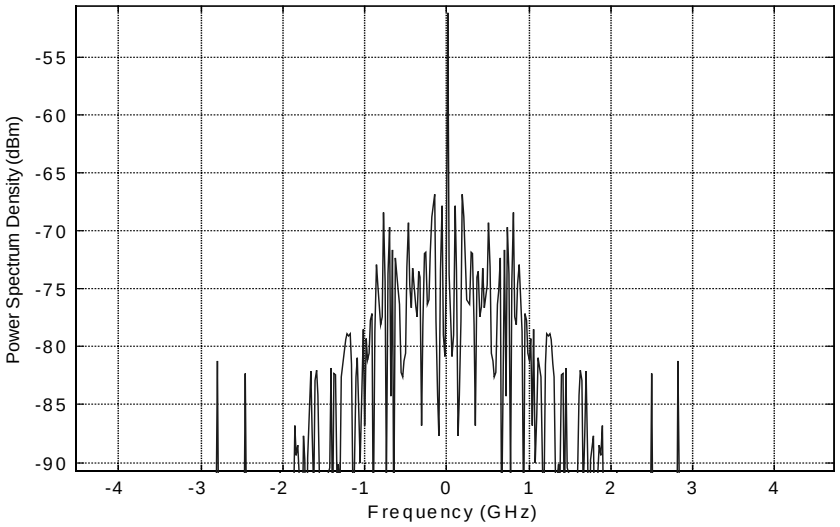

Figure 3.15, waveform, eyediagram and electrical spectrum after the electrical filter

3.3.1 The impact of FP filter bandwidth

The Bandwidth of the FP filter is very critical in such a direct detection receiver using optical filter. If the bandwidth is too large, the interference from adjacent channels will be strong; on the contrary, a small bandwidth will result in signal waveform distortion. In order to find the optimal optical bandwidth, we can vary the bandwidth of the FP filter in the simulation and determine the best bandwidth through sensitivity calculation. Figure 3.16 shows the receiver sensitivity vs the FP filter bandwidth. OMI of 0.3 and 35dB carrier suppression were used in this simulation. The fiber length is 0.

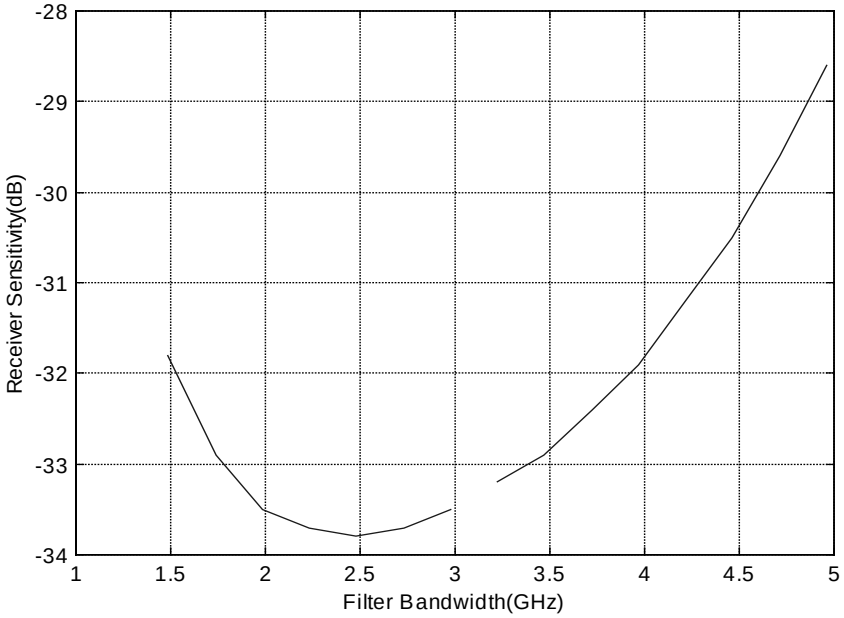

Figure 3.16, sensitivity as the function of FP filter bandwidth

From Figure 3.16 we can see the best receiver sensitivity is achieved when the bandwidth is 2.5 GHz which is exactly the bit rate of the channel.

We also find that the best achievable sensitivity is only –34 dBm by numerical simulation. In the calculation of the SNR for ASK SCM systems, the sig-spon beat noise is proportional to the power of the selected subcarrier tone. The power used to calculate the sensitivity showing in Figure 3.16 is the total power which includes all 4 subcarriers. If the optical power of each subcarrier is used in the calculation, the sensitivity will be about -40 dB. This value is still about 6 dB worse than the theoretical limit of –46 dB which is analytically calculated in chapter 2 for IMDD systems. The discrepancy is partly due to the nonlinearity of MZ modulation and partly due to non-ideal optical filtering and waveform distortion.

3.3.2 Optical modulation index and the suppression ratio.

Because the carrier is absolutely useless in this system, it is desirable to suppress the carrier totally. Similar to what we did in PSK system, we will vary the

carrier suppression and the optical modulation index to make the parameter optimization. Since practically it is difficult to achieve very strong carrier suppression, it is not wise to use too small optical modulation index, we only considered using 0.3,0.4,0.5 as the OMI since high OMI results in small carrier amplitude. Figure 3.17 shows the calculated receiver sensitivity for these three OMI values. The sensitivity reported in Figure 3.17 represent the worst case of four subcarrier channels. In the simulation, all the subcarrier channels have same RF modulation index.

From these three curves shown in Figure 3.17, we can see that as the suppression ratio increases, the sensitivity is improved because of the increase of signal modulation efficiency. If the suppression ratio is smaller than a certain value, the sensitivity will deteriorate dramatically. At very high carrier suppression ratio, sensitivity improvement stops and the curves become flat, where the carrier component is already negligible. In the following simulations, we will use OMI 0.3 with 35 dB carrier suppressions.

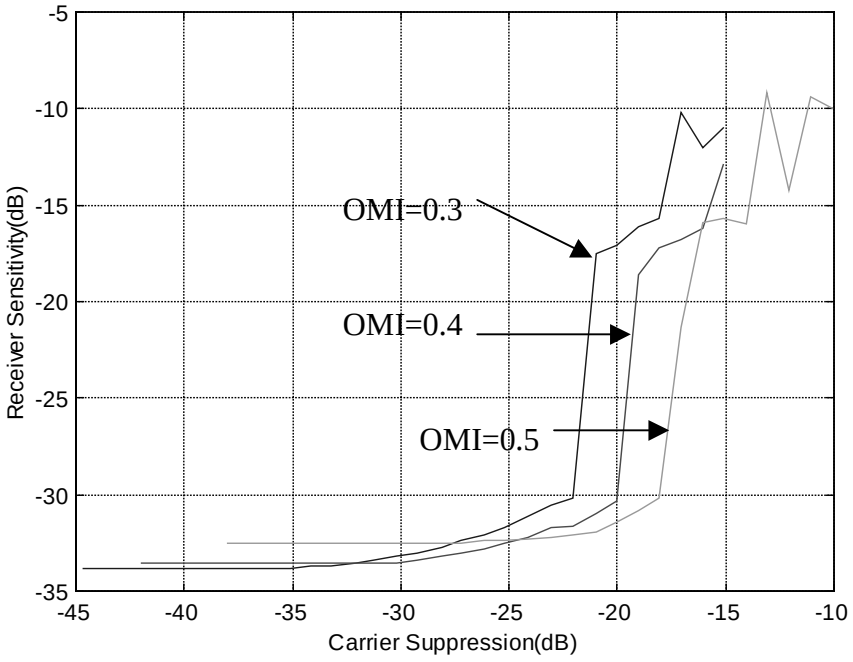

Figure 3.17 sensitivity vs the carrier suppression ratio for different OMI

3.3.3 Effect of optical power

For back to back simulation, the system performance is independent of optical power level because there is no optical fiber. When transmission fiber is introduced, nonlinear effect of the fiber has to be considered and we have to decide the optical power level to be used. We vary the optical power levels and run the simulation for different fiber lengths. The optical powers we used are 5dBm, 3dBm, 0dBm, -3dBm, Figure 3.18 shows the calculated receiver sensitivity versus fiber length at different optical power levels:

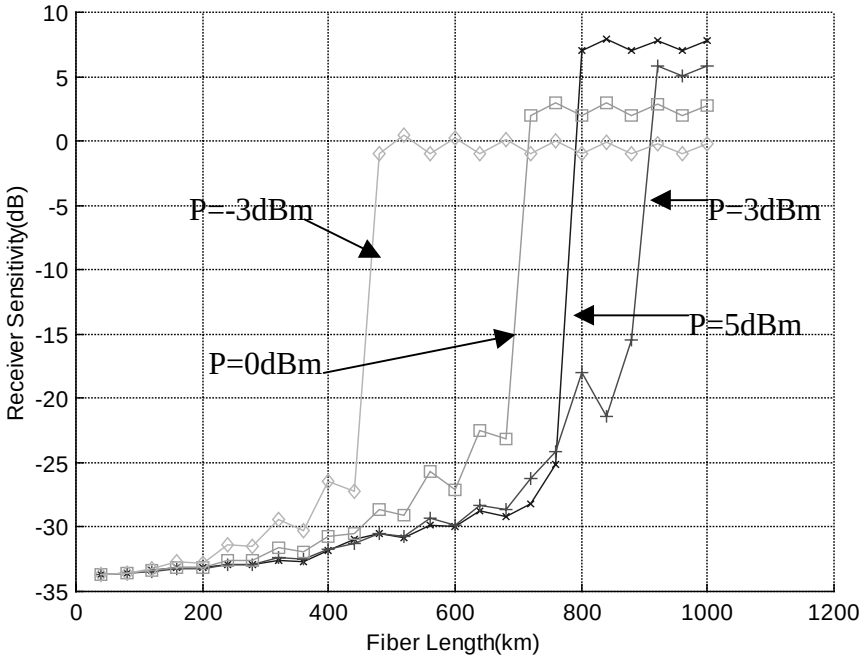

Figure 3.18 sensitivity curves with different optical power

It is obviously that system with optical power of 3dBm has the longest transmission distance which is about 880km. 5dBm is worse than 3dBm because the nonlinearity of the fiber becomes significant which causes waveform distortion of the signal. –3dBm system can transmit less than 440km, that is because the signal noise ratio at receiver is not large enough.

3.3.4 four wavelength system results

In the last section, we have discussed the performance of single wavelength, 4 subcarrier SCM system using direct detection through an optical filter. Now we extend our simulation into multi wavelengths. In a multi-wavelength system, the interference both between wavelengths and between subcarriers in the same wavelength channel have to be considered. Therefore additional performance degradation may be introduced. Table 3.3 summarizes the major results of simulation for a 4 wavelength ASK SCM system. Please see appendix 4 for the corresponding plots.

Due to the nonlinear interference between wavelength channels, the optimum optical power for a multiple wavelength WDM/SCM system is lower than that for a single wavelength SCM system. From table 3.3, we found the dispersion compensation does not help the system performance. This system is not dispersion limited, instead, it is crosstalk noise limited. The longest transmission distance is 550km with 0dBm optical power and no dispersion compensation is used.

DC	OMI	OP(dBm)	RFMI	L(km)
Yes	0.3	3	1 1 1 1	50
Yes	0.3	0	1 1 1 1	200
Yes	0.3	-3	1 1 1 1	250
Yes	0.3	-6	1 1 1 1	250
No	0.3	3	1 1 1 1	250
No	0.3	0	1 1 1 1	550
no	0.3	-3	1 1 1 1	500
No	0.3	-6	1 1 1 1	350

Table 3.3 longest transmission distance for ASK SCM systems with different parameters

3.4 system performance for a traditional four wavelength OC192 system

In order to make comparison, we also did simulations on a traditional four wavelengths ASK OC192 TDM system, the bit rate of each wavelength is 10Gbps. NRZ modulation format was used in this simulation. The result presented here does not consider the PMD effect.

As shown in table 3.4, without dispersion compensation, the transmission distance of a 10Gb/s TDM system is limited to approximately 100km due to the high bit rate. With dispersion compensation, the distance can be 1100 km with the optical power per channel is 0dBm.

DC	OMI	OP(dBm)	L(km)
Yes	0.5	3	950
Yes	0.5	0	1100
Yes	0.5	-3	800
Yes	0.5	-6	500
No	0.5	3	100
No	0.5	0	100
No	0.5	-3	100
No	0.5	-6	100

Table 3.4 longest transmission distance for traditional OC192 systems with different parameters

Chapter Four

BPSK SCM system experiments

In the laboratory, a single-wavelength four-subcarrier BPSK SCM system experiment was conducted. The experiment configuration is shown in figure 4.1.

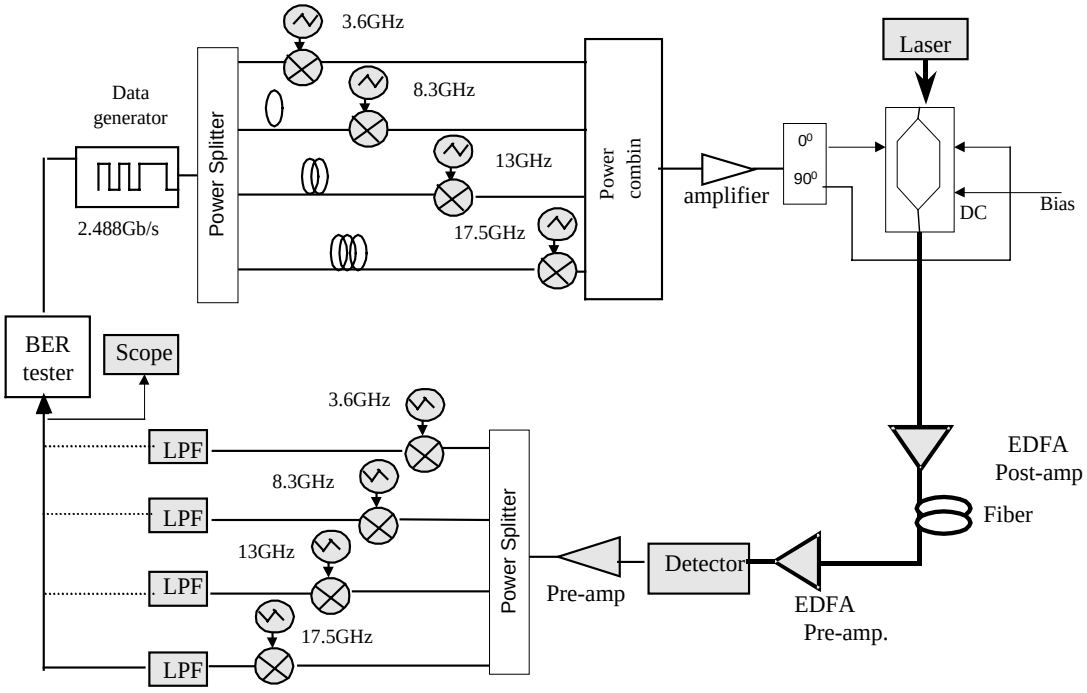

Figure.4.1, Basic configuration of an SCM/WDM optical system

In this setup, the 2.5Gb/s digital signal output from the BERT were split into 4 channels by a microwave power splitter. Then these four channels were delayed each by a different time and then individually mixed with a microwave carrier at 3.6 GHz, 8.3 GHz, 13 GHz and 18 GHz respectively. They were then combined and amplified.

In order to generate optical single-side band signal, the amplified composite RF signal was fed into a 90^o hybrid splitter. One output of this splitter has a 90-degree phase advance than the other output. This hybrid splitter has a frequency bandwidth

of 18GHz. The two outputs of the splitter were applied to the two arms of a dual electrode $LiNbO_3$ Mach-Zehnder modulator with 20 GHz bandwidth. A DC bias was applied to one arm of the MZ modulator and set the modulator at the quadrature operating point.

Figure 4.2 shows the SSB optical spectrum measured by a scanning Fabry-Perot interferometer with 1GHz resolution bandwidth. The carrier is about 15 dB higher than the subcarriers. And the subcarriers only appear on one side of the carrier. The suppression is larger than 15 dB.

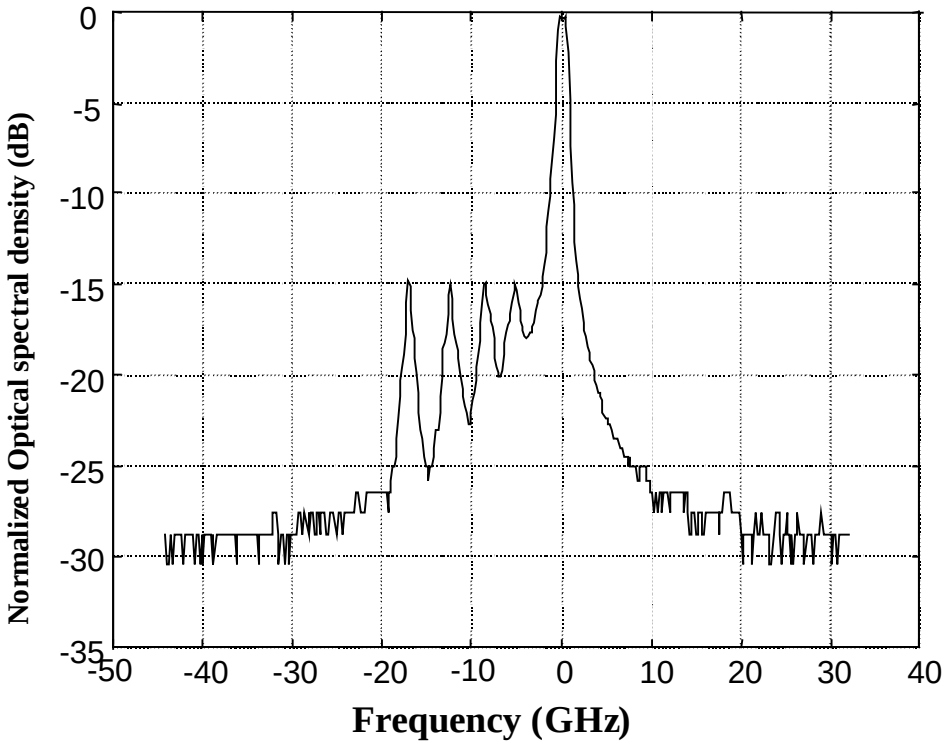

Figure 4.2 spectrum of generated OSSB signal by the MZ modulator

Then the optical signal is amplified by a post optical amplifier and launched into a 75 km strand single mode fiber. At the receiver, the signal is amplified by an EDFA preamplifier and then detected by a high-speed photo diode. The bandwidth of the detector is larger than 20GHz. Figure 4.3 shows the electrical spectrum after O/E conversion.

The signal to noise ratio is larger than 20dB for the high frequency subcarriers, but it is only 15dB for the low frequency subcarrier. This is similar to what we saw in the simulation: lower frequency subcarriers are subject to more distortion.

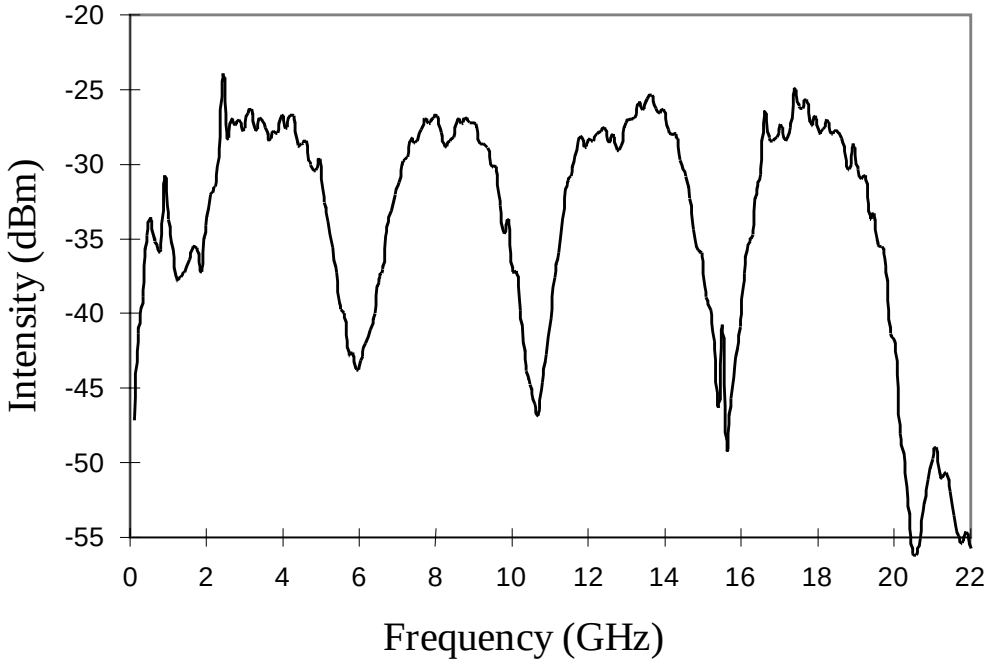

Figure 4.3, Detected composite signal RF spectrum

After photo detection, there is an electrical amplifier where signal is amplified and then split by a power splitter into four ports. The output of each port is mixed with four microwave carriers at 3.6 GHz, 8.3 GHz, 13 GHz and 18 GHz to perform frequency down-conversion. The phase of the local oscillators are adjusted by RF delay lines in order to get maximum signal outputs. Then the demodulated signal is filtered by a 1.75GHz low pass filter. Fig. 4.4 gives an example of the demodulated baseband spectrum.

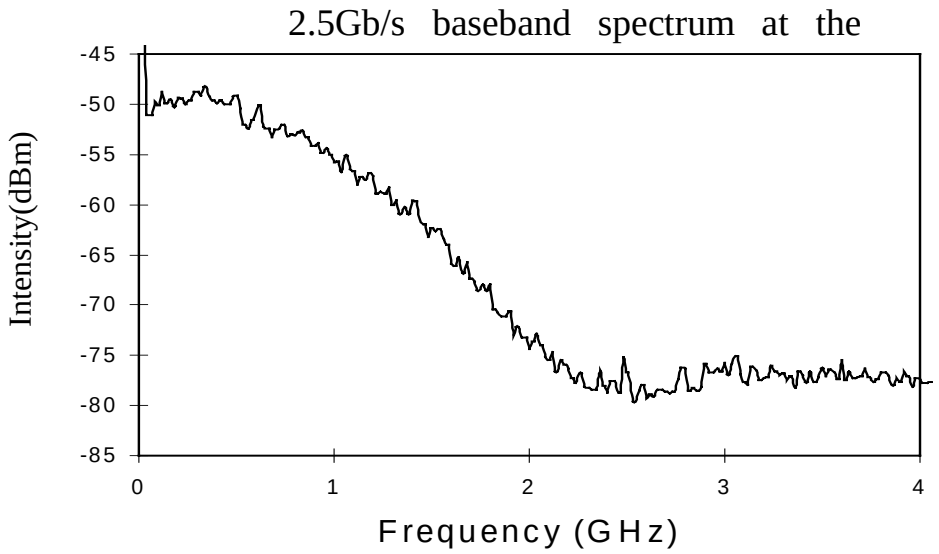

Figure 4.4, electrical spectrum of a baseband signal after demodulation.

Fig. 4.5 shows eyediagrams of all the four-subcarrier channels for both back-to-back (left column) and over 75km SMF (right column). All the eye diagrams were measured at the bit-error rate of 10^{-10}.

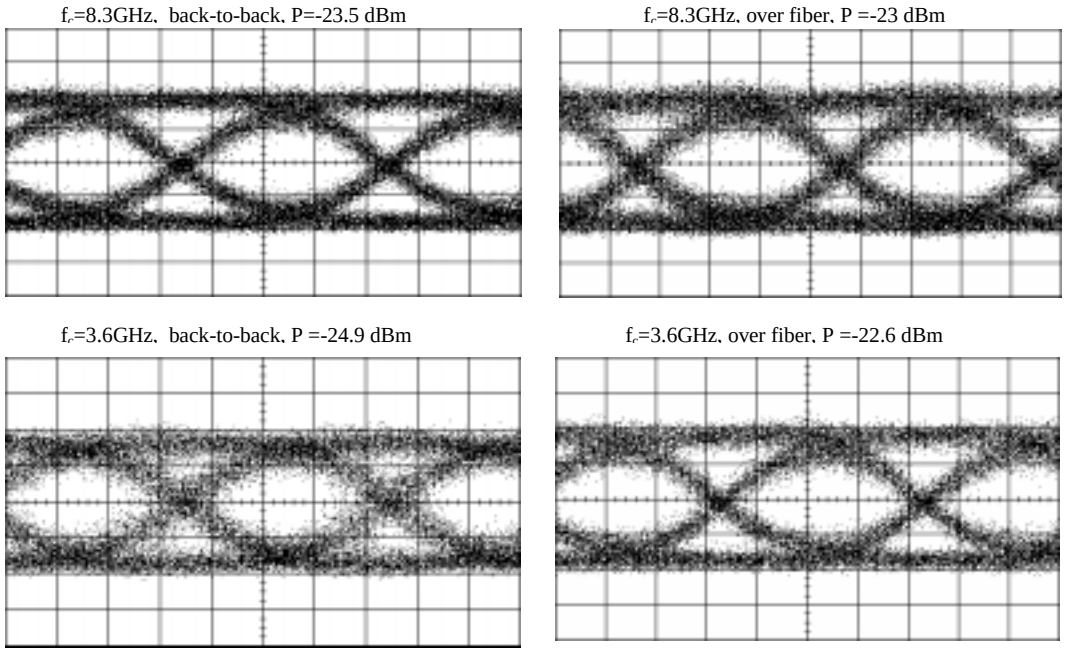

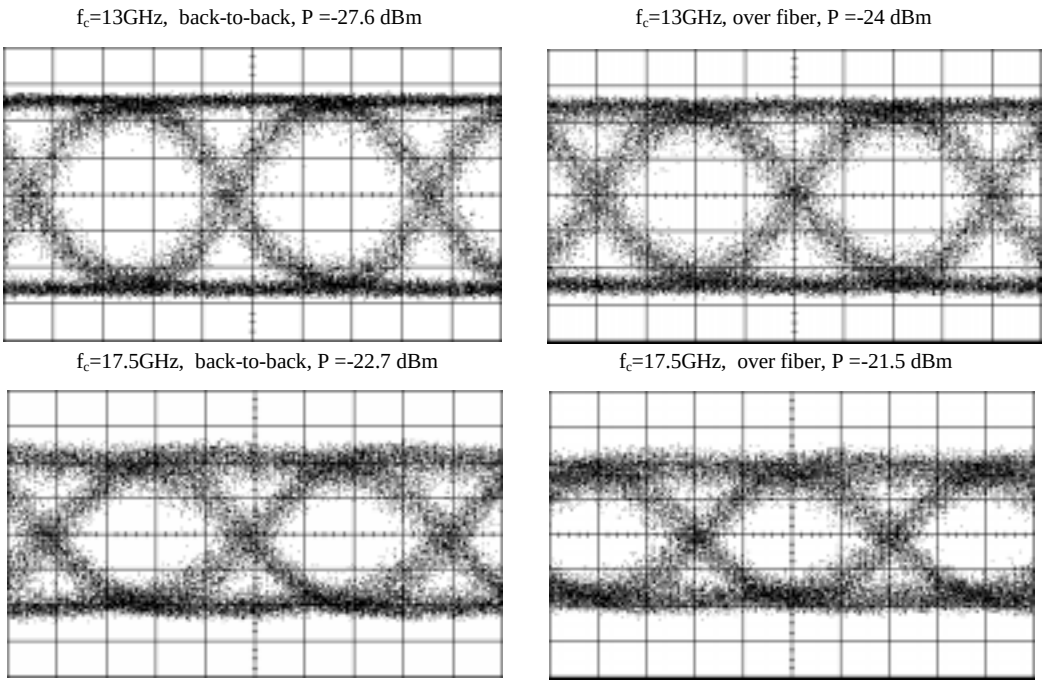

Figure 4.5, Measured eye diagrams of 3.6GHz, 8.3GHz, 13GHz and 17.5GHz channels at the receiver for back/back (left column) and after 75km SMF transmission (right column).

4.1 BER test

Bit error rate measurement was also performed for all four channels for both back-to-back and over 75km standard SMF as shown in Figure 4.6. For back-to-back, the sensitivity (for a BER of 10^{-9}) ranges from –24dBm to –27dBm for different channels mainly due to the ripples in the microwave devices. This value is about 4 to 7 dB less than we found with the simulation, this is mainly attributed to imperfect devices and that the phase of the local oscillator may not be the optimum.

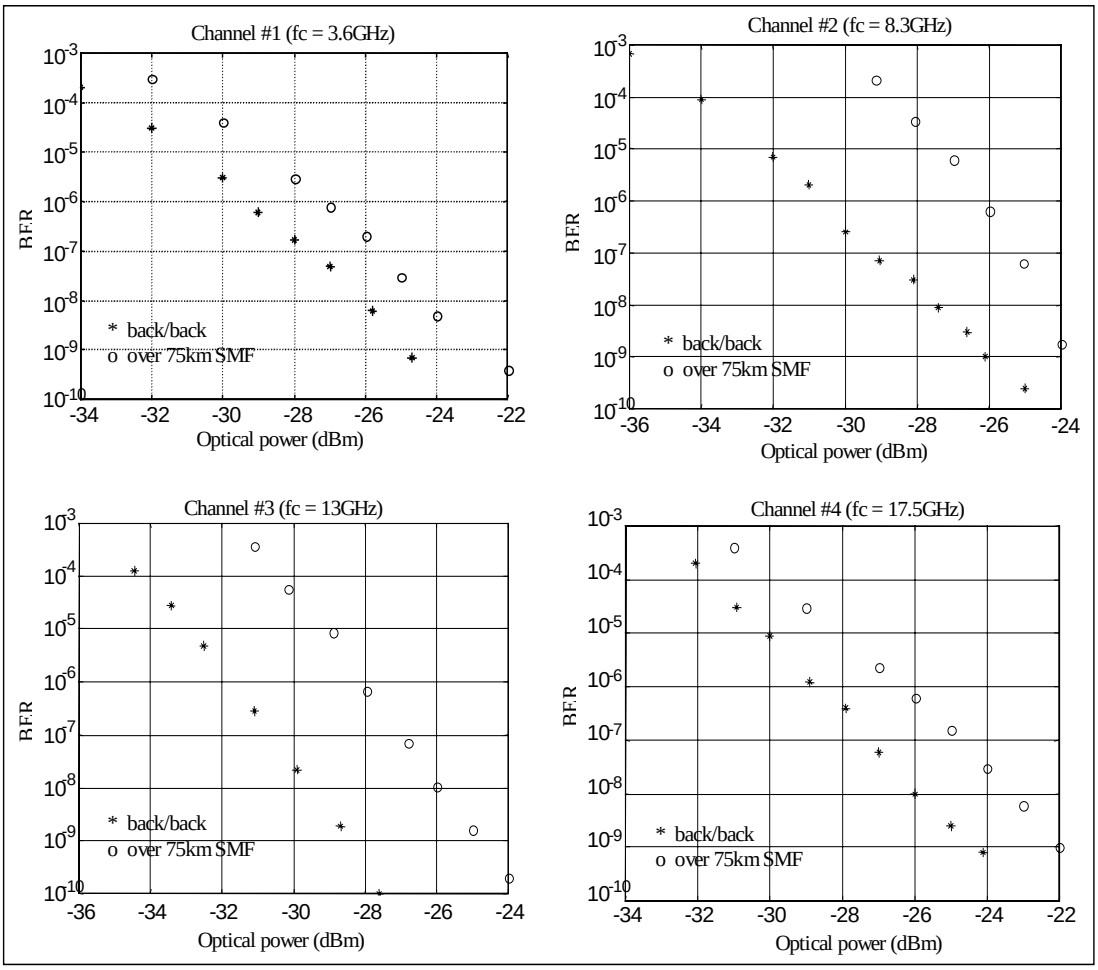

Figure 4.6, Measured BER versus received optical power for all four channels both back-to-back (stars) and over 75km SMF (circles).

After transmission of 75km of SMF, the sensitivity degraded by typically 2dB. The reason for this degradation is partly due to fiber nonlinearity and partly due to the frequency instability of the local oscillators. In our experiment, the same RF oscillators are shared by both the transmitter and the receiver (as local oscillators). A fiber length of 75km corresponds to a time delay of approximately 0.38ms. Over this time delay, the oscillators change their frequency (or phase) due to phase noise. This caused a phase mismatch between RF carriers and local oscillators at the receiver and thus resulted in measurable sensitivity degradations. However, in real commercial systems, this problem can be solved by carrier recovery and phase-locked-loop.

Although special customer designs are generally required for the specific carrier frequencies, both of these microwave techniques are commercially available.

4.2 Channel spacing

In order to pack all the four channels into a 20GHz modulator bandwidth, channel spacing needs to be as narrow as possible. Since each channel carries a 2.5Gb/s traffic, its double side electrical bandwidth is approximately 1.75*2 = 3.5GHz (information bandwidth). Figure 4.7 shows the receiver sensitivity versus channel spacing for a 2 subcarriers system. The minimum channel spacing is found to be about 4.7GHz in our experiment. Below this limit, significant sensitivity degradation cased by inter-channel crosstalk is observed. This minimum channel spacing largely depends on the quality of the baseband filter. A sharp cut off outside the passband is desired to reduce the inter-channel crosstalk and to reduce channel spacing. The reason why this experimentally determined minimum channel spacing number is larger than we got from the simulation is because in the simulation, the electrical filter was ideal which has a sharp cut off outside the passband.

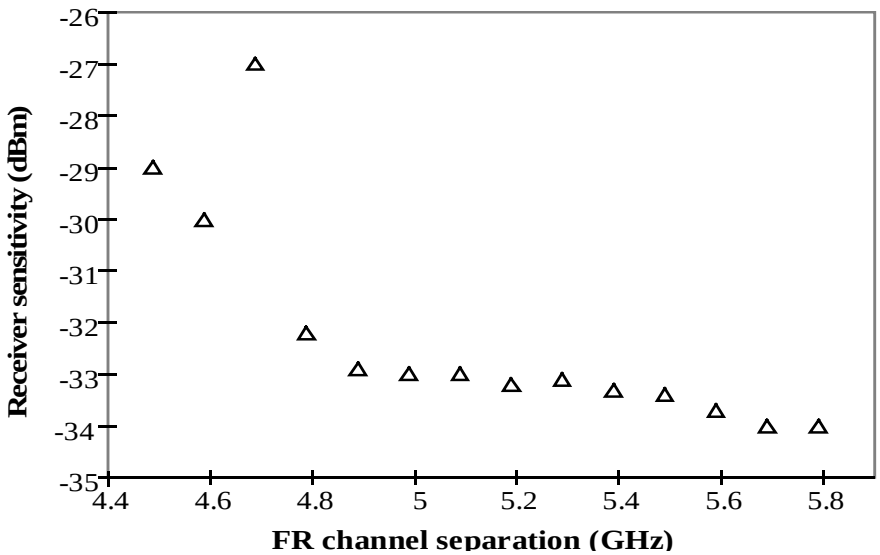

Figure 4.7, Impact of channel spacing on the receiver sensitivity

4.3 Carrier suppression

We also investigated the effect of optical carrier suppression experimentally. Fig.4.8 shows the experimental set-up for carrier suppression. A fabry-Perot Interferometer (FPI) was used as a wavelength dependent reflector and an optical circulator was used to re-direct the optical signal. The wavelength of the FPI was tuned by its electrical bias in order to obtain an appropriate amount of carrier suppression.

As discussed in the chapter 2, receiver sensitivity can be improved by optical carrier suppression approximately on a dB per dB base. Fig.4.9 shows a measured BER plot to demonstrate the effect of carrier suppression. This was performed in a single channel system with the carrier suppression of approximately 5dB. Clearly the receiver sensitivity was improved by approximately 3dB in this case.

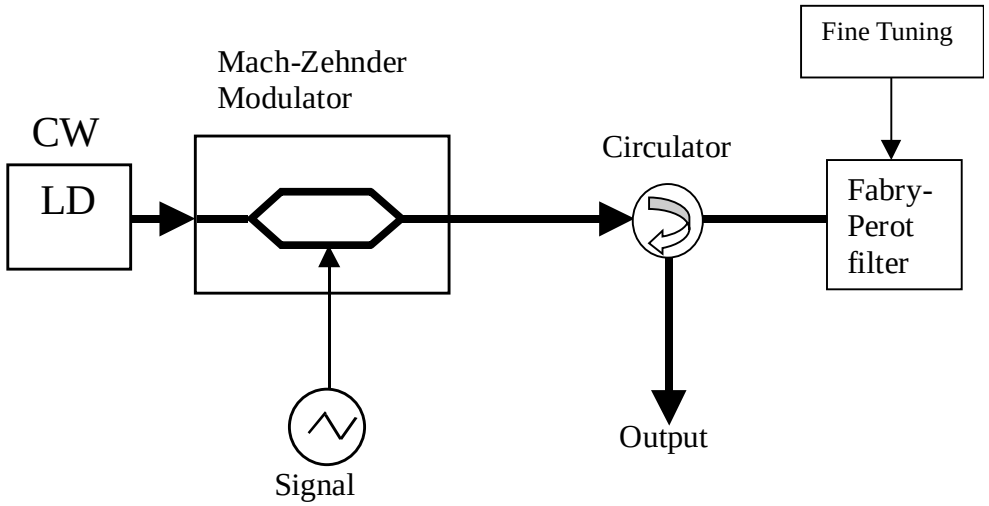

Figure 4.8, Experimental set-up for optical carrier suppression.

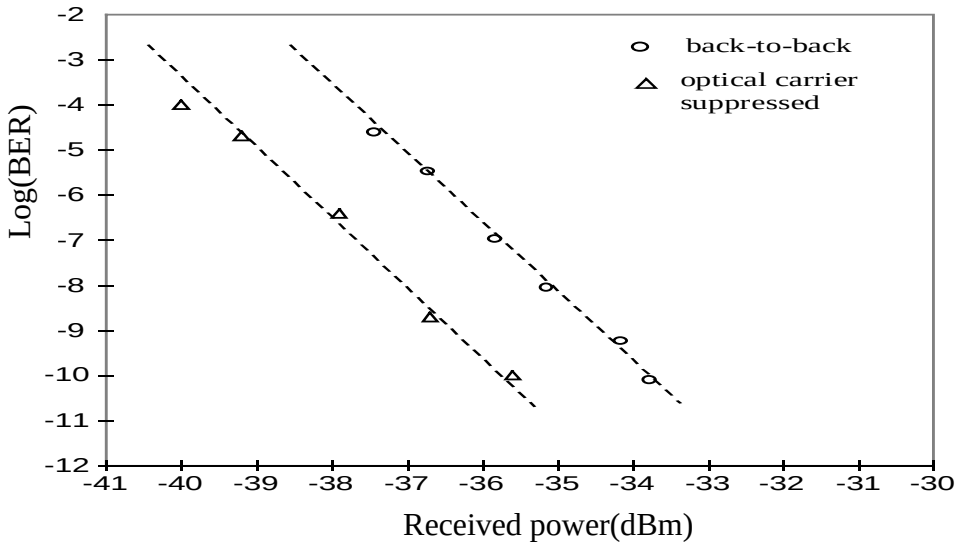

Figure 4.9, Comparison of system performance with and without optical suppression.

The effect of modulation index on the sensitivity improvement due to carrier suppression is demonstrated in Figure 4.10. As the RF power increases, the sensitivity improvement due to carrier suppression is decreased. This is exactly what we saw in the simulation.

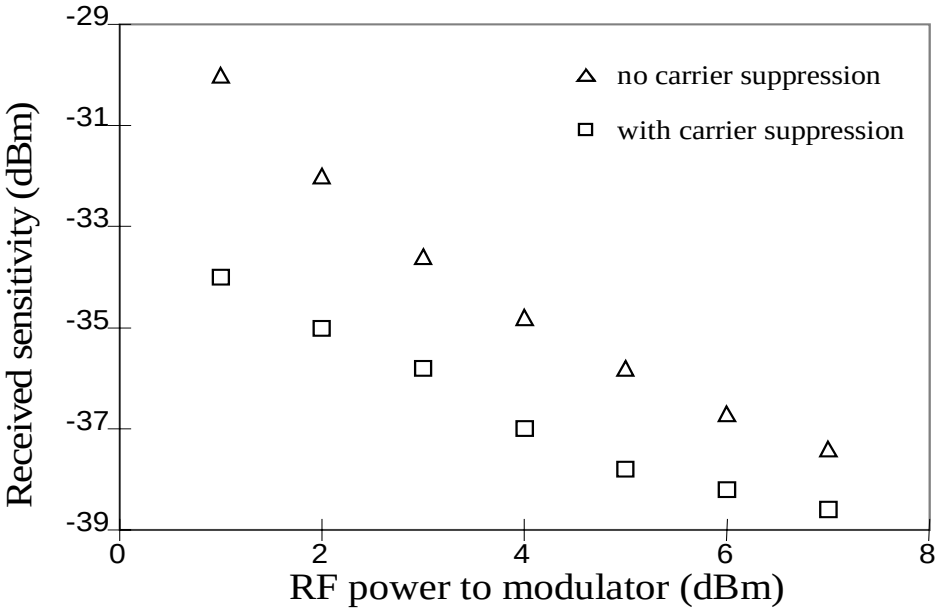

Figure 4.10, Effect of modulation index on the sensitivity improvement due to a 7 dB carrier suppression.

4.4 Comparison between SCM and TDM at OC192 Rates

With standard SMF, chromatic dispersion alone limits the transmission distance of an uncompensated OC192 system to approximately 100km. On the other hand, the dispersion limited transmission distance for an OC48 system is typically 500km with standard SMF. For the reason of comparison, we did a OC192 sensitivity measurement with variable system accumulated dispersion. In the following Fig. 4.11, the curve with solid squares represents the sensitivity of an OC192 system and the curve with triangles represents the sensitivity of a 4-channel OC48 BPSK SCM system.

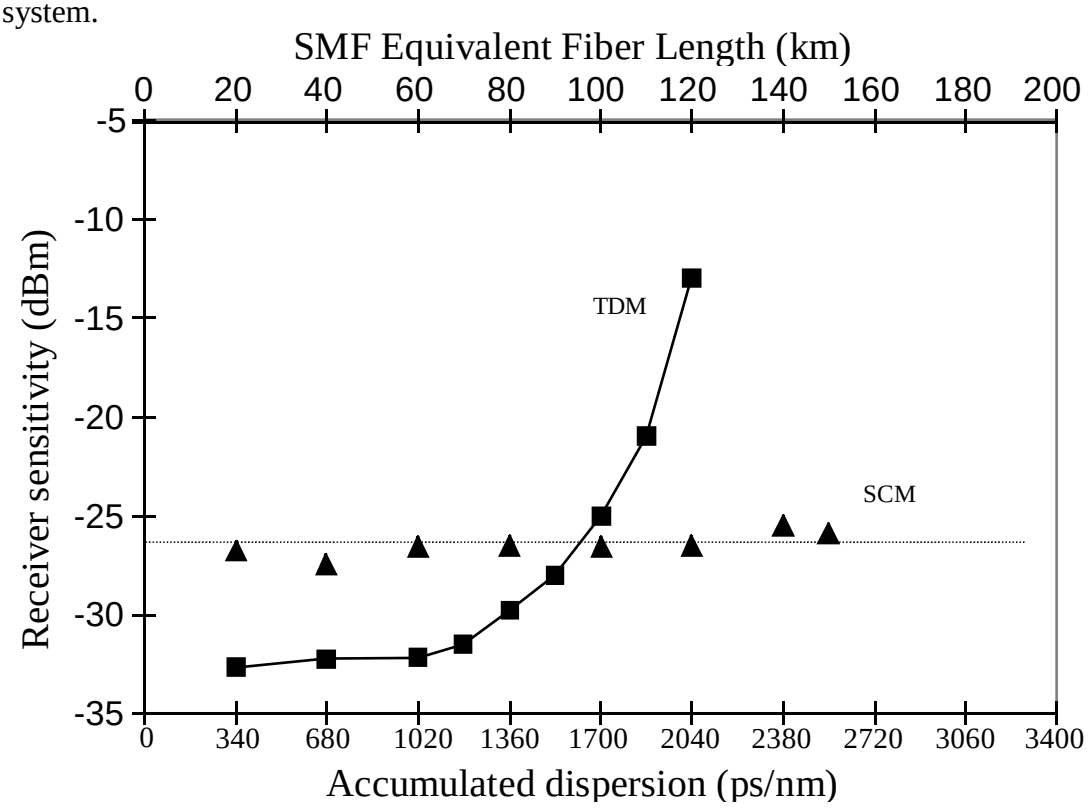

Figure 4.11, sensitivity of traditional OC192 and a 4 channels OC48 BPSK SCM system vs the accumulated dispersion

Due to the limitation of fiber availability, the experiment was performed with negative dispersion DC fibers (dispersion compensating fiber), which have large dispersion values. Assume that the dispersion value for a standard SMF is 17ps/nm/km, we can convert the accumulated dispersion in the experimental system

into an equivalent length of standard SMF. At back-to-back, the sensitivity of the SCM system is about 6dB worse compared to its TDM counterpart. With the accumulated dispersion of higher than 1700ps/nm (corresponds to 100km of SMF), the performance of the TDM system deteriorates rapidly with the increase of the dispersion, while the performance of the SCM system remains unchanged.

Because of the limitation of the fiber availability in the laboratory, we only measured the system with the equivalent SMF length of up to 150km.

Although dispersion induced distortion penalty in TDM systems can be reduced by dispersion compensation, however, attenuation of dispersion compensating module is typically 6 to 8dB for each 80km equivalent SMF span. This attenuation adds to the system link budget. In addition, dispersion compensation increases the cost of system equipment and system design engineering and thus makes systems less flexible.

Chapter Five
Conclusion and future work

In conclusion, we have studied some possible applications of subcarrier multiplexing and optical-single-side-band modulation in transporting high-speed data through standard single mode fiber. The targeted data speed per wavelength is 10Gbps or OC192 speed. Three different types of optical SCM system were simulated and the results are presented by sensitivity and eye opening vs transmission distance. These three types of SCM systems are: 4-subcarrier BPSK SCM system, 2-subcarrier QPSK SCM system, 4-subcarrier ASK SCM system. They all have 4 wavelengths with 10Gbps capacity on each wavelength. The wavelength spacing is 50GHz.

In order to obtain these sensitivity values, for each setup, parameters' optimization are had to be done for optical modulation index, carrier suppression ratio, RF modulation index, channel spacing, frequency allocation, electrical filter bandwidth, and optical filter bandwidth.

We demonstrated that optical carrier suppression is an effective way to improve the receiver sensitivity when the modulation index is relatively low and it can improve system performance by reducing the nonlinearity of the modulation process.

We discussed the impact of PMD effect and considered 2 effects: PMD-induced polarization walkoff and PMD-induced waveform distortion. We considered the first effect in our simulation and estimated the second effect, analytically.

We simulated the system performance for different optical power levels in order to find the optimal optical power range for each system configuration. We selected two different PMD coefficients of optical fibers and investigated the compact of dispersion compensation. Table 5.1 below gives the transmission distance limit for each type of system.

System type	Dispersion Compensation	PMD coefficient $ps/\sqrt{km}$	Distance limit (km)	Power range (dBm)
BPSK SCM	DC	0.1	450	5dBm
BPSK SCM	No DC	0.1	350	0 to 3dBm
BPSK SCM	DC	0.5	350	3 to 5dBm
BPSK SCM	No DC	0.5	300	0 dBm
QPSK SCM	DC	0.1	1200	3 to 5 dBm
QPSK SCM	No DC	0.1	450	3 dBm
QPSK SCM	DC	0.5	750	3 to 5 dBm
QPSK SCM	No DC	0.5	450	3 to 5 dBm
ASK SCM	DC	0.1	250	-3 to –6dBm
ASK SCM	No DC	0.1	550	-3 to 0dBm
OC192	DC	0.1	1100	0 dBm
OC192	No DC	0.1	100	-6 to 3dBm

Table 5.1, Transmission distance limit for different type of systems

From the simulation, BPSK system is most suitable for applications within 300 to 350 km with no dispersion compensation. QPSK system is suitable for application up to 750 km with dispersion compensation and 450 without dispersion compensation. ASK system is not recommended because the maximum distance is only 550 km while the narrow band optical fiber is very difficult to implement and stabilize.

In addition to numerical simulations, we have demonstrated a four-channel digital SCM system with the aggregated capacity of 10Gb/s. Compare to TDM OC192 systems, this SCM system is less sensitive to chromatic dispersion. Also it is more flexible in terms of channel add/drop.

Through this extensive study, we believe that to upgrade optical systems from OC48 rate to OC192, sub-carrier multiplexing is feasible and practical. SCM has

several advantages over TDM as mentioned above, especially in systems with standard single mode fibers.

Future work

Recently, some WDM system vendors are starting to use a channels spacing of 6.25 GHz for OC48 channel and they are using Raman amplification to reduce the noise and optical power and thus reduced the nonlinearities. From the simulation results, we found that when optical power is small, the SCM system would not incur much distortion even after long distance transmission. It is only limited by ASE noise. So SCM system also can be used with Raman amplification and with a small optical power. It can reduce the number of optical sources in the system. It would be interesting to see the system performance with Raman amplification.

Multilevel signal such as QAM could be used to further increase the spectrum efficiency. Microwave single sideband modulation could also be used for this purpose. And it is very likely that they will have good application in short distance applications.

The PMD effect is only estimated in this study. Detailed analysis of PMD effect is necessary and it should be implemented into the simulation in order to get more accurate result.

From the simulation, we found single wavelength SCM system has much better performance than a same type four wavelengths SCM system. We need setup up a multi-wavelength SCM test bed in the laboratory and verify it experimentally. Experimental investigation of QPSK and M-ary SCM may also be necessary.

References

1. Paul D. Sargis etc. 10Gb/s subcarrier multiplexed transmission over 490km of ordinary single mode fiber without dispersion compensation., IEEE PTL, Dec,1997
2. Anthony P. Foord etc, Optical demultiplexing for subcarrier multiplexed systems, IEEE Transactions on Microwave theory and techniques. 2324-2329,1995,9
3. P.M. Hill etc. ,8 Gb/s subcarrier multiplexed coherent lightwave system, IEEE PTL, Aug,1991
4. Bandwidth efficient transmission of 4Gb/s on two microwave QPSK subcarriers over a 48 km optical link, IEEE PTL, july, 1990
5. P.D. Sargis etc. Dispersion reduction technique using subcarrier multiplexing. Proc. SPIE. Oct. 1995. Vol. 2614, pp 244-251
6. Subcarrier multiplexing with dispersion reduction and direct detection. EL, Sept. 28, 1995
7. Javier Marti etc, modeling optically prefiltered AM Subcarrier Multiplexed systems, IEEE Transactions on Microwave theory and techniques. 2249-2256,1993,9
8. Anthony P. Foord, optical demultiplexing for subcarrier multiplexed system, IEEE Transactions on Microwave theory and techniques. 2324-2329,1995,9
9. Mike Sieben, Jan Conradi, Optical single sideband transmission at 10 Gb/s using only electrical dispersion compensation. JLT, OCT. 1999
10. Moshe Nazarathy, etc. Progress in externally modulated AM CATV transmission systems, JLT, Jan. 1993
11. M.R. Phillips etc. Nonlinear distortion generated by dispersive transmission of chirped intensity modulated signals PTL, May, 1991
12. M.C. Wu etc. CSO distortions due to the combined effects of self and external phase modulation, OFC 96, TuP1-1
13. Sen Lin Zhang etc. Assessment of the nonlinearity tolerance of different modulation schemes for millimeter wave fiber radio systems using MZ modulators, IEEE Transactions on Microwave theory and techniques. Aug, 1997
14. G. P. Agrawal, Nonlinear Fiber optics. New York: Academic, 1995
15. G. P. Agrawal, Fiber communication systems. John wiley &sons, 1997

16. L.W. Couch II, Digital and analog communication systems, Prentice Hall, 1997
17. Michel C. Jeruchim etc. Simulation of communication systems.
18. P. Kaminow etc. optical fiber telecommunications. IIIA, Academic, 1997
19. F.S.Yang etc., Nonlinear crosstalk and SBS reduction by carrier suppression in SCM-WDM optical communication system, OFC99

Appendix 1

Some considerations for the simulation of communications system

Low pass equivalent signals and systems

The signal in this simulation is represented by the complex envelope of the real signal. Below is some explanation.

Computer simulation of communications signal and systems are always being done in the sampled or digital domain. Because a continuous signal is uniquely represented by a discrete model only if that the sampling frequency is at least twice the highest frequency in the signal spectrum. So Because the optical frequency is so high, you can not sample the signal directly, even for one bit of signal of a OC48 channel, direct sampling will generate more than 7.7e4 samples, you have to find a equivalent way to simulate the signal with much less sampling rate,

One technique is the so-called complex envelope method, which makes use of the concepts of low pass equivalent signals and systems.

For any carrier modulated signal $x(t)$, if the signal bandwidth is much less than the carrier frequency, we can write

$x(t) = \mathrm{Re}[r(t)e^{j\phi(t)}e^{j\omega_c t}]$, here $r(t)$ is the amplitude modulation and $\phi(t)$ is the phase modulation of the signal. And ω_c is the carrier frequency

$r(t)e^{j\phi(t)}$ contains all of the information related variations and has low pass nature. It is often called the complex envelope or complex low pass equivalent of the signal. For optical signal, the bandwidth of the signal is always much less than the carrier frequency and thus can be written into this format.

For a LTI (linear time invariant) system, the system output for an input $x(t)$ is

$y(t) = x(t) * h(t)$, $h(t)$ is the impulse response of the system. It can be proved that we also have $y_L(t) = \frac{1}{2} x_L(t) * h_L(t)$, the suffix L represent the low pass equivalent signal. And we have $y(t) = \mathrm{Re}[y_L(t) e^{j\omega_c t}]$

This is to say that the processing and transmission of the bandpass signal can be evaluated through its low pass envelope. So the whole simulation can be done with this complex envelope if the system is LTI. In our program, we represent the microwave signal with its directly sampled signal. When it is goes to the optical domain, we will use complex envelope for that optical signal. the transform is done at the optical modulator and detector.

Power relationship of complex envelope and the real signal

Because we use complex envelope in the simulation, we have to know the power relationship of complex envelope and the real signal. it is very important for the calculation of the sensitivity.

For a passband signal $s(t) = x(t)\cos(\omega_c t + \phi) - y(t)\sin(\omega_c t + \phi)$. Its time averaged power is $\frac{1}{2} Avg[x^2(t)] + \frac{1}{2} Avg[y^2(t)]$. The complex signal of the signal is $z(t) = x(t) + jy(t)$, time averaged power in the envelope is $Avg[x^2(t) + y^2(t)]$ and it is two times the power of the real passband signal. In the simulation , you should be very careful about this.

Power spectrum (PSD) estimation

If a random process is ergodic, it can be shown that its PSD can be defined in terms of a time average as

$$S_{xx}(f) = \lim_{M->\infty} E\{\frac{1}{(2M+1)dT} | dT \sum_{n=-M}^{M} x(n) \exp(-j2\pi fndT) |^2\}$$

If we eliminate the limiting operation by assuming a finite data set of N samples for $x(n)$ and eliminates the expectation operation by restricting our attention to a single sample function, it becomes $S_{xx}(f) = \frac{dT}{N} |\sum_{n=0}^{N-1} x(n) \exp(-j2\pi fndT)|^2\}$.

If we let f ->k, dT->1/N, then we have

$$S_{xx}(k) = \frac{1}{N^2} |\sum_{n=0}^{N-1} x(n) \exp(-j2\pi kn/N)|^2 = \frac{1}{N^2} |\, fft(x(n))|^2 \ .$$

Estimating the sampling rate for nonlinear systems

The SCM system is not a strict linear system. The optical fiber and the photon detector are not linear at all. We should know that the spectrum of the output of a nonlinear system does not generally have the same frequency components as the input. The processing of a band-limited baseband signal by a nonlinear system will increases the bandwidth greatly.

If we expand the output into a power series, it is easy to show if the input is limited to the bandwidth B, the output is limited to $n*B$, n is the highest order in the series

In practical, we don't have to use $n*B$ because the small coefficient of those high order terms, another reason is a phenomenon called self concentration which means the resulted spectrum will concentrated around the input spectrum in most nonlinear system. But some increase in sampling rate will be required to keep the aliasing error at an acceptably low level.

Filtering: Butterworth and Bessel filter

Bessel filters are a class of all pole filters that are characterized by the system function $H(s) = 1/B_N(s)$, where $B_N(s)$ is the N th-order Bessel polynomial. These polynomials can be expressed in the form.

$B_N(s) = \sum_{k=0}^{N} a_k s^k$, where the coefficients a_k are given as

$a_k = \frac{(2N-k)!}{2^{N-k} k!(N-k)!}$, $k = 0,1,....,N$,

alternatively the Bessel polynomials may be generated recursively form the relation $B_N(s) = (2N-1)B_{N-1}(s) + s^2 B_{N-2}(s)$, with $B_0(s) = 1$ and $B_1(s) = s+1$ as initial conditions.

You have to find the 3 dB frequency first and then translate the filter into your desired frequency.

An important characteristic of Bessel filters is the linear phase response over the passband of the filter.

The expression of Butterworth filter is $H(f) = 1/\sqrt{1+(f/f_{3dB})^{2*m}}$. m is the order of the Butterworth filter, f3db is the 3 dB bandwidth of the filter. Butterworth filter usually have a narrower transition bandwidth compared to the Bessel filter

Appendix 2 : BPSK SCM results

In the titles of following plots, DC means 100% dispersion compensation, CS means subcarriers suppression, the parameters from left to right are dispersion compensation, PMD coefficient, optical power of each wavelength, frequency of first subcarrier, optical modulation index and carrier suppression ratio. In appendix 3,4 and 5 , we will use the same abbreviation.

1. DC, 0.1 $ps/\sqrt{km}$ PMD, 5dBm, 2.6GHz, 0.3 and 5 dB CS

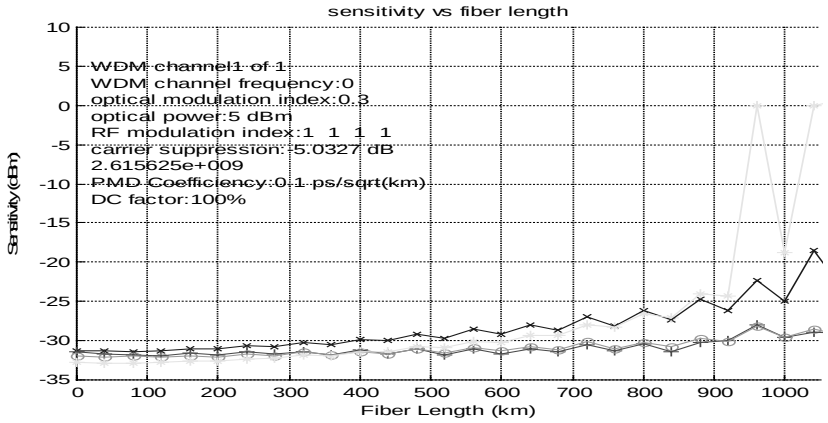

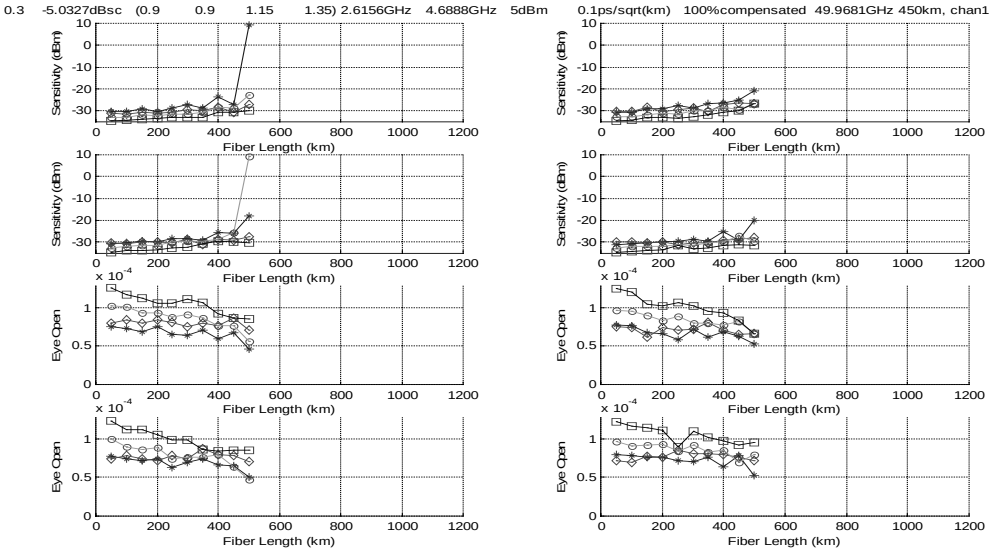

2. DC, 0.1 $ps/\sqrt{km}$ PMD, 5dBm, 2.6GHz, 0.4 and 0 dB CS

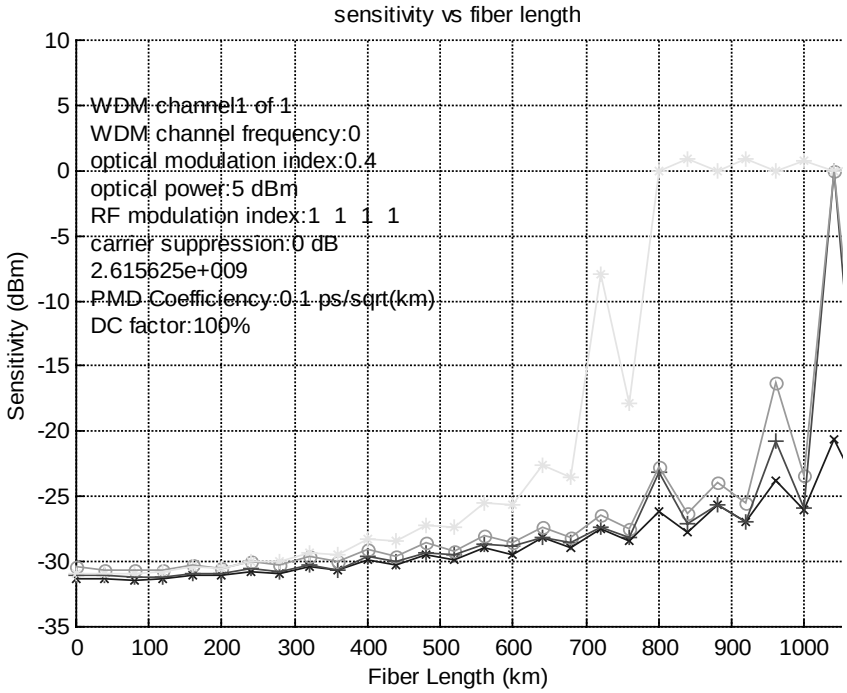

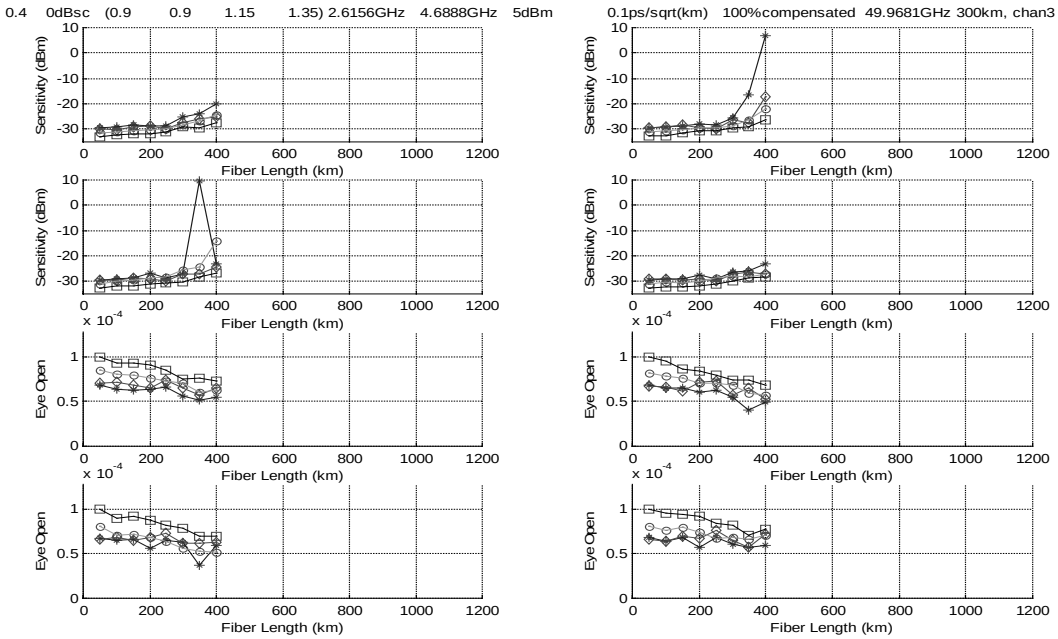

3. DC, 0.1 $ps/\sqrt{km}$ PMD, 3dBm, 2.6GHz, 0.3 and 5 dB CS

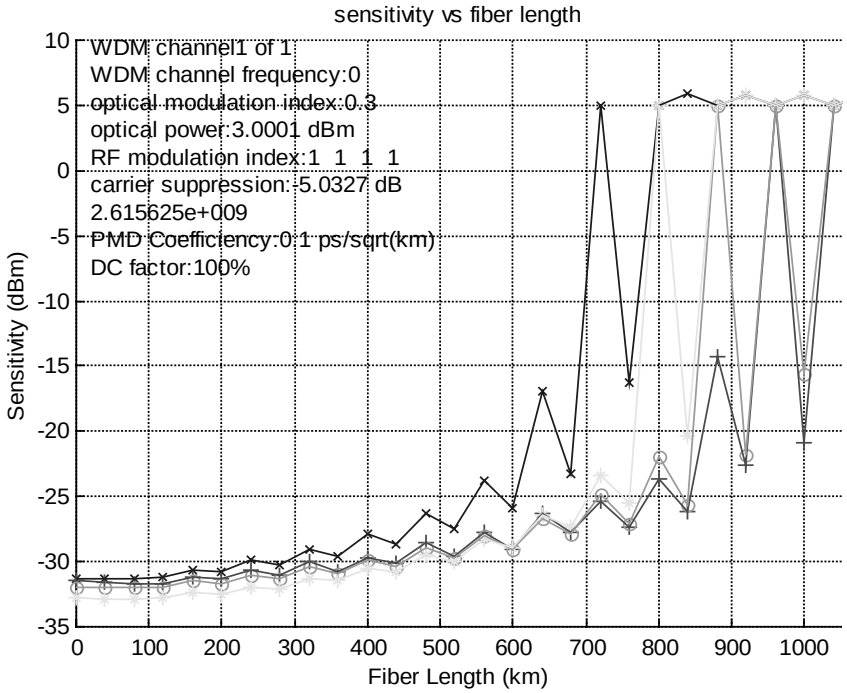

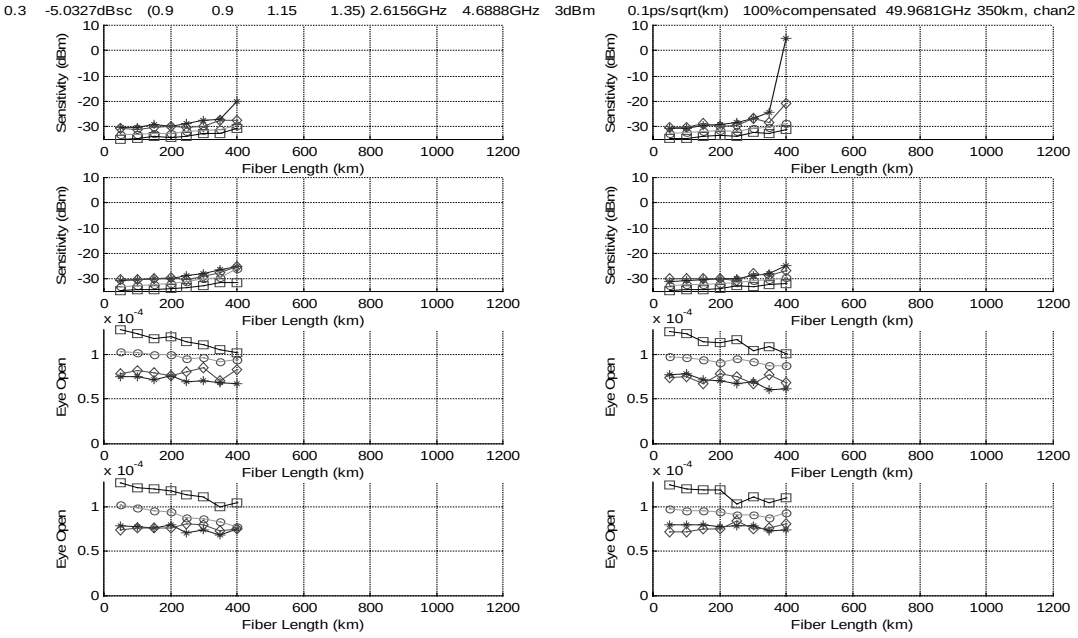

4. DC, 4. 0.1 $ps/\sqrt{km}$ PMD, 3dBm, 2.6GHz, 0.4 and 0 dB CS

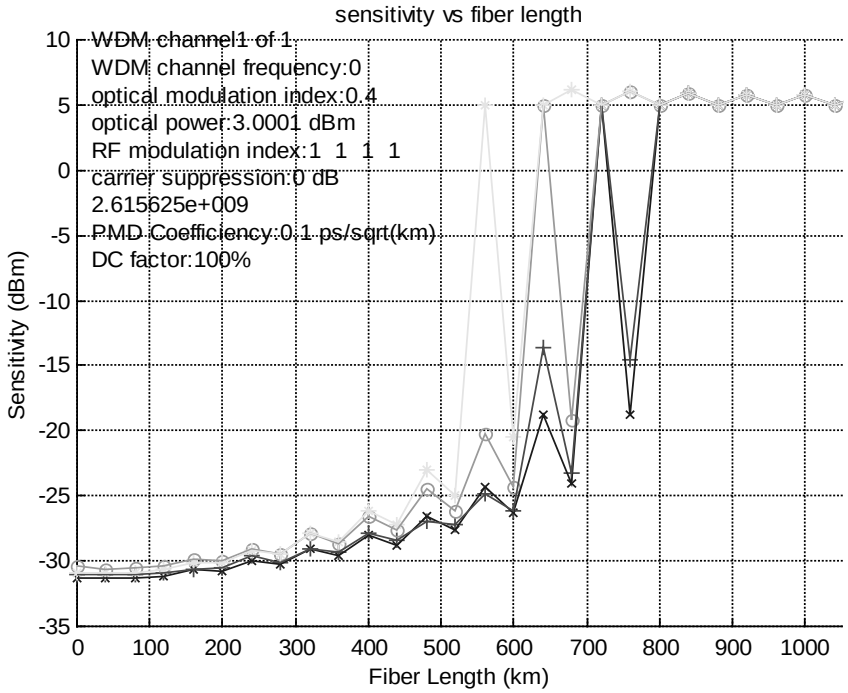

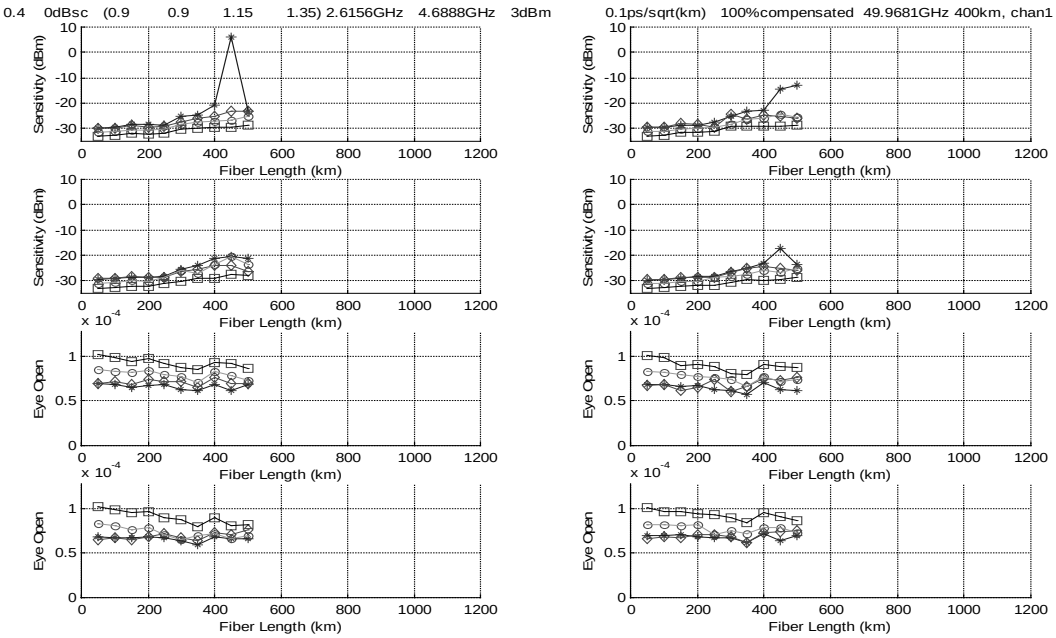

5. DC, 0.1 $ps/\sqrt{km}$ PMD, 0dBm, 2.6GHz, 0.3 and 5 dB CS

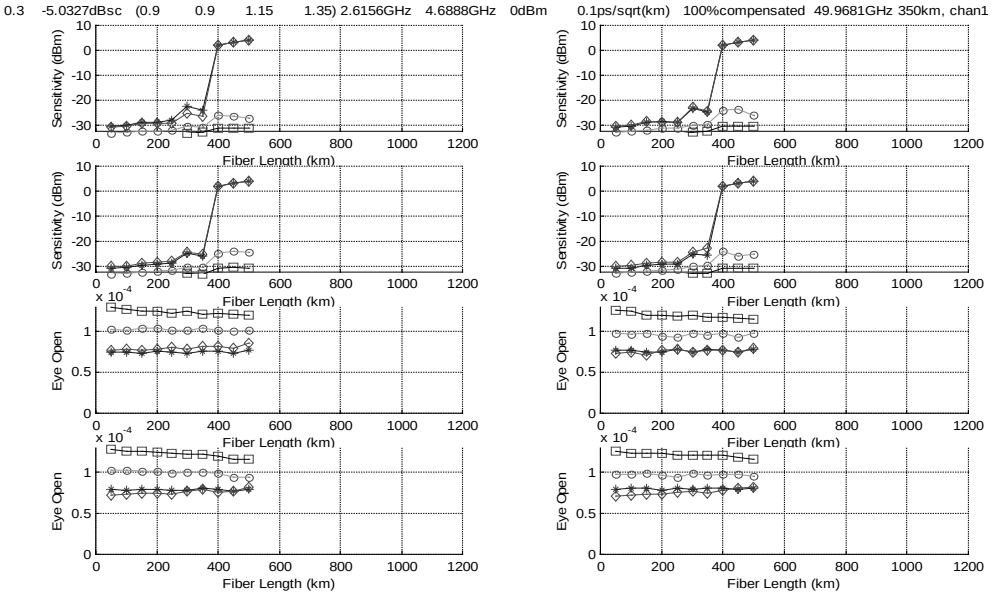

6. No DC, 0.1 $ps/\sqrt{km}$ PMD, 5dBm, 2.6GHz, 0.3 and 5 dB CS

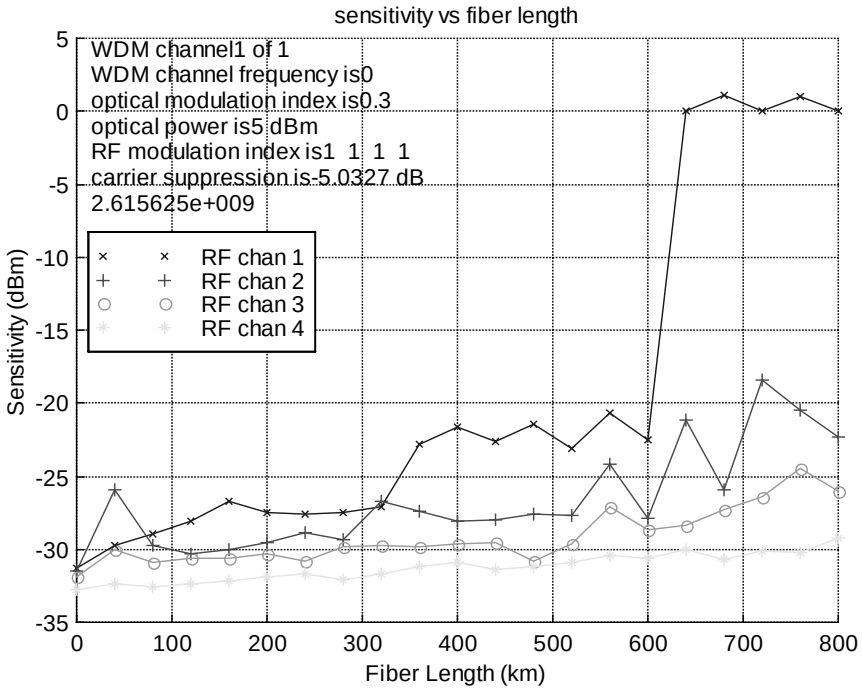

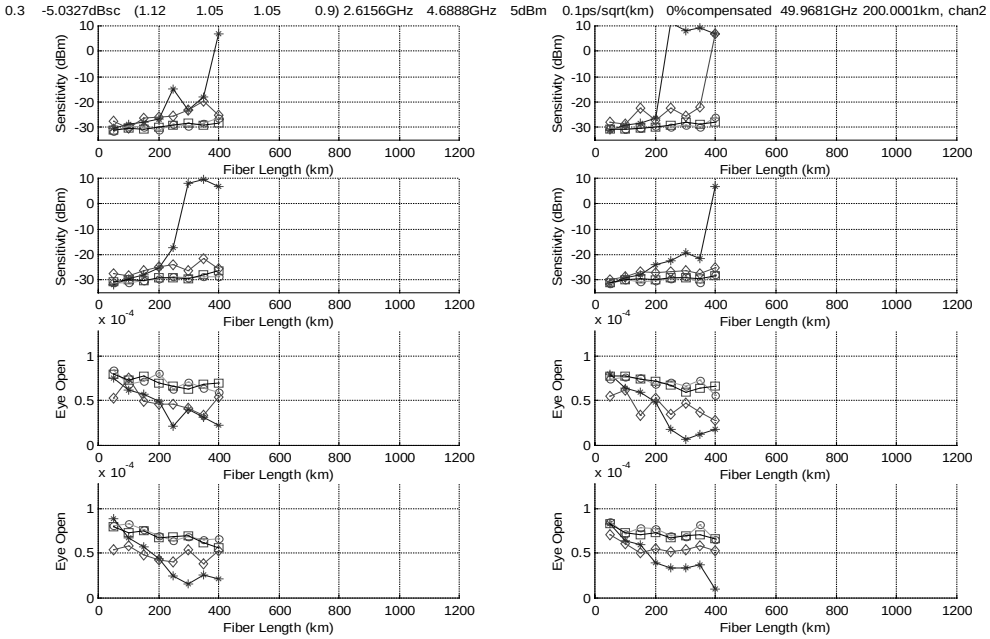

7. DC, 0.1 $ps/\sqrt{km}$ PMD, 0dBm, 2.6GHz, 0.4 and 0 dB CS

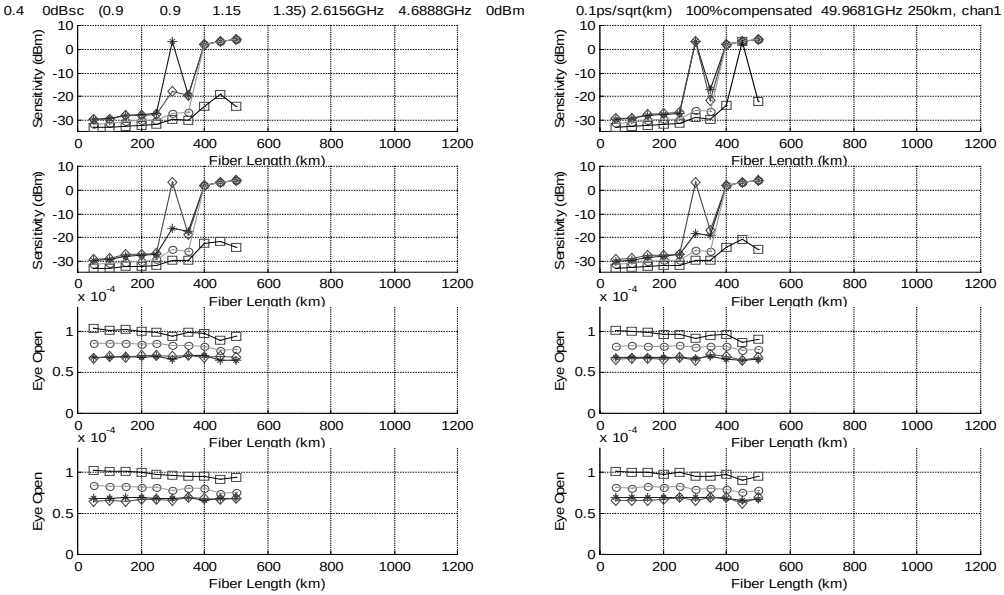

8. DC, 0.1 $ps/\sqrt{km}$ PMD, -3dBm, 2.6GHz, 0.3 and -5 dB CS

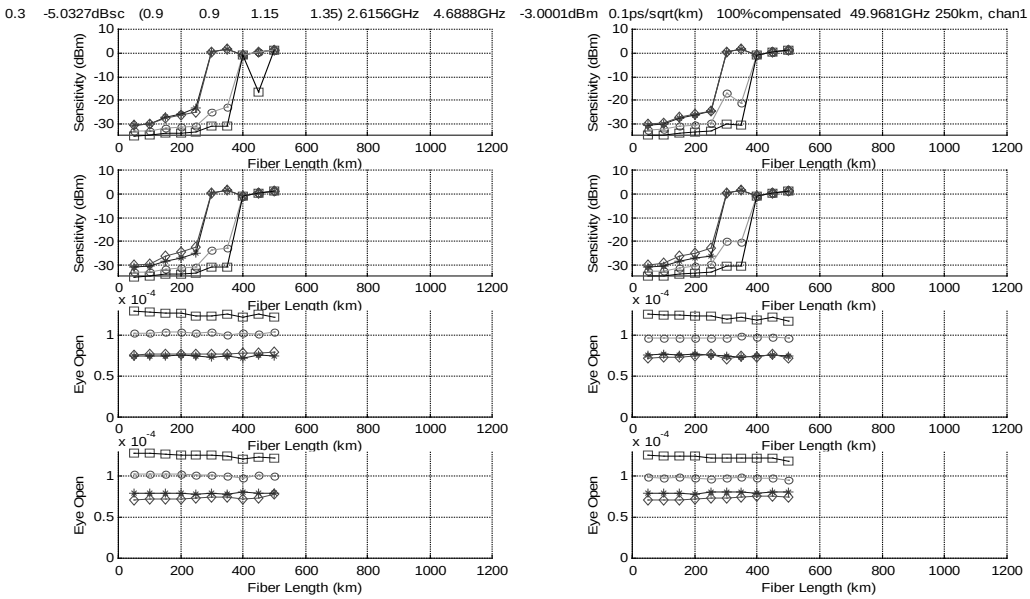

9. DC, 0.1 $ps/\sqrt{km}$ PMD, -3dBm, 2.6GHz, 0.4 and 0 dB CS

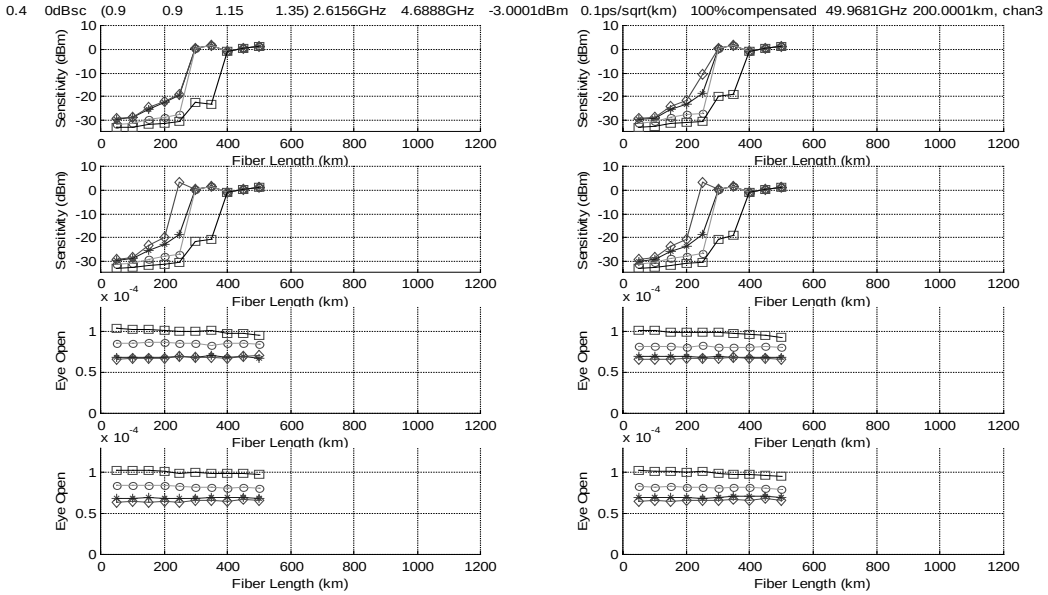

10. No DC, 0.1 $ps/\sqrt{km}$ PMD, 5dBm, 2.6GHz, 0.4 and 0 dB CS

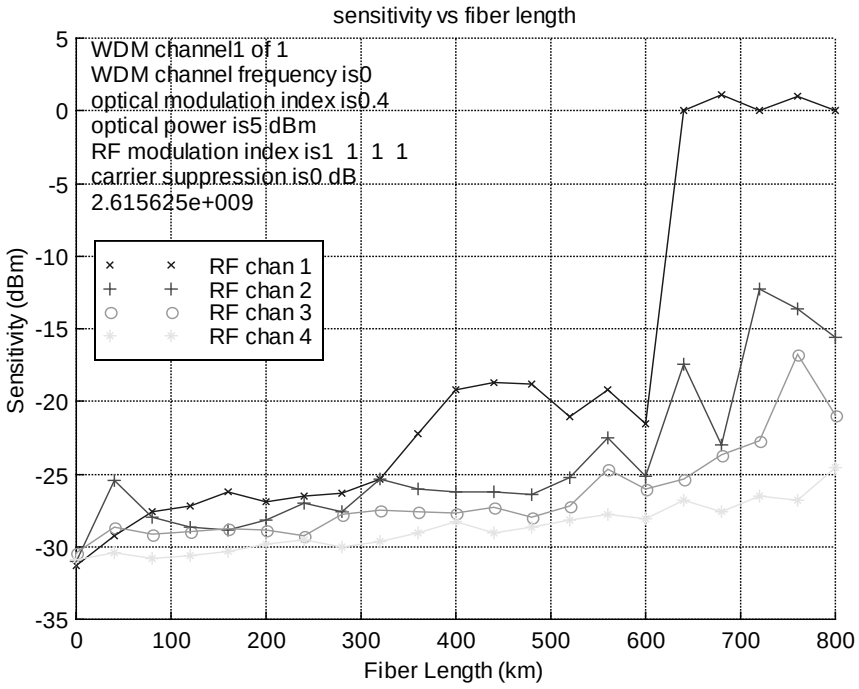

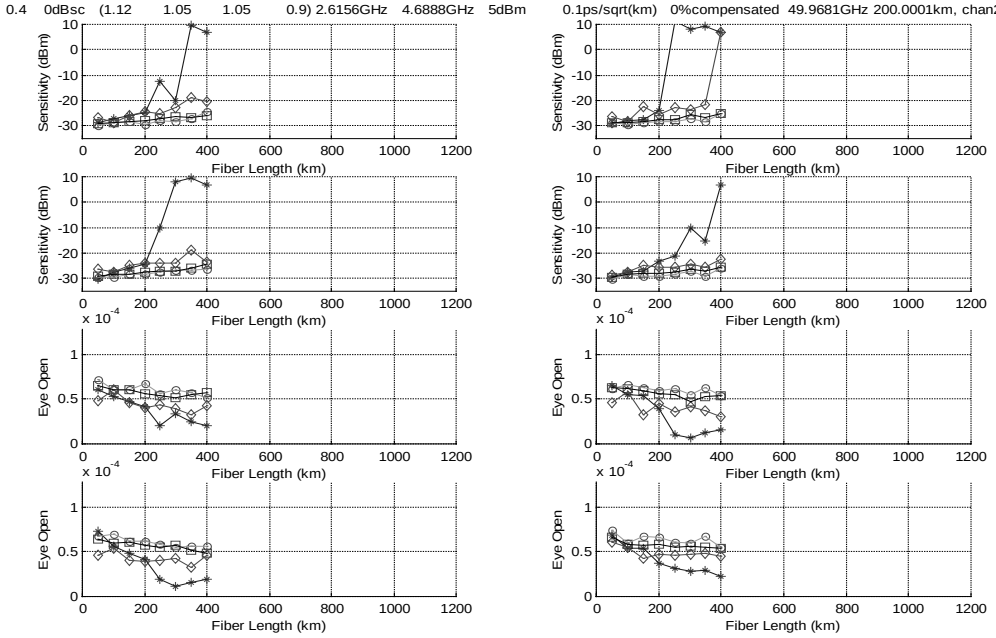

11. No DC, 0.1 $ps/\sqrt{km}$ PMD, 3dBm, 2.6GHz, 0.3 and 5 dB CS

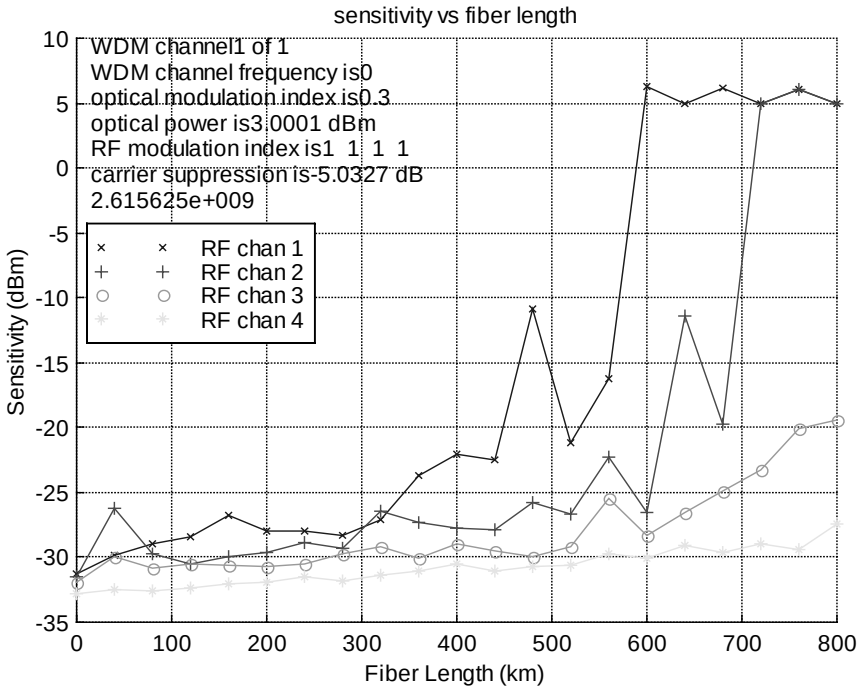

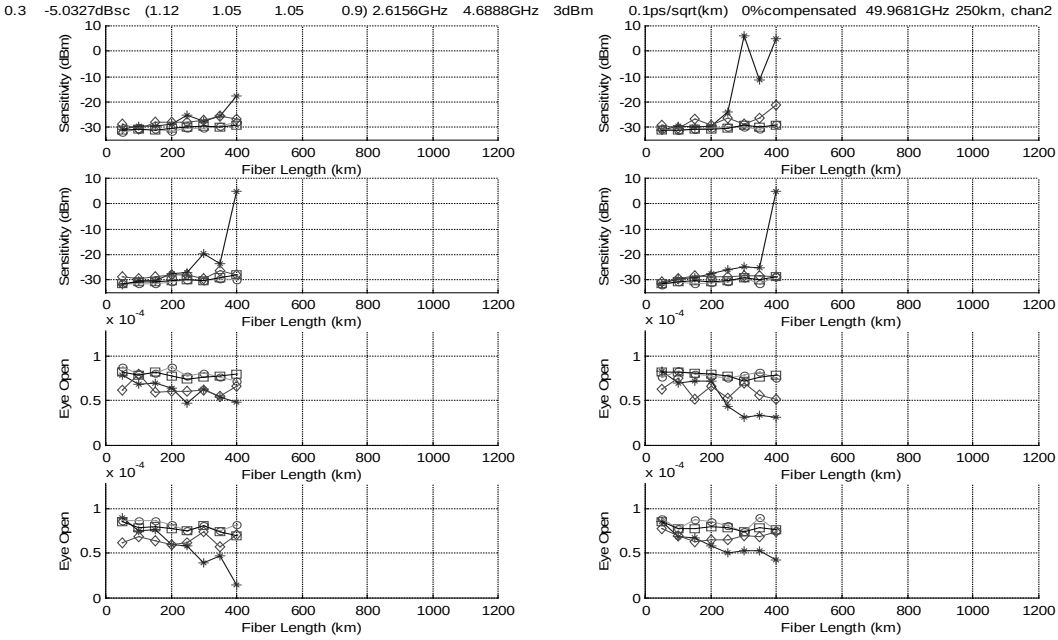

12. No DC, 0.1 $ps/\sqrt{km}$ PMD, 3dBm, 2.6GHz, 0.4 and 0 dB CS

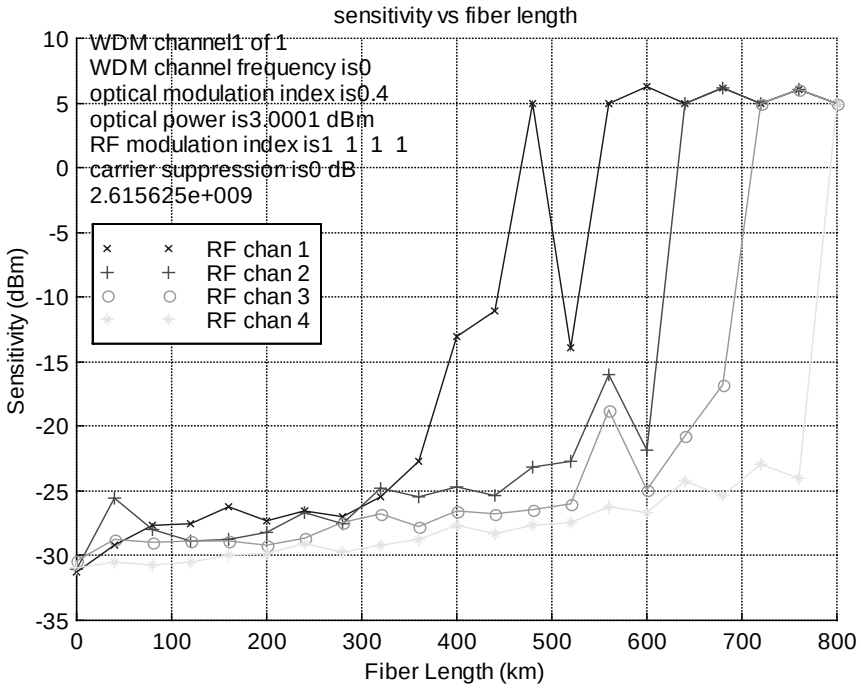

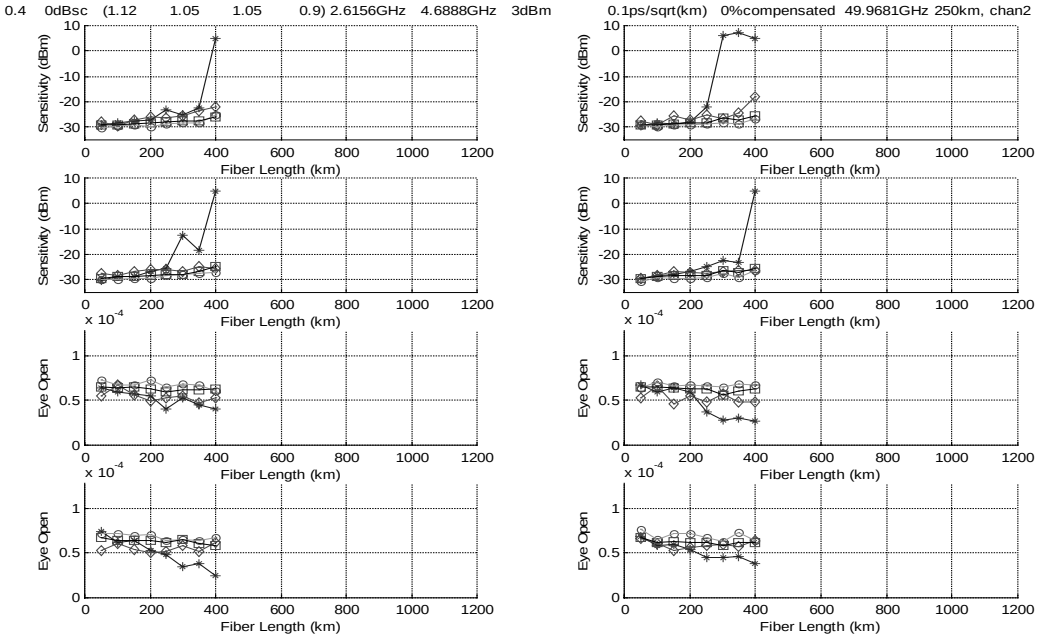

13. No DC, 0.1 $ps/\sqrt{km}$ PMD, 0dBm, 2.6GHz, 0.3 and 5 dB CS

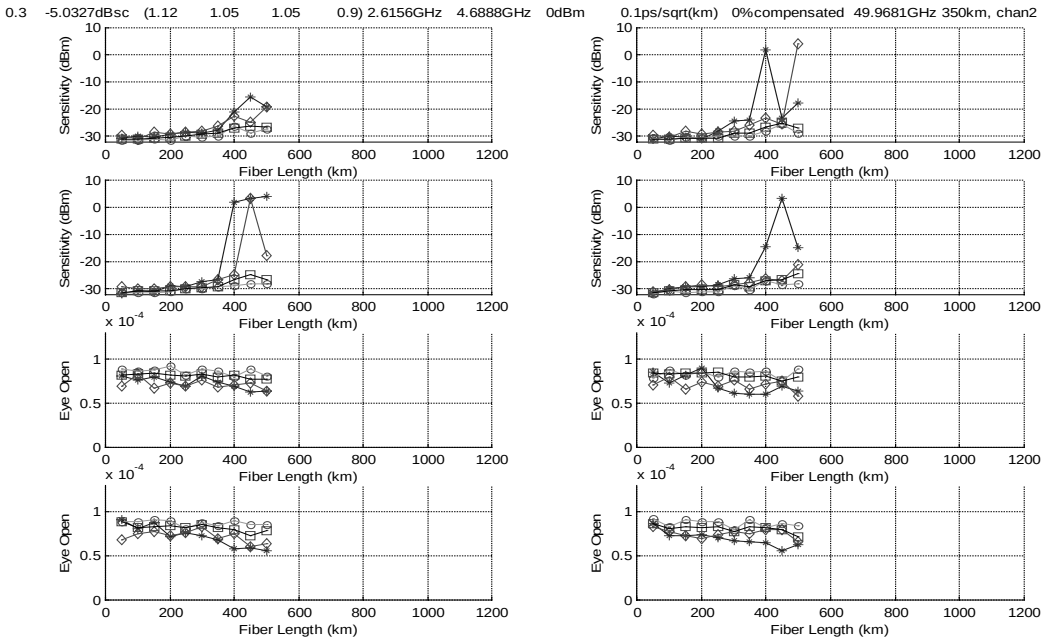

14. No DC, 0.1 $ps/\sqrt{km}$ PMD, 0dBm, 2.6GHz, 0.4 and 0 dB CS

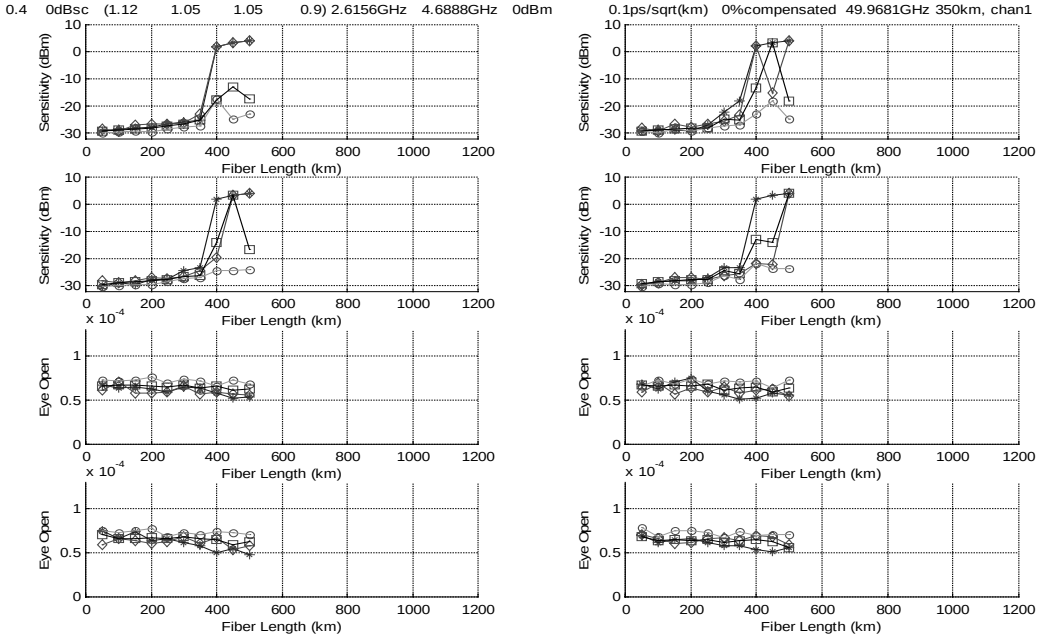

15. No DC, 0.1 $ps/\sqrt{km}$ PMD, -3dBm, 2.6GHz, 0.3 and 5 dB CS

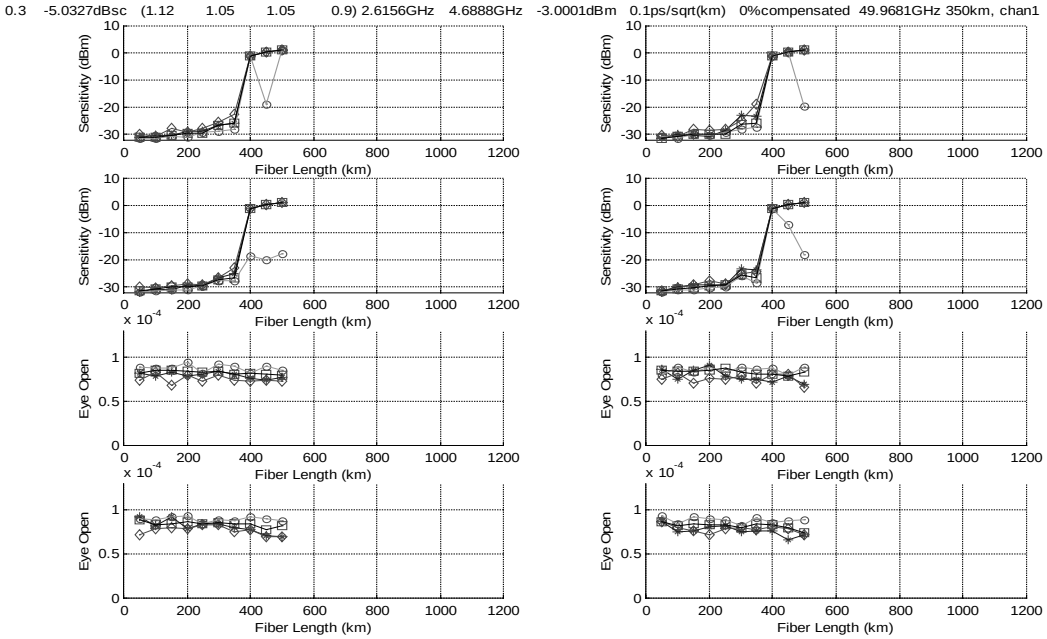

16. No DC, 0.1 $ps/\sqrt{km}$ PMD, -3dBm, 2.6GHz, 0.4 and 0 dB CS

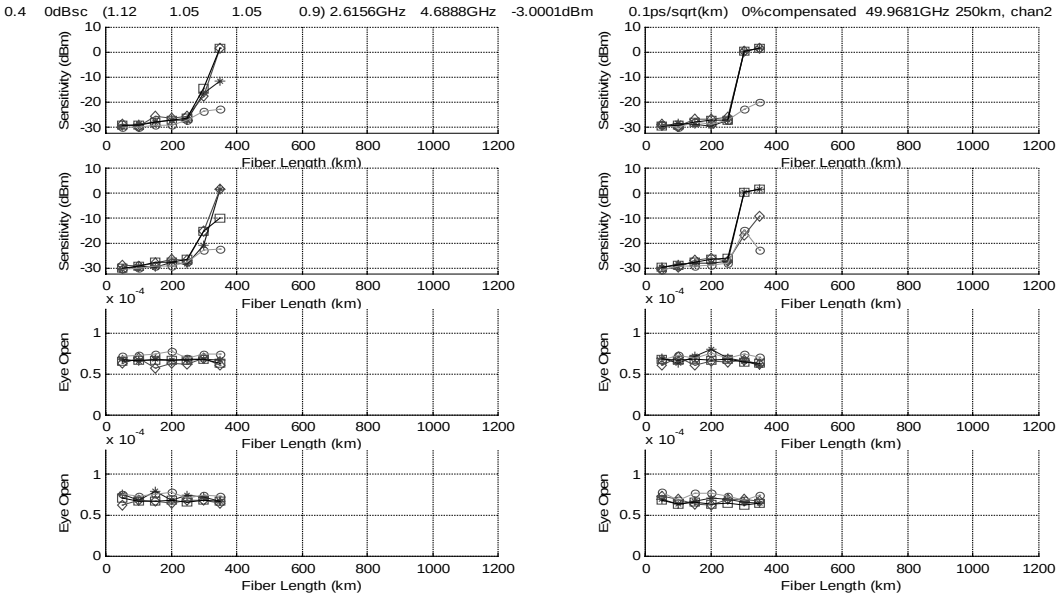

17. DC, 0.5 $ps/\sqrt{km}$ PMD, 5dBm, 2.6GHz, 0.3 and 5 dB CS

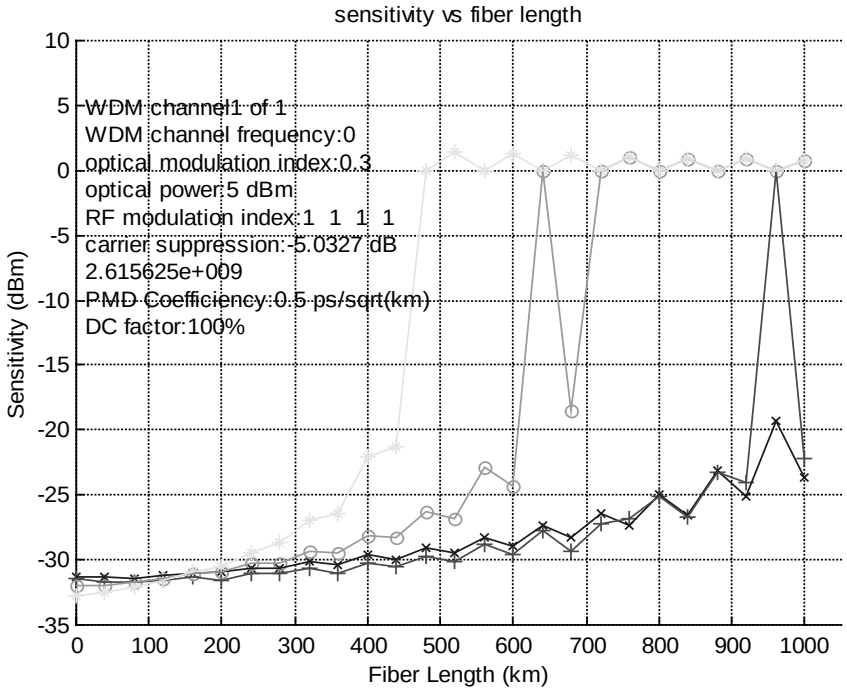

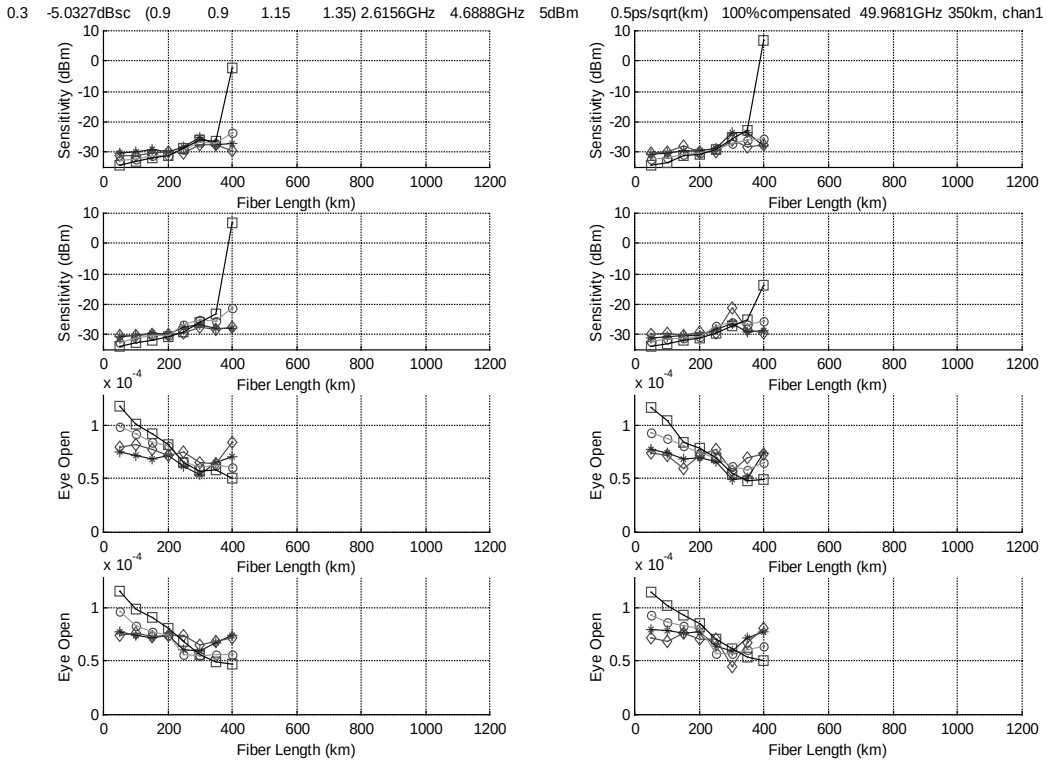

18. DC, 0.5 $ps/\sqrt{km}$ PMD, 5dBm, 2.6GHz, 0.4 and 0 dB CS

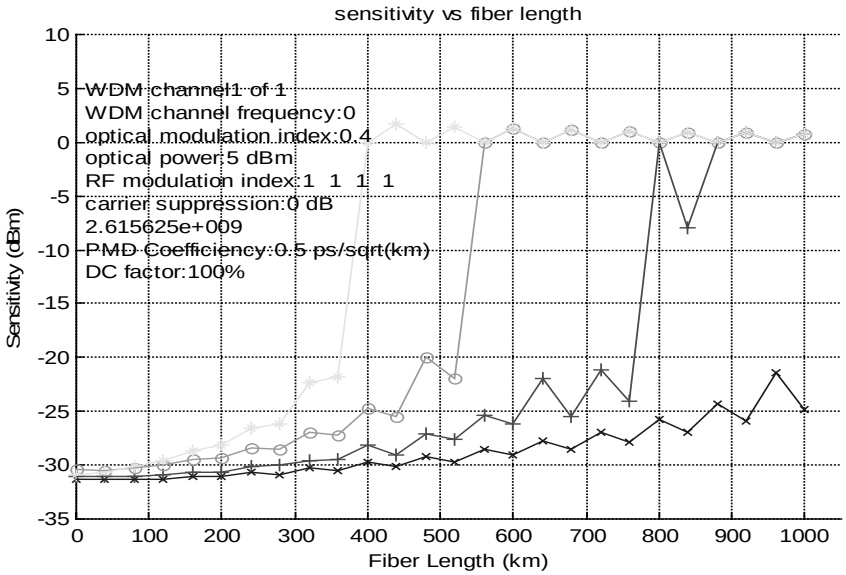

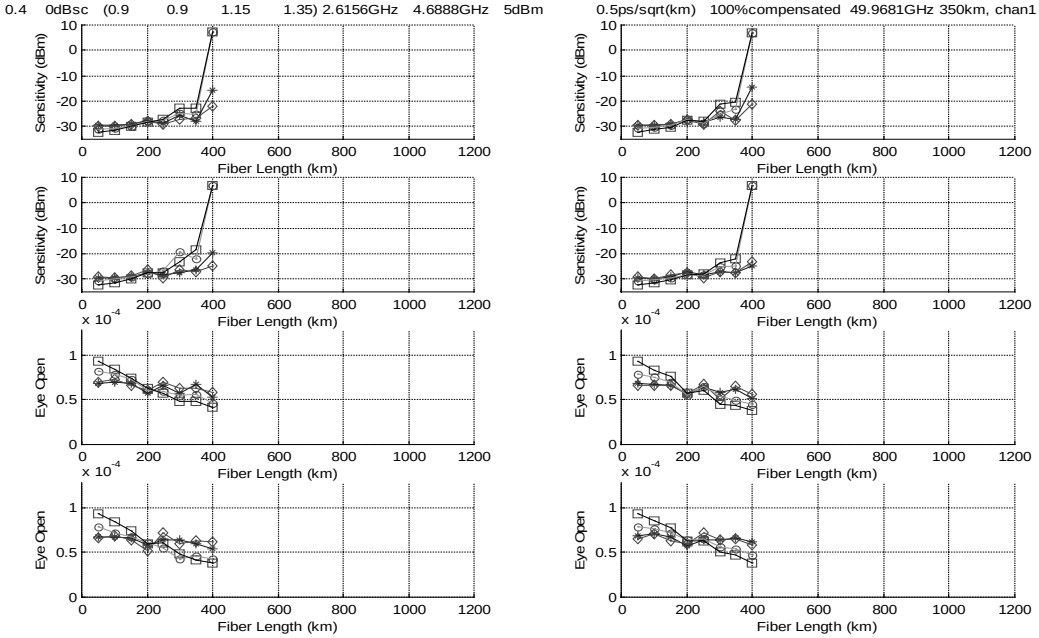

19. DC, 0.5 $ps/\sqrt{km}$ PMD, 3dBm, 2.6GHz, 0.3 and 5 dB CS

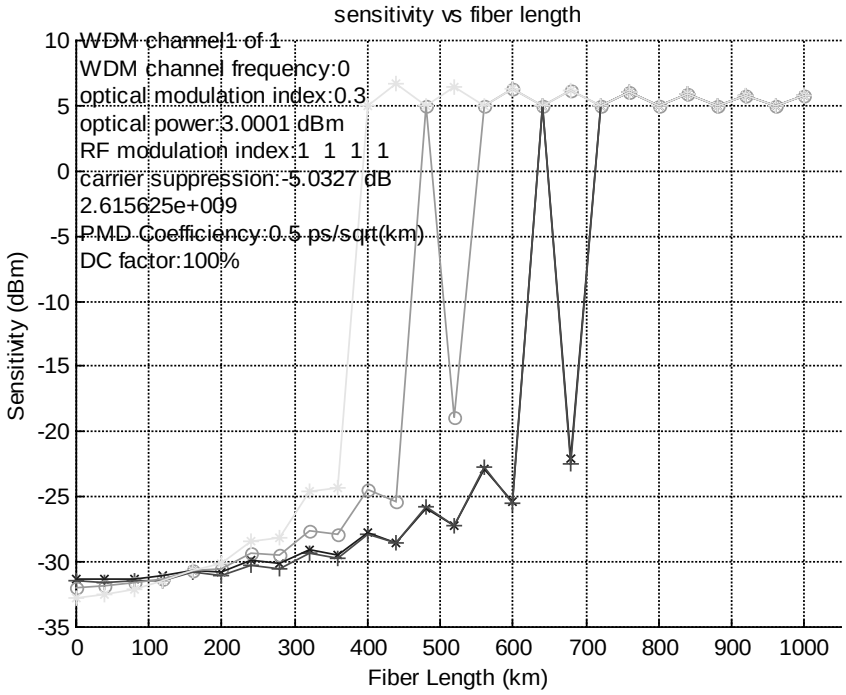

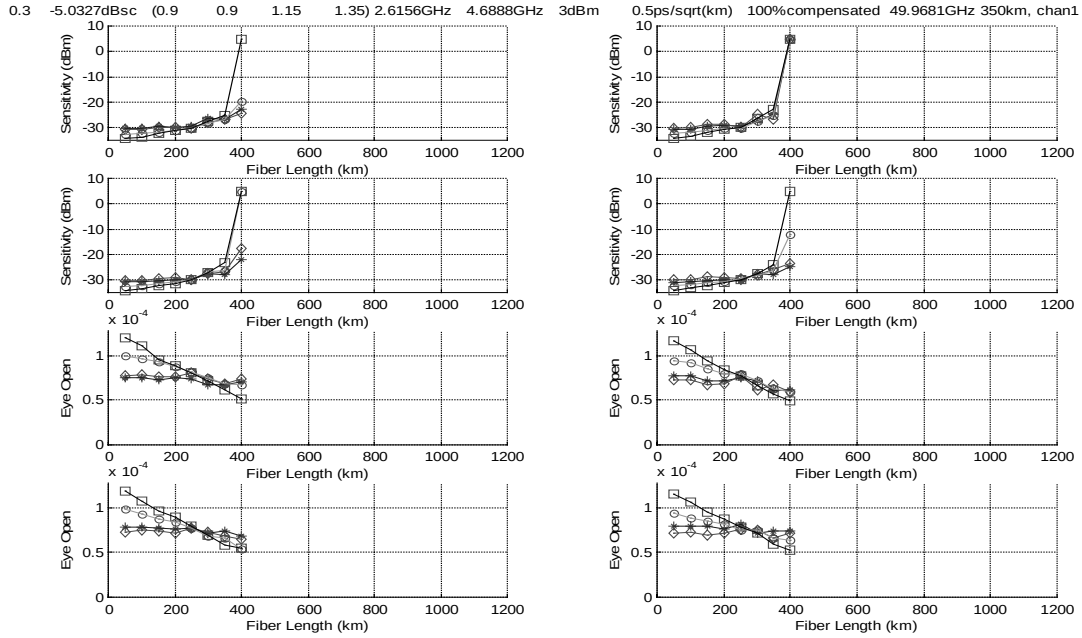

20. DC, 0.5 $ps/\sqrt{km}$ PMD, 3dBm, 2.6GHz, 0.4 and 0 dB CS

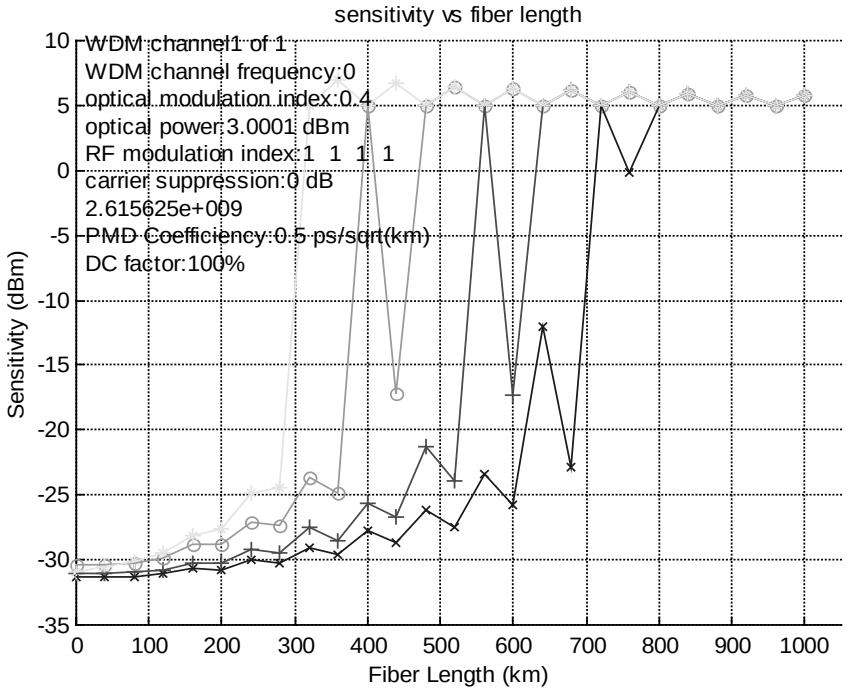

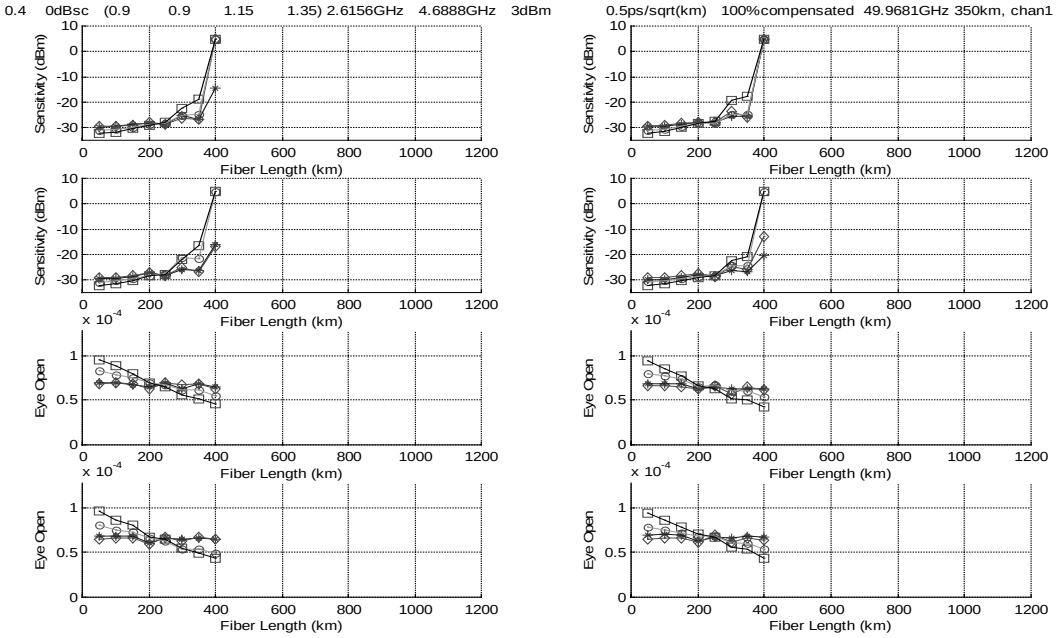

21. DC, 0.5 $ps/\sqrt{km}$ PMD, 0dBm, 2.6GHz, 0.3 and 5 dB CS

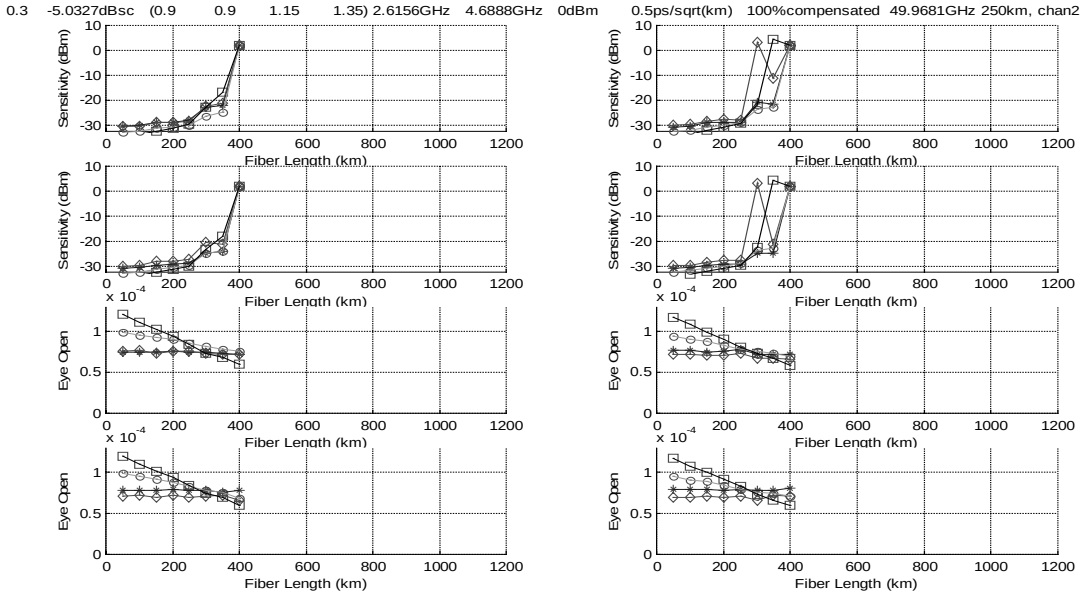

22. DC, 0.5 $ps/\sqrt{km}$ PMD, 0dBm, 2.6GHz, 0.4 and 0 dB CS

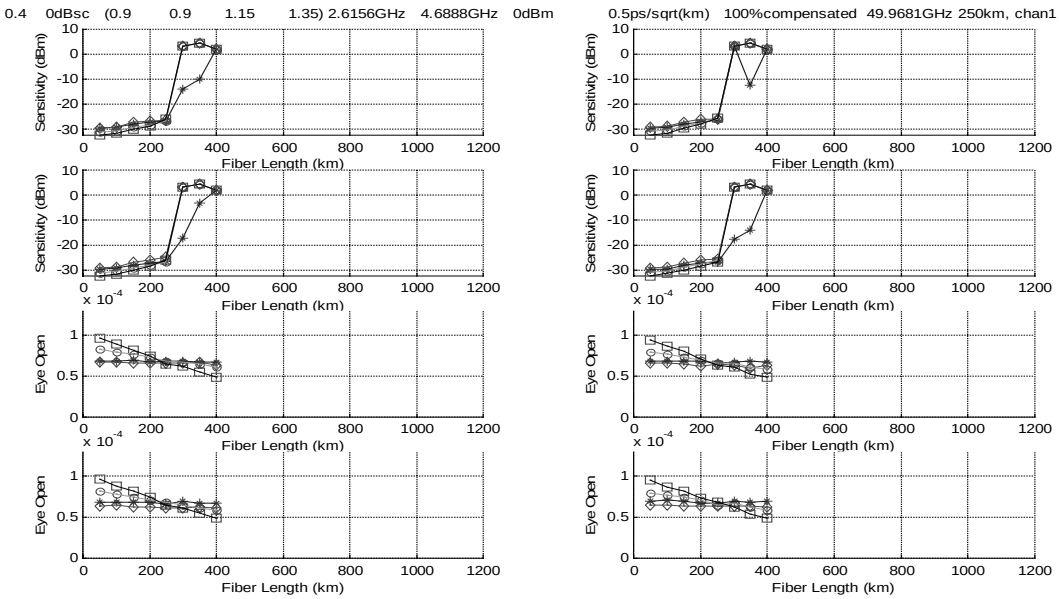

23. DC, 0.5 $ps/\sqrt{km}$ PMD, -3dBm, 2.6GHz, 0.3 and 5 dB CS

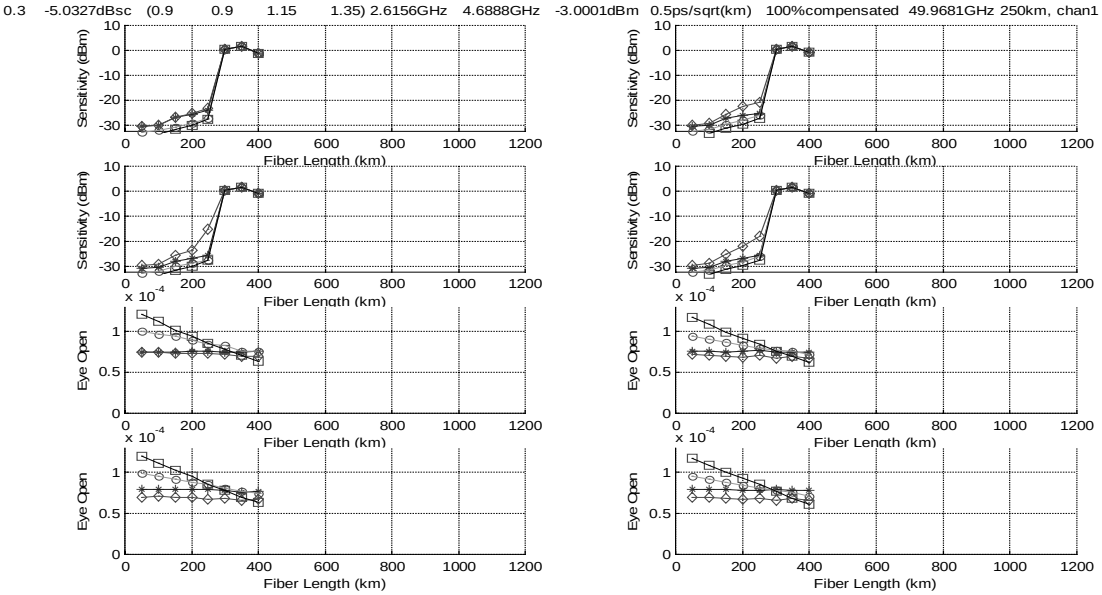

24. DC, 0.5 $ps/\sqrt{km}$ PMD, -3dBm, 2.6GHz, 0.4 and 0 dB CS

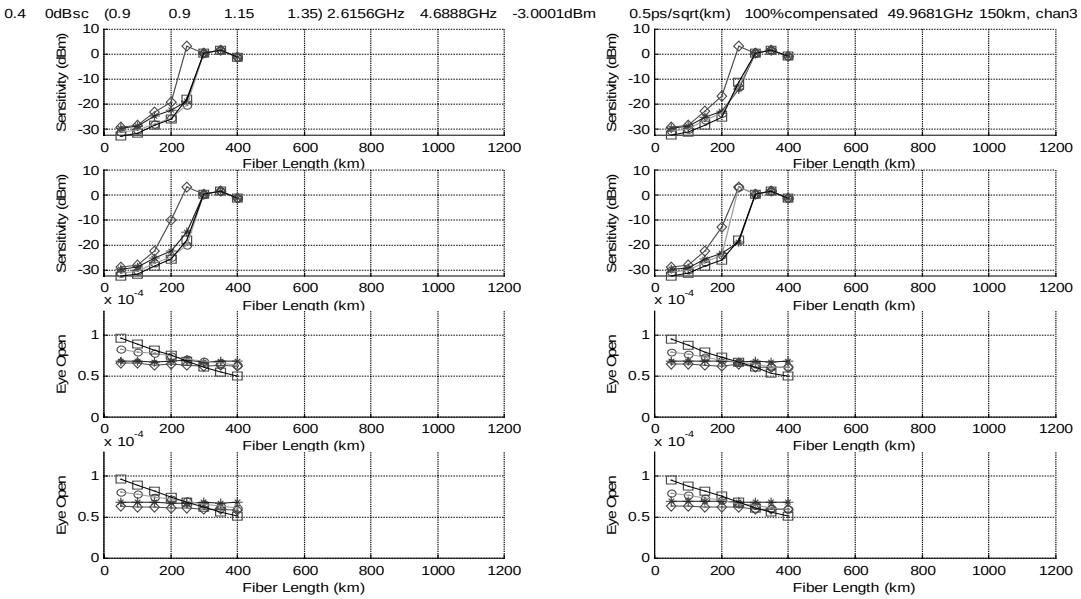

25. No DC, 0.5 $ps/\sqrt{km}$ PMD, 5dBm, 2.6GHz, 0.3 and 5 dB CS

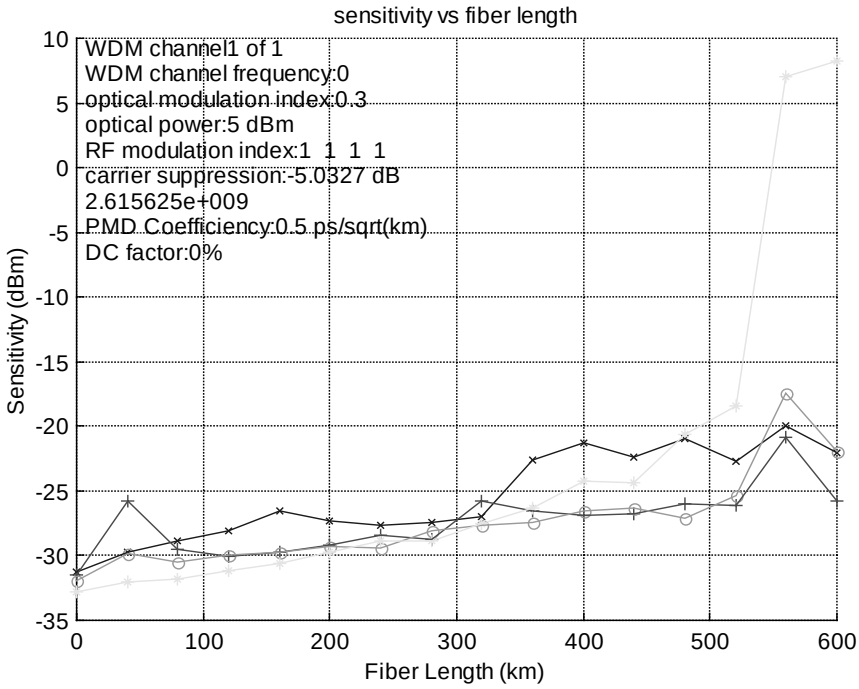

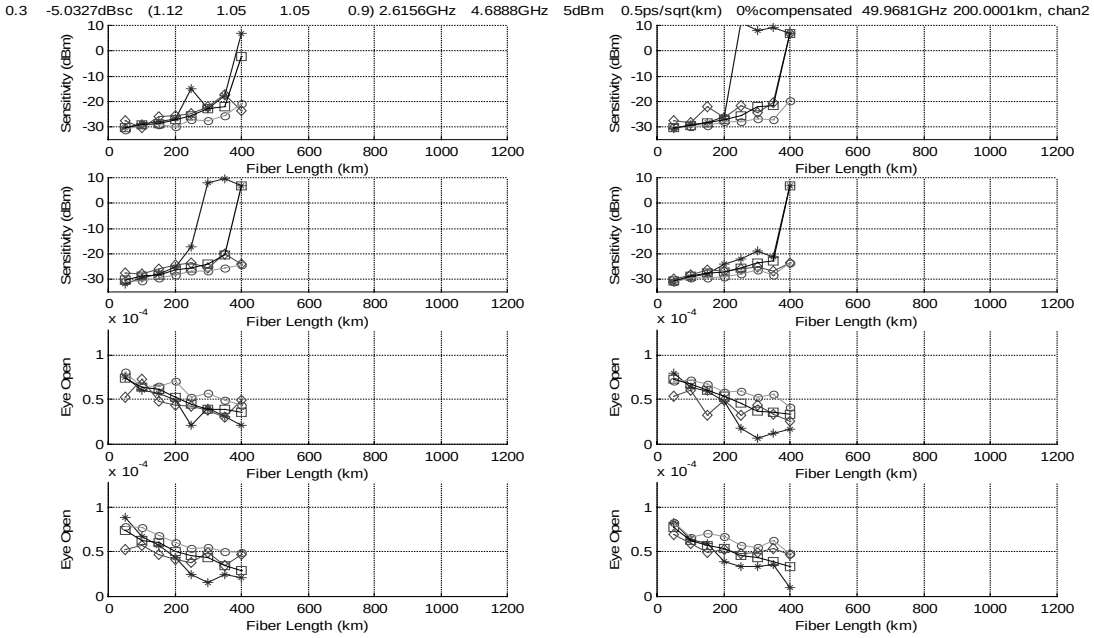

26. No DC, 0.5 $ps/\sqrt{km}$ PMD, 5dBm, 2.6GHz, 0.4 and 0 dB CS

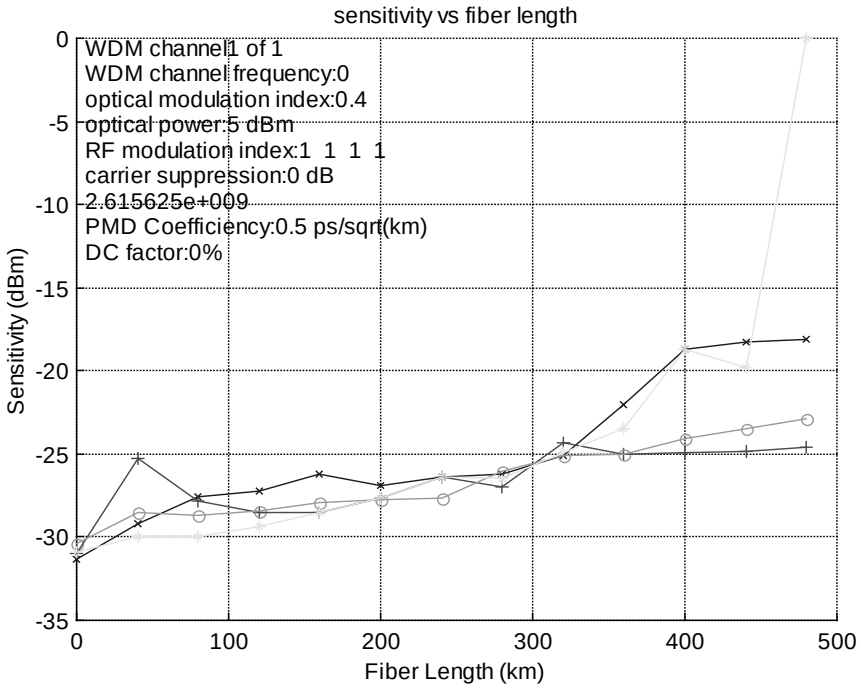

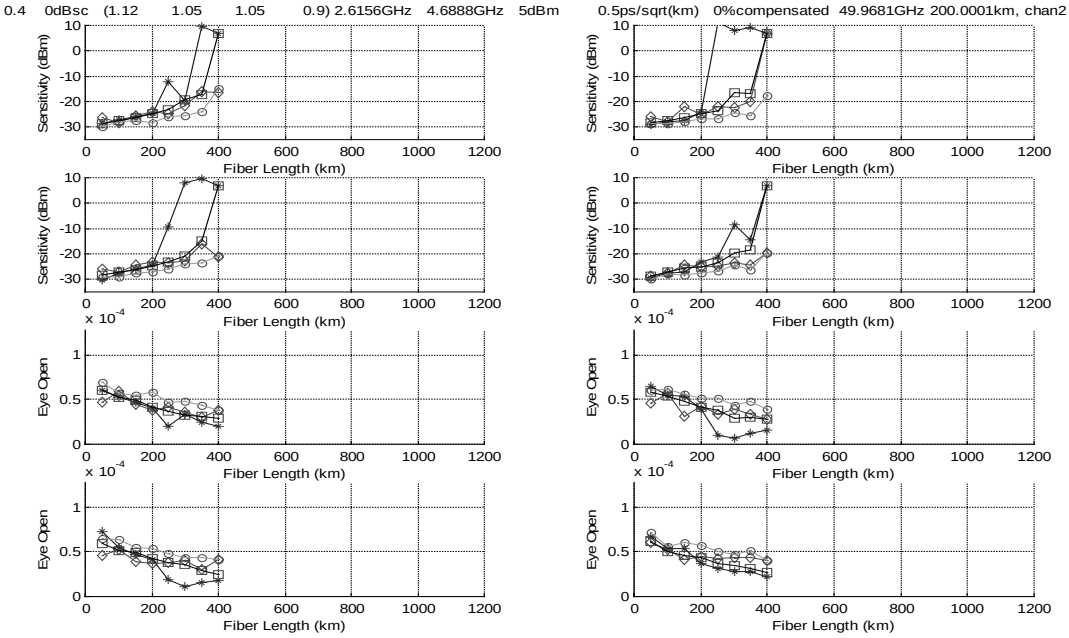

27. No DC, 0.5 $ps/\sqrt{km}$ PMD, 3dBm, 2.6GHz, 0.3 and 5 dB CS

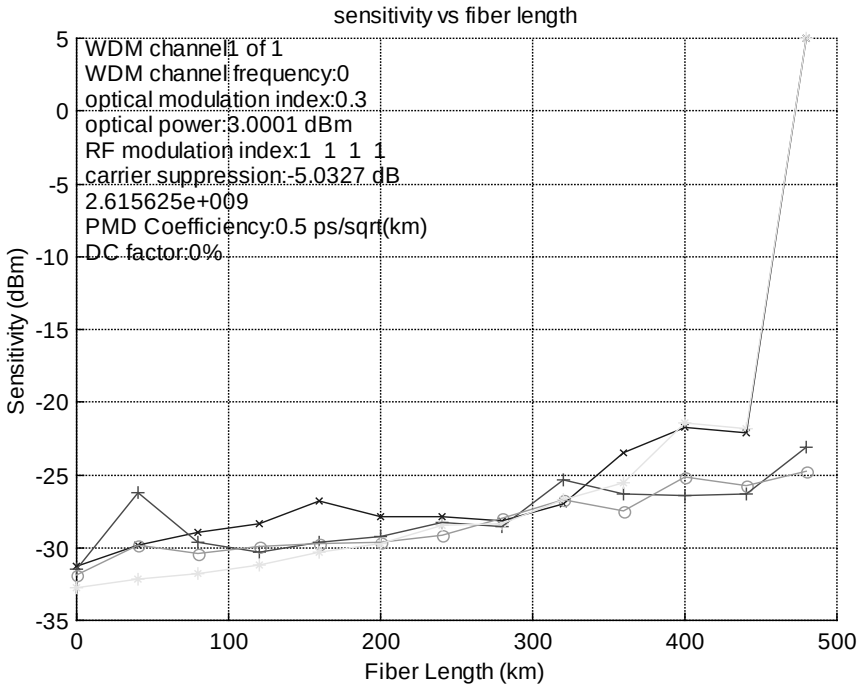

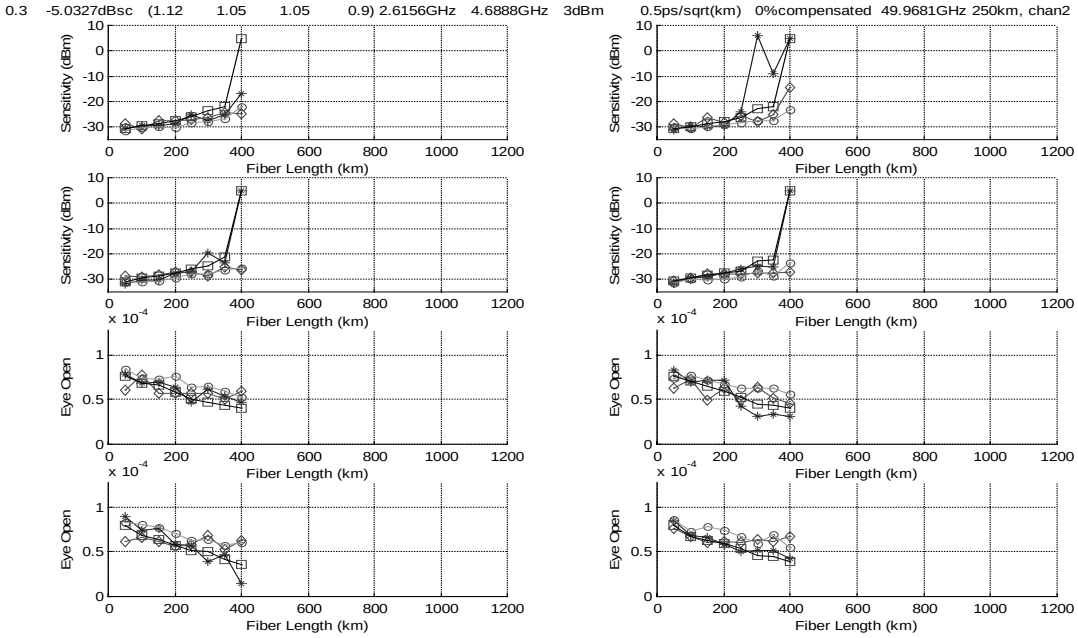

29. No DC, 0.5 $ps/\sqrt{km}$ PMD, 3dBm, 2.6GHz, 0.4 and 0 dB CS

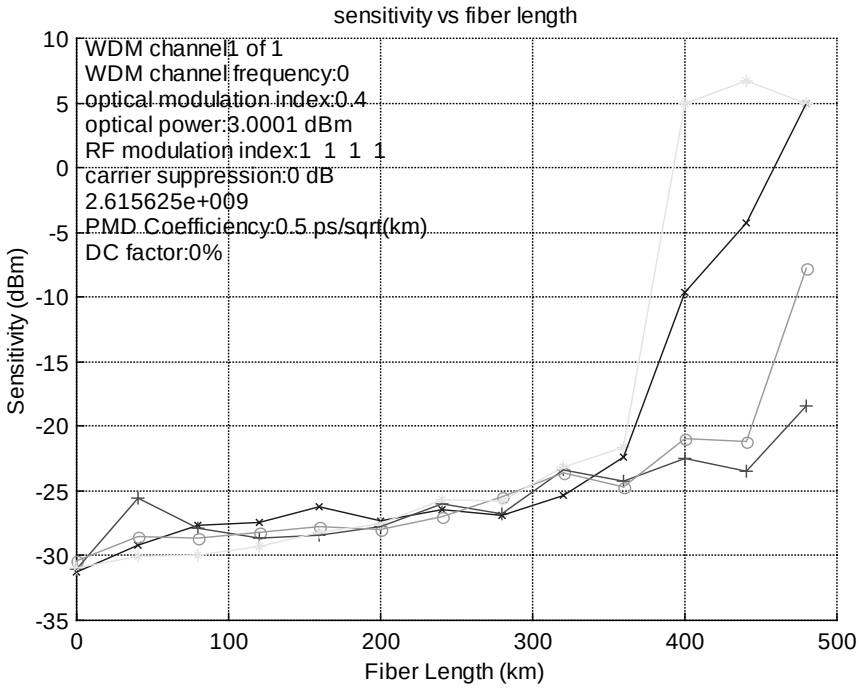

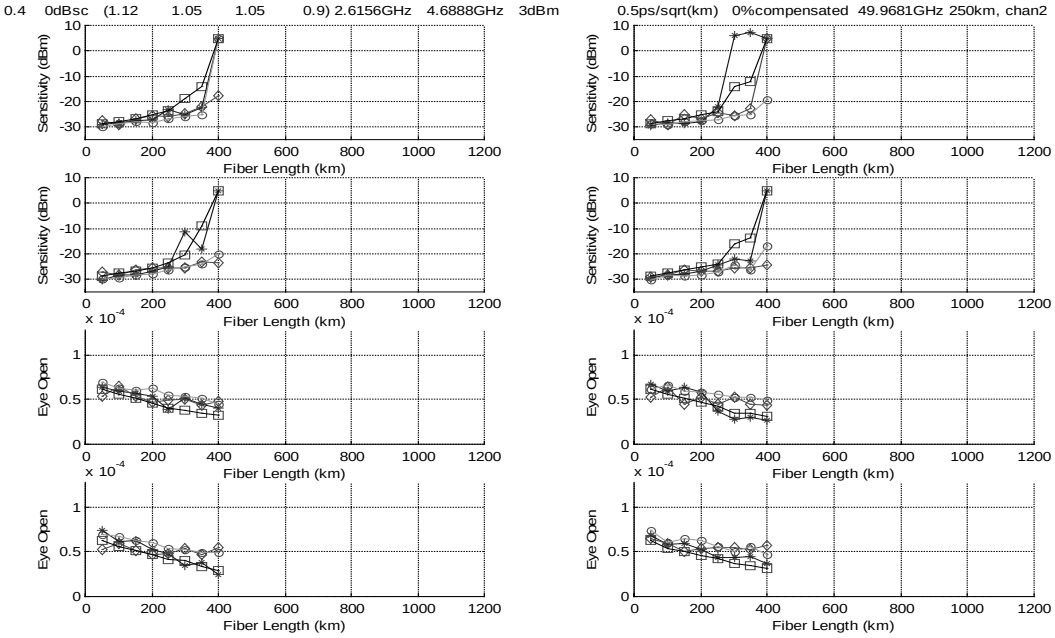

30. No DC, 0.5 $ps/\sqrt{km}$ PMD, 0dBm, 2.6GHz, 0.3 and 5 dB CS

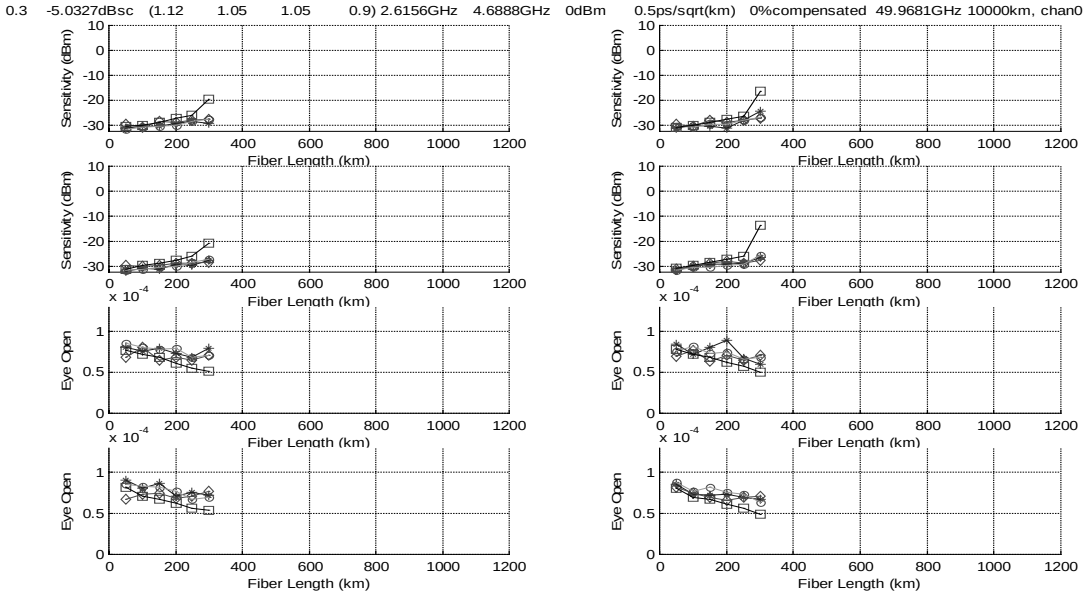

31. No DC, 0.5 $ps/\sqrt{km}$ PMD, 0dBm, 2.6GHz, 0.4 and 0 dBCS

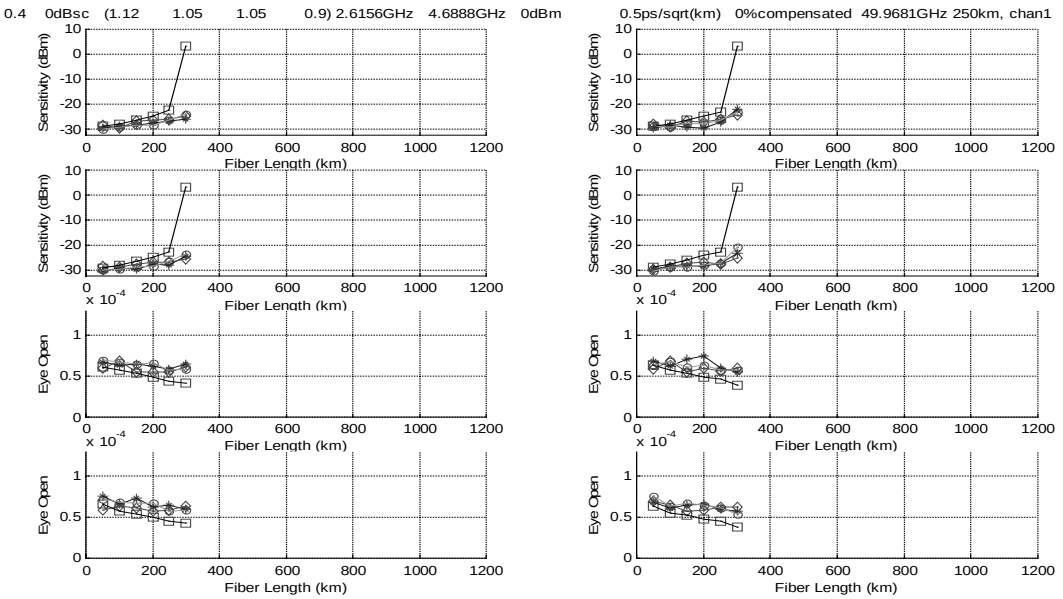

32. No DC, 0.5 $ps/\sqrt{km}$ PMD, -3dBm, 2.6GHz, 0.3 and 5 dB CS

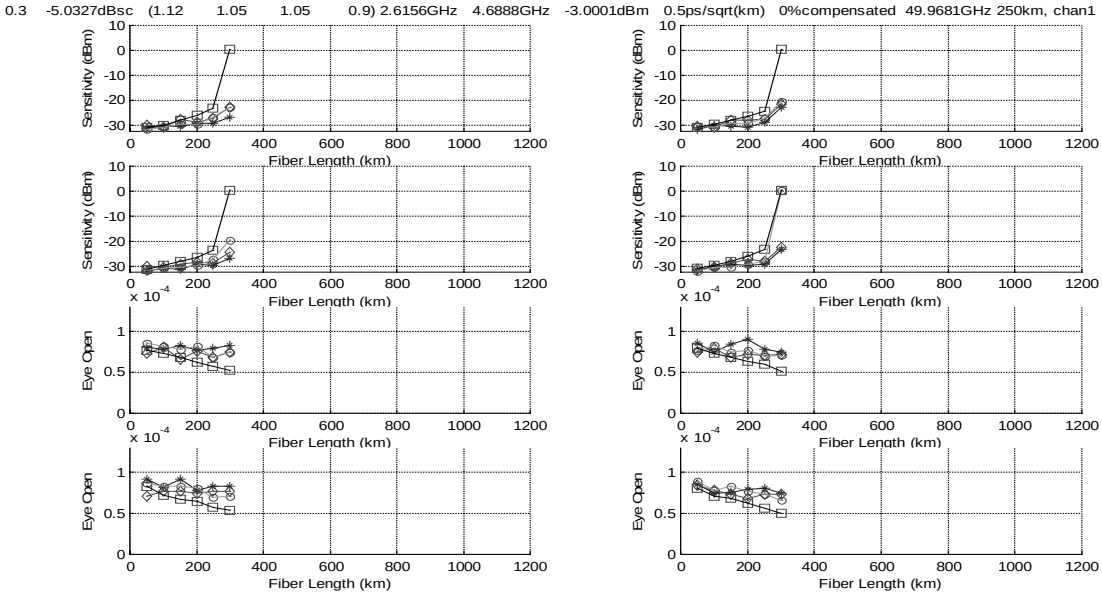

33. No DC, 0.5 $ps/\sqrt{km}$ PMD, -3dBm, 2.6GHz, 0.4 and 0 dB CS

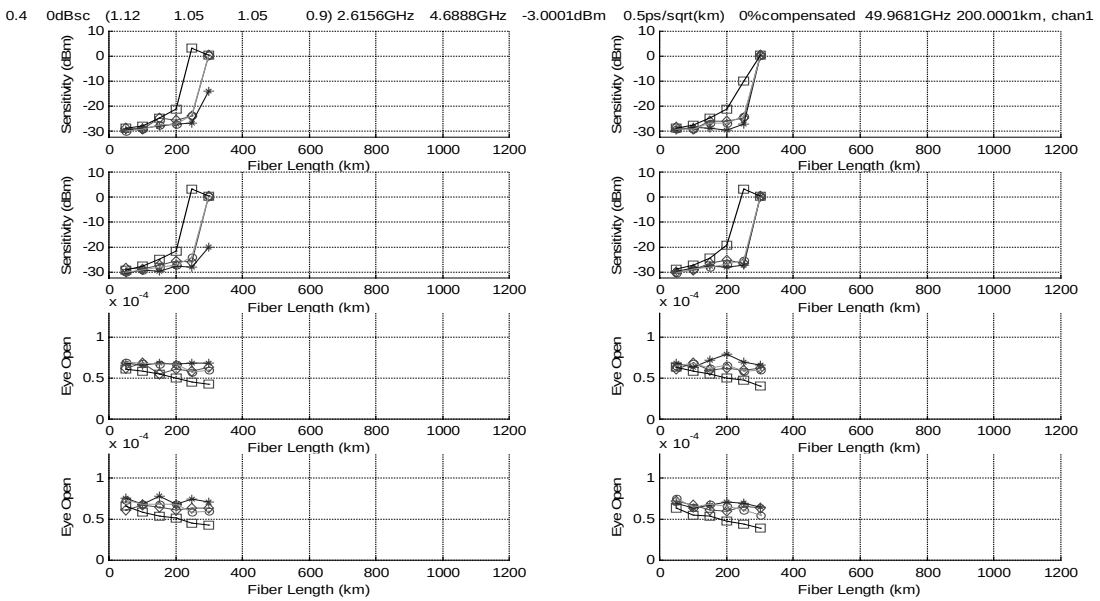

Appendix 3: QPSK SCM results

1.DC, 0.1 $ps/\sqrt{km}$ PMD, 5dBm, 0.3 and 5 dB CS

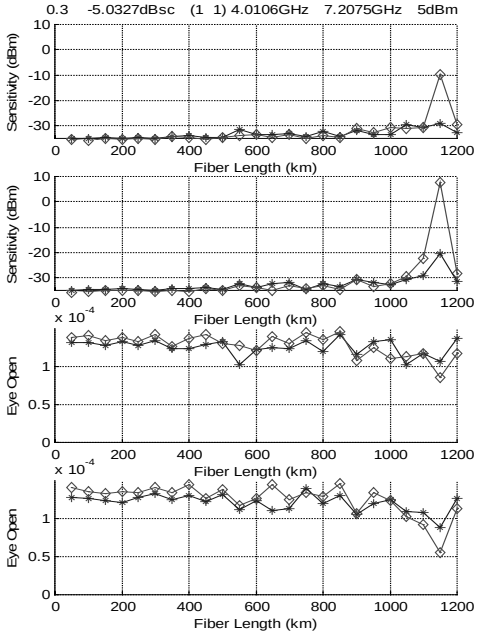

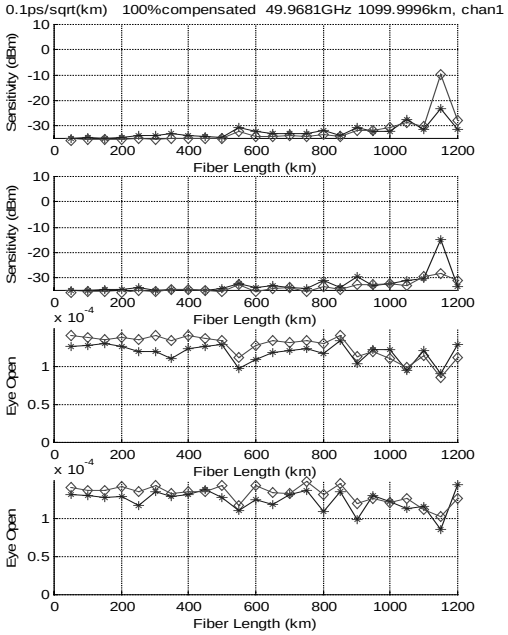

2. DC, 0.1 $ps/\sqrt{km}$ PMD, 5dBm, 0.4 and 0 dB CS

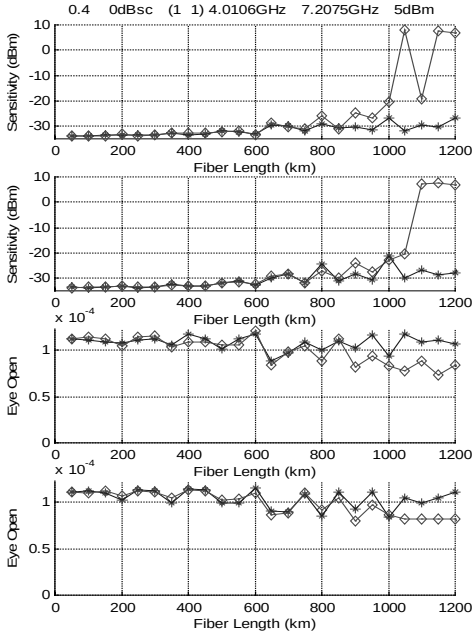

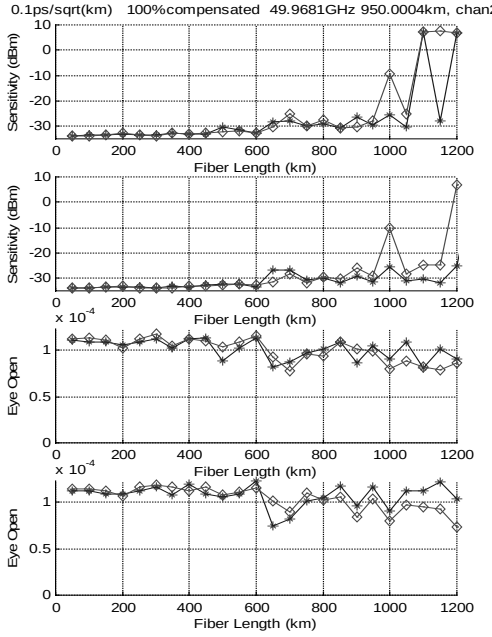

3. DC, 0.1 $ps/\sqrt{km}$ PMD, 3dBm, 0.3 and 5 dB CS

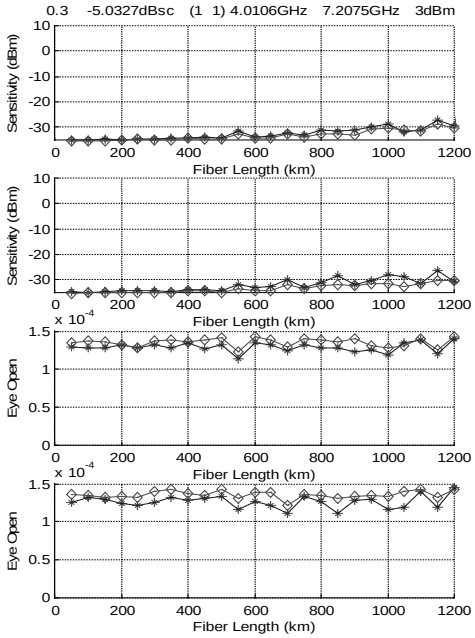

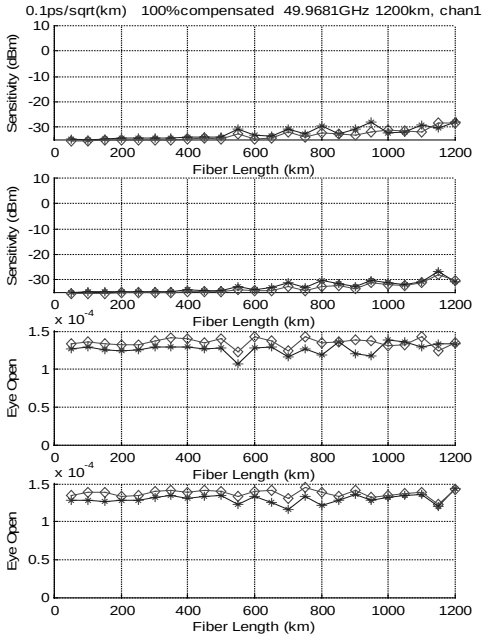

4. DC, 0.1 $ps/\sqrt{km}$ PMD, 3dBm, 0.4 and 0 dB CS

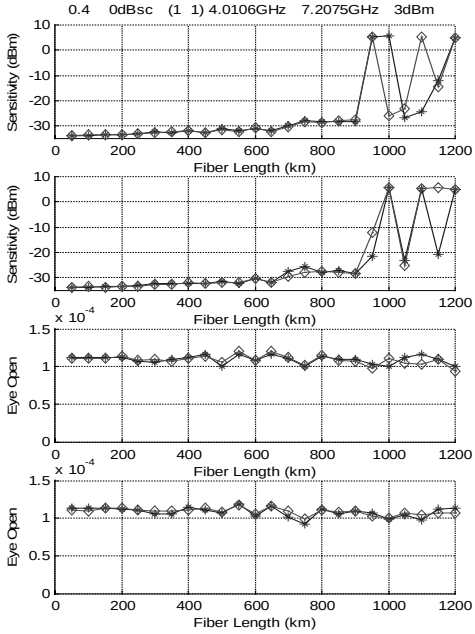

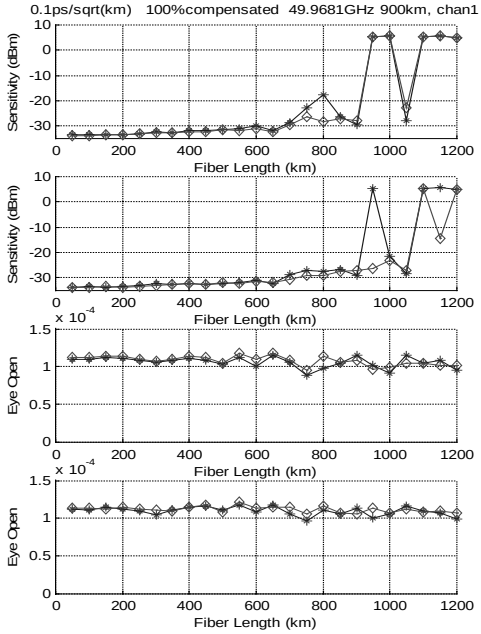

5. DC, 0.1 $ps/\sqrt{km}$ PMD, 0dBm, 0.3 and 7 dB CS

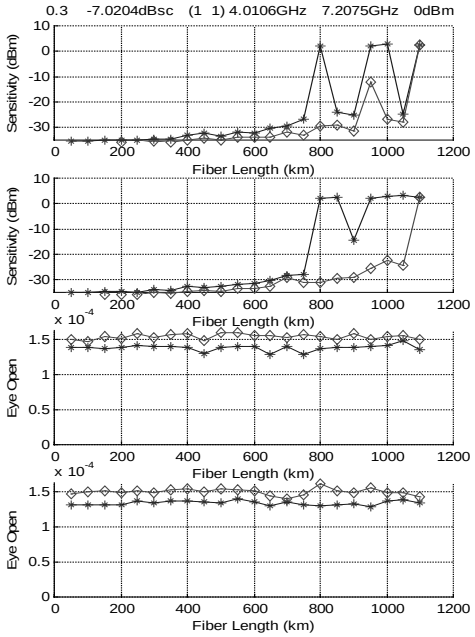

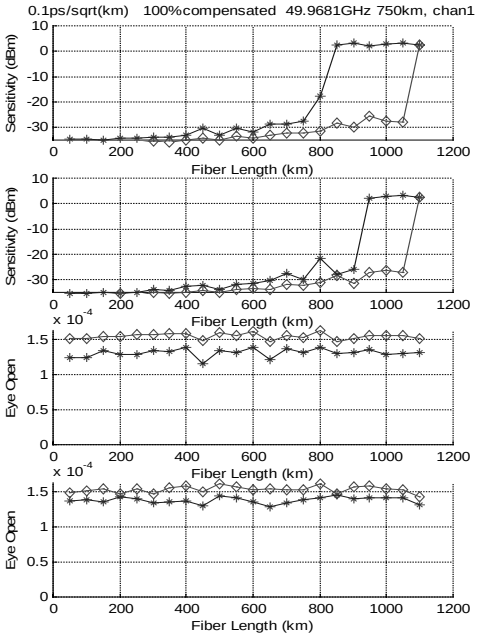

6. DC, 0.1 $ps/\sqrt{km}$ PMD, 0dBm, 0.4 and 0 dB CS

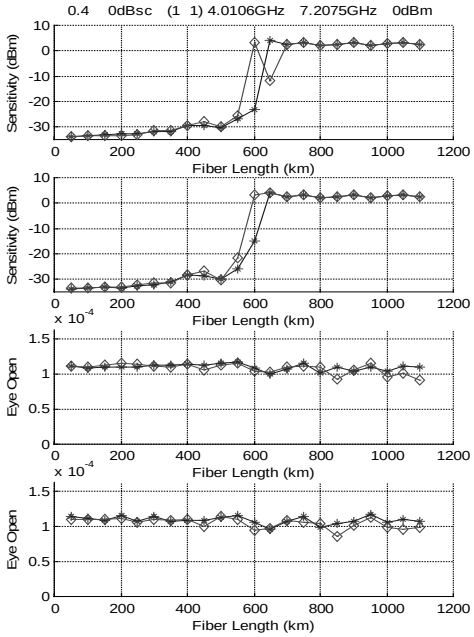

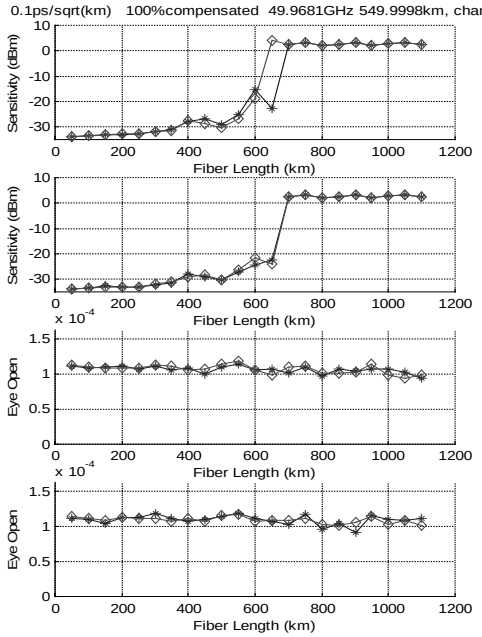

7. DC, 0.1 $ps/\sqrt{km}$ PMD, -3dBm, 0.3 and 7 dB CS

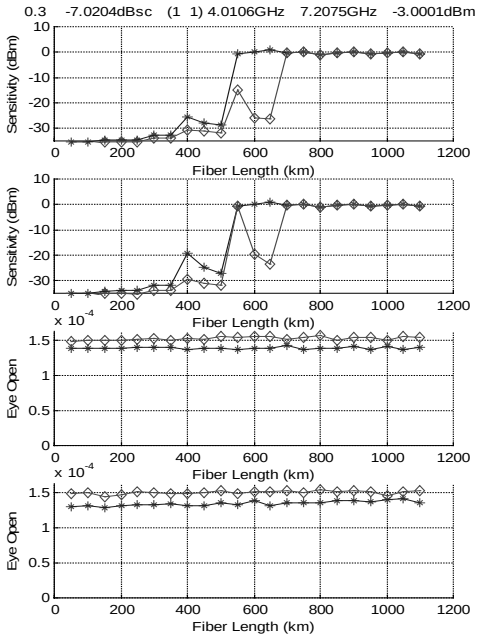

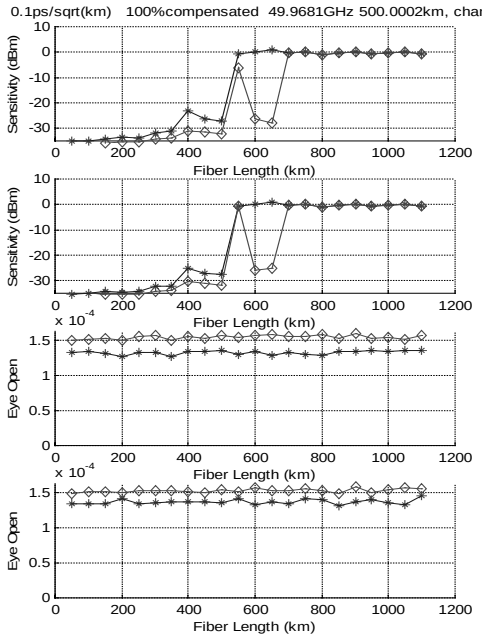

8. DC, 0.1 $ps/\sqrt{km}$ PMD, -3dBm, 0.4 and 0 dB CS

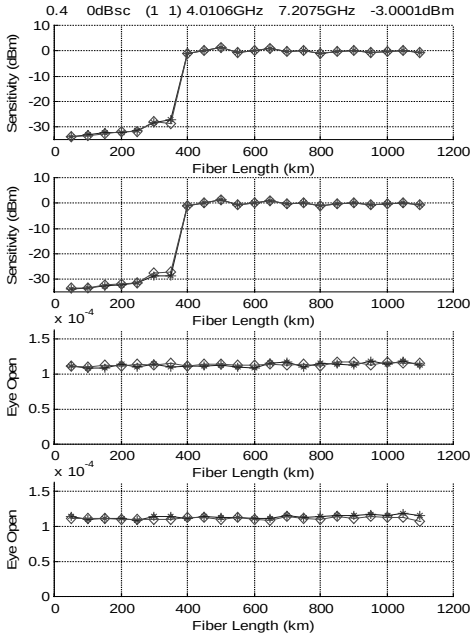

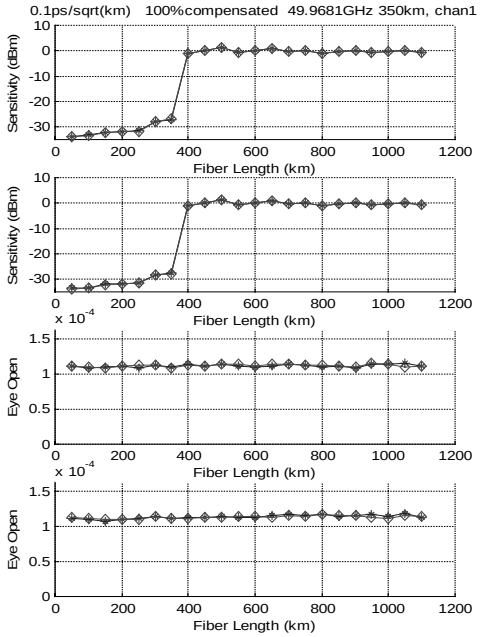

9. No DC, 0.1 $ps/\sqrt{km}$ PMD, 5dBm, 0.3 and 5 dB CS

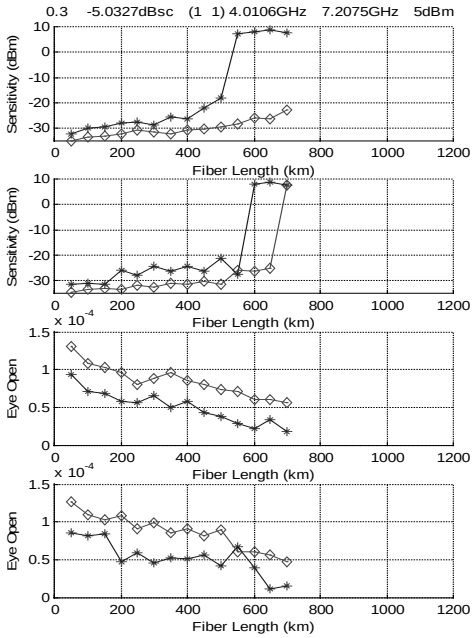

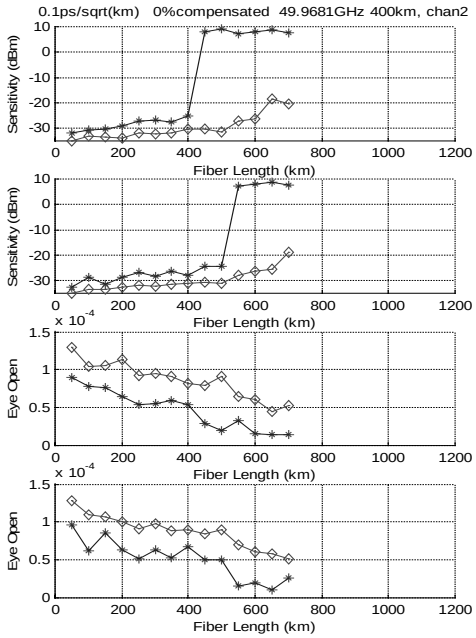

10. No DC, 0.1 $ps/\sqrt{km}$ PMD, 5dBm, 0.4 and 0 dB CS

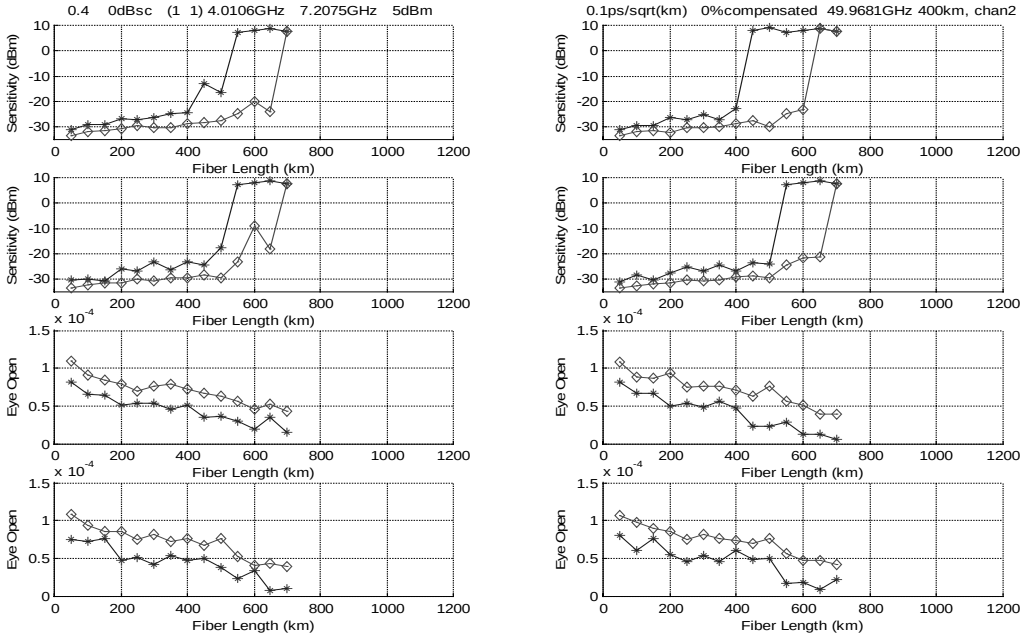

11. No DC, 0.1 $ps/\sqrt{km}$ PMD, 3dBm, 0.3 and 5 dB CS

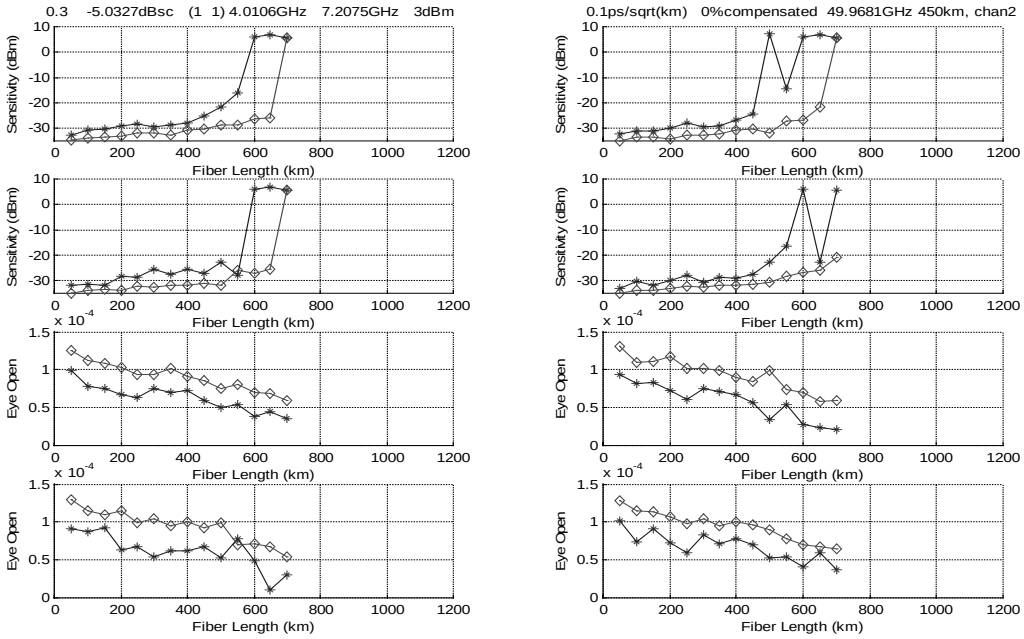

12. No DC, 0.1 $ps/\sqrt{km}$ PMD, 3dBm, 0.4 and 0 dB CS

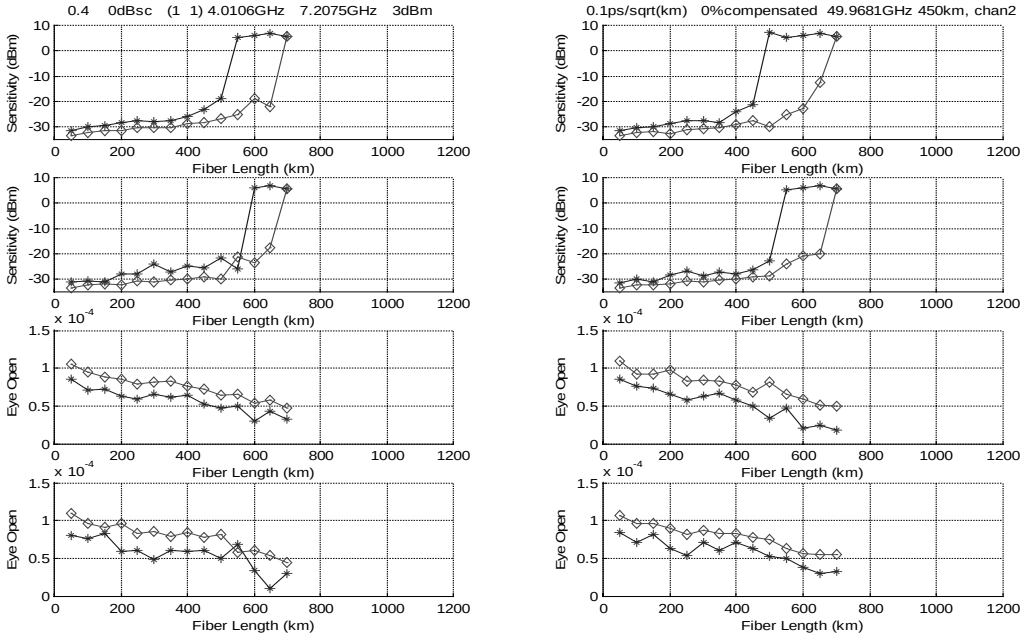

13. No DC, 0.1 $ps/\sqrt{km}$ PMD, 0dBm, 0.3 and 7 dB CS

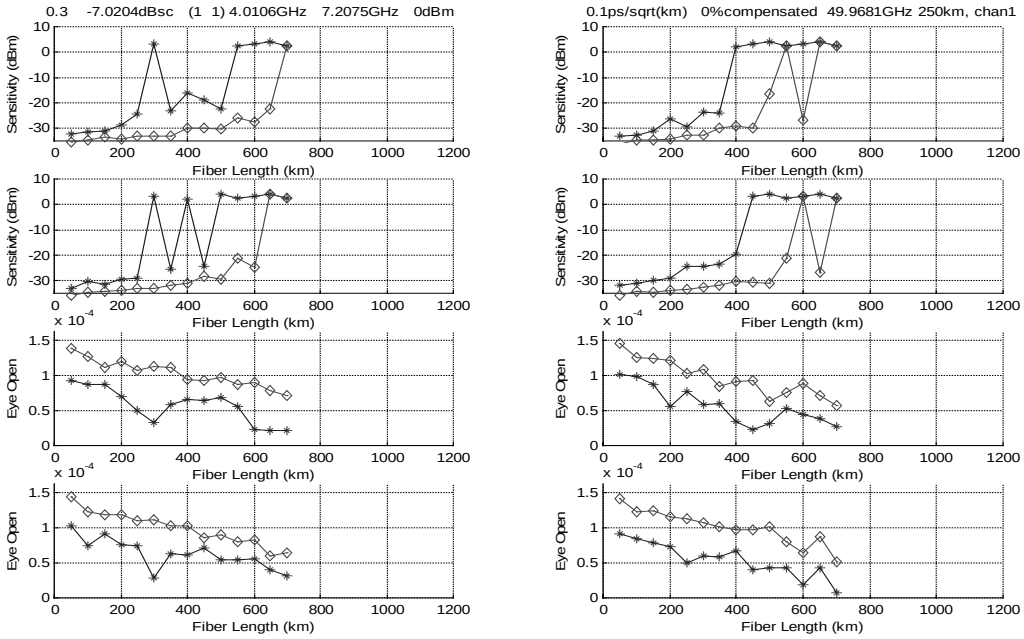

14. No DC, 0.1 $ps/\sqrt{km}$ PMD, 0dBm, 0.4 and 0 dB CS

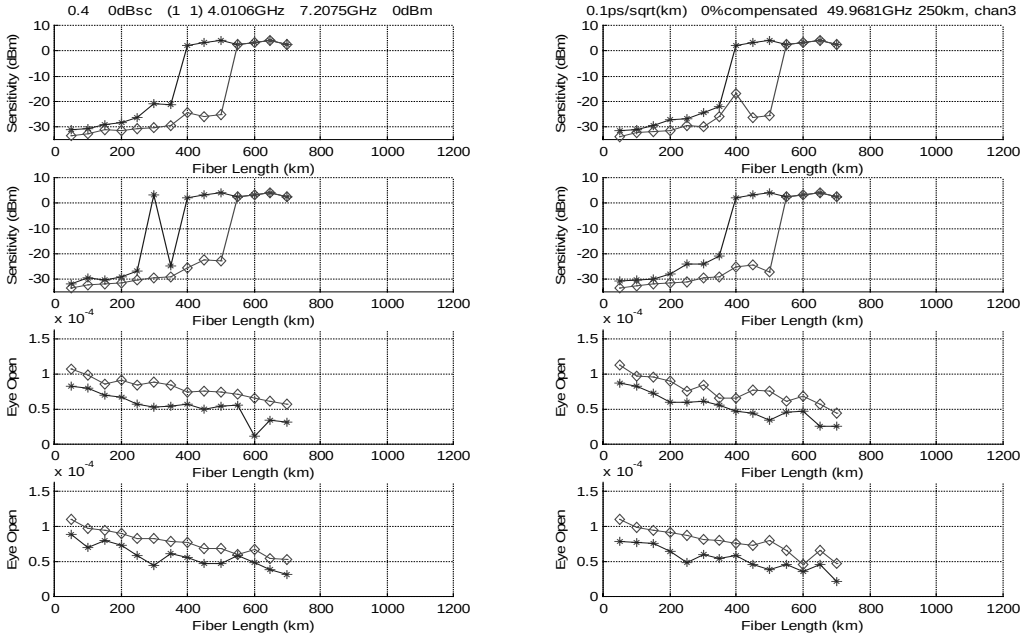

15. No DC, 0.1 $ps/\sqrt{km}$ PMD, -3dBm, 0.3 and 7 dB CS

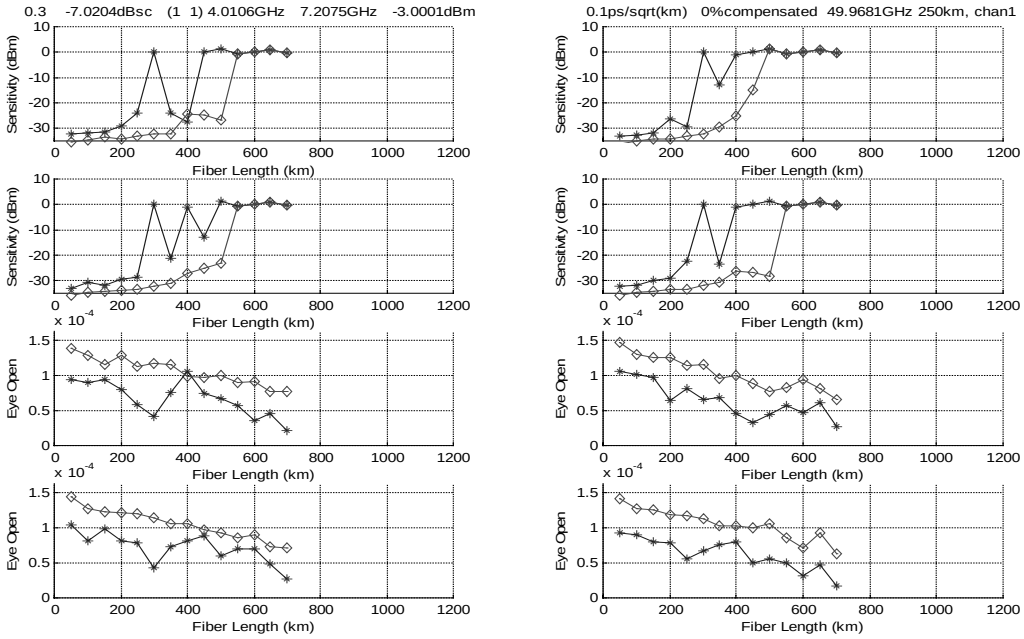

16. No DC, 0.1 $ps/\sqrt{km}$ PMD, -3dBm, 0.4 and 0 dB CS

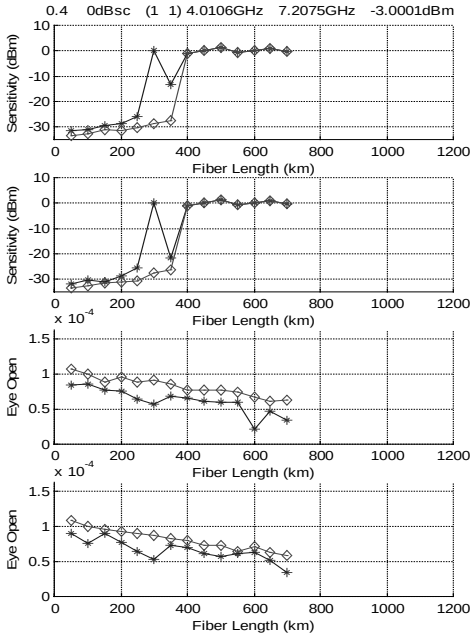

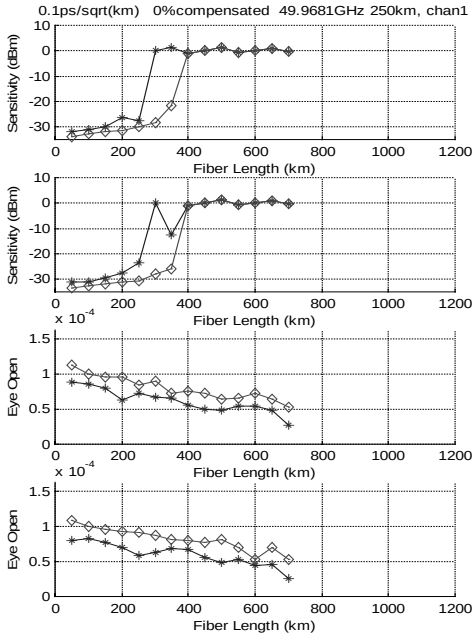

17. DC, 0.5 $ps/\sqrt{km}$ PMD, 5dBm, 0.3 and 5 dB CS

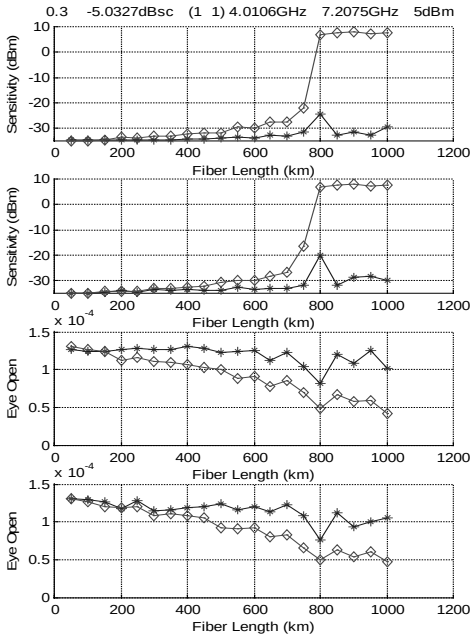

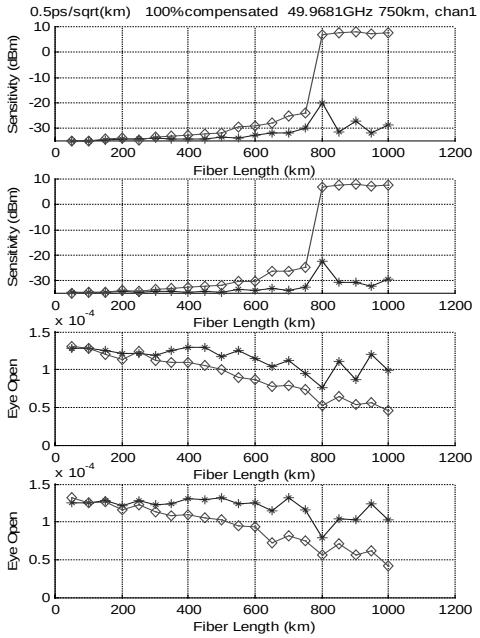

18. DC, 0.5 $ps/\sqrt{km}$ PMD, 5dBm, 0.4 and 0 dB CS

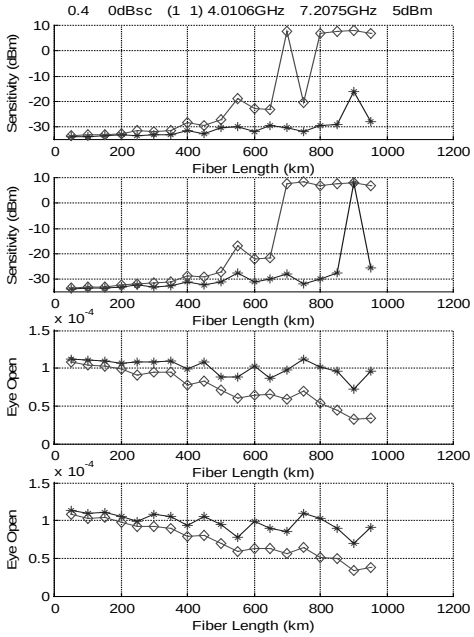

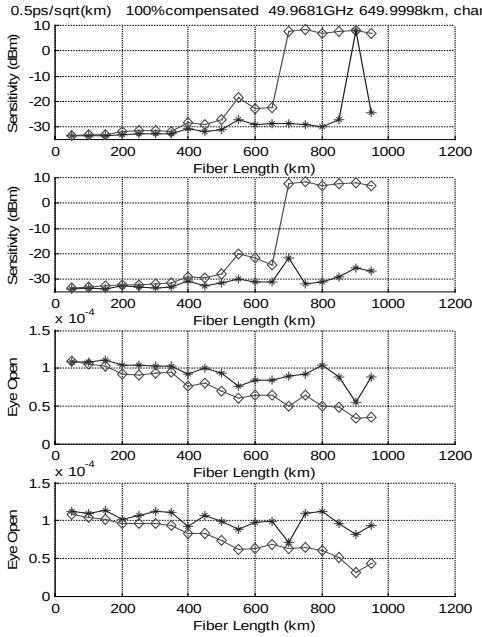

19. DC, 0.5 $ps/\sqrt{km}$ PMD, 3dBm, 0.3 and 5 dB CS

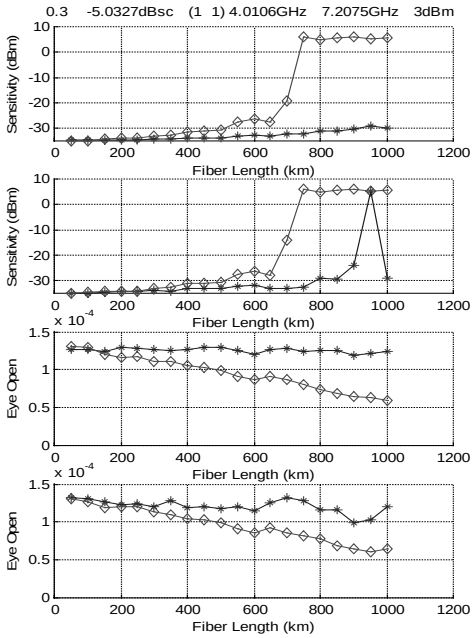

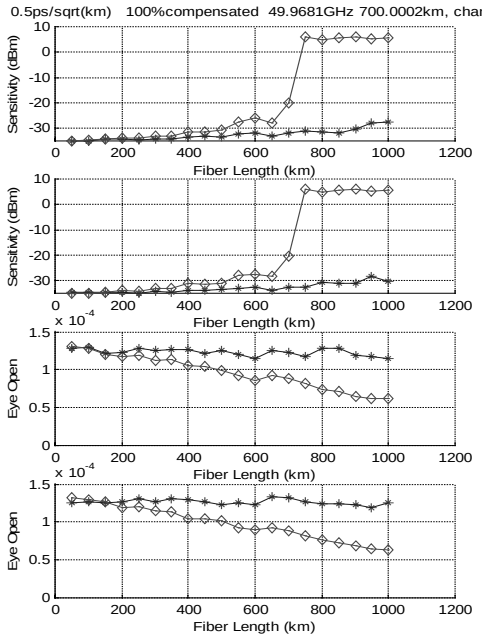

20. DC, 0.5 $ps/\sqrt{km}$ PMD, 3dBm, 0.4 and 0 dB CS

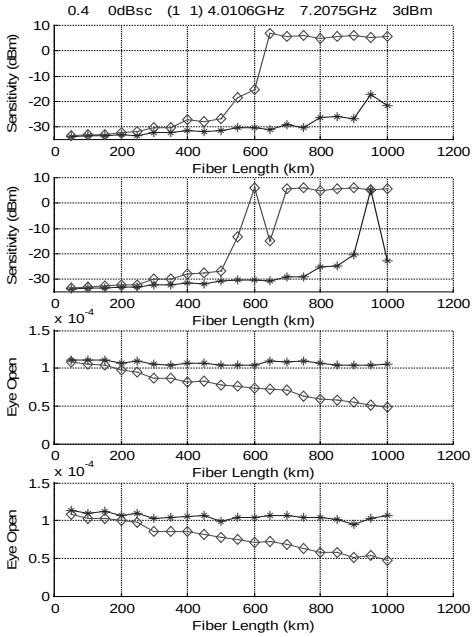

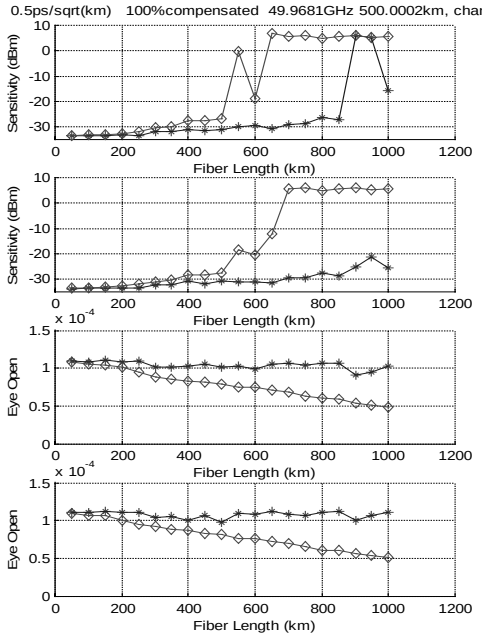

21. DC, 0.5 $ps/\sqrt{km}$ PMD, 0dBm, 0.3 and 7 dB CS

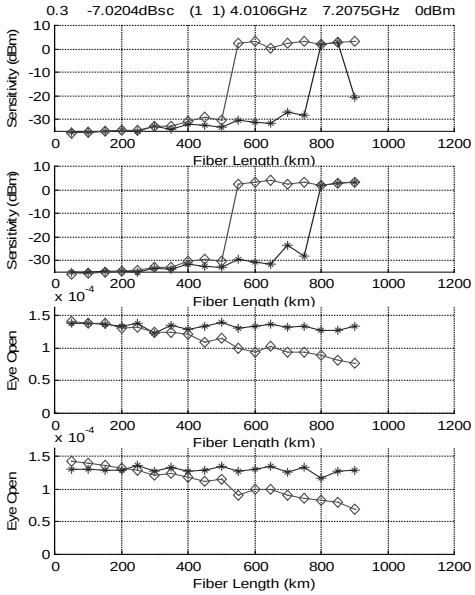

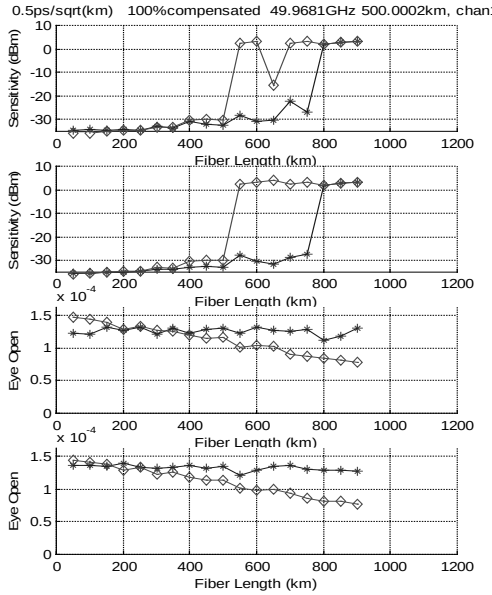

22. DC, 0.5 $ps/\sqrt{km}$ PMD, 0dBm, 0.4 and 0 dB CS

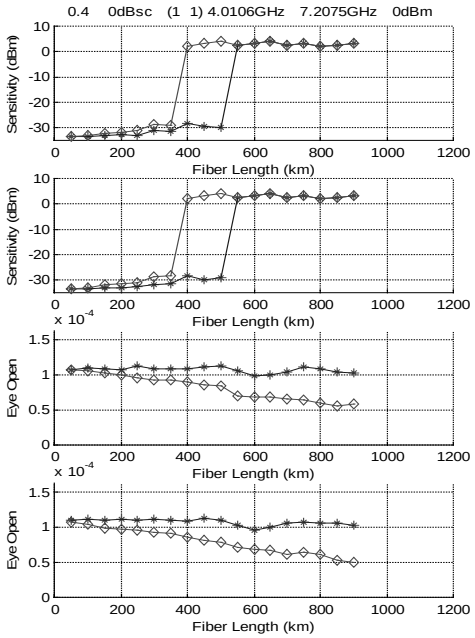

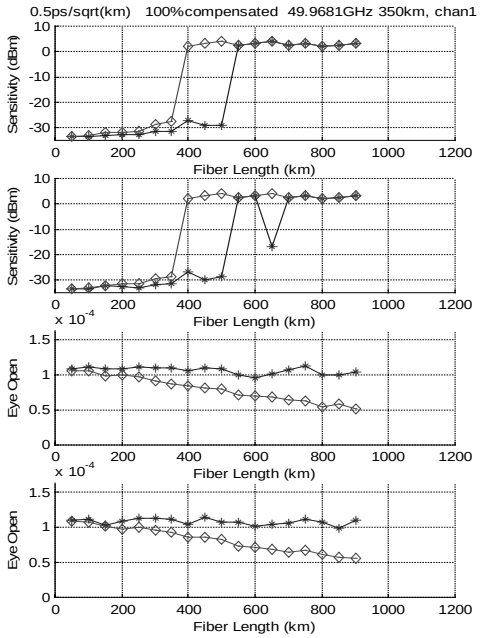

23. DC, 0.5 $ps/\sqrt{km}$ PMD, -3dBm, 0.3 and 7 dB CS

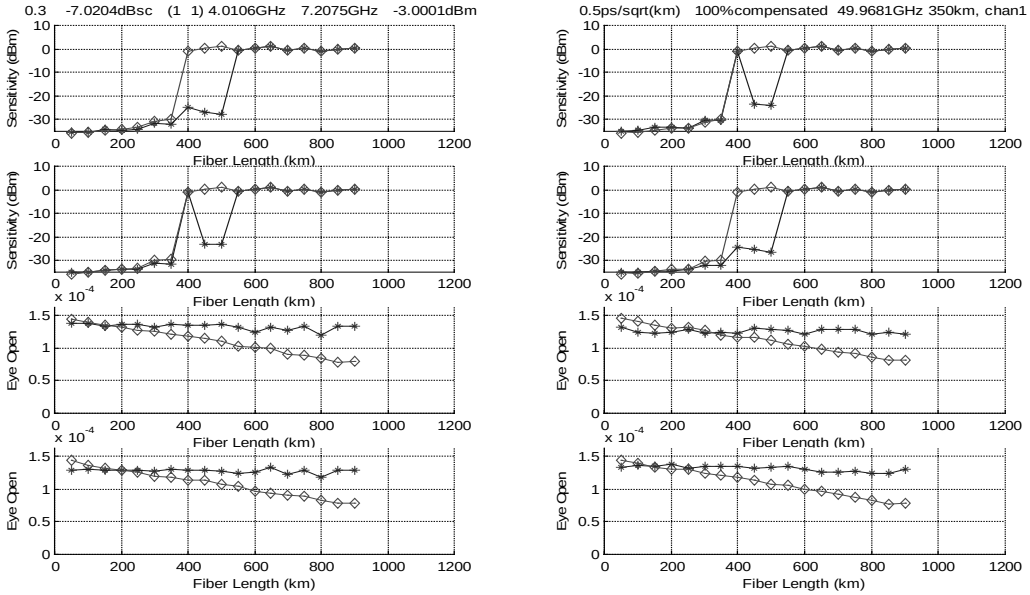

24. DC, 0.5 $ps/\sqrt{km}$ PMD, 0dBm, 0.4 and 0 dB CS

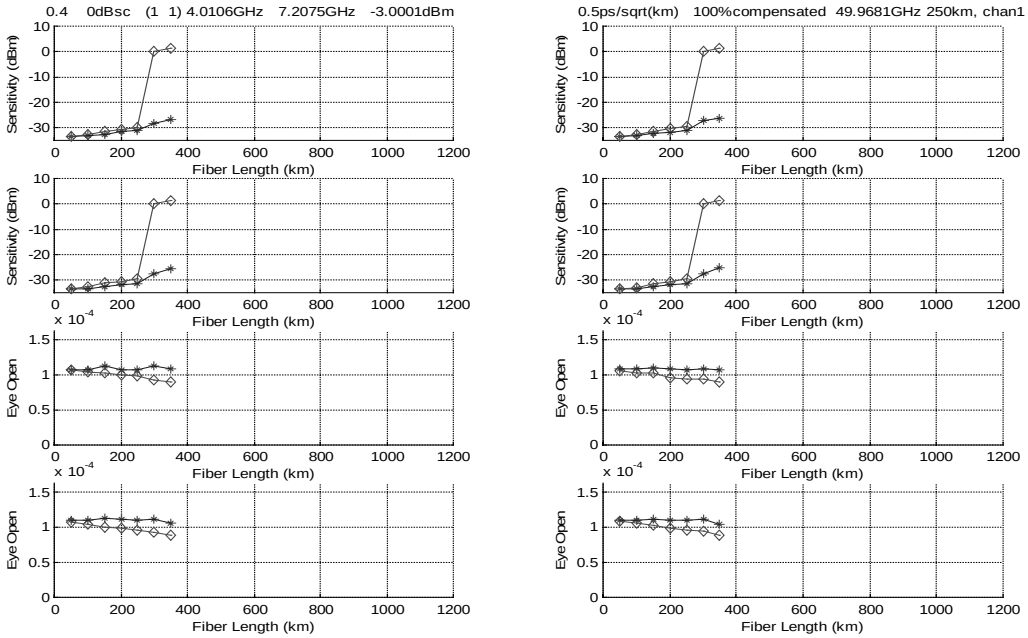

25. No DC, 0.5 $ps/\sqrt{km}$ PMD, 5dBm, 0.3 and 5 dB CS

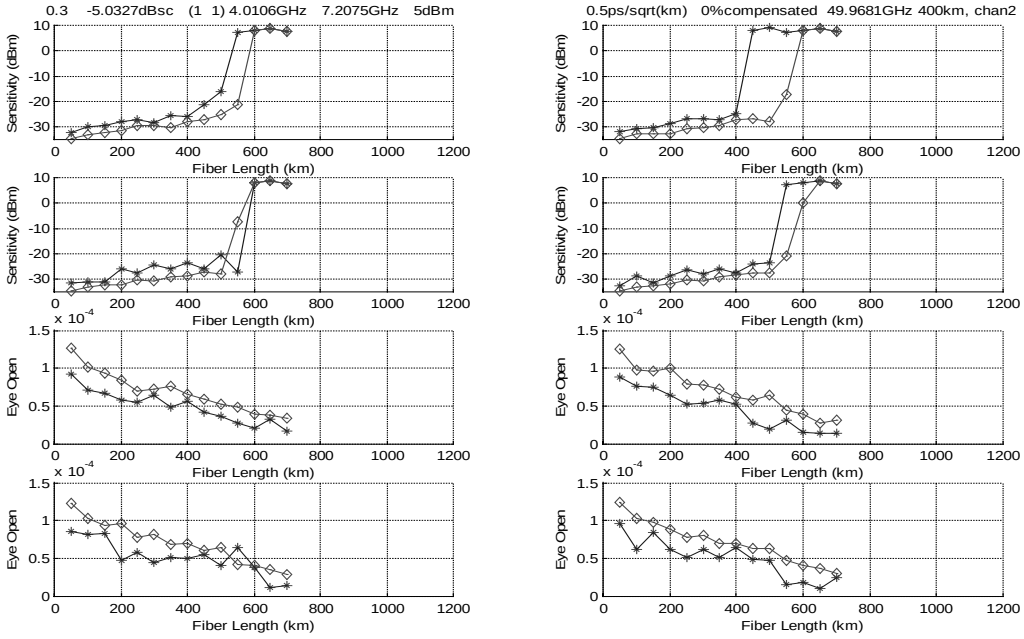

26. No DC, 0.5 $ps/\sqrt{km}$ PMD, 5dBm, 0.4 and 0 dB CS

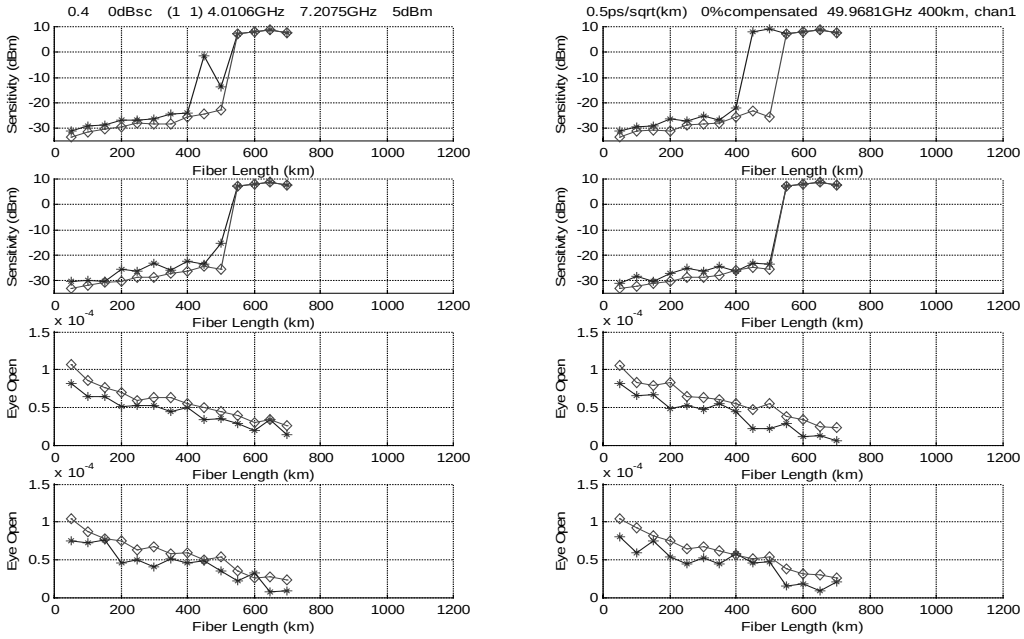

27. No DC, 0.5 $ps/\sqrt{km}$ PMD, 3dBm, 0.3 and 5 dB CS

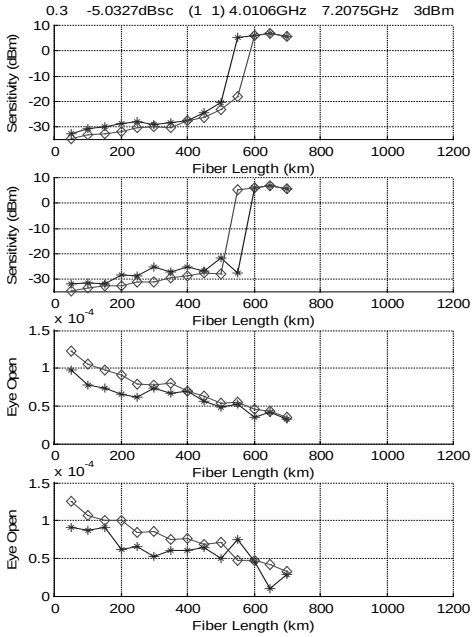

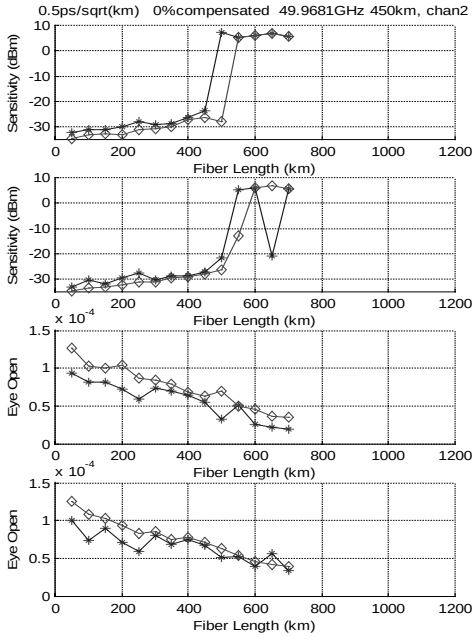

28. No DC, 0.5 $ps/\sqrt{km}$ PMD, 3dBm, 0.4 and 0 dB CS

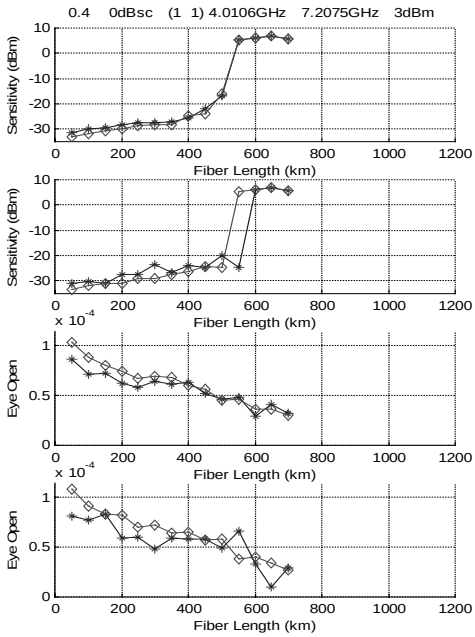

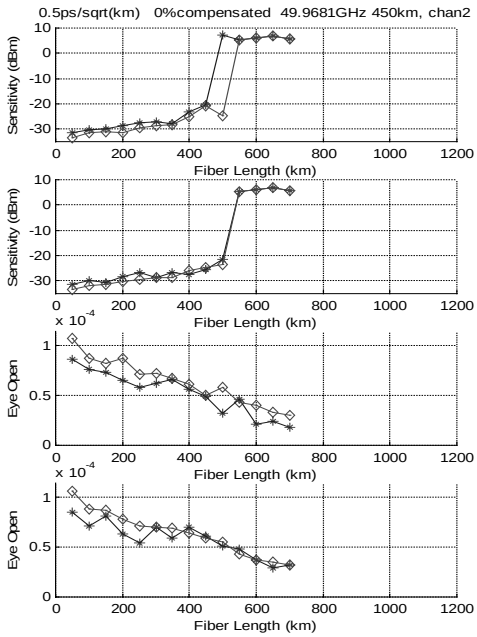

29. No DC, 0.5 $ps/\sqrt{km}$ PMD, 0dBm, 0.3 and 7 dB CS

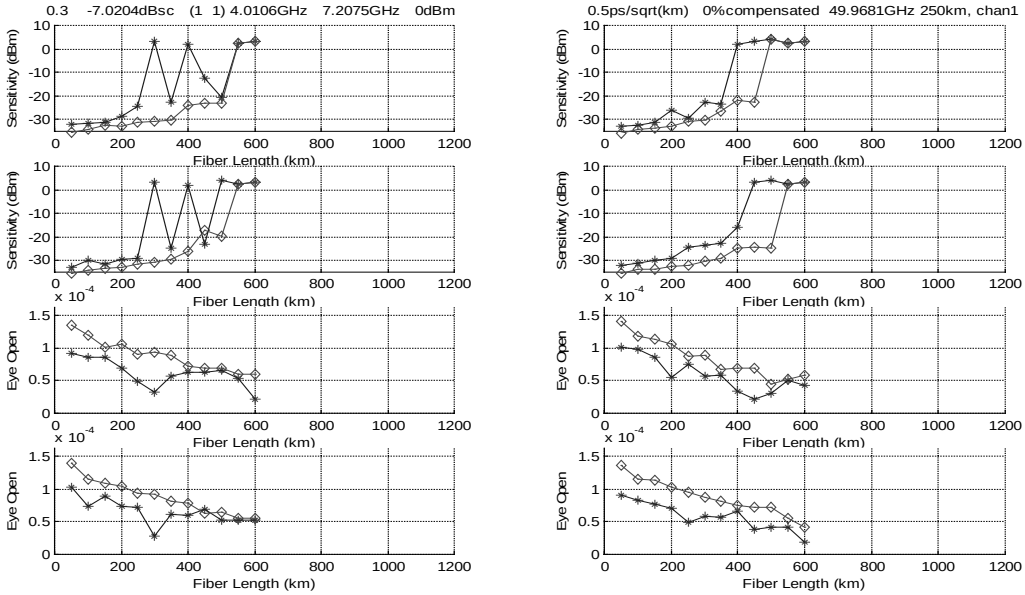

30. No DC, 0.5 $ps/\sqrt{km}$ PMD, 0dBm, 0.4 and 0 dB CS

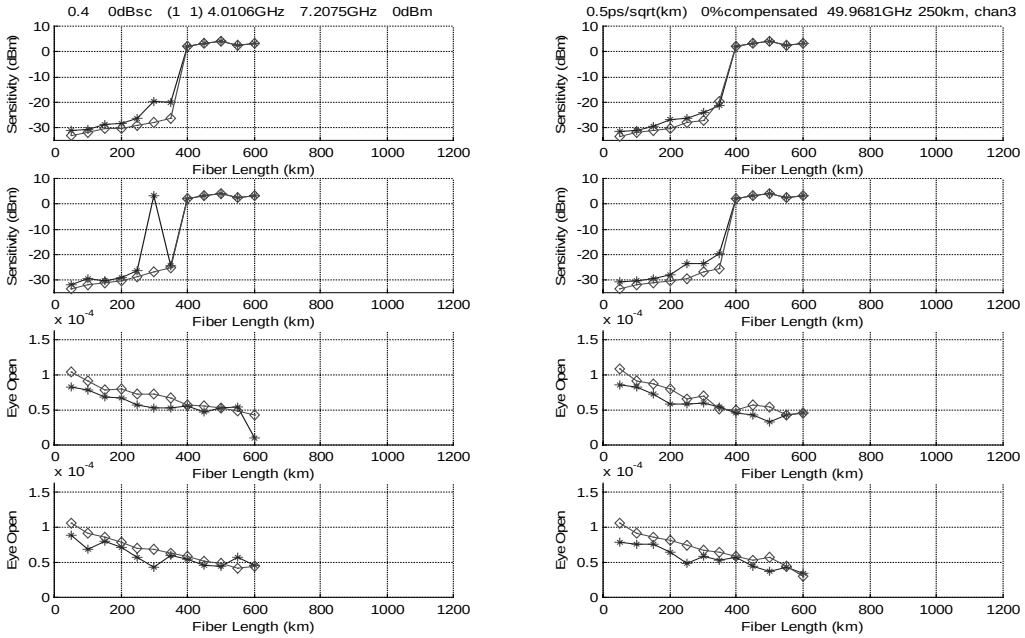

31. No DC, 0.5 $ps/\sqrt{km}$ PMD, -3dBm, 0.3 and 7 dB CS

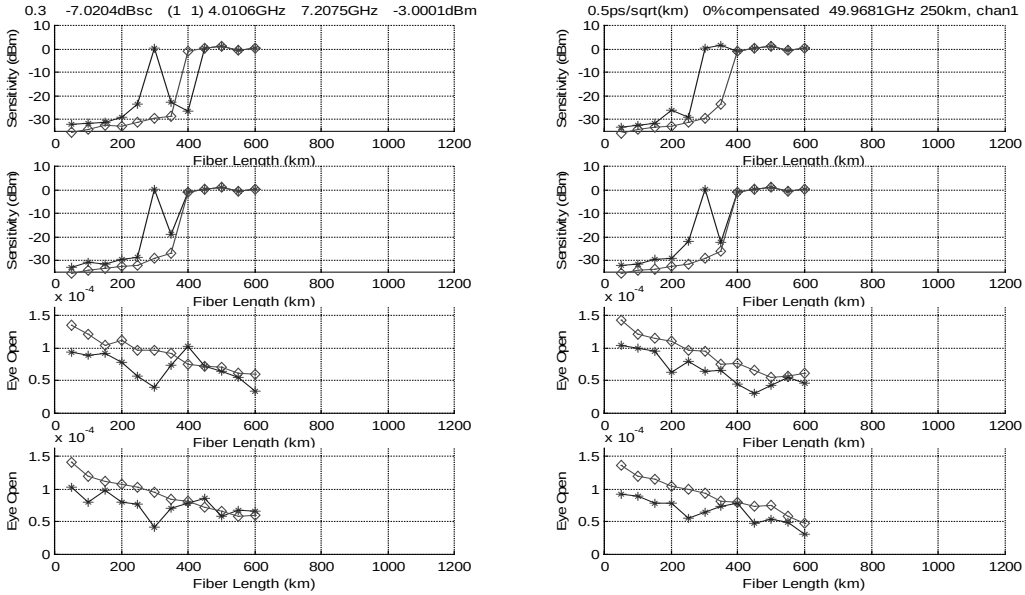

32. No DC, 0.5 $ps/\sqrt{km}$ PMD, -3dBm, 0.4 and 0 dB CS

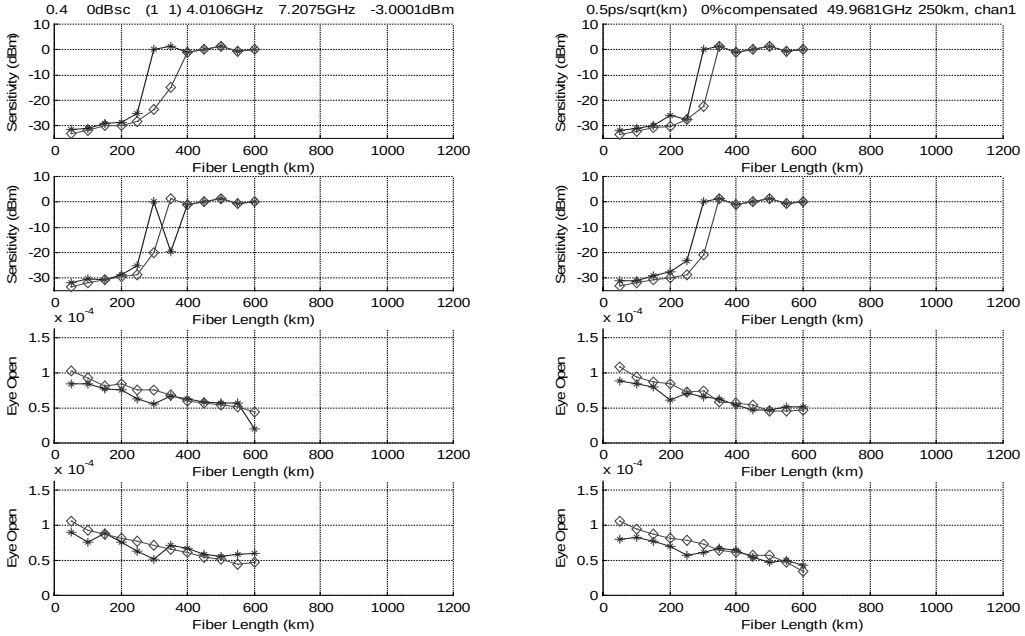

Appendix 4: ASK SCM results

DC, 0.1 $ps/\sqrt{km}$ PMD, 3dBm, 0.3 and -35 dB CS

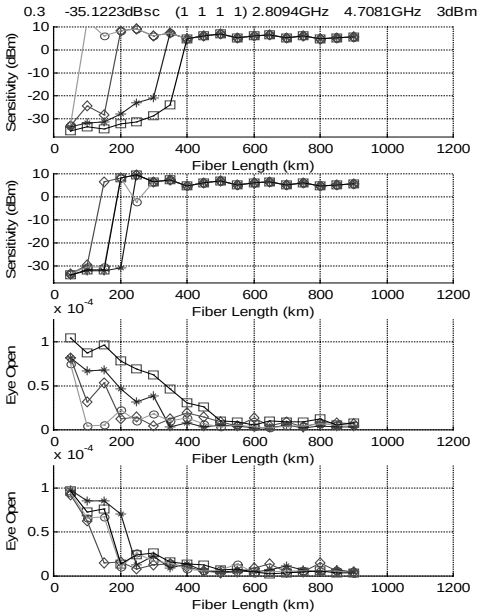

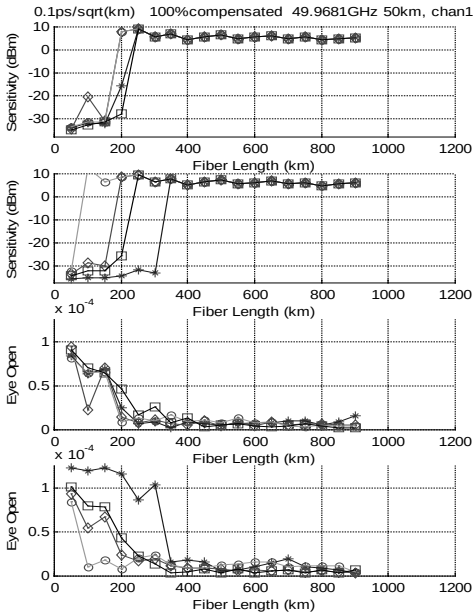

DC, 0.1 $ps/\sqrt{km}$ PMD, 0dBm, 0.3 and -35 dB CS

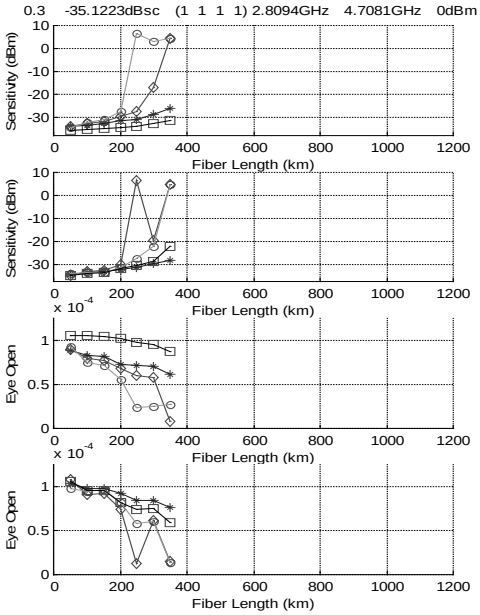

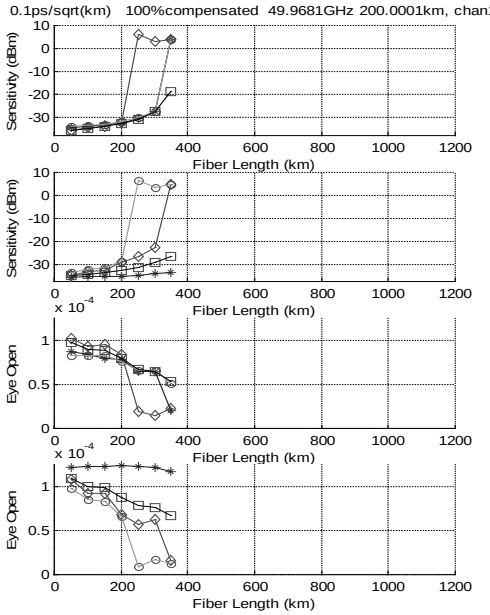

DC, 0.1 $ps/\sqrt{km}$ PMD, -3dBm, 0.3 and -35 dB CS

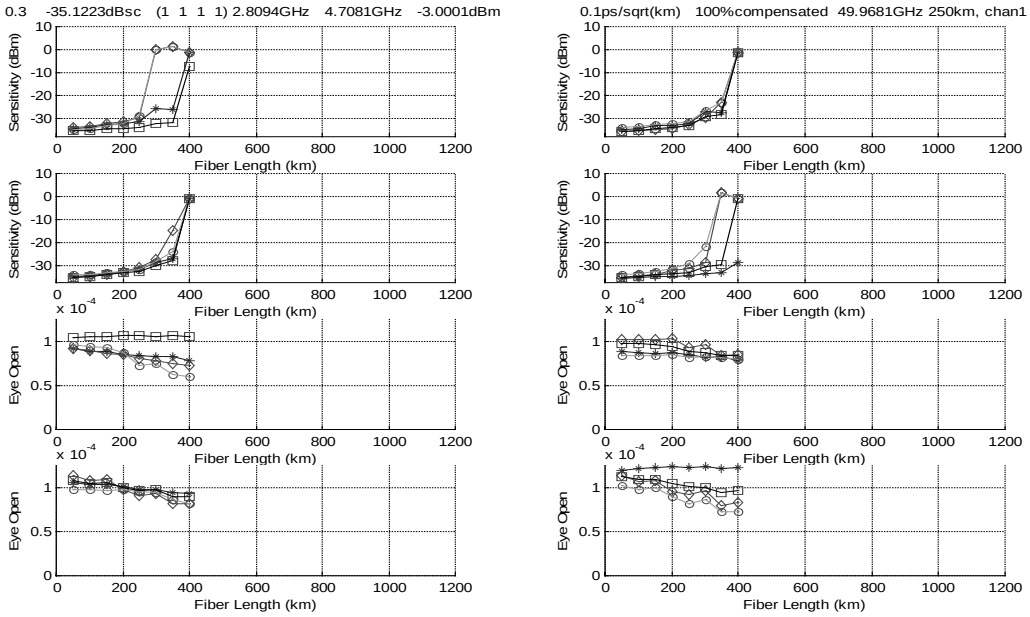

DC, 0.1 $ps/\sqrt{km}$ PMD, -6dBm, 0.3 and -35 dB CS

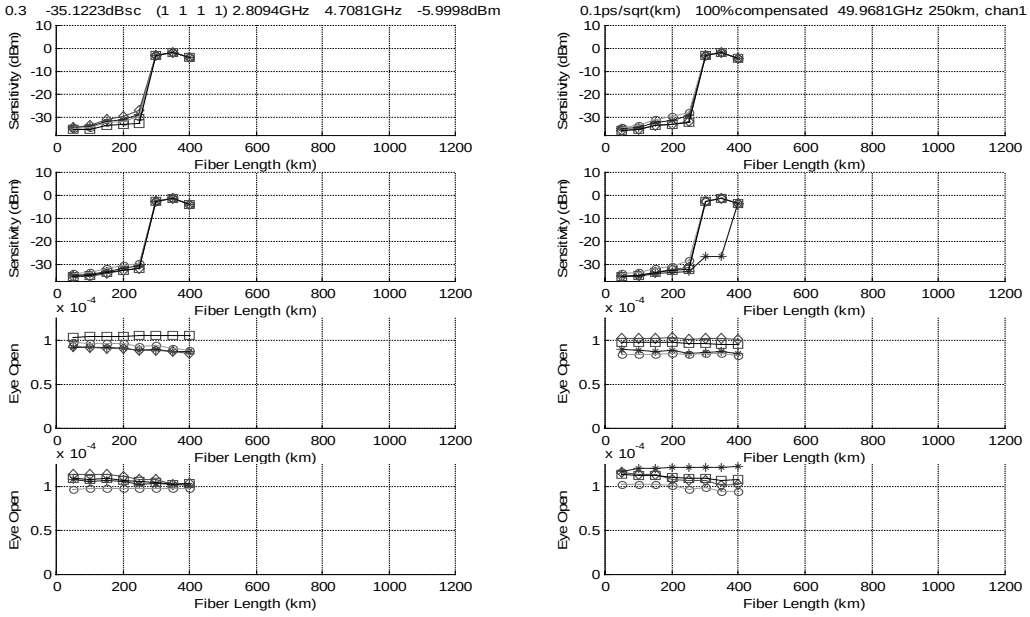

No DC, 0.1 $ps/\sqrt{km}$ PMD, 3dBm, 0.3 and -35 dB CS

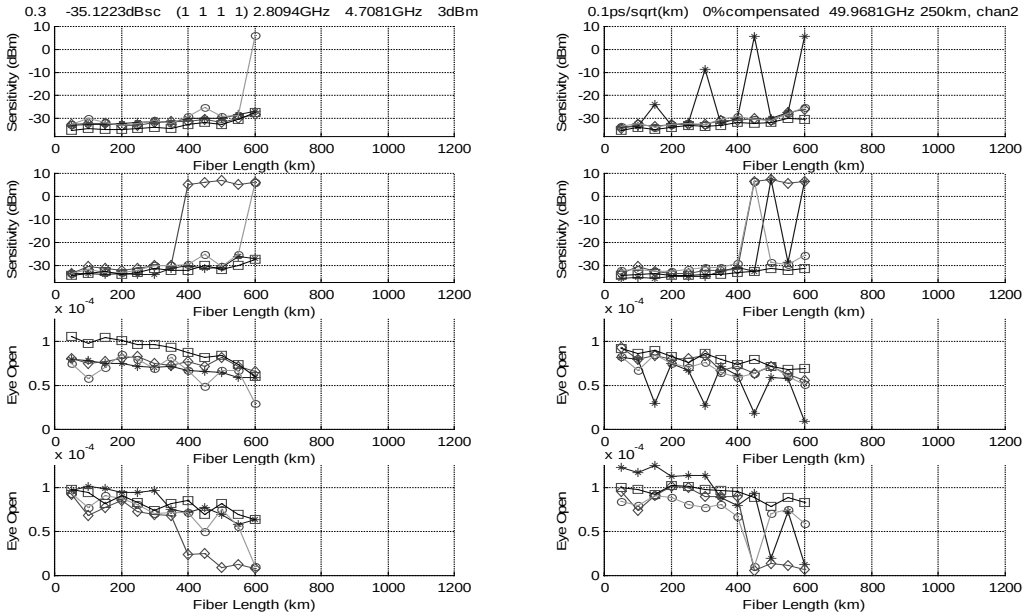

No DC, 0.1 $ps/\sqrt{km}$ PMD, 0dBm, 0.3 and -35 dB CS

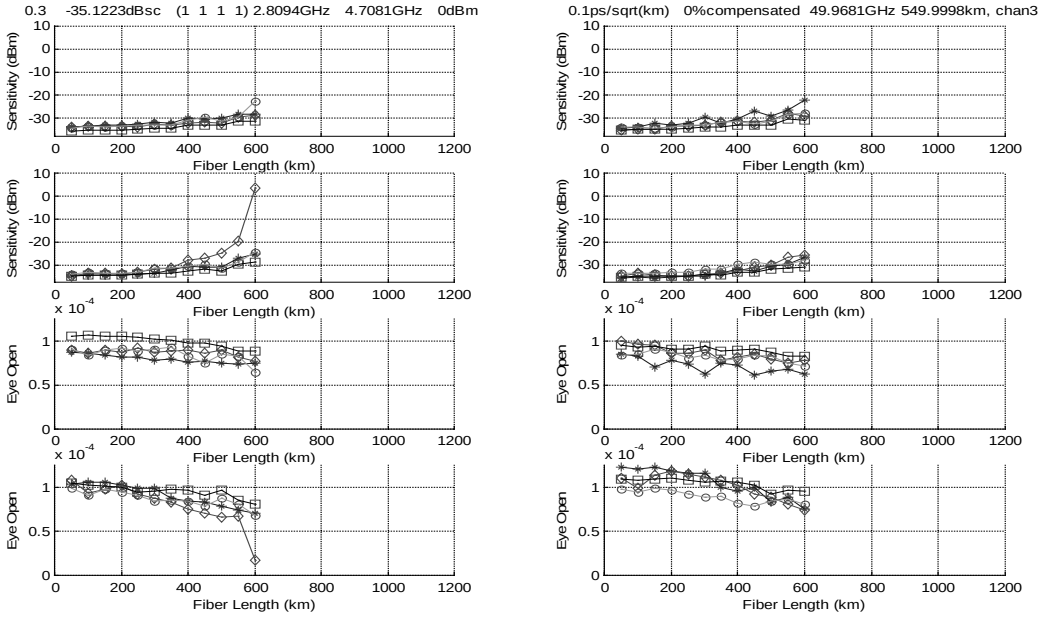

No DC, 0.1 $ps/\sqrt{km}$ PMD, -3dBm, 0.3 and -35 dB CS

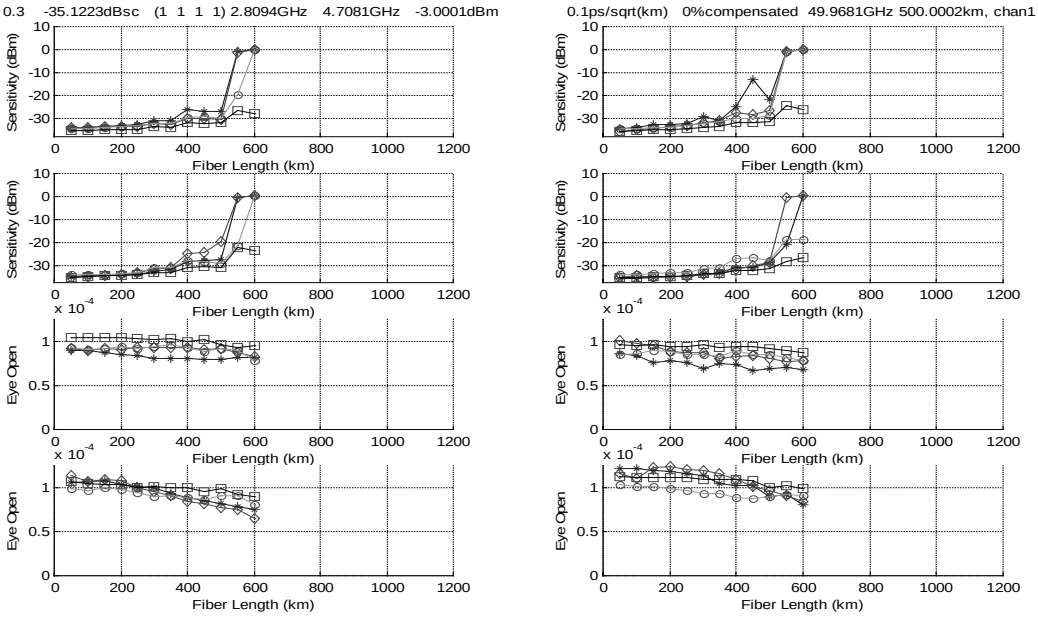

No DC, 0.1 $ps/\sqrt{km}$ PMD, -6 dBm, 0.3 and -35 dB CS

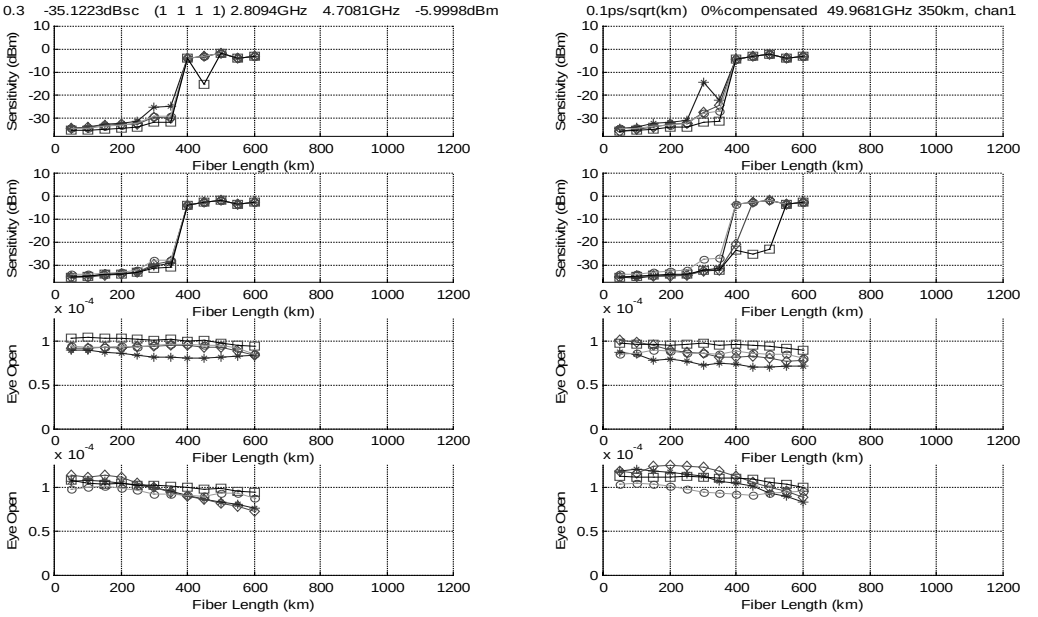

Appendix 5: OC192 results

DC, 0.1 $ps/\sqrt{km}$ PMD, 3dBm, 0.5 and 0 dB CS

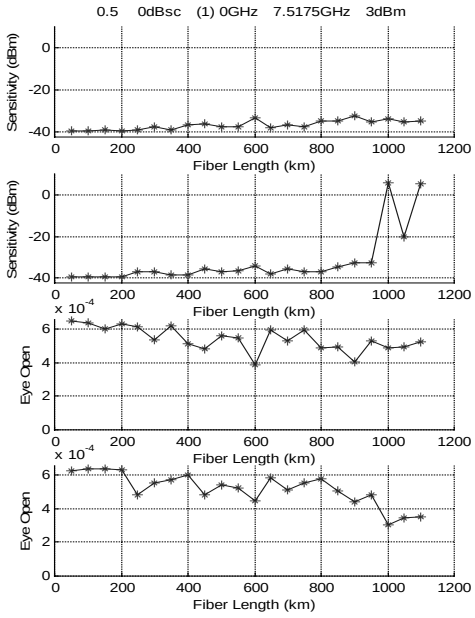

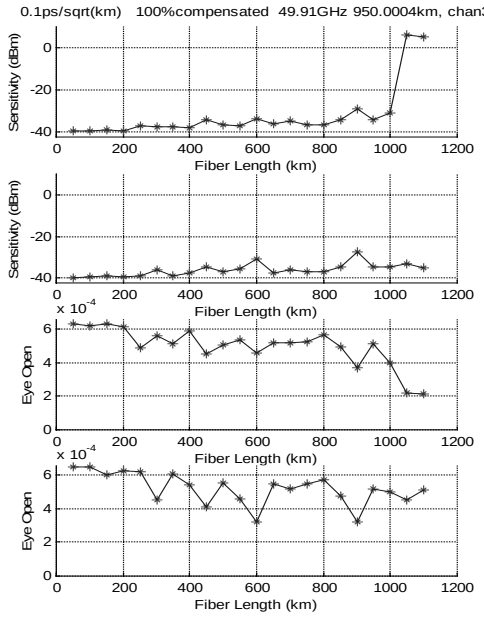

DC, 0.1 $ps/\sqrt{km}$ PMD, 0 dBm, 0.5 and 0 dB CS

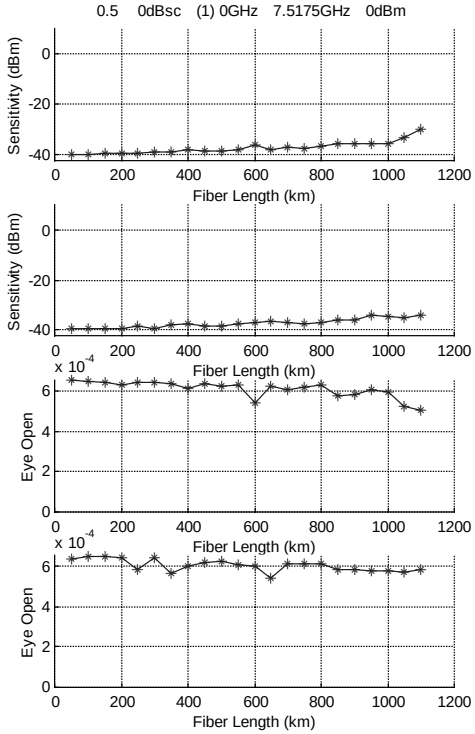

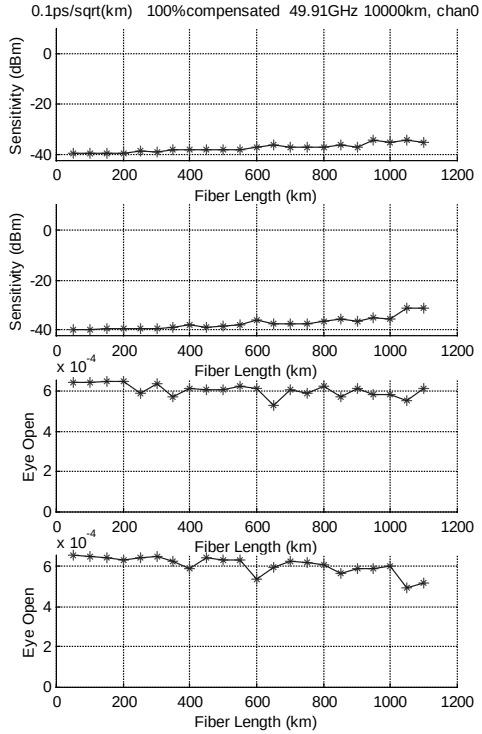

DC, 0.1 $ps/\sqrt{km}$ PMD, -3 dBm, 0.5 and 0 dB CS

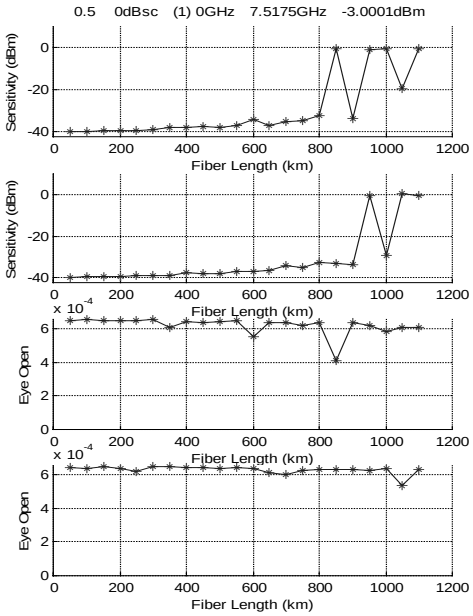

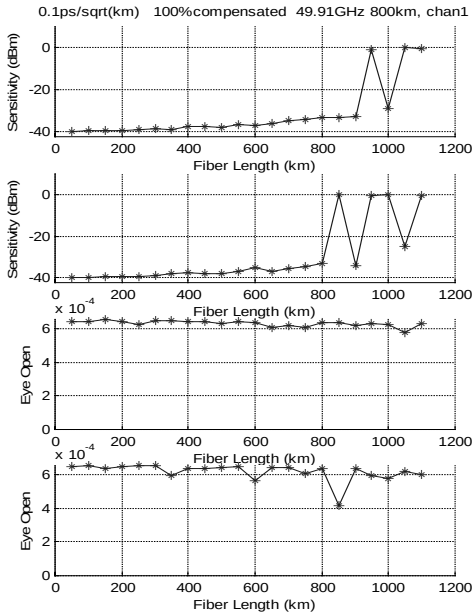

DC, 0.1 $ps/\sqrt{km}$ PMD, -6 dBm, 0.5 and 0 dB CS

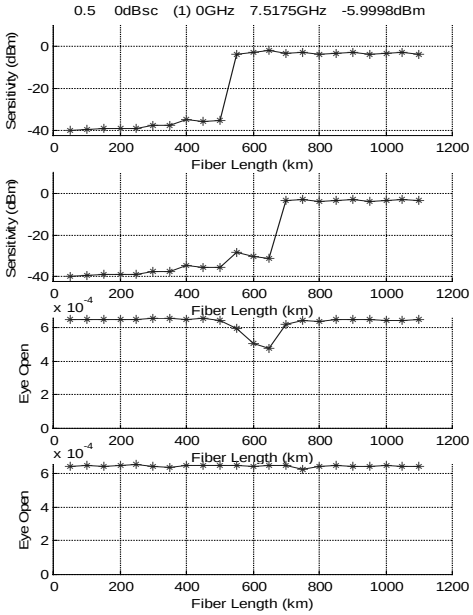

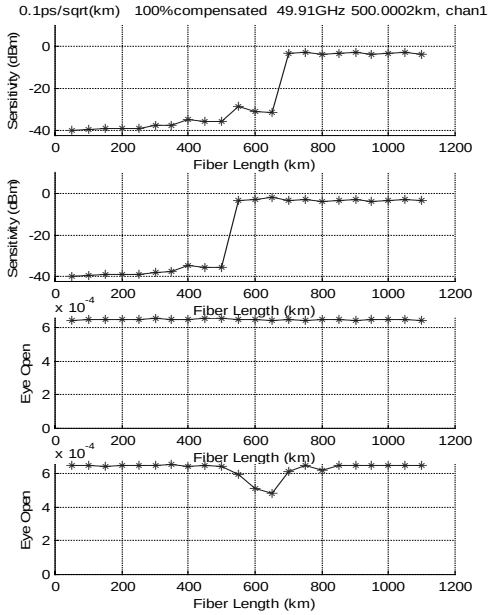

No DC, 0.1 $ps/\sqrt{km}$ PMD, 3dBm, 0.5 and 0 dB CS

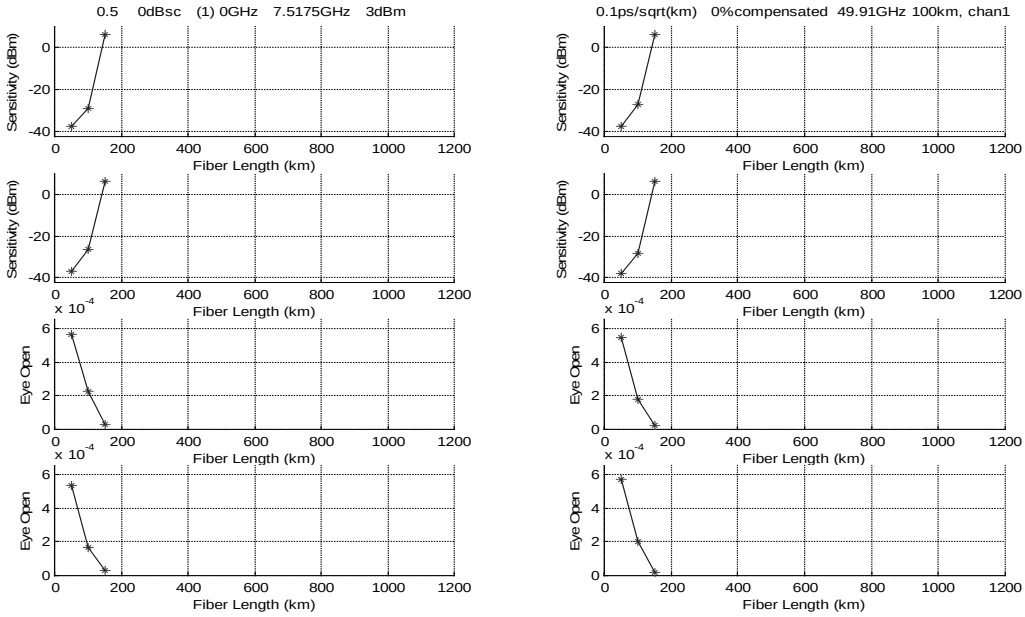

No DC, 0.1 $ps/\sqrt{km}$ PMD, 0 dBm, 0.5 and 0 dB CS

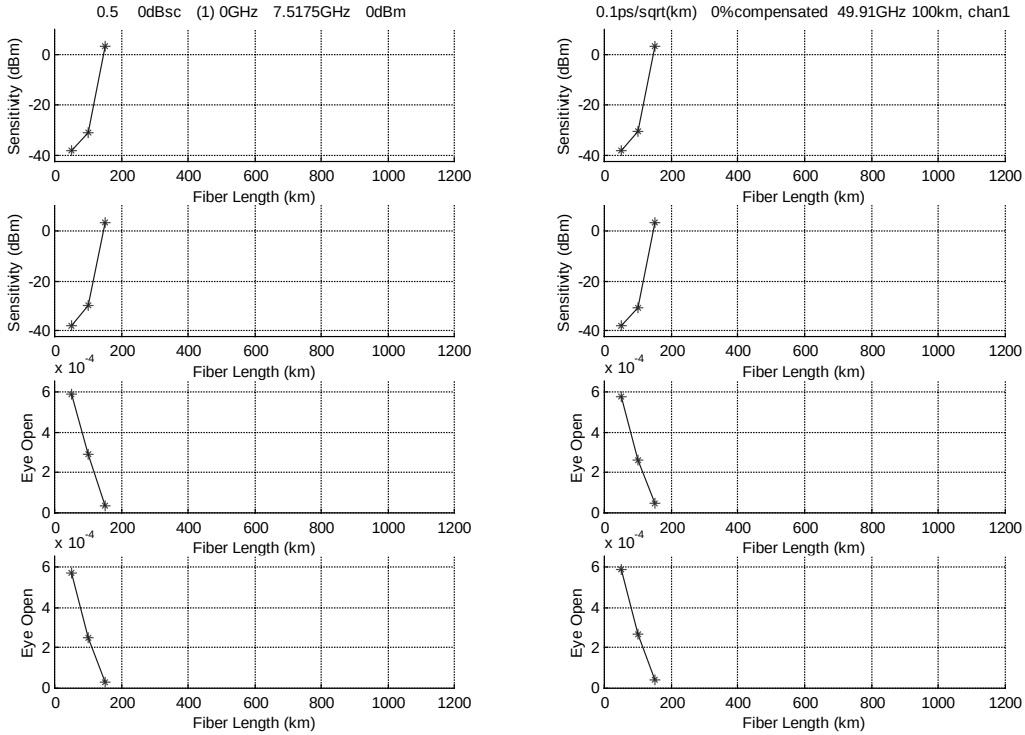

No DC, 0.1 $ps/\sqrt{km}$ PMD, -3dBm, 0.5 and 0 dB CS

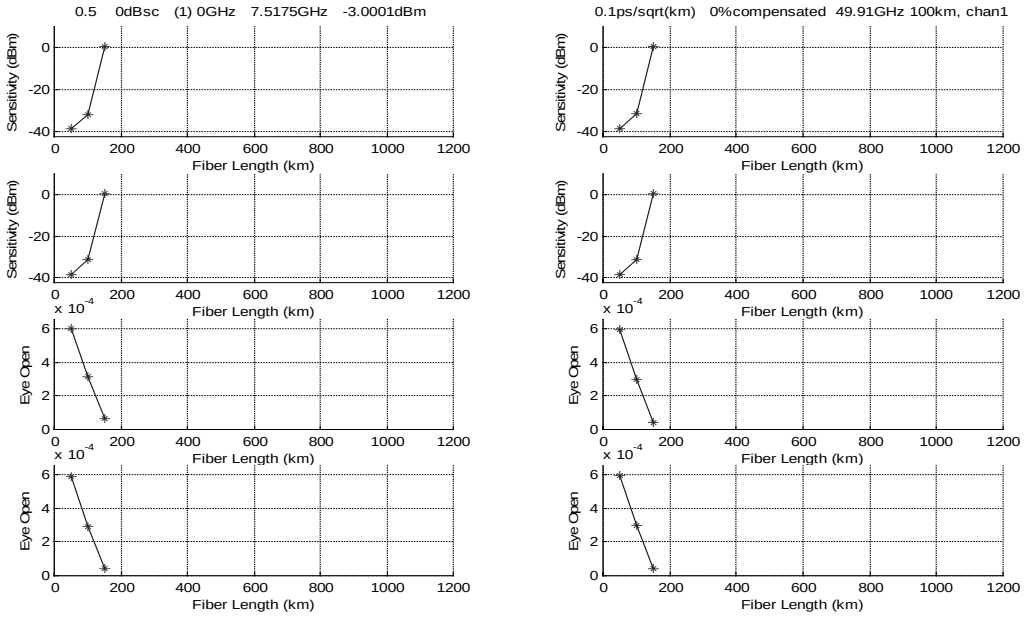

No DC, 0.1 $ps/\sqrt{km}$ PMD, -6 dBm, 0.5 and 0 dB CS